1.0

2.8 | 2.5

3.2 | 2.2

3.6

4.0 | 2.0

1.1

1.8

1.25 | 1.4 | 1.6

MICROCOPY RESOLUTION TEST CHART
NATIONAL BUREAU OF STANDARDS 1963 A

ARL-STRUC-REPORT-384

LEVEL

AR-002-237

DEPARTMENT OF DEFENCE

DEFENCE SCIENCE AND TECHNOLOGY ORGANISATION

AERONAUTICAL RESEARCH LABORATORIES

MELBOURNE, VICTORIA

STRUCTURES REPORT 384

DTIC
ELECTE
DEC 8 1981

LOW LEVEL WIND STUDY
BALD HILLS — THUNDERSTORM SEASON 1976-77

by

C. K. RIDER, D. J. SHERMAN and M. R. THOMSON

Approved for Public Release.

COPY No 21

OCTOBER 1980

81 12 08197

AR-002-237

DEPARTMENT OF DEFENCE
DEFENCE SCIENCE AND TECHNOLOGY ORGANISATION
AERONAUTICAL RESEARCH LABORATORIES

STRUCTURES REPORT 384

LOW LEVEL WIND STUDY
BALD HILLS — THUNDERSTORM SEASON 1976-77

by

C. K. RIDER, D. J. SHERMAN and M. R. THOMSON

SUMMARY

*At Bald Hills, Queensland, a 200 metre tower has been instrumented with anemo-
meters at levels 50 metre apart. Data were recorded each second for about 100 days
during the 1976-77 thunderstorm season, although night-time data for the hours mid-
night to 5 a.m. were generally not recorded.*

The strongest wind gusts were found to occur during thunderstorm gust front situations.

*The strongest wind shears occurred in a wider range of meteorological conditions.
In order of severity these were:*

  (a) *thunderstorm gust fronts*
  (b) *thunderstorms not associated with significant gust fronts*
  (c) *conditions associated with high temperatures, strong gusty but statistically
       stationary winds and active vertical wind component.*

*All the shears obtained using long averaging times (of the order of 10 minutes) were
only of slight to moderate intensity. Strong and severe shears occurred fairly frequently
but in short bursts, generally little more than 2 minutes in duration. This is a sufficient
period to appear as a steady shear to an aircraft pilot during an individual landing, but
not long enough to enable measurements made during one landing to be of use during
subsequent landings. As an indication of the scattered nature of the high shear incidents,
it was found that shears in excess of $0 \cdot 1$/second (i.e. wind speed differences greater than
5 m/s over the lowest 50 metre) occurred for only $0 \cdot 7\%$ of the time, but they occurred
for at least 6 seconds in $2 \cdot 5\%$ of the minutes of recorded data, and on more than 90%
of the days of the experiment.*

POSTAL ADDRESS: Chief Superintendent, Aeronautical Research Laboratories,
Box 4331, P.O., Melbourne, Victoria, 3001, Australia.

DOCUMENT CONTROL DATA SHEET

1. Document Numbers
   (a) AR Number:
   AR-002-237
   (b) Document Series and Number:
   Structures Report 384
   (c) Report Number:
   ARL-Struc-Report-384

2. Security Classification
   (a) *Complete document:*
   Unclassified
   (b) *Title in isolation:*
   Unclassified
   (c) *Summary in isolation:*
   Unclassified

3. Title: LOW LEVEL WIND STUDY
   BALD HILLS—THUNDERSTORM SEASON 1976-77

4. Personal Author(s):
   Rider, C. K.
   Sherman, D. J.
   Thomson, M. R.

5. Document Date:
   Published: October 1980
   Written: June 1978

6. Type of Report and Period Covered:

7. Corporate Author(s):
   Aeronautical Research Laboratories

8. Reference Numbers
   (a) Task:
   DST 76/154

9. Cost Code:
   24 7011

   (b) Sponsoring Agency:
   DST

10. Imprint:
    Aeronautical Research Laboratories,
    Melbourne

11. Computer Program(s)
    (Title(s) and language(s)):

12. Release Limitations (of the document)
    Approved for Public Release

12.0. Overseas:	N.O.	P.R.	1	A	B	C	D	E	

13. Announcement Limitations (of the information on this page):
    No Limitations

14. Descriptors:

		15. Cosati Codes:
Thunderstorms	Towers	0402
Gusts	Turbulence	
Gust fronts	Velocity distribution	
Wind shear	Airports	
Aircraft landing	Hazards	
Wind pressure	Wind (meteorology)	

16. *ABSTRACT*

See Reverse.

At Bald Hills, Queensland, a 200 metre tower has been instrumented with anemometers at levels 50 metre apart. Data were recorded each second for about 100 days during the 1976–77 thunderstorm season, although night-time data for the hours midnight to 5 a.m. were generally not recorded.

The strongest wind gusts were found to occur during thunderstorm gust front situations.

The strongest wind shears occurred in a wider range of meteorological conditions. In order of severity these were:

(a) *thunderstorm gust fronts*
(b) *thunderstorms not associated with significant gust fronts*
(c) *conditions associated with high temperatures, strong gusty but statistically stationary winds and active vertical wind component.*

All the shears obtained using long averaging times (of the order of 10 minutes) were only of slight to moderate intensity. Strong and severe shears occurred fairly frequently but in short bursts, generally little more than 2 minutes in duration. This is a sufficient period to appear as a steady shear to an aircraft pilot during an individual landing, but not long enough to enable measurements made during one landing to be of use during subsequent landings. As an indication of the scattered nature of the high shear incidents, it was found that shears in excess of $0 \cdot 1$/second (i.e. wind speed differences greater than 5 m/s over the lowest 50 metre) occurred for only $0 \cdot 7\%$ of the time, but they occurred for at least 6 seconds in $2 \cdot 5\%$ of the minutes of recorded data, and on more than 90% of the days of the experiment.

CONTENTS

1. INTRODUCTION

The Aeronautical Research Laboratories are concerned with any atmospheric conditions which are hazardous or which cause significant loads on aircraft. Aircraft are most vulnerable to unusual wind conditions during landing and take-off, and moreover the variability of the wind is greatest at low levels. Special attention is therefore being given to low level winds. A 200 m high radio transmission tower at Bald Hills, Brisbane, has been fitted with anemometers, direction vanes, vertical axis propellers and temperature sensors. (See Fig. 1.) A rain gauge and a number of anemometer/direction vane pairs mounted on 10 m masts in a "T" array have also been installed in the open paddock at the base of the mast. Readings from all these instruments are recorded each second on a magnetic tape recorder. The instrumentation is more fully described by Patterson *et al.* (1975), and the computer control of the system is described by Thomson (1975).
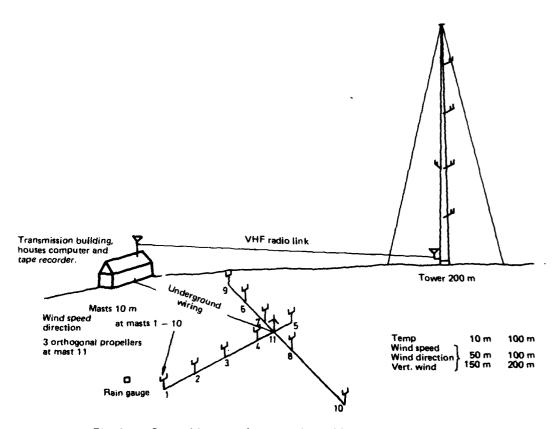
Fig. 1   General layout of meteorological instruments at Bald Hills.

1.1 Wind Shear

At low altitudes there are, apart from orographic effects, three (non-exclusive) categories of wind conditions which are commonly recognized as hazardous to aircraft. These are wind shear (see for example the review by Schrage, 1977), turbulence and thunderstorms. They are non-exclusive categories because in fact many of the aircraft accidents attributed to wind shear

or turbulence have in fact occurred during thunderstorms. A wind shear situation is either one where the mean horizontal wind velocity at one height is different from that at another height, or else one where the mean vertical wind component at a given point differs from the mean vertical wind at another point in the same horizontal plane. This second type is often associated with updrafts and downdrafts in thunderstorms. According to Fujita (1976) and Fujita and Caracena (1977) the principal cause of the Boeing 727 accident at John F. Kennedy airport on 24 June 1975 was a severe downburst associated with a thunderstorm. Such downbursts are *in the first place a horizontal shear of the vertical velocity*, though near the ground the spreading out of the downburst also causes a vertical shear of the horizontal wind vector. The magnitude of the vertical changes in the horizontal wind which cause difficulties to aircraft have been considered by ICAO, and recommendation 6 : 2/34 of the Fifth Air Navigation Conference, 1976, classifies shear as follows:

Light	0–4 knots per 30 m	(< 0·07/sec)
Moderate	5–8 knots per 30 m	(< 0·13/sec)
Strong	9–12 knots per 30 m	(< 0·19/sec)
Severe	above 12 knots per 30 m	(> 0·19/sec)

The time for which a shear acts on an aircraft is also relevant to the severity of its effect. This time is closely related to the height band over which the shear is acting, since the descent rates of most aircraft are usually fairly similar. Once a large aircraft has descended to the "decision height" of around 50 m it is committed to touch the ground. This is not, however, a valid argument for considering shears over a 50 m height band, for airspeed changes due to changing wind speed can occur very much faster than those due to pilot actions which are limited by speed of engine response and aircraft inertia. Aviation experts quoted by Sparks and Keddie (1971) have suggested that the most critical height band for an aircraft is that between 30 m and 15 m. Typically an aircraft such as a Boeing 727 will land on a 3 degree glide slope with an approach speed of 130 knots. This corresponds to a sink rate of 3–4 m/s and a time of 4·5 seconds to descend through 15 m. During this time the aircraft travels approximately 300 m, so that Sparks and Keddie suggest that wind speeds of significance to an aircraft are those averaged over a 300 m wind run. Sparks and Keddie then consider the problem of predicting the wind speed at a subsequent time and for this purpose they recommend a fairly long averaging period, at least four minutes. However such long averaging periods may smooth out peaks which may be critical in an individual landing, so here the problem of the forecaster has been ignored. The data from Bald Hills have been analysed for their potential effect on an aircraft, and this according to Sparks and Keddie, depends on an averaging time of around 4–5 seconds for the wind seen by the aircraft. The same order of magnitude for the averaging times of significance can be found by considering the work of Snyder (1968). Snyder gives some graphs of aircraft responses to step changes in horizontal and vertical winds which show some parameters reaching extrema within 1–2 seconds of the change, and returning to original values within 2–4 seconds. It appears then that wind shears acting for a fraction of a second are not very important, but that shears acting for several seconds are highly significant. We conclude that the averaging time for the wind seen by an aircraft should be in the range 1–5 seconds, which corresponds to an averaging distance of about 60–300 metres.

When measurements are made by a ground based anemometer, the wind passes the anemometer at a speed which is of the order of 10 m/s. The corresponding averaging time that would need to be applied to the anemometer record is in the range 6–30 seconds. For most of the data presented here an averaging time of 6 seconds has been adopted, but for certain problems a study has been made of the effect of varying the averaging time. One reason for choosing the shorter averaging time is that Hall *et al.* (1976) state that many thin high shear layers cannot be defined if an averaging time of about one minute is adopted, but with a shorter averaging time (they used 10 seconds) it is possible to delineate them.

There are very few measurements of wind shear probabilities of occurrence. In America Snyder (1968) quotes studies by Roberts (1964) and Scoggins (1967), and in England Pearce (1972) has made a study of wind shears measured by balloon soundings in the lower 1400 m of the atmosphere over a 12 month period. In Australia there are few known statistics on wind shear. Brook (1970) obtained 141 hours of data from anemometers at the 50 ft and 150 ft levels on a tower at Melbourne's Tullamarine airport. He classified the data by mean wind speed and

2

by gust class, using for the latter classification the five classes described by Singer and Smith (1953) based on the appearance of the wind direction trace. His data were biased by the rejection of any data for which one of the wind speeds failed to maintain a level above the threshold of the anemometer (about 4 knots). On the basis of his sample he estimated that a wind speed difference of 6 knots in 100 feet (i.e. $0\cdot1$/sec) would be exceeded, for 10 seconds or more at a time, for $81\cdot17$ hours per year—i.e. for about 1% of the time. For the case of an atmosphere with C-class gustiness and hence a neutral lapse rate, Brook and Spillane (1968) considered the shears that would occur in normal turbulent conditions, but excluding such singular events as thunderstorm squalls and sea breeze fronts. In regular turbulence they found the shear to be approximately normally distributed. They estimated the peak shear in an hour by adding to the mean shear a variability allowance which was proportional to both the mean wind speed at the upper level, and to a tabulated function of the averaging time over which the shear was measured. They found that if a power law was used to describe the variation of velocity, U, with height, z,

$$U/U_0 = (z/z_0)^m \tag{1.1}$$

where the parameters U_0 and z_0 are sometimes referred to as the gradient wind and gradient height respectively, the index m varied from $0\cdot08$ to $0\cdot25$ even with the data restricted to C class gustiness (neutral stability). Brook and Spillane's conclusion was that such formulae were not adequate to predict the mean shear in any situation, but that the mean shear should be measured each time. Blackman (1972) studied the velocity profile, in a suburban environment, using a 30 m tower. His tower was situated among shrubs, so he used a modification of equation (1.1) to allow for a roughness displacement, z'.

$$\frac{U}{U_0} = \left(\frac{z - z'}{z_0 - z'}\right)^m \tag{1.2}$$

Using, generally, 6 minute average velocities, he found z' and m to both vary from occasion to occasion. z' tended to be constant for winds coming from bearings between $90°$ and $270°$, though there was considerable scatter for winds coming from the $0 \div 30°$ sector. Using the appropriate value of z' for each run, Blackman found that m varied from $0\cdot12$ to $0\cdot27$. This scatter is rather similar to that found by Brook and Spillane.

Deacon (1955) measured wind speeds at three levels (40 ft, 210 ft and 503 ft) on a tower situated in grassland near Sale, Victoria. He obtained 24 runs, with an average duration of 8 minutes per run, in strong wind conditions. Using the mean wind velocities of each run he obtained an average exponent value of $m = 0\cdot16$. He also considered for each run the peak gust at each height irrespective of the time of occurrence at the various heights. When the peak gusts were fitted to a power law of the form 1.1, he obtained a much lower exponent, $m = 0\cdot08$. This he attributed to the fact that peak gusts are generally caused by eddies bringing a parcel of upper level air with high momentum down to the ground. Until the parcel has been retarded by friction and mixing, the velocity is very close to the general velocity at high levels. Nowadays Deacon's method of handling the peak gust has been superseded by a separate treatment of the profiles of mean velocity, and the profiles of some measure of the deviation of the instantaneous velocity from the mean at each level. A simple model which is commonly used assumes the standard deviation of the wind speed at any point is constant, independent of height.

Some climatological studies of wind shear, using 1 hour average values of wind speed are being carried out on data obtained from N. W. Cape, W.A., and Black Mountain, Canberra. (Stuart Allen, private communication). About two years data are available from each source but at present only the Black Mountain data have been published (Allen, 1980).

In summary, then, the available wind shear data for Australia are either based on a very small and biased sample, or use averaging times which are so long that they smooth out most peaks of significance to aircraft.

The Bald Hills tower data offers some opportunity to improve the available statistics for Australia, but even so the data available in the present season only cover 100 days. Moreover the sample is still biased in that it covers only one season of the year, and in general data were not recorded for the midnight to dawn period each day due to absence of power when the radio transmitter was turned off. On the other hand the starting velocity of the anemometers was so

3

low that there was no necessity to censor data by removing occasions when the wind speed was zero. It would probably be possible to use Brook's technique of classifying data according to wind speed and gustiness category (the latter is basically a classification according to lapse rate) and then to find an overall probability distribution of wind shear by weighting the probability distribution of shear for each speed, gustiness category by the long term average probability of occurrence of that category. This would, however, involve a rather large amount of manual work, so at this stage a simpler though less satisfying procedure has been adopted. The probability distribution of wind shear in the 100 day sample has been related to the probability distribution of wind speed in the same sample. Then the long term probability distribution of wind shear may be estimated from the known long term probability distribution of wind speed.

1.2 Thunderstorm Gust Fronts

Wind velocities that change with time (gusts or turbulence) can cause as much difficulty to a pilot as winds that change with height (wind shear). In fact, during an individual landing it is not possible to distinguish between the two phenomena on the basis of the aircraft behaviour. As with wind shear the strongest gusts are usually associated with thunderstorms. The strongest shears and gusts associated with a thunderstorm frequently occur at the "gust front". When a gust front occurs, mid-tropospheric air is cooled by melting hail and evaporating water. This cooled, denser air sinks to the ground and tends to spread out in all directions, but especially in the forward direction as the cooled air tends to carry mid-tropospheric momentum with it. (The total storm also tends to move in the direction of the mid-tropospheric wind but at a somewhat slower speed.) Actually the gust front will often, especially in severe local storms, be found to lie ahead but on one flank of the storm. The explanation of this is discussed by Browning (1968).

In a gust front situation, the magnitude of the wind speeds and shears depends on the momentum of the outflowing air which is a function of the density or temperature difference between the ambient air and the downdraft. Fawbush and Miller (1954) have obtained a statistical correlation between the peak wind gust and the temperature drop as the gust front passes. They have also recommended the use of Brancato's (1942) method of predicting the downrush temperature, i.e. the temperature which a parcel of air would have if it was moved from the wet bulb freezing level to ground level following a saturated adiabatic compression law.

The relation between air density and temperature is affected by the presence of moisture, since moist air has a lower density than dry air. In order to preserve the form of equations in which density differences are expressed as fractional differences in temperature, the concept of "virtual temperature" is introduced. Haurwitz (1941) defines the virtual temperature of a mass of moist air as the temperature which dry air should have in order to be of the same density as the actual moist air under the same pressure. If the total pressure of the air is p, the partial pressure of the water vapour is e, and the temperature is T, then the virtual temperature T^* is

$$T^* = T/(1 - 0.379\,e/p). \tag{1.3}$$

The recent literature on thunderstorm gust fronts has made little, if any, use of the concept of virtual temperature. The temperature drop commonly recorded is just the drop in actual temperature. Assuming that the downdraft, which has been subjected to evaporative cooling, has a temperature of 20°C and a relative humidity of 100% it is possible to compute the following table of virtual temperature drops corresponding to various actual temperature drops in ambient air of various relative humidities.

Table of Virtual Temperature Drops

R.H.	Actual temperature drop (°C)		
	4·0	8·0	12·0
80"	4·1	8·9	13·9
60"	3·4	8·0	12·7
40"	2·8	7·1	11·6

4

It is seen that generally the virtual temperature drop is very close to the actual drop. However the occasional large differences may be important in the explanation of differences in behaviour of otherwise similar gust fronts.

Fig. 2(a) Observed form of gravity current (after Keulegan, 1958).
(The head is moving to the left with velocity c.)
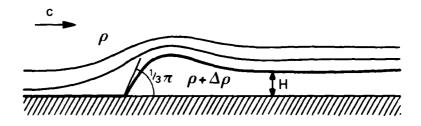
Fig. 2(b) Theoretical model proposed by von Kármán.
(The head is brought to rest by superimposing a velocity c to the right.)

Fig. 2 Head of density current outflow.

Classical fluid mechanics (see e.g. Benjamin, 1968) has considered the case of a density current head of density $\rho + \Delta \rho$ flowing inviscidly beneath a lighter fluid of density ρ. The speed of movement of the head, c, is given by

$$c = \alpha \sqrt{gH\Delta\rho/\rho} \qquad (1.4)$$

where H is the depth of the dense fluid layer well upstream from the head (see Fig. 2) and the coefficient α is theoretically equal to the square root of 2 in an ideal fluid, and experimentally is found to be around $1 \cdot 1$ in a real fluid. As noted above the density difference is related to the temperature drop. Hall et al. (1976) used this approach and assuming a linear velocity profile through a boundary layer around 100 m thick in a density current of depth $H = 500$ m, estimated wind shear as a function of gust front temperature drop. They presented data on how wind shears observed in a number of thunderstorm gust fronts varied with the temperature drop and found the data to agree fairly well with their simple model.

The static pressure beneath a density current is slightly higher than ambient. Consider, for example, an ambient environment with a temperature of 27°C (300 K) and a downdraft with a fairly small temperature drop of 3°C. The fractional density difference is $3/300 = 1^{o}{}_{o}$. The speed of travel of the front is approximately $c = \sqrt{2g} \, H \, \Delta\rho/\rho$ and for $H = 500$ m this gives $c = 10$ m/s. The ultimate pressure rise is $\Delta p = \Delta \rho g H = 0 \cdot 6$ mbar. However the head of the outflow is usually (see Fig. 2) about twice as high as the ultimate thickness of the outflow. This suggests an initial rise of about $1 \cdot 2$ mbar in the time the outflow takes to travel about 1 km, i.e. in about 100 seconds. Presumably a fast response high resolution pressure transducer would tend to give a trace which showed the shape of the head of the density current, but this might be modified by three different factors. Firstly the flow is dynamic rather than static, so that pressure rise will not occur exactly under the dense air as a sharp discontinuity, but will

5

propagate ahead as a pressure wave and in so doing will be modified somewhat in shape. Secondly the pressure will be increased by the impact pressure which will also occur due to the falling downdraft striking the ground. Thirdly Charba and Sasaki (1971) indicate that at least in some situations a low level stable layer may exist, and when the downdraft disturbs this it may cause a surge wave at the top of this stable layer which, with an associated pressure rise, may propagate ahead quite independently of the gravity current outflow. It has been proposed (Bedard et al., 1977, several papers) to use the pressure rise as the basis of a gust front warning system. An experimental system has been developed at Dulles airport using pressure switches which trigger an alarm system if a pressure rise exceeding 0.5 mbar occurs when the pressure time history is filtered by a high pass filter with a 3 minute time constant.

A few authors have studied detailed flow within and around density current heads. Goff (1975, 1977) has made a detailed study of 20 thunderstorms, and, with data from vertical wind measurements at three levels and horizontal wind measurements at seven levels on a 480 m tower, has obtained streamlines showing the shape of the gust front and the flow before and after the front for each storm. Mitchell and Hovermale (1977) have made a numerical simulation of a thunderstorm gust front, and Simpson (1969, 1972) has carried out model tests with flow visualisation on density currents in water. Sinclair et al. (1973) have tried to obtain a similarity description of the variations in the local mean wind speeds (averaged over 130 seconds) during six gust front passages.

Charba and Sasaki (1971) have described an Oklahoma storm in which the gust front reached 20 mile ahead of the main weather radar echo. The possibility that the gust front may be so far ahead is rather alarming from the pilot warning point of view, but such a large outrun has not been described in Australia. Colmer (1971) states that the gross features of gust fronts are different throughout the world, and it is assumed that the actual structures of the fronts may also be different. Therefore one important field of study is to determine for various thunderstorm-prone regions in Australia, a probability distribution of distances by which the gust front may outrun the thunderstorm cell. At present the Australian Bureau of Meteorology uses weather radar to monitor the approach of thunderstorms around major airports. The Terminal Area Severe Turbulence (TAST) service is a service provided to Department of Transport air traffic controllers to assist in the direction of aircraft away from convective turbulence within 60 nautical miles of an airport. Areas of possible severe and extreme turbulence are determined by delineating echoes on the radar which exceed a reflectivity* value, z, of 10^5 mm^6 m^{-3} and which extend to over 35,000 ft (10,500 m) in height. An extra buffer area may be added by the forecaster using his skill and knowledge of special circumstances. In practice this usually amounts to allowing 5 nautical miles around the $z = 10^5$ mm^6 m^{-3} reflectivity contour together with a further area to cover probable movement during the forecast period. Also if more than one storm centre exists, even though they may be as much as 20 nautical miles apart, the area between the storms may also be restricted. These turbulence warnings are prepared at 10 minute intervals. This Australian procedure has been examined by Barclay (1974) and compared with American FAA procedures, and with aircraft responses in the vicinity of Brisbane thunderstorms. Barclay did not give special consideration to gust front occurrences, which are a low level phenomena generally encountered only during landing or take-off, but he did find that the criteria used appeared to be effective in avoiding severe turbulence, and that moderate turbulence could be encountered as much as 20 nautical miles ahead of a thunderstorm echo. On this ground he indicated that it was preferable to divert behind a storm rather than ahead.

2. EXPERIMENTAL APPARATUS AND PROCEDURE

The ABC radio transmitter tower at Bald Hills, Queensland, was fitted with anemometers at heights of 58.2 m, 104.5 m, 153.3 m and 189.9 m. For convenience these heights were commonly referred to throughout the experiment as 50 m, 100 m, 150 m, and 200 m and this designation is continued in this report. (For example the wind speed at the 58.2 m level will be

---

* Actually z is a factor proportional to the radar reflectivity. It is defined as the sum, for all diameters, of $N_D.D^6$, where N_D is the number of hydrometeors of diameter D per unit volume. For further details see the entry under "radar reflectivity" in the Glossary of Meteorology edited by Huschke (1959).

6

denoted S_{50}.) Because of shielding due to an adjacent tuning hut building, it was not possible to place an anemometer at the 10 m level on the tower, and because of the mat of earth wires buried in the ground around the tower it was not possible to install one of the 10 m masts any closer than the network shown in Figure 1. The nearest of these anemometers was 270 m from the tower. A line through the anemometer at the 50 m (actually 58·2 m) level and the top of the nearest 10 m mast makes an angle of 10° to the horizontal. Wind shears* determined from anemometer readings at these two levels are not therefore typical of pure vertical shears. They are, however, typical of what an aircraft landing or taking off on a 10 flight path would encounter. This angle is fairly typical of take off angles, but is steeper than the landing approach path of the scheduled aircraft currently in use. (Three degrees is more typical.) It is however applicable to a landing STOL aircraft (such as the Australian designed NOMAD), and this is of some importance as STOL aircraft are particularly susceptible to gusts during landing and take-off. In a later section it is argued that in homogeneous turbulence at 10 m altitude the gusts at separations significantly greater than 100 m are uncorrelated. It could be expected that in such homogeneous conditions the probability distribution of shears measured between 50 m and 10 m on a 10° glide slope would be identical to the probability distribution measured on a 3° glide slope.

The terrain around the tower is open grassland, with only an occasional tree or bush. However in some directions suburban housing may be found as close as 400 m away. Thus the terrain is intermediate in roughness between that typical of an open airport, and that typical of Australian suburban housing.

The instrumentation system, shown in outline in Figure 1, was broadly as described by Patterson *et al.* (1975) except that the direction vanes described in that report were found to be rather insensitive, and were replaced by the Anderson vanes shown in Figure 3. Special levelling devices were used to ensure that the shafts of the vertical wind propellers were vertical to within 0·5 degree. The pressure transducer and humidity sensor connected to the computer network
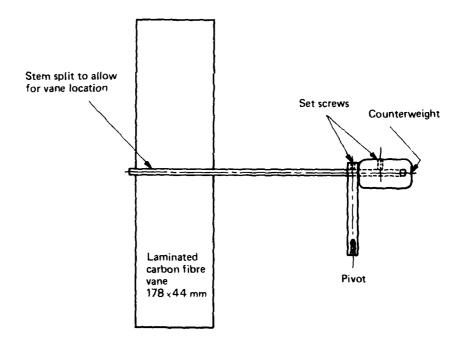
Fig. 3   Anderson direction vane.

---

* To avoid excessive classification, in this report wind shear has been measured as the difference in speed at two locations.

7

were not working, and so there was no possibility of evaluating virtual temperature. Due to a lightning strike on Monday 8 November 1976, only anemometers at positions 1, 4, 7, 9, 10 and 11 in the 10 m Tee array were working. Anemometer 7 was used in this study for S_{10}.

The radio transmitter station was generally not operating between midnight and 5 a.m. During those hours power for the instrumentation system was switched off, so that recordings were not available on a full 24 hour basis. The recording period covered by this report was from 12 November 1976 to 5 March 1977, which corresponds fairly well with the expected thunderstorm season at Bald Hills. Because of certain failures in the instrumentation system, recordings were obtained for only 100 days of this 113 day period.

The radio transmission tower at Bald Hills is fairly close to the Brisbane airport at Eagle Farm. A meteorological radar is located at the airport 13·6 km away on a bearing of 153° from the tower, and on some occasions it was possible to obtain tracings of the PPI screen.

3. INCIDENCE OF THUNDERSTORMS

In Australia the occurrence of thunderstorms is recorded at Meteorological observing stations. However there can be difficulty in distinguishing a large thunderstorm from several small thunderstorms, so routine statistics do not record numbers of storms but simply those days on which some thunderstorm activity was observed. Since 1964 the practice adopted has been to note those days on which thunder was heard at the observing station. Prior to 1964 a dual classification was used.

(a) "Thunderstorm in the vicinity of the observing station" was noted if lightning and thunder were observed with less than 10 seconds between. (Australian Meteorological Observers Handbook, 1954, p. 61.) With a speed of sound of 340 m/s this corresponds to a range of less than 3·4 km.

(b) "Distant thunderstorm" was noted if lightning and thunder were observed with more than 10 seconds between.

The cases when thunder was heard without lightning being observed might be expected to be rare, so that the sum of the two classifications prior to 1964 might be expected to give the same average incidence of thunderstorms as the "thunder heard" classification adopted since 1964. This is born out in the case of the Eagle Farm meteorological observing station as may be seen in Table 3.1.

In the period before 1964 there were many days on which both a near and a distant thunderstorm were recorded. Presumably on these days the storms were so far separated that two (or more) storms could be clearly distinguished as separate entities. What would not show up in the table is the occasions when two distinct storms occurred but both fell into the same category of near or distant. However, if it is assumed that no more than two distinct storms occurred in any one day, it may easily be shown that the figures in the table can be explained if on 46% of thunderdays two distinct thunderstorms occur, and for any observed thunderstorm there is a probability of 62% that it will pass "in the vicinity" of the station.

TABLE 3.1

Eagle Farm—Near and Distant Thunderstorms

Dates	Average number of days per year for	
1950–1963	Thunderstorms in vicinity *only*	11·9
	Thunderstorms in vicinity *and* distant thunderstorms	5·1
	Distant thunderstorms *only*	6·4
	TOTAL	23·4
1964–1976	Thunder heard	22·9

8

Because the two categories prior to 1964 jointly give the same information as the thunderday category adopted since 1964, it is possible to pool all the available data to obtain the monthly incidence of thunderdays. This is shown in Table 3.2 for both Amberley and Eagle Farm.

TABLE 3.2

Monthly Incidence of Days on which Thunder was Heard

(a) Amberley—Average over 1955 to 1976

Month	Jan.	Feb.	Mar.	Apr.	May	June	July	Aug.	Sep.	Oct.	Nov.	Dec.	Year
Ave	4·45	3·23	2·18	0·77	0·36	0·32	0·32	0·68	1·73	3·68	5·00	6·27	29·0
S.D.	2·46	1·95	2·50	0·92	0·73	0·57	0·57	0·78	1·35	1·84	2·60	2·73	4·82

(b) Eagle Farm—Average over 1950 to 1976

Month	Jan.	Feb.	Mar.	Apr.	May	June	July	Aug.	Sep.	Oct.	Nov.	Dec.	Year
Ave	3·00	2·19	1·41	0·81	0·48	0·26	0·15	0·81	1·41	3·30	4·67	4·70	23·19
S.D.	1·88	1·64	1·82	1·04	0·80	0·45	0·36	0·83	1·28	2·03	2·53	2·71	5·80

(c) Eagle Farm—Actual incidence during November 1976 to February 1977

Month	Jan.	Feb.	Mar.	Apr.	May	June	July	Aug.	Sep.	Oct.	Nov.	Dec.
Year												
1976											12	3
1977	1	2										

Note: "Ave" and "S.D." are the mean and standard deviation of the number of thunderdays per month (or per year).

Table 3.2 also shows the actual number of thunderdays which occurred during the period of the present study. The number of thunderdays may differ from the number of days on which TAST watches were declared because a thunderstorm may be too small for a TAST to be declared or it may occur late at night when no aircraft are flying, or a TAST may be declared because a thunderstorm is detected by radar, but the thunderstorm may never approach close enough to the station for thunder to be heard. Table 3.3 shows, for the period of the present study, the incidence of thunderdays and days on which TASTs were declared.

TABLE 3.3

Thunderdays and TASTs at Eagle Farm

12 November 1976 to 5 March 1977

Date	Thunderday?	TAST Time
1976 Nov. 12	No	1445–2055
13	Yes	0805–1115
14	Yes	0750–0810
15	Yes	—
21	Yes	1230–1715
25	Yes	—
26	Yes	1605–2000
28	Yes	1030–1805
29	Yes	1410–1940
30	Yes	1405–1730
Dec. 4	Yes	1425–2200
12	No	1715–1855
16	Yes	1520–2000
27	Yes	—
1977 Jan. 3	Yes	—
Feb. 22	Yes	—
26	Yes	1340–1640

9
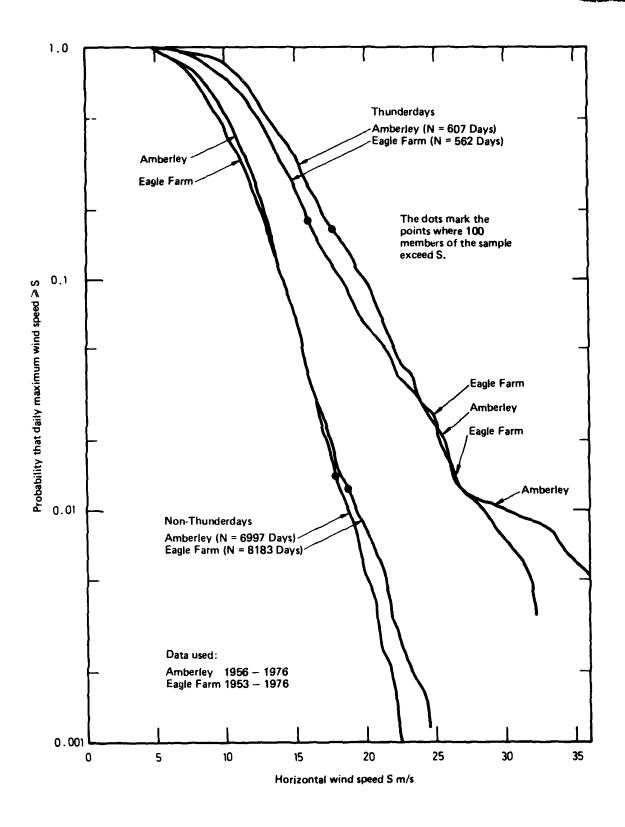
Fig. 4   Probability distribution of daily maximum wind speeds at Eagle Farm and Amberley.
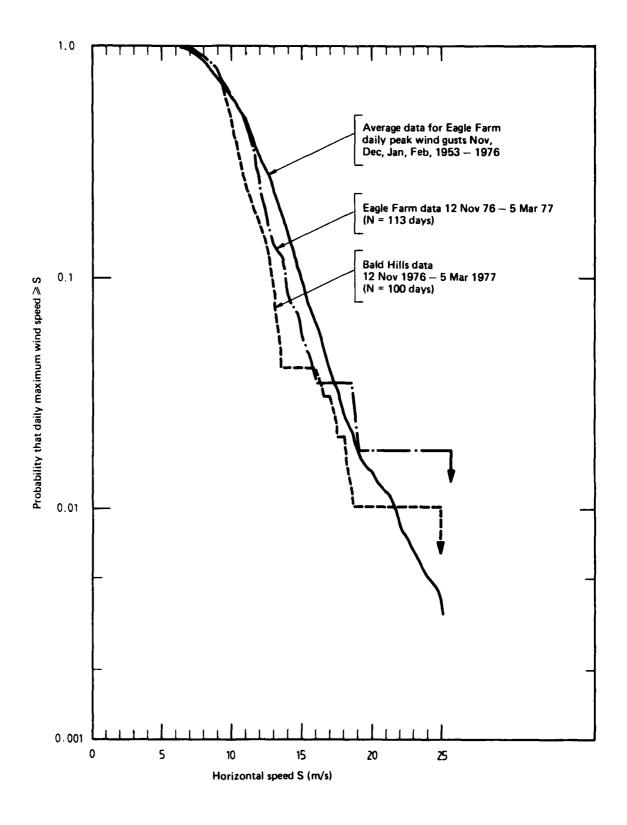
Fig. 5   Probability distributions of daily maximum wind speeds during thunderstorm season.

11

4. LONG TERM WIND SPEED STATISTICS

The long term (horizontal) wind speed data which are readily available are insufficient to give accurate estimates of the probability of occurrence of some of the higher (and rarer) speeds. To obtain some assessment of the stability of the available statistics it was decided to compare the data for Eagle Farm with the data for Amberley, which is situated about 45 km SW of Eagle Farm, and so is about 45 km further inland. Amberley has a slightly higher incidence of thunderdays (see Table 3.2) and temperature extremes, but as shown in Figure 4 the wind speed statistics seem fairly similar. At the low wind speed, high probability end, the curves are smooth and corresponding curves are similar in shape. The slight differences are probably due to differences in anemometer exposure and to local climatic variations. At the higher wind speeds (beyond that wind speed which is exceeded on less than 100 days of the relevant sample) the curves become more irregular and differ in shape from each other, presumably due to random factors. The difference between thunderdays and non-thunderdays is nevertheless clearly established.

In order to compare the period of this study (12 November 1976 to 5 March 1977) with the long term average data in the same area, Figure 5 has been prepared. This shows the probability distribution of daily maximum wind speeds at Eagle Farm, for the months of November to February, averaged over the years 1953 to 1976, with thunderdays and non-thunderdays taken together. The same figure also shows the probability distribution of maximum wind speeds from 12 November 1976 to 5 March 1977 at Eagle Farm and at Bald Hills. The Bald Hills sample size of 100 days is smaller than the Eagle Farm sample of 113 days because there were certain days, randomly distributed throughout the period, when Bald Hills data were unobtainable. The Eagle Farm data show that apart from one or two storms, wind speeds during the season were quieter than average. The Bald Hills curve falls below the Eagle Farm curve for the same period, and this may be attributed mainly to variations in the exposure of the two sites, but also in small part to the fact that on most days the Bald Hills system was not operating between midnight and 5 a.m.

5. STATISTICS OF WIND SHEARS

The wind speed differences or shears were computed each 6 seconds from the 6 second average wind speeds, and the maximum or peak value each minute was noted. The probability distribution of the peak shear each minute is plotted, for several height intervals, in Figure 6 together with the corresponding distribution of wind speed at the 10 m level. Shears between the 200 m and 150 m levels were not included because of a fault in the 200 m anemometer during some of the study period. The similarity in the shape of all these curves suggests that the wind shear has the same distribution as the wind speed, apart from a scaling factor. Table 5.1, obtained by reading values from Figure 6, shows that this is approximately so.

TABLE 5.1

Various Percentile Values of One Minute Maxima of Wind Speed and Wind Shear

Probability of exceedance p	Maximum 6-sec value each minute which is exceeded $p\%$ of minutes						
	Wind Speed S_{10}	Wind Shear $S_{50}-S_{10}$		Wind Shear $S_{100}-S_{50}$		Wind Shear $S_{150}-S_{100}$	
$\%$	m/s	m/s	Fraction of S_{10}	m/s	Fraction of S_{10}	m/s	Fraction of S_{10}
50	3·7	2·1	0·57	1·3	0·35	0·9	0·24
10	7·1	3·8	0·54	2·9	0·41	2·4	0·34
2·5	8·6	5·0	0·58	4·0	0·47	3·4	0·40
0·5	10·1	6·2	0·61	5·0	0·50	4·6	0·46
0·25	10·8	6·7	0·62	5·3	0·49	5·0	0·46
Adopted Values			0·6		0·5		0·45

TABLE 5.2

Various Percentile Values of Daily Maximum Wind Speed and Daily Maximum Shear

Probability of Exceedance P	Daily maximum 6-second average value of P-percentile of:		
	Wind Speed S_{10}	Wind Shear $S_{50}-S_{10}$	
%	m/s	m s	Fraction of S_{10}
50	10	6·5	0·65
10	13	8·3	0·64
2·5	16·4	10·0	0·61

Figure 6 also shows that a moderate shear of $0 \cdot 1$/sec (5 m/s wind speed difference in a vertical height of 50 m) is exceeded at least once per minute in approximately $2 \cdot 5\%$ of minutes in the lowest 50 m of the atmosphere, in $0 \cdot 5\%$ of minutes in the 50–100 m band, and in $0 \cdot 25\%$ of minutes in the 100–150 m band. (Note that because of the differences between nominal heights and actual heights, mentioned at the beginning of section 2, $S_{50}-S_{10}$ is actually the shear over a 48 metre height band and not over the 40 metre band that would be derived from the nominal heights.) These high shear bursts occur as many, widely scattered, brief incidents, for, as Figure 7 shows, the wind speed difference of 5 m/s is exceeded on 90% of the days even though such exceedences only occur in $2 \cdot 5\%$ of minutes. Similarly a severe shear of 10 m/s is exceeded on $2 \cdot 5\%$ of days even though extrapolation of Figure 6 shows that it is only exceeded in $0 \cdot 002\%$ of minutes. Figure 23 will be introduced later, but it shows a typical time history of shears in a fairly steady situation. Especially at the lowest levels the shear is quite variable but a wind speed difference of 5 m/s is only occasionally exceeded. There are periods of two or three minutes where the shear remains fairly constant, and a landing aircraft would experience a steady large shear. However a following aircraft a few minutes later may experience quite different shears, even though the mean velocity at all levels has not changed at all.

Figure 7 shows histograms of daily maxima of wind speed and shear. The distribution of wind shear has approximately the same form as the distribution of wind speed which suggests, as an empirical relation, that a fractional multiple of the wind speed has the same distribution as the wind shear. The fractional multiple or scale factor is evaluated in Table 5.2.

Both Tables 5.1 and 5.2 support the approximate relation that the probability of exceeding a wind speed difference of $0 \cdot 6\ S$ in the lowest 50 m is the same as the probability of exceeding a wind speed S at the 10 m level. Some such sort of correlation is to be expected between wind speed and shear, but the correlation bears a closer study both on an incident by incident basis and on the basis of plausible mechanistic types of arguments.

6. CHOICE OF INCIDENTS

6.1 Criteria Used and Classification of Incidents

The available Bald Hills data, amounting to 100 days, were searched for any occurrences of:

(a) A temperature drop or rise exceeding 2 C,

(b) A wind speed difference, between adjacent levels in excess of $7 \cdot 5$ m s,

(c) A squall, or sudden sustained rise in wind speed.

The details of how these phenomena were defined are given in Appendix 1. Table 6.1 lists the incidents chosen for further examination, and Appendix 3 contains, for each incident, a graph
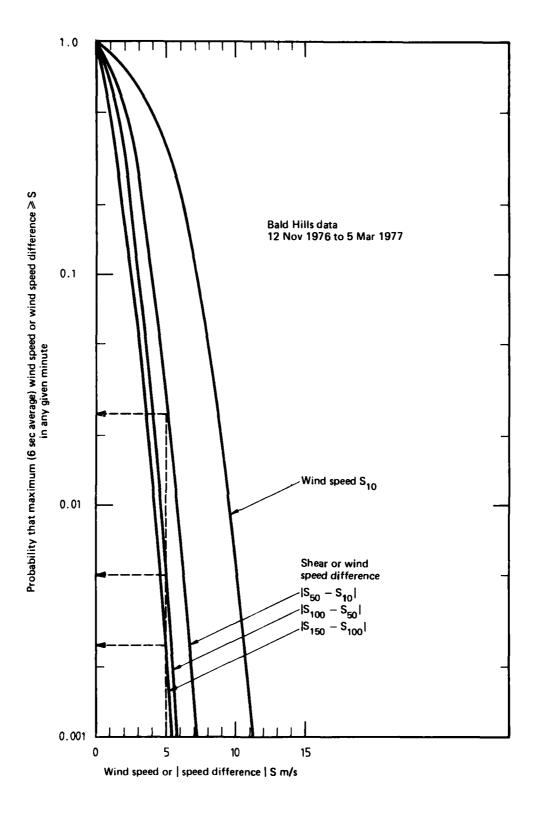
Fig. 6   Probability distribution of one minute maxima of wind speed and shear.

14
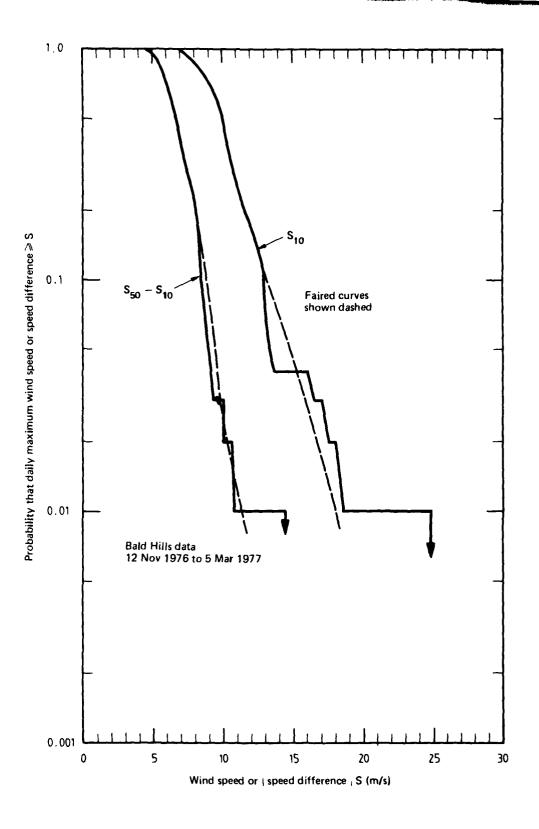
Fig. 7   Probability distribution of daily maximum wind speed and shear.

of several representative parameters recorded during the incident. The incidents were classified, as shown in one of the columns of the table, according to the following criteria:

Classification of incident	Meaning
1.	Temperature drop of not less than 2°C in 9 minutes, plus a squall at any two or more levels.
2.	Temperature drop of not less than 2°C but no squall, or a squall at only one level.
3.	A squall at any level(s) but no accompanying temperature drop of significance. A (3) in parentheses indicates that a squall was only noted at one level. Otherwise it occurred at two or more levels.
4.	High shear was observed but no squall or temperature change.
5.	Temperature rise of at least 2°C plus at least one other phenomenon. (A temperature rise without any accompanying phenomenon was ignored.)

Notes on TABLE 6.1

A figure (usually a 1) in columns 8, 9 or 10 represents an occurrence of the corresponding phenomenon during the course of the incident. A "1" in the squall column indicates that the wind speed rose by at least 5 m/s to at least $7 \cdot 5$ m/s within 9 minutes, and a "2" in the column indicates that the wind speed rose by at least 8 m/s to at least 11 m/s within 9 minutes.

Columns

1	Date of incident
2	Time of start of incident
3	"T" denotes the existence of a simultaneous TAST.
4	Duration of incident in minutes
5	Magnetic tape number
6	Identification at start of incident
7	Classification of incident
8	Squall at level 1 = 10 m, 2 = 50 m, 3 = 100 m, 4 = 150 m
9	High shear between two levels A = 50–10 m, B = 100–50 m, C = 150–100 m
10	Significant temperature drop (D) or rise (R)
11	Magnitude of temperature drop
12	Maximum 6-sec average wind speed (m/s) at 10 m level
13	Max. and min. 6-sec average vert. wind speed at 50 m level
14	6-sec average shear $(S_{50}-S_{10})$ of maximum magnitude (m/s)
15	Peak 2-minute rainfall in mm.

TABLE 6.1

Incidents Chosen for Study

1 Date	2 Start Time	3 T	4 Dur. Inc. Min.	5 Tape No.	6 Ident.	7 Cla.	8 Squall at				9 High Shear			10 Temp.		11 Temp. Drop °C	12 Peak Wind Speed	13 Vert. Wind Up/Down	14 Peak Shear	15 Peak 2 min. Rain
							1	2	3	4	A	B	C	D	R					
1976																				
12 Nov.	2050	T	120	203	122042	3	—	—			—						11·6	2·63/1·24	10·5	2
13 Nov.	0859	T	60	203	130851	1	—	—	—		—	—				4·3	15·4	3·43/1·99	9·5	4·3
13 Nov.	2131		60	204	132119	1		—	—		—					3·0	15·8	3·64/2·68	9·8	0·3
14 Nov.	0627		60	204	140615	3	—	—	—					—			9·4	1·95/1·73	6·4	
15 Nov.	0419		60	205	150403	(3)			—								6·2	1·11,0·62	5·4	
15 Nov.	0948		60	205	150932	3			—	—							10·1	3·07/1·74	5·9	
15 Nov.	1307		60	205	151251	3				—							10·4	2·63/2·41	6·8	
15 Nov.	1705		260	206	151704	4	—				—	—		—			11·2	4·84/2·34	8·5	
16 Nov.	1305		60	207	161246	4		—					—	—			12·5	3·19/2·71	8·0	
21 Nov.	1150	T	60	212	211100	3		—	—		—			—		4·9	8·0	1·87/1·56	4·8	7·1
21 Nov.	1436	T	60	212	211346	3			—		—			—		2·9	6·5	1·39/0·74	4·4	3·3
23 Nov.	1758		60	214	231702	2				2	—			—			5·8	2·76/1·02	5·1	
26 Nov.	1721	T	60	217	261619	1	2	2	2	2	—			—			16·5	3·11/2·96	7·9	2
28 Nov.	1124	T	60	219	281012	2		2			—			—		4·9	8·3	2·43/1·24	3·7	1·3
30 Nov.	1554	T	60	221	301423	1	2	2	2		—		—	—		11·5	24·9	4·69/1·73	14·2	2·3
4 Dec.	1654	T	120	225	341524	1	—	—			—			—		5·2	17·7	5·74/2·92	7·9	2·3
5 Dec.	0849		60	226	350714	(3)											8·6	2·56/1·56	5·7	
11 Dec.	1231		60	232	411020	2		—									7·4	2·53/1·72	3·7	
12 Dec.	1802	T	180	233	421515	3		—	—		—						12·1	2·79/2·85	8·3	
15 Dec.	1547		60	236	451243	4					—						9·9	2·92/1·46	7·7	
16 Dec.	1140		80	237	460833	5					—				—	−2·4	9·7	3·17/2·73	−7·7	
23 Dec.	1034		60	244	530105	2		1						—		2·2	8·9	2·29/1·37	6·2	
23 Dec.	1513		60	244	531144	(3)			—								7·8	1·73/1·42	6·7	0·3
24 Dec.	0530		60	245	540201	(3)				—				—			6·1	2·43/1·65	6·2	0·8
24 Dec.	1100		60	245	540731	1				—				—		4·0	8·1	2·53/1·82	6·4	0·5
28 Dec.	1121		60	249	580751	2								—		2·8	5·0	1·91/1·24	−3·4	0·5
30 Dec.	0955		60	251	600621	5								—	—	−3·6	4·3	3·27/1·62	−2·6	

TABLE 6.1 (Continued)

Incidents Chosen for Study

1 Date	2 Start Time	3 T	4 Dur. Inc. Min.	5 Tape No.	6 Ident.	7 Cla.	8 Squall at 1	2	3	4	9 High Shear A	B	C	10 Temp. D	R	11 Temp. Drop °C	12 Peak Wind Speed	13 Vert. Wind Up/Down	14 Peak Shear	15 Peak 2 min. Rain
1977																				
02 Jan.	1544		90	254	631142	3		1									8·9	2·56/1·31	6·7	
04 Jan.	1110		60	256	650649	2		1	1					1		4·0	10·9	3·36/1·56	6·6	
04 Jan.	1330		60	256	650909	4	1				1						10·0	3·32/1·97	7·7	
04 Jan.	1803		60	256	651342	4					1						12·0	3·28/1·80	7·5	
07 Jan.	1218		60	259	680750	3				1				1			10·0	2·38/2·00	6·2	
16 Jan.	1137		60	268	011135	2		1								4·5	8·1	2·31/1·49	4·0	
23 Jan.	1422		180	275	041405	4		1			1						12·0	3·12/2·53	8·3	
24 Jan.	1145		60	276	051124	2		1						1		4·4	6·1	2·57/1·65	—3·0	
24 Jan.	1857		60	276	051836	3	1			1	1						8·5	1·71/1·35	5·9	3·3
24 Jan.	2015		60	276	051954	(3)					1						12·0	2·85/1·82	8·1	
25 Jan.	1205		180	277	061139	5					1				1	—2·0	11·5	3·90/3·10	8·7	
26 Jan.	1301		60	278	071234	4					1						10·0	3·71/1·72	7·6	
02 Feb.	1202		60	285	141107	4					1						12·5	3·78/1·78	8·4	
02 Feb.	1734		60	285	141639	2				1	1			1		2·2	8·8	2·41/1·07	5·3	
02 Feb.	1930		60	285	141835	3		1			1						10·8	2·97/4·47	10·4	1·0
04 Feb.	0654		60	287	160555	4					1						11·6	2·38/1·85	7·9	3·6
04 Feb.	1148		60	287	161049	4					1						10·3	3·16/1·87	7·5	0·3
07 Feb.	1108		60	290	190958	2			1					1		2·7	6·5	1·82/1·83	5·3	0·3
11 Feb.	0735	T	60	294	230613	(3)					1						9·6	2·29/1·65	6·4	
11 Feb.	1056		60	294	230934	4					1						10·5	2·84/1·82	8·1	
12 Feb.	1257		60	295	241132	5					1			1		—2·6	11·1	3·56/1·86	8·0	0·1
12 Feb.	1513		60	295	241348	4					1						10·6	2·85/1·73	7·7	
15 Feb.	1043		60	298	270902	4					1						8·6	3·10/2·19	8·6	
25 Feb.	0957		60	308	370736	5					1			1		—2·2	4·5	1·89/2·65	4·0	0·3
26 Feb.	1443		60	309	381222	1	2	2		2	1			1	1	5·5	12·7	2·20/1·24	8·9	1·0
27 Feb.	1505		140	310	391240	4					1						11·5	3·11/2·10	7·9	
01 Mar.	1625		60	312	411353	4					1						9·4	2·73/2·55	7·8	

6.2 Type 1 Incidents

(i.e. Temperature drop of 2°C or more and a squall at two or more levels.)

A total of 7 type 1 incidents occurred as follows:

Date	Start of incident	Onset of Temp. Drop	TAST?
13 Nov.	0859	0917	Yes
13 Nov.	2131	2149	–No–
26 Nov.	1721	1736	Yes
30 Nov.	1554	1610	Yes
4 Dec.	1654	1710 and 1730	Yes
24 Dec.	1100	1118	–No–
26 Feb.	1443	1502	Yes

(Note: Times of start and onset are in hours and minutes, using local standard time.)

It is probably safe to conclude that all of the type 1 incidents occurred because of gust fronts associated with thunderstorm passages. All but two of the incidents occurred during TAST watch periods, and one of the exceptions occurred on a thunderday (13 Nov.) but late at night after scheduled airline flights had ceased and TAST operations had become unnecessary. The other exception (24 Dec.) had all the hallmarks of a thunderstorm with a sudden increase in wind, a bearing change, a significant temperature drop and simultaneous onset of rain. It may represent a storm whose radar echo did not become severe enough to trigger a TAST watch, and whose path was too far from the Eagle Farm observatory for thunder to be heard.

TABLE 6.2

Date	Onset of Temp Drop	Time of Tracing	Distance from Bald Hills to Radar Echo (n.mile)		
			$z = 10^4$ $R = 12\cdot5$ mm/hr	$z = 9*10^4$ $R = 50$ mm hr	$z = 8*10^5$ $R = 150$ mm hr
13 Nov.	0917	0915	0·5	0·5	1·8
13 Nov.	2149	NO TAST			
26 Nov.	1736	1740	1·2	5·8	—
30 Nov.	1610	1605	3·4	5·2	—
4 Dec.	1710	1715	6·1	8·2	9·5
24 Dec.	1118	NO TAST			
26 Feb.	1502	1500	0·2	2 5	5·2

Notes

1. A negative distance means the echo had already passed the station when the gust front was observed.

2. Distances are distances to the *nearest* point of an echo, not distances parallel to the storm movement.

3. R is estimated rainfall rate corresponding to given z values.

It is desirable to relate the gust front position to the radar echoes from the weather radar. Unfortunately simultaneous photographs of the weather radar screen were not taken during the experiment. It has been possible to obtain manual tracings of the radar screen which are made during TAST procedures, but as the tracing has to be done in haste, it may represent a considerable simplification of the complex structure of a real storm. The simplified tracings, though quite adequate for TAST purposes, may be quite inaccurate for the purpose of determining distances between gust fronts and radar echoes. For each of the five type 1 incidents for which TAST tracings are available, the tracing was chosen whose time was closest to the time the gust front passed Bald Hills. These tracings are shown in Figures 8 to 12. For each case the distance between the radar echo contours and Bald Hills has been read off and tabulated in Table 6.2.

Storm movement T6 — T9

$\overline{W}$

$\overline{S}$ = 20 knot

Relative upwind

$\overline{W}$

$\overline{S}$ = 14 knot

$\frac{6H}{420}$

Tracing No: T8
Date/Time : GMT 12/2315 Z
: Local 13/0915 L
Nov. 1976

$\frac{6H}{430}$

$\frac{6H}{400}$

$Z = 10^4, 9 \times 10^4, 8 \times 10^5$

Notes: (1) $\frac{6H}{420}$ Denotes $\frac{\text{Rainfall intensity (e.g. 6''/hr) Hail}}{\text{Max. height of radar echo (42000 ft)}}$

(2) $\overline{S}$ = Mean speed of storm centres from tracing T6 to tracing T9

(3) $\overline{W}$ = Mean wind speed over heights 0-25000 ft from radiosonde at 12 Nov/2200 GMT
$\overline{W}$ = 270°/16 knot

12/2200 Z
Mean wind 0-25000
$\overline{W}$ = $\frac{270°}{16 \text{ knots}}$
Circle is 15n mile rad.

Bald Hills — ▽

Fig. 8   Manual tracing of weather radar P.P.I. 13 Nov. 1976 at 0915 EST.

Tracing No. T10
Date/Time : GMT 26/0740 Z
: Local 26/1740 L
Nov. 1976

6H / 500

5 / 490

4 / 350

3H / 450

Fig. 9   Manual tracing of weather radar P.P.I.
26 Nov. 1976 at 1740 EST.

Storm movement $T_{11} — T_{14}$

Tracing No. T12
Date/Time : GMT 30/0605 Z
: Local 30/1605 L
Nov. 1976

6H / 490

$\overline{W}$

10 kn

Relative
upwind

6H / 450

6H / 530

6H / 550

30/0400 Z
Mean wind 0-15000
$\overline{W}$ = 270°
31 knots
Circle is 15n mile rad.

Fig. 10   Manual tracing of weather
radar P.P.I. 30 Nov. 1976
at 1605 EST.

Storm movement T_{17} — T_{20}

$\dfrac{6H}{640}$

$\dfrac{6H}{570}$

$\dfrac{6H}{550}$

$\dfrac{6H}{510}$

$\overline{W}$

3 kn

$\overline{S}$ = 7 knots

W

3 kn

Relative
upwind

Relative
upwind

Mean wind 0-20000
$\overline{W} = \dfrac{285^\circ}{24 \text{ knots}}$

Tracing No. T18
Date/Time : GMT 04/0715 Z
: Local 04/1715 L
Dec. 1976

Fig. 11   Manual tracing of weather radar P.P.I. 4 Dec. 1976 at 1715 EST.

4

4

Storm movement T_7 — T_{10}

Tracing No. T9
Date/Time : GMT 26/0500 Z
:   26/1500 L
Feb. 1977

$\overline{W}$ 5kn

$\dfrac{6H}{4}$

5kn

Relative
upwind

$\overline{W}$

4

$\overline{S}$ = 10 knots

4

$\dfrac{6H}{300}$

4

$\dfrac{6H}{220}$

$\dfrac{6H}{250}$

Mean wind 0-20000
$\overline{W} = \dfrac{270^\circ}{11 \text{ knots}}$

4
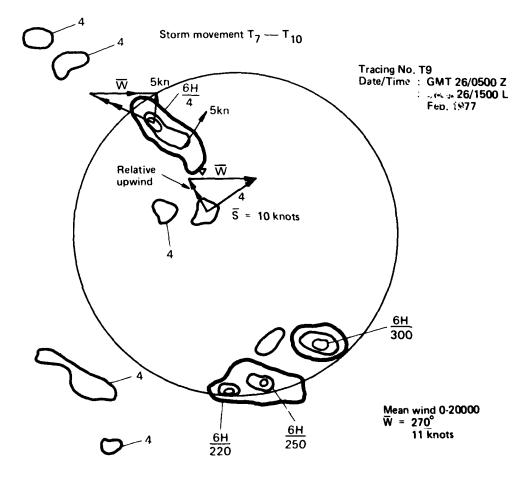
Fig. 12   Manual tracing of weather radar P.P.I. 26 Feb. 1977 at 1500 EST.
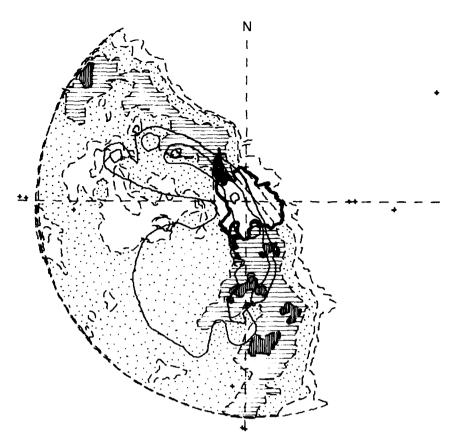
Fig. 13   Comparison of VIP photograph on 7 Nov. 1977 at 1845 EST with manual P.P.I. tracing at 1840 EST.
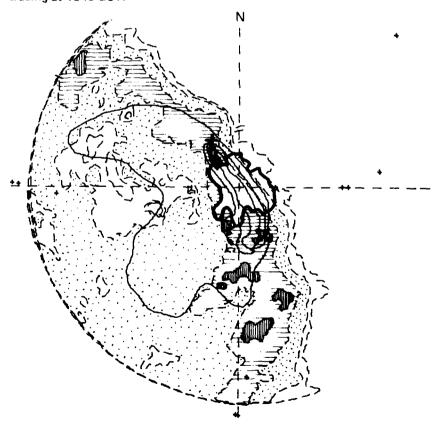
Fig. 14   Comparison of VIP photograph on 7 Nov. 1977 at 1845 EST with manual P.P.I. tracing at 1850 EST.

23

As well as the errors inherent in tracing the screen there are two other possible causes of error.

(a) Radar calibrations tend to drift with time.

(b) In the case of the two storms of 26 November and 30 November, only two levels of echoes are shown. It is likely that the $\geq 10^1$ echo may have covered so much of the screen that it was not drawn in. In this case the distances for these two storms should all be moved one column to the right.

A measure of the simplifications possibly involved in TAST tracings can be obtained from the comparison in Figures 13 and 14. Both of these figures show the same underlying radar picture obtained at 1840 local time on 7 November 1977, using a WF 44 10 cm weather radar specially modified by the addition of a Video Integrator Processor (VIP) so as to display a maximum of six levels of reflectivity (see Meighen *et al.*, 1978). Figure 13 shows, superimposed, the TAST tracing taken 5 minutes previously from a normal 3 level display, and Figure 14 shows, superimposed the TAST tracing taken 5 minutes after the 6-level photograph. It is to be expected that the levels chosen in the two systems will not match, so that the lines will not coincide. However it is also to be expected that the lines of the 3-level TAST tracing should generally interpolate (and smooth) the lines of the 6-level VIP display. The actual correlation in the two figures is in fact quite surprisingly poor, though it is not known at this stage whether the poor correlation was due to incorrect setting up of the VIP (which had only recently been installed), misadjustment of the normal PPI, or the speed required in tracing the echoes. However, at this time it may be necessary to treat the data in Table 6.2 with some caution. Distances from the centre of the storm may be more accurate than the distances from particular contours. It may one day be possible to provide automatic pictures of the radar screen on a facsimile machine. In fact this is presently possible under the CAPPI system, which has the additional advantage of providing Constant Altitude sections through the storm. With such pictures, and several accurately timed Dines anemometer charts from different stations in the area covered by the storm, it would be possible to obtain a very good idea of the probability distribution of distances from the gust front to the radar echo.
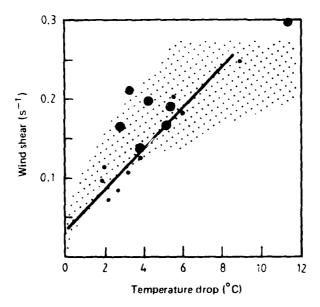
Fig. 15   Correlation between temperature drop and wind shear for type 1 incidents (after Hall et al). The emphasised points were obtained at Bald Hills, the others are the ones shown by Hall et al.

The relation between the peak 6-sec average shear and the temperature drop for the seven type 1 incidents is shown in Figure 15. The same figure also shows the points obtained or cited by Hall *et al.* (1976). The data differ slightly in that here a 6-sec average shear is used rather than the 10-sec average used by Hall *et al.* The method used here to define the temperature dr*.*) is in Appendix 1. Hall *et al.* do not supply any information of the method they used to define the temperature drop. Even with the slight variations in definitions, the present data plot generally within the scatter band chosen by Hall *et al.* (based on a simplified physical model) and shown in Figure 15 as a stippled zone. The equations of this scatter band are 0.057_χ $\Delta T <$ shear $< 0.114_\chi$ ΔT. (There is a discrepancy between the scatter band shown by Hall *et al.* and the coefficients in the inequalities they quote. Here the scatter band adopted is the one shown in their figure.)

The correlation between peak wind speed and temperature drop for the type 1 incidents is shown in Figure 16, which also shows the points used by Fawbush and Miller (1954). The scatter of the present points is quite similar to that of the points they showed. It is also of interest to compare the observed downrush temperatures that would be predicted by the Brancato method recommended by Fawbush and Miller. Radiosondes measure profiles of temperature, pressure and mixing ratio (i.e. water content expressed in gram of water per kg of air) at Eagle Farm at 8 a.m. local time each morning. From these soundings it is possible to determine the level at which the wet bulb temperature is zero, and from the wet adiabatic lines marked on the standard aerological diagrams it is possible to obtain the surface temperature of a parcel of air moved wet adiabatically from the level of the wet bulb zero to ground level.

Fig. 16 Correlation between measured temperature drop and peak wind gust for type 1 incidents (after Fawbush and Miller). The emphasised points were obtained at Bald Hills, the others are the ones shown by Fawbush and Miller.

25
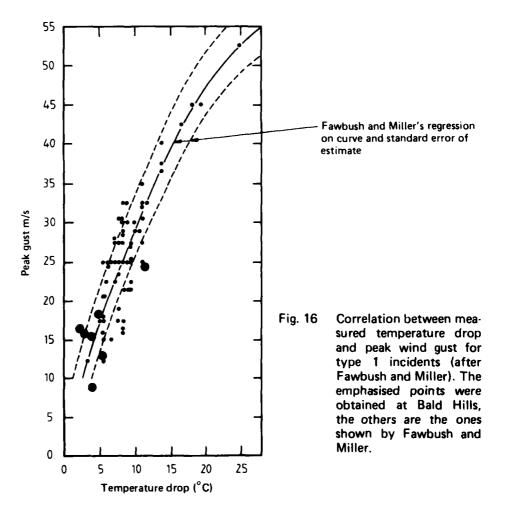
TABLE 6.3

Date	Local Time	Balloon Soundings		Surface Observations	
		Height of wet bulb zero (mbar)	Predicted downrush temp. (°C)	Actual temp. before downrush (°C)	Actual temp. after downrush (°C)
13 Nov.	0800	675	16·5		
13 Nov.	0859			25·3	21·0
13 Nov.	2131			24·8	21·8
14 Nov.	0800	640	18·25		
26 Nov.	0800	695	15·5		
26 Nov.	1721			28·0	25·1
27 Nov.	0800	675	16·5		
30 Nov.	0800	655	17·5		
30 Nov.	1554			31·4	19·9
1 Dec.	0800	720 appr.	≥14·5		
4 Dec.	0800	670	16·7		
4 Dec.	1654			26·7	21·5
5 Dec.	0800	695	15·5		
24 Dec.	0800	645	18·0		
24 Dec.	1100			25·9	21·9
25 Dec.	0800	690 appr.	≥15·7		
26 Feb.	0800	620	19·0		
26 Feb.	1443			28·9	23·4
27 Feb.	0800	670	16·7		

Table 6.3 shows these predicted downrush temperatures for soundings taken before and after each of the type 1 storms. The actual temperatures observed before and after the downrush at the 10 m level on the Bald Hills tower are also shown. (The method of definition of these temperatures is given in Appendix 1.) In all cases the observed downrush temperature is greater than the predicted one. Fawbush and Miller concluded that "strong gusts associated with thunderstorms may be expected only in those areas where the wet-bulb zero is less than 11,000 ft above the earth's surface." The 670 mbar surface corresponds to an altitude of approximately 11,000 ft so most of the occurrences in the table are right at the limit of this condition. Thus the high observed downrush temperatures may be because air from the level of the wet-bulb-zero never reached the surface. Alternatively they may be due to entrainment and mixing of air during the downdraft's descent and outflow over the surface. With the limited information available it is not possible to choose between these two alternatives.

The most severe of the type 1 incidents was the storm on 30 November, with the gust front passing at 1605 local time. The peak gust of 28·5 m/s corresponded to a 5 year return period for the Brisbane area. The graph of a sample of significant recorded parameters during the storm is shown in Figure 17, and Figures 18 and 19 show surface charts preceding and at the time of the storm. It is apparent from these that the storm is associated with a pre-frontal trough depression. Figure 20 shows the aerological diagram produced at the morning sounding, and the balloon measurements of the upper winds before and after the storm are plotted as hodographs in Figure 21. Note that for the hodographs presented here and later, the convention is that the wind vector is from the origin to the hodograph.
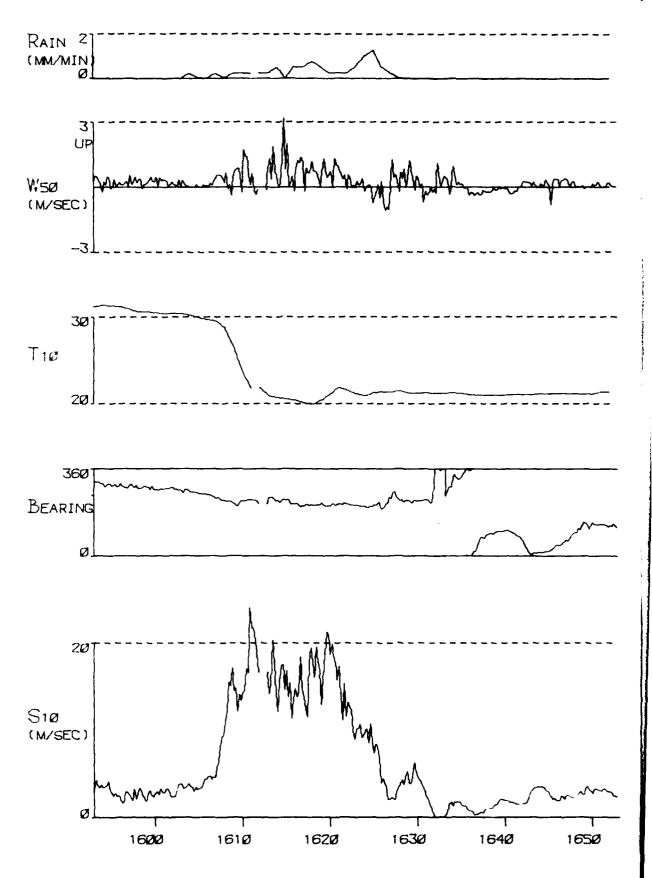
Fig. 17(a) A selection of parameters recorded during the thunderstorm and gust front passage on 30 Nov. 1976.

27
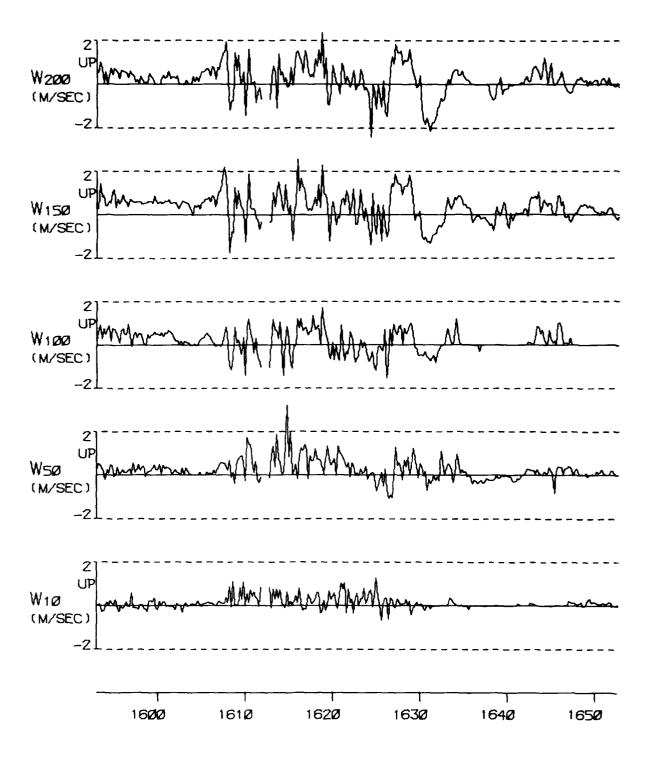
Fig. 17(b) Vertical wind component recorded during the thunderstorm and gust front passage on 30 Nov. 1976.

28
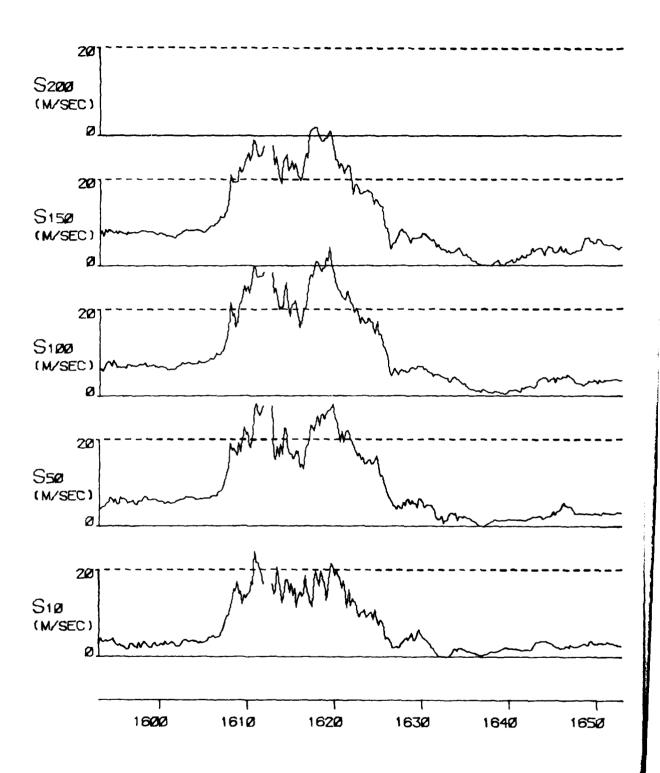
Fig. 17(c) Wind speeds recorded during the thunderstorm and gust front passage on 30 Nov. 1976.
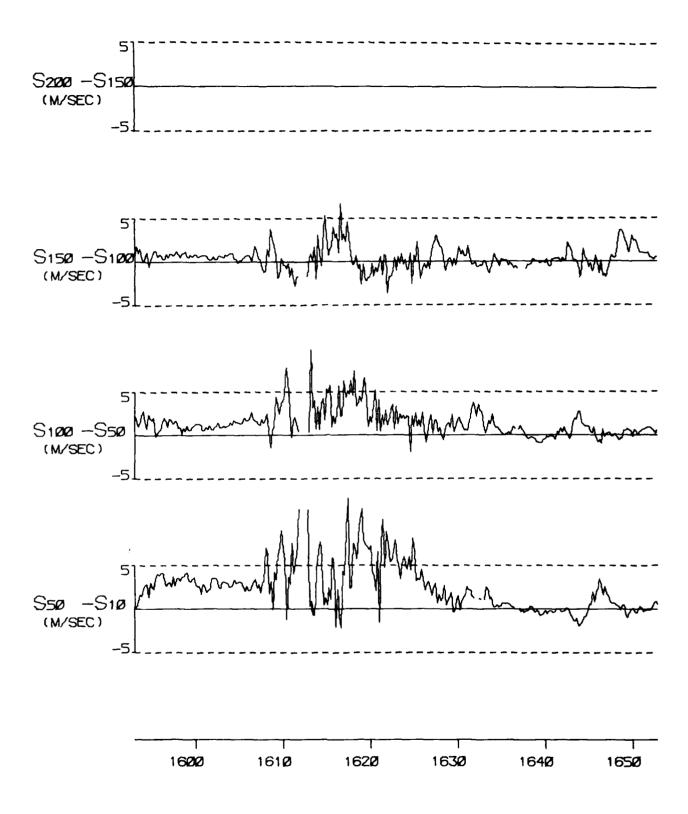
Fig. 17(d) Shears recorded during the thunderstorm and gust front passage on 30 Nov. 1976.

30
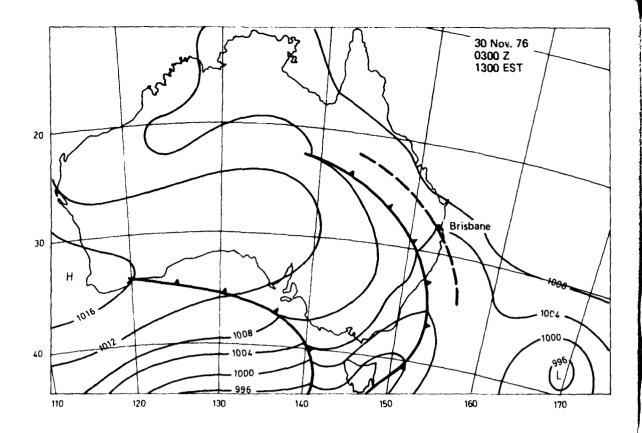
Fig. 18   Surface chart preceding storm on 30 Nov. 1976.
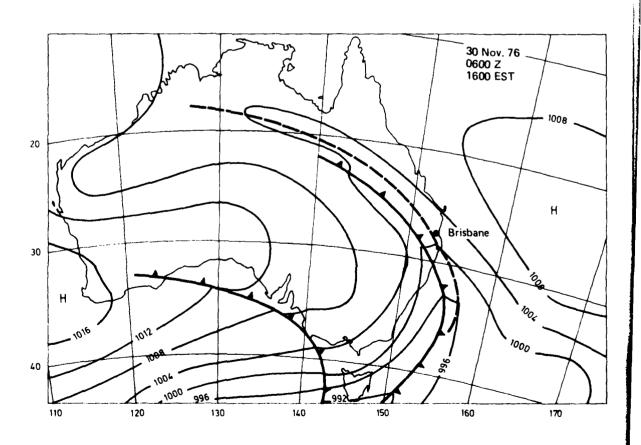
Fig. 19   Surface chart at time of storm on 30 Nov. 1976.

31
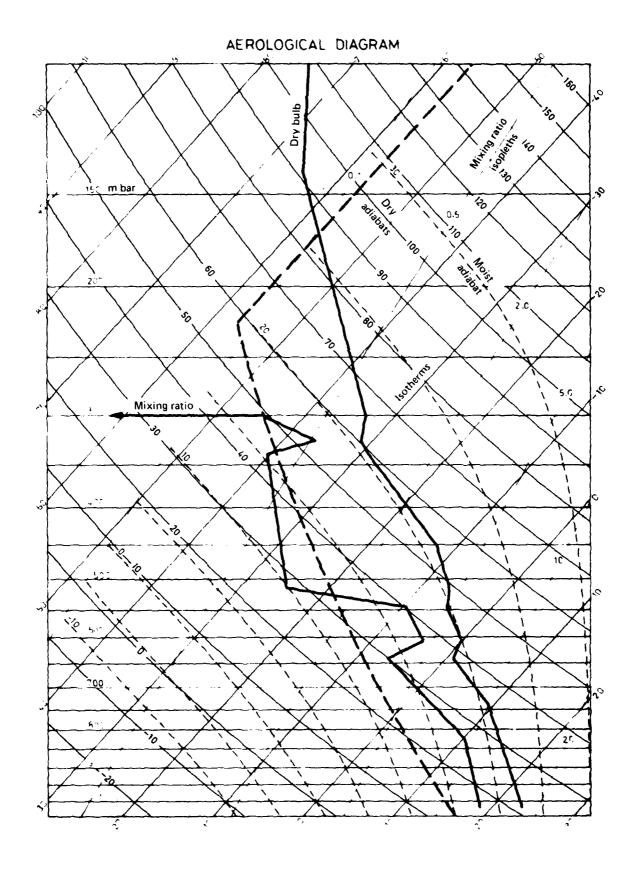
Fig. 20 Aerological diagram on 30 Nov. 1976 at 0800 EST.
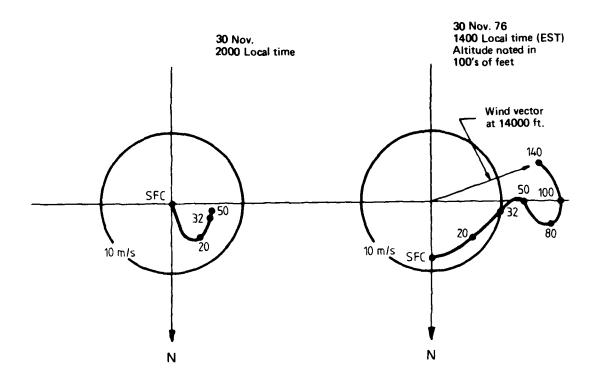
Fig. 21   Hodographs of wind velocity at different altitudes at Eagle Farm on 30 Nov. 1976.
Altitudes are noted in 100's of feet.

6.3 Type 2 Incidents

(i. e. a temperature drop not accompanied by squalls or with a squall at not more than one level.)
A total of 10 type 2 incidents occurred as follows:

(a) Sea breeze fronts

23 Nov.	1758
11 Dec.	1231
28 Dec.	1121
4 Jan.	1110
24 Jan.	1145
7 Feb.	1108

(b) Mild Thunderstorm

28 Nov.	1124

(c) Evaporative cooling associated with small falls of rain

23 Dec.	1034
2 Feb.	1734

(d) Unknown cause

16 Jan.	1137

33

The major cause of type 2 incidents seems to be the passage of a sea breeze front. Such incidents are marked by a temperature drop, a moderate but sudden increase in wind, and a change of bearing, with winds before the change generally being from the west (land breeze) and swinging to the east (i.e. from the sea) as the temperature drop becomes established. It is of interest to note that all but one of these fronts occurred around midday, which is the usual time for the sea breeze to come in at Brisbane. The one exception at around 6 p.m. has been included in this group because it also shows a significant temperature drop and mild wind speed rises at all levels, associated with a wind direction change from west to east and later north-east.

The case occurring on 28 November has been attributed to a thunderstorm because it occurred on a thunderday and during a TAST watch.

The two incidents associated with evaporative cooling are both marked by fairly sudden temperature drops at about the same time as a small fall of rain, followed by a gradual return to normal temperatures over the next half hour.

The remaining temperature drop case for which it has not been possible to suggest a cause occurred on 16 January at 1137. The temperature drop was quite large (4·5 C) and was preceded by 15 minutes of almost continuous updraft measured at all levels on the tower. However winds were almost continuously from the North and showed very little tendency to increase suddenly during the incident. No rain occurred.

6.4 Type 3 Incidents

(i.e. a squall at any level or levels without any accompanying significant temperature change.)

A total of 17 type 3 incidents occurred, the majority of which appear to be associated with storms or rain, although there is one sea breeze incident, and a few events which it has not been possible to find an explanation for. A classification of type 3 incidents follows:

(a) Occasions when a TAST was declared just before, during, or shortly after the incident.

12 Nov.	2050-2250
14 Nov.	0627 0727
21 Nov.	1150-1250
21 Nov.	1436-1536
12 Dec.	1802 2102

(b) Incidents occurring on a thunderday although a TAST was not declared.

15 Nov.	0419-0519
15 Nov.	0948 1048
15 Nov.	1307-1407

(c) Other incidents associated with rain.
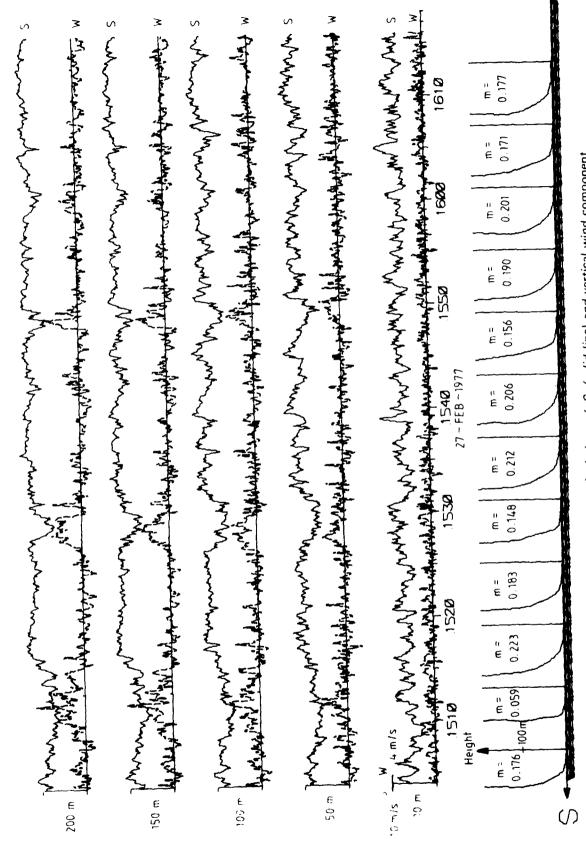
23 Dec.	1513-1613	(intermittent gentle rain)
24 Dec.	0530-0630	(gentle rain before and just after a front)
24 Jan.	1857 1957	(fairly heavy rain following a small temperature drop)
2 Feb.	1930 2030	(heavy rain)

(d) Sea breeze incident (a small temperature drop occurred.)
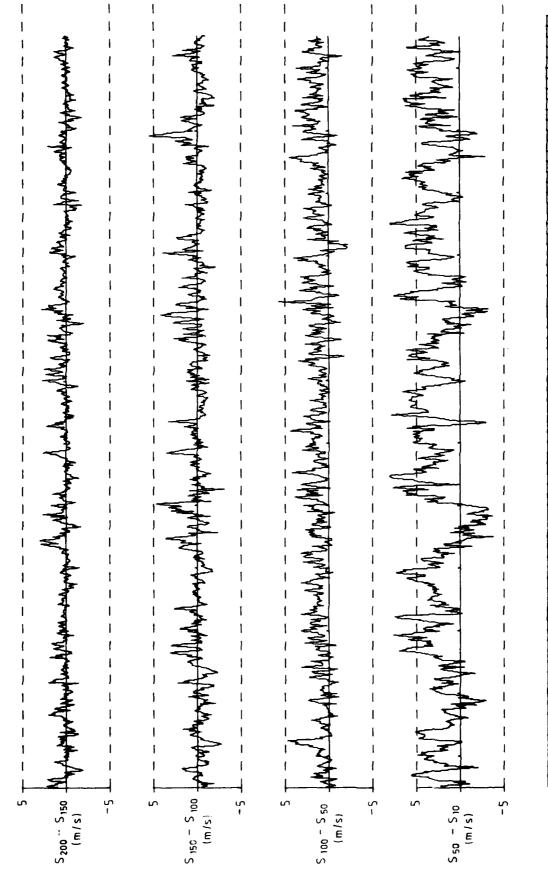
| 7 Jan. | 1218-1318 |

(e) Other incidents.

5 Dec.	0849-0949
2 Jan.	1544-1714
24 Jan.	2015-2115
11 Feb.	0735-0835

Fig. 22 6-second average values of wind speed, S, (solid line) and vertical wind component, W, (broken line) at various levels on the tower. The scale unit is 10 m/s for S and 4 m/s for W. Positive W is upward. The lower part of the figure shows 6 minute mean vertical profiles of wind speed.

Fig. 23   Time history of shears during type 4 incident on 27 Feb. 1977.

27 - FEB - 1977

36

6.5 Type 4 Incidents

(i.e. Strong shear not accompanied by squalls or significant temperature changes.)

A total of 15 such incidents occurred. All are characterised by a steady wind direction and a steady temperature. Only one of the incidents (4 February at 0645) was accompanied by rain, and that was only slight. The wind is generally fairly strong and turbulent. In most cases the speed fluctuated between 5 m/s and 8 m/s. That is probably because higher wind speeds happen so rarely as scarcely to have been encountered during the 100 day period except in storms. On only one occasion (15 February at 1043) was the wind lower, at 3-6 m/s, and this was only accompanied by one or two small bursts of shear. There were two occasions (16 Nov. at 1305 and 23 January at 1422) when the wind was slightly stronger at 6-10 m/s.

The type 4 incidents are of some interest in that flow conditions have remained steady for a considerable time, allowing fairly steady boundary layer conditions to become established. For example the case on 27 February at 1505 (see Fig. 22) is of some interest in that there are quiescent periods when the flow becomes fairly steady with a typical vertical profile of wind speed. Interspersed are periods of vertical updrafts, generally stronger at greater altitude. The updrafts carry up air with lower momentum, causing notable drops in the wind speed at higher altitude during these periods. Figure 22 shows the graphs of wind speed and vertical wind component, using a 6 second averaging time, and below these graphs are successive vertical profiles of wind speed based on 6-minute average speeds. Below each profile is the best fit value of m to describe the profile by equation 1.1. The time history of wind shears is shown in Figure 23. The shear in the lowest height band is by no means steady even during the steady periods of the tower wind speed traces. However the big sudden changes in shear appear to be related to the updrafts as indicated by the wind speed profiles.

Three of the type 4 incidents were chosen for detailed study. They were all incidents (see Table 8.2) in which the 30 second average shear fell into the "strong" or "severe" category. For each incident, figures are reproduced here which show:

(a) A time history of a sample of parameters recorded during the incident.

(b) A surface pressure chart or charts.

(c) Balloon measurements of upper winds.

(d) Radiosonde profiles of temperature and mixing ratio.

The figure numbers for the various figures for the three incidents are shown in the following table:

Type 4 Incidents Described in Detail

Date of incident	4 Jan. 77	2 Feb. 77	27 Feb. 77
Time of incident	1330-1430	1200-1300	1505-1725
Time History figures	24	28	32
Surface Chart figures	25	29	33, 34, 35
Upper Wind figures	26	30	36
Radiosonde Profile figures	27	31	37

Examination of the surface charts for these incidents shows that they are all associated with a ridge of high pressure extending from the south whilst a pressure trough runs parallel but some distance inland.
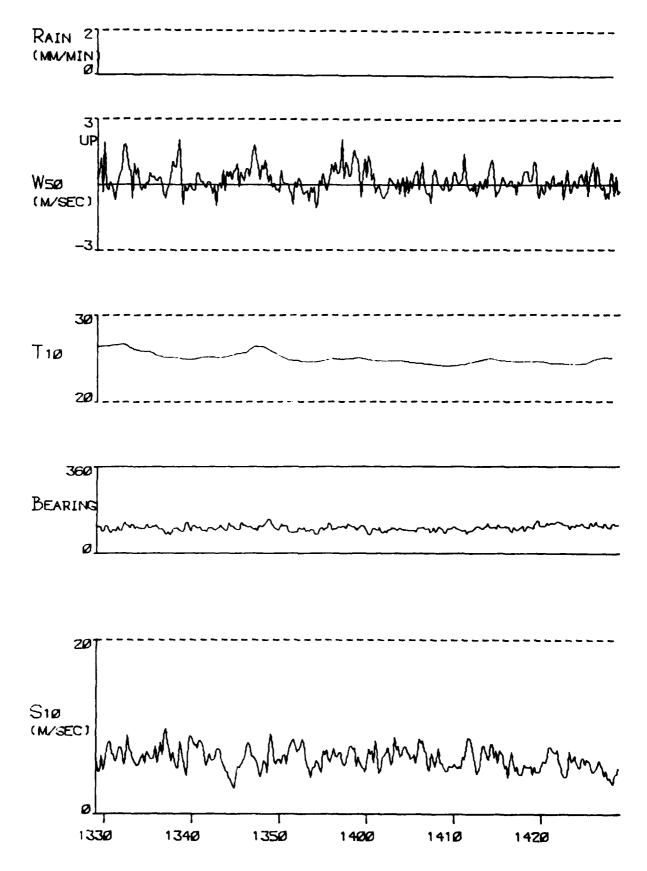
Fig. 24   A selection of parameters recorded during the type 4 incident on 4 Jan. 1977.
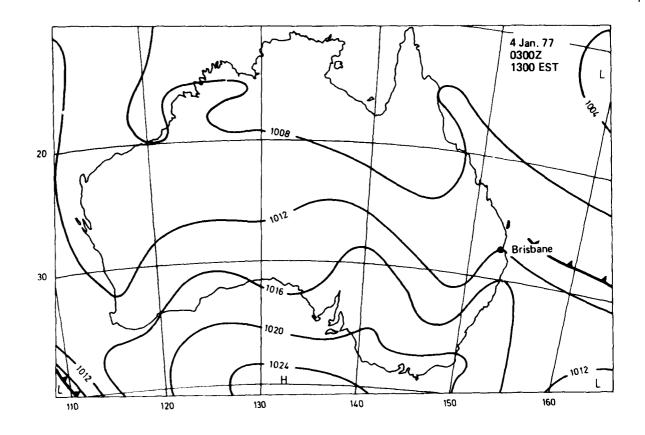
Fig. 25   Surface chart at time of type 4 incident on 4 Jan. 1977.
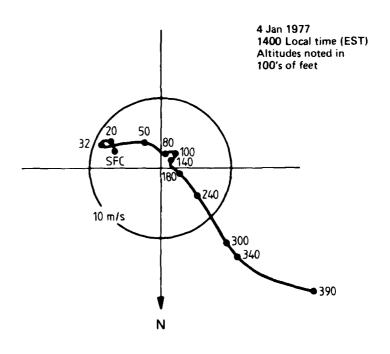
Fig. 26   Hodograph of wind velocity on 4 Jan. 1977 at 1400 EST, at Eagle Farm. Altitudes are noted in 100's of feet.

AEROLOGICAL DIAGRAM
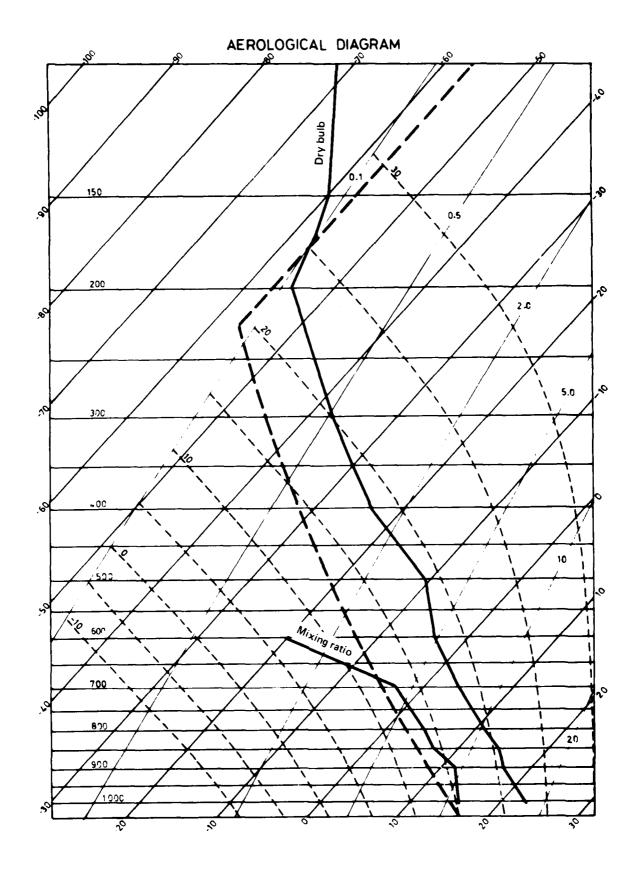
Fig. 27   Aerological diagram on 4 Jan. 1977 at 0800 EST.

40
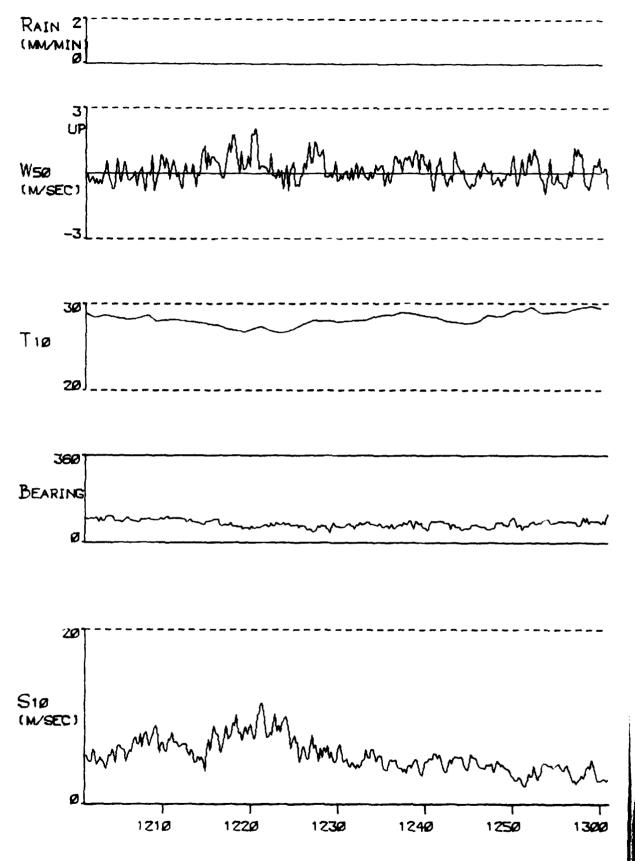
Fig. 28   A selection of parameters recorded during the type 4 incident on 2 Feb. 1977.
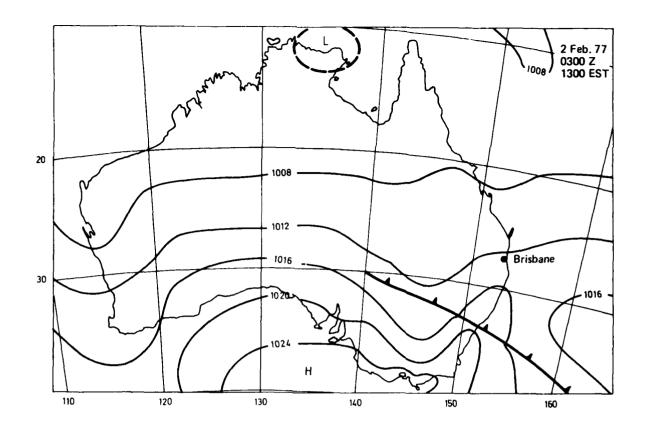
Fig. 29   Surface chart at time of type 4 incident on 2 Feb. 1977.
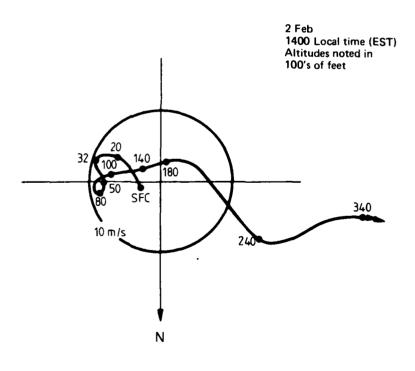
Fig. 30   Hodograph of wind velocity at Eagle Farm on 2 Feb. 1977 at 1400 EST. Altitudes are noted in 100's of feet.

AEROLOGICAL DIAGRAM
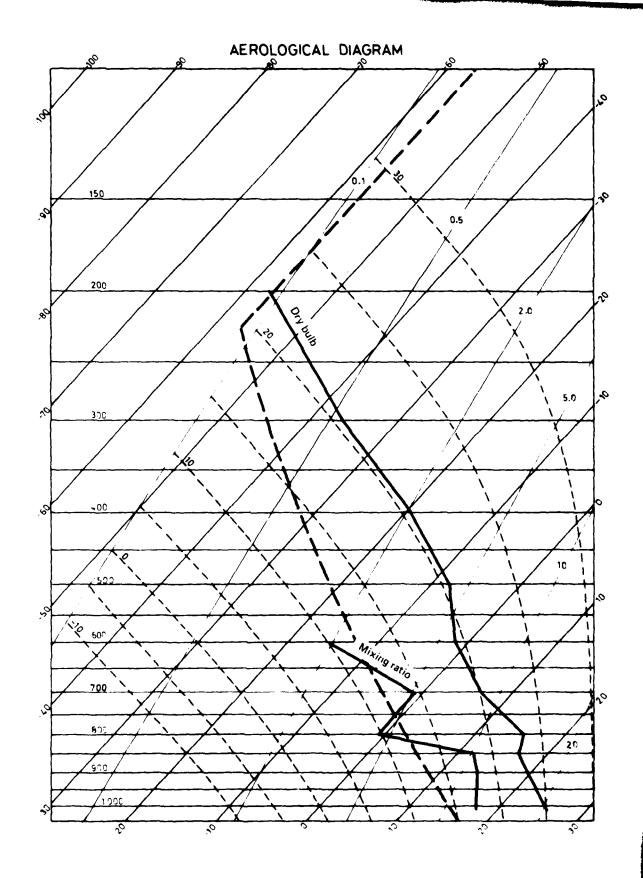
Fig. 31   Aerological diagram on 2 Feb. 1977 at 0800 EST.

43
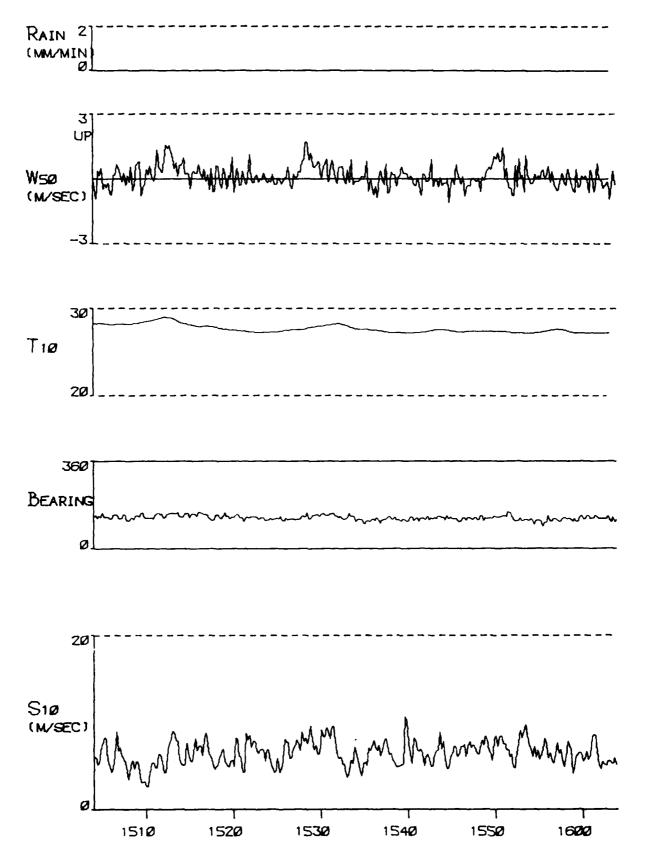
Fig. 32   A selection of parameters recorded during the type 4 incident on 27 Feb. 1977.

44
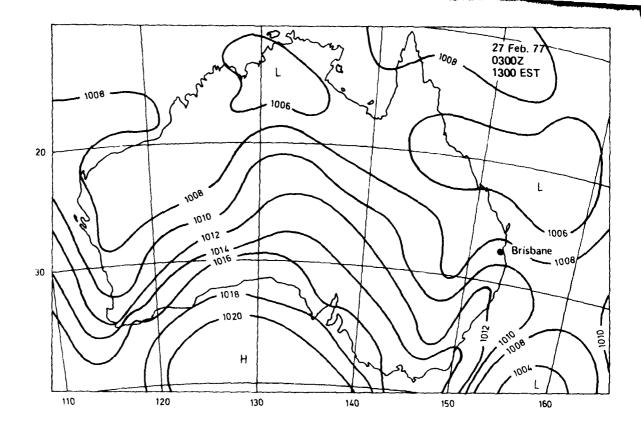
Fig. 33   Surface chart preceding type 4 incident on 27 Feb. 1977.
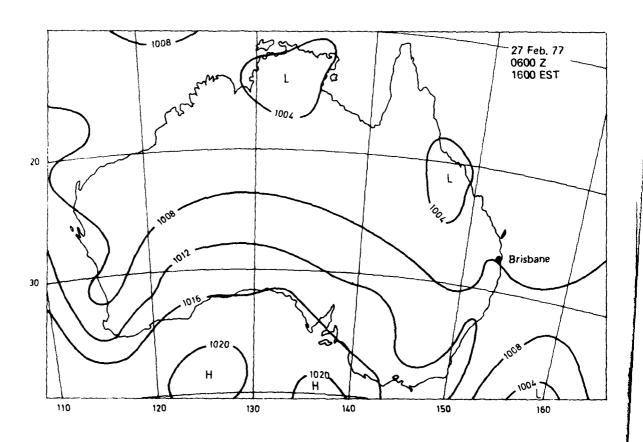
Fig. 34   Surface chart at time of type 4 incident on 27 Feb. 1977.
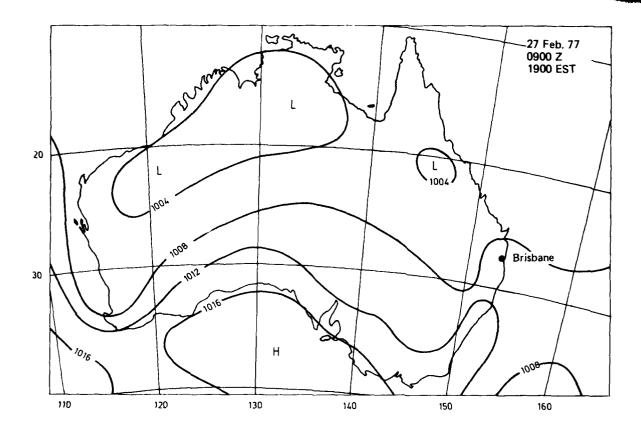
Fig. 35   Surface chart following type 4 incident on 27 Feb. 1977.
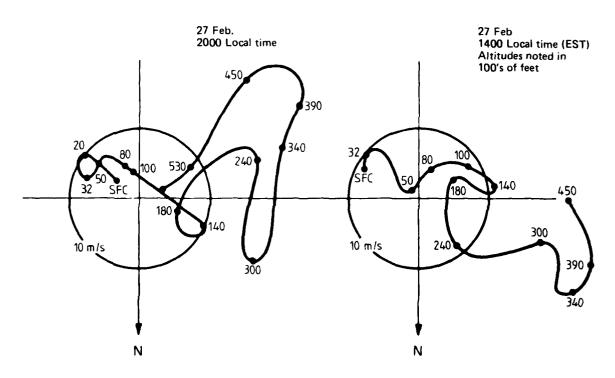
Fig. 36   Hodographs of wind velocity at Eagle Farm on 27 Feb. 1977. Altitude noted in 100's of feet.

AEROLOGICAL DIAGRAM
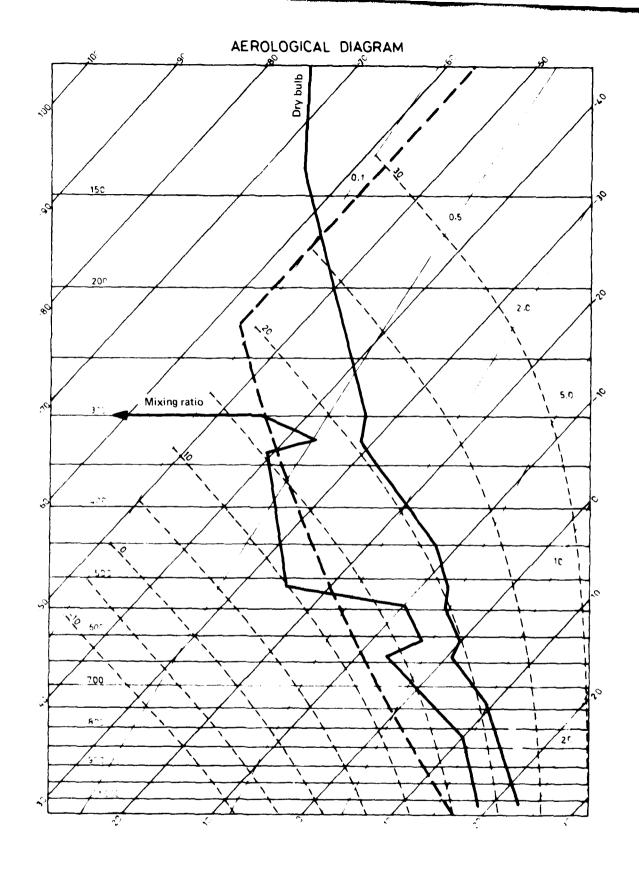
Fig. 37   Aerological diagram on 27 Feb. 1977 at 0800 EST.

6.6 Type 5 Incidents

(i.e. A temperature rise accompanied by at least one other phenomenon)

A total of 5 such incidents occurred, two in which the temperature rise was associated with significant temperature drops, and three in which the temperature rise was associated with high shears. The incidents associated with temperature drops occurred on 30 December at 0955 and 25 February at 0957. Both incidents were associated with high temperatures (around $35^\circ C$), low wind speed (around 2 m/s) and fairly active vertical wind components. They appear to be convective situations, and their main effect on aircraft would be the updrafts which can suddenly rise to 2 m/s for periods of the order of 3 minutes.

The other three incidents in this category are all associated with high shear. They occurred on

16 Dec. at 1140,

25 Jan. at 1205,

12 Feb. at 1257,

and are associated with fairly warm irregularly varying temperatures, and moderate wind speeds. For these three incidents the time histories, surface charts and balloon measurements were obtained and are presented in the figures indicated in the following table:

Date of incident	16 Dec. 76	25 Jan. 77	12 Feb. 77
Time of incident	1140–1300	1205–1505	1257–1357
Time History figures	38	43	49
Surface Chart figures	39, 40	44, 45, 46	50, 51
Upper Wind figures	41	47	52
Radiosonde Profile figures	42	48	53

The incident on 16 December was associated with a frontal type change in wind direction, but the concurrent wind speed changes were only minor. The surface chart shows that a cold front was approaching Brisbane at this time. All of the incidents were associated with fairly active vertical winds, which in the case of the 12 February incident (see Fig. 54) included an updraft which exceeded 5 m/s at the 150 m level. Such conditions in conjunction with high shears may represent a hazardous situation for aircraft. The vertical activity is presumably convective in nature.
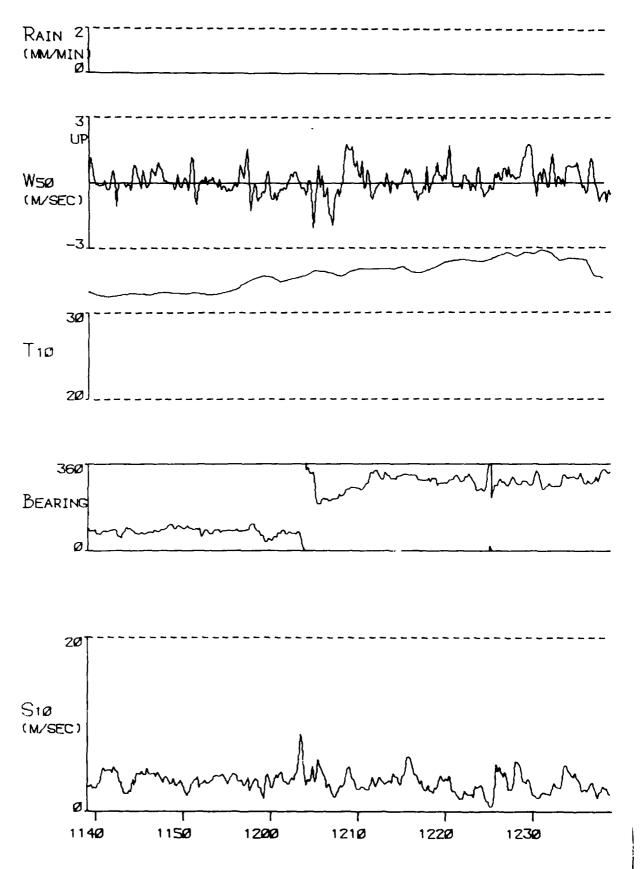
Fig. 38   A selection of parameters recorded during the type 5 incident on 16 Dec. 1976.
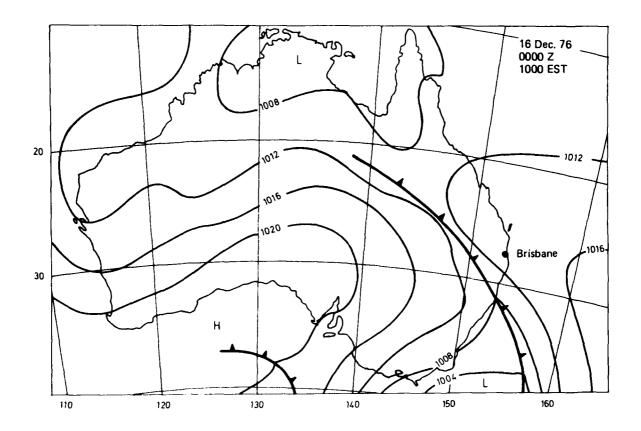
Fig. 39   Surface chart preceding type 5 incident on 16 Dec. 1976.

Fig. 40   Surface chart at time of type 5 incident on 16 Dec. 1976.
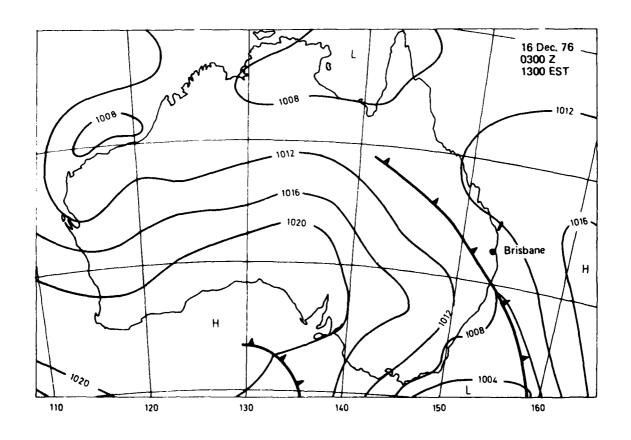
16 Dec.
0800 Local time (EST)
Altitude noted in
100's of feet

16 Dec.
1400 Local time
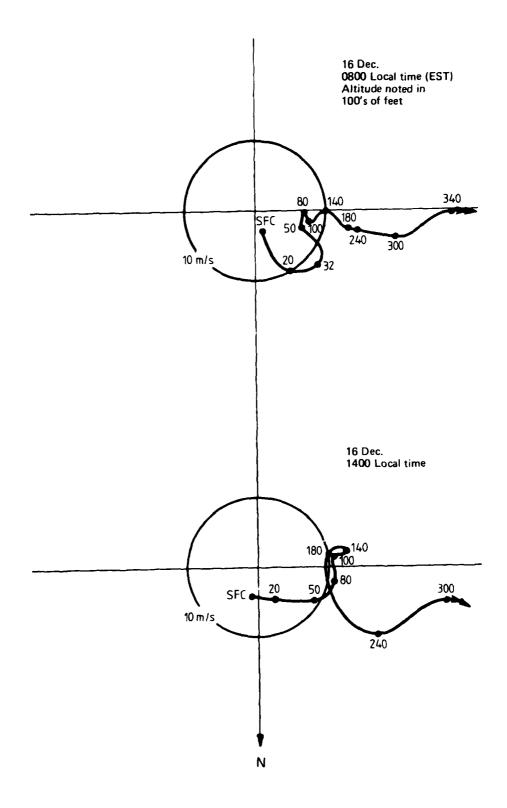
Fig. 41   Hodographs of wind velocity at Eagle Farm, for type 5 incident on 16 Dec. 1976.

AEROLOGICAL DIAGRAM
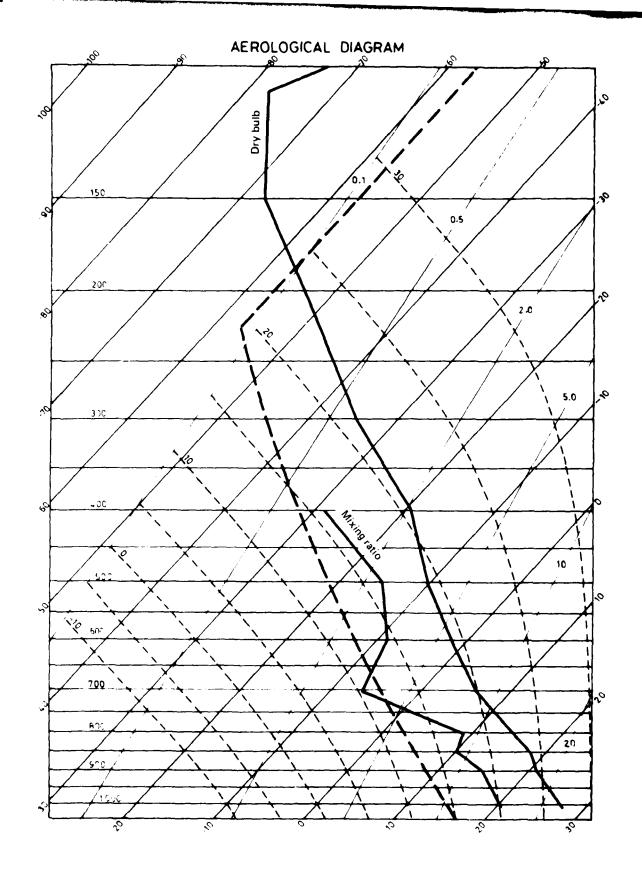
Fig. 42   Aerological diagram on 16 Dec. 1976 at 0800 EST.
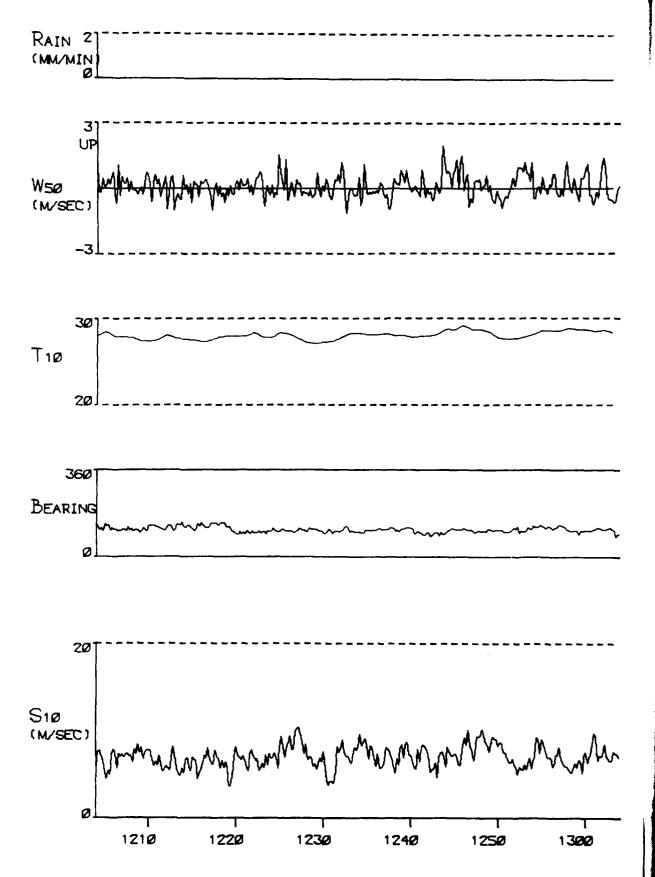
Fig. 43   A selection of parameters recorded during the type 5 incident on 25 Jan. 1977.
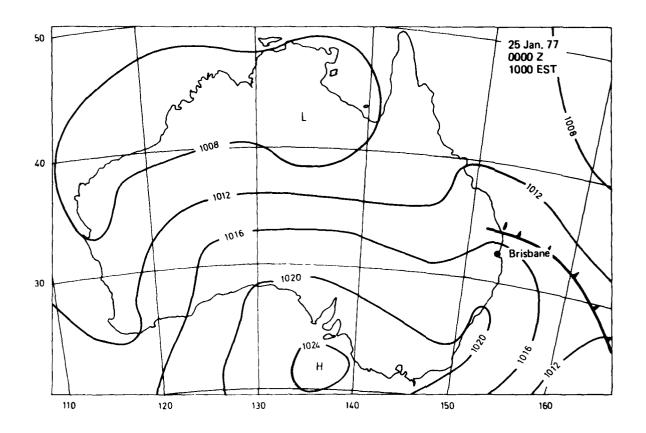
Fig. 44   Surface chart preceding type 5 incident on 25 Jan. 1977.
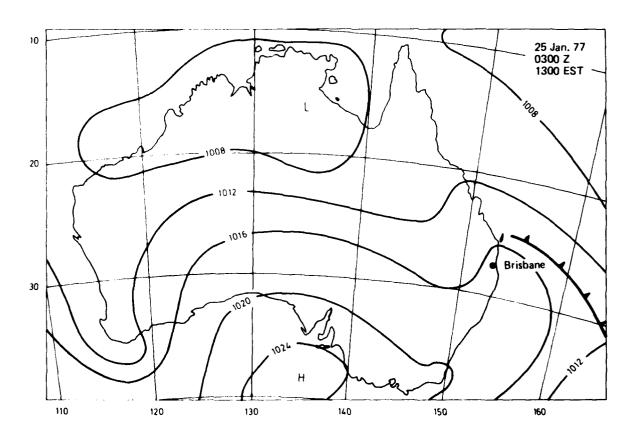
Fig. 45   Surface chart at time of type 5 incident on 25 Jan. 1977.
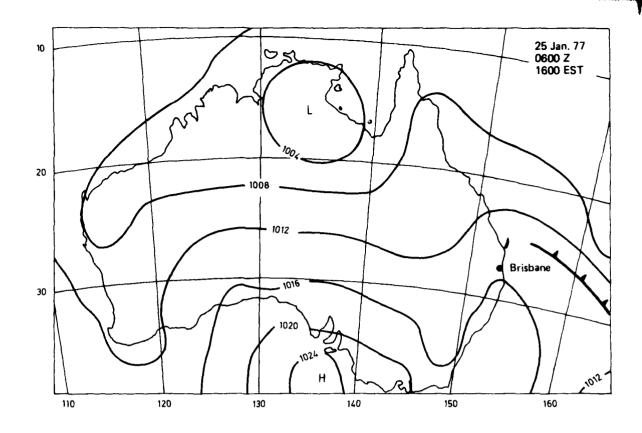
Fig. 46   Surface chart following type 5 incident on 25 Jan. 1977.
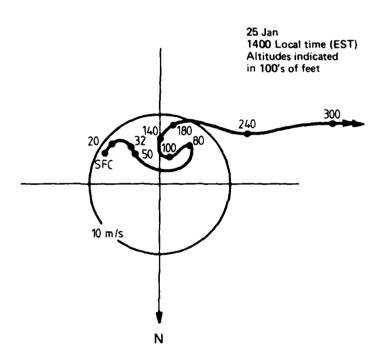
Fig. 47   Hodograph of wind velocity at Eagle Farm for type 5 incident on 25 Jan. 1977.
Altitudes noted in 100's of feet.

AEROLOGICAL DIAGRAM
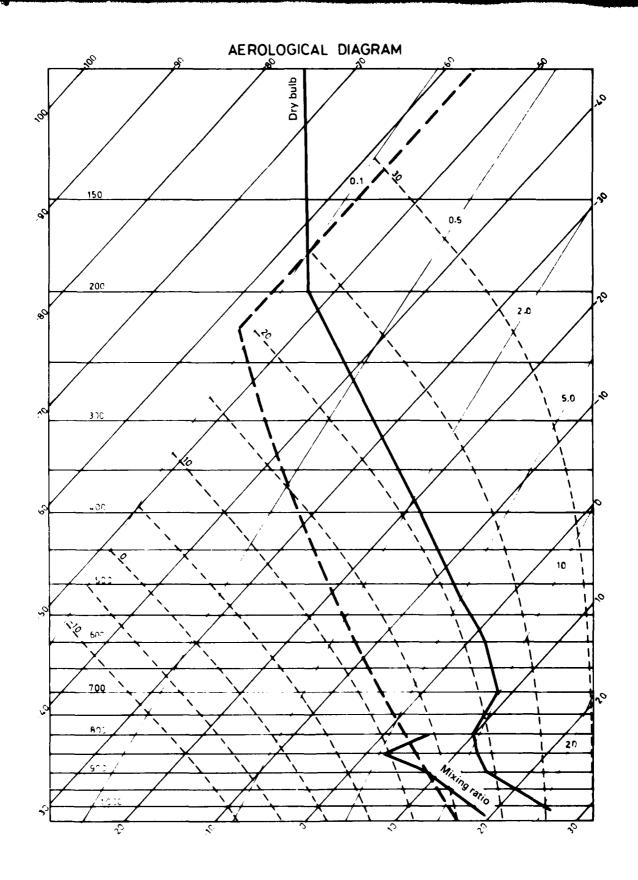
Fig. 48   Aerological diagram on 25 Jan. 1977 at 0800 EST.
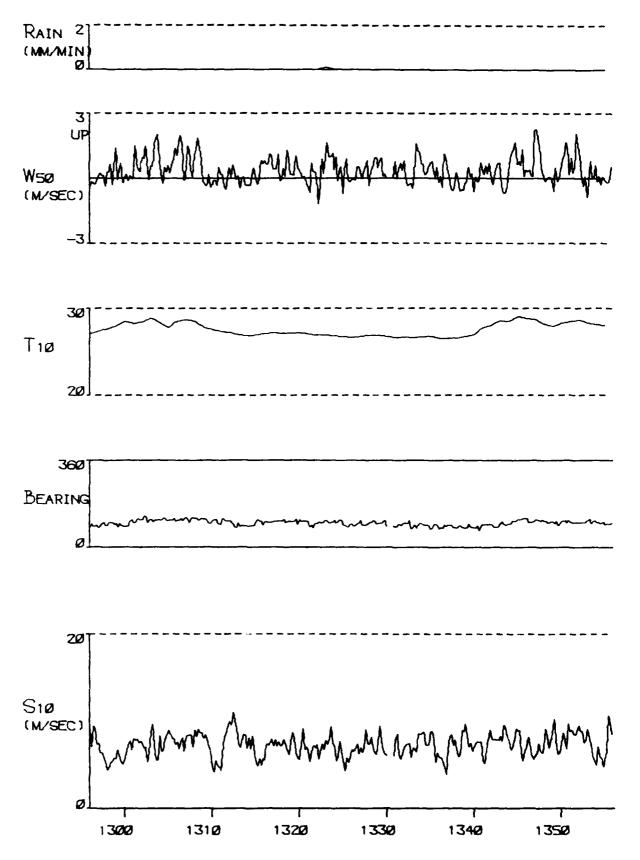
Fig. 49   A selection of parameters recorded during the type 5 incident on 12 Feb. 1977.
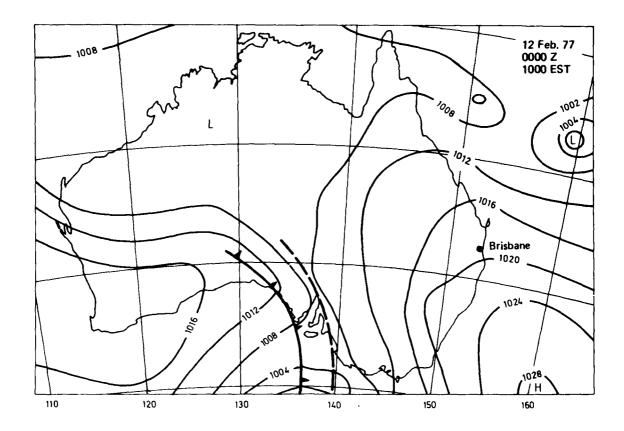
Fig. 50   Surface chart preceding type 5 incident on 12 Feb. 1977.

Fig. 51   Surface chart at time of type 5 incident on 12 Feb. 1977.
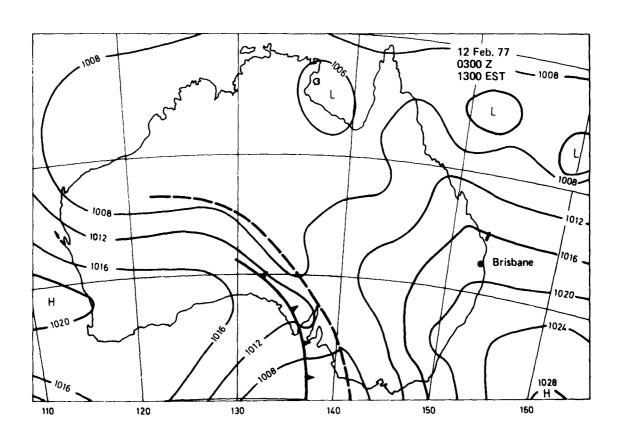
12 Feb
1400 Local time (EST)
Altitudes noted in
100's of feet
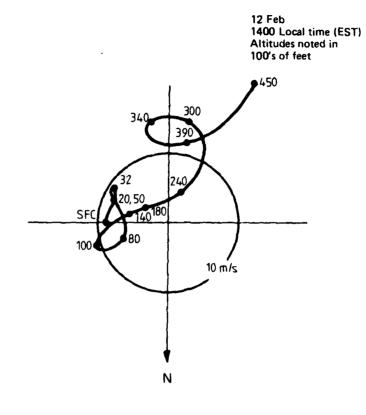
Fig. 52   Hodograph of wind velocity at Eagle Farm at time of type 5 incident on 12 Feb. 1977.
Altitudes noted in 100's of feet.

59

AEROLOGICAL DIAGRAM
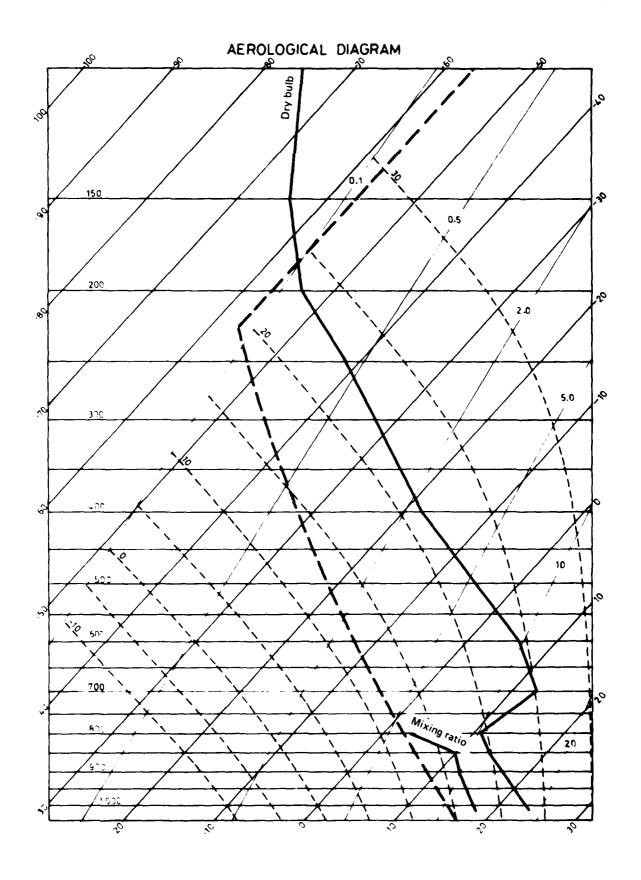
Fig. 53   Aerological diagram on 12 Feb. 1977 at 0800 EST.
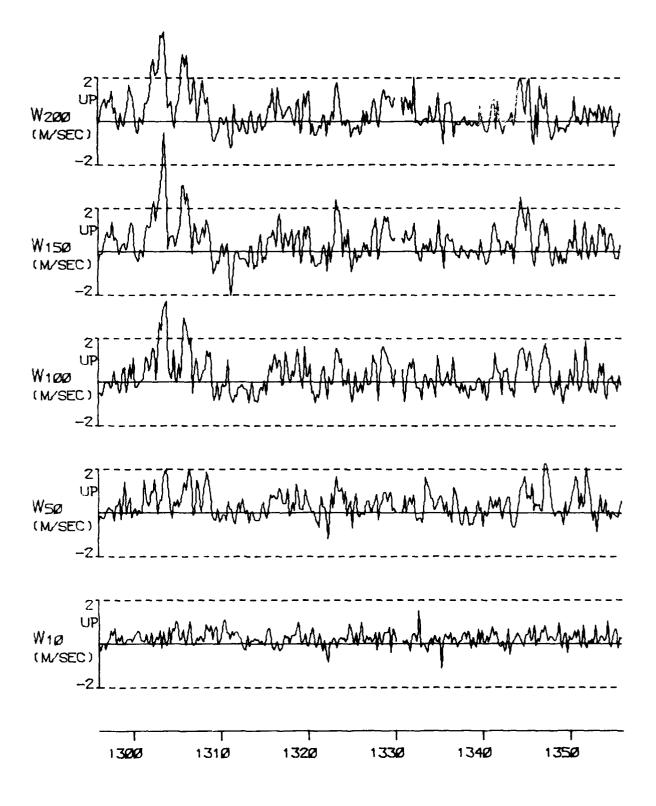
Fig. 54   Vertical wind component recorded at various levels during the type 5 incident on
12 Feb. 1977.

61

7. WIND SPEED PROFILES

The conventional power law velocity profile for horizontal wind speed, S, is given by the equation

$$S/S_0 = (z/z_0)^m \tag{7.1}$$

which for the purpose of fitting the parameter m can be written in the form

$$\ln S = m \ln z + C \tag{7.2}$$

and using a conventional least squares technique the parameters m and C can be calculated. Writing Y for $\ln S$ and X for $\ln z$ we have for the best fit to N sets of X, Y pairs

$$m = (N\Sigma XY - \Sigma X\Sigma Y)/(N\Sigma X^2 - (\Sigma X)^2) \tag{7.3}$$

$$C = (\Sigma Y - m\Sigma X)/N \tag{7.4}$$

and the goodness of fit of the equation is measured by the correlation coefficient

$$r = (N\Sigma XY - \Sigma X\Sigma Y)/\sqrt{((N\Sigma X^2 - (\Sigma X)^2)(N\Sigma Y^2 - (\Sigma Y)^2))}. \tag{7.5}$$

In the following discussion any data set for which the correlation coefficient, r, was less than 0·9 was ignored. The wind speed data used were moduli of the 6 minute average of the horizontal wind vectors at the nominal levels 10 m, 50 m, 100 m, 150 m and (when available) 200 m. Naturally in calculating m the exact values of z were used.

The m values were calculated at 6 minute intervals for all the data in the incidents tabulated in Section 6.1. This totalled 67·5 hours of data. The velocity profile will depend on the degree of turbulence (which influences mixing and lapse rate) and possibly the bearing from which the wind comes. There is a fair correlation between wind speed and degree of turbulence so here we have analysed the data as a function of wind speed and approach bearing. Figure 55 shows how m varies with wind speed at the 10 m level. For wind speeds above about 8 m/s the mean value of m appears fairly steady at about 0·16 to 0·18 as might be expected for a fairly open
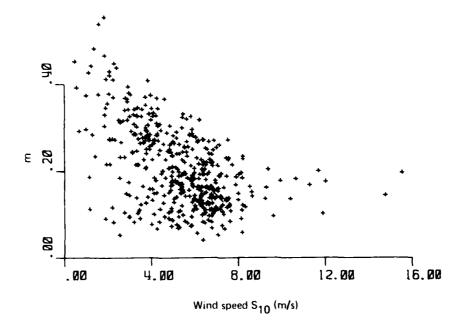
Fig. 55　Values of the wind speed profile exponent, m, as a function of mean wind speed.
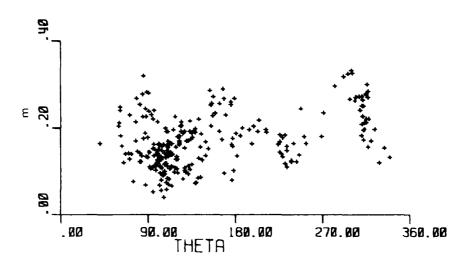
Fig. 56   Value of the wind speed profile exponent, m, for cases where the mean wind speed
          exceeds 5 m/s as a function of bearing from which wind approaches the Bald Hills
          site.

site. Brook and Spillane (1968) and Blackman (1972) both find similar values and a similar
scatter of values for somewhat similar terrain. There is however insufficient of this data to attempt
any analysis by direction of wind approach. If wind speeds above about 5 m s are considered
there are more data available, although the scatter is somewhat worse. However the mean value
is still somewhere around 0·16 to 0·18 so a classification by bearing was attempted for these
data. Figure 56 shows the result. There is perhaps a slight tendency to lower values of m when
the wind comes from a bearing around 120 degrees, and to higher values of m when the wind
comes from about 300 degrees but little more than this can be said concerning the bearing effect.

A question of interest concerns the value of m in thunderstorms. It is possible that because
the strong winds in thunderstorm gust fronts originate from downdrafts, and do not usually
travel very far horizontally, a normal velocity profile will not develop to any appreciable extent.
However this hypothesis is not supported by the present data. In fact all the points shown in
Figure 55 corresponding to wind speeds greater than 9 m s are due to the following type 1
incidents:

                    13 Nov. 1976   0859 0959

                    13 Nov. 1976   2131-2231

                    26 Nov. 1976   1721-1821

                    30 Nov. 1976   1554 1654

                    4 Dec. 1977   1654 1854

and it is precisely these points which show the least scatter and a close approach to the value
of m which would be expected for this type of moderately open terrain.

8. EFFECT OF HEIGHT, PEAK VALUE STATISTICS, AND AVERAGING TIME

Figure 57 shows how the probability distribution of the wind speed varies with height.
For computational convenience the distribution of peak 6-second average wind speed each
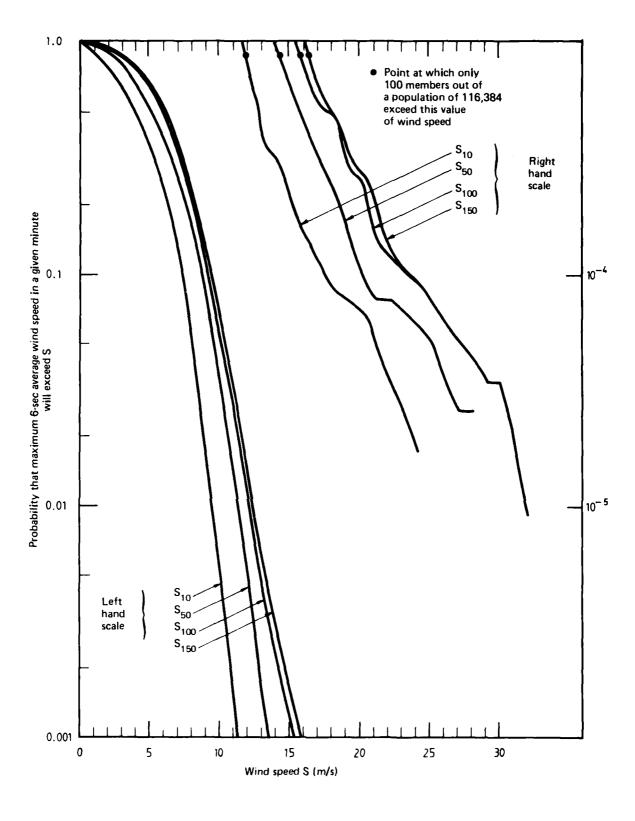
Fig. 57   Probability distribution of one minute maximum wind speeds at various levels on the tower.
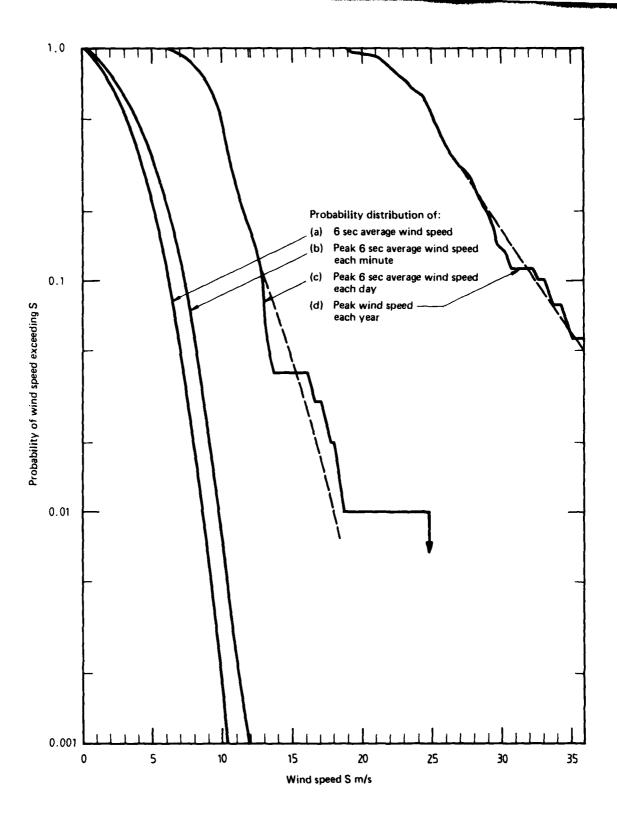
Fig. 58 Comparison of wind speed probability distribution and various extreme value distributions.

The figure shows a plot with "Probability of wind speed exceeding S" on the vertical (logarithmic) axis ranging from 0.001 to 1.0, and "Wind speed S m/s" on the horizontal axis ranging from 0 to 35.

Probability distribution of:

(a) 6 sec average wind speed

(b) Peak 6 sec average wind speed each minute

(c) Peak 6 sec average wind speed each day

(d) Peak wind speed each year

minute is shown. At the midrange probability levels (and with less certainty at the low probability extreme value end) we have for the wind speed encountered with a given probability:

$$S_{50} \qquad 1 \cdot 2 \, S_{10}$$

$$S_{100} \qquad 1 \cdot 3 \, S_{10}$$

For comparison, the Australian Standard Loading Code for wind forces (CA 34 Part 2) gives:

Terrain category 2 e.g. airport		Terrain category 3 e.g. suburban housing	
S_{50}	$1 \cdot 15 \, S_{10}$	S_{50}	$1 \cdot 25 \, S_{10}$
S_{100}	$1 \cdot 21 \, S_{10}$	S_{100}	$1 \cdot 37 \, S_{10}$

The tower data are therefore compatible with a terrain category intermediate between category 2 and category 3. It should however be noted that there is a small discrepancy between the values of the exponent m assumed by the Australian code (0·085 and 0·14 for terrain categories 2 and 3 respectively) and the general mean value of 0·16 to 0·18 found for the Bald Hills site for the strongest wind cases. It is possible that for the strong wind cases at Bald Hills a compensatingly smaller gradient height, z_0, would be found than that in the code.

In Figure 58 the probability distribution of 6-second average wind speed is compared with the extreme value distributions for the peak 6-second average wind speed each minute, each day and each year. (The data for the annual maxima were not obtained from the Bald Hills network. They are given in Appendix 2.) If $S(p)$ is the p-percentile value of wind speed, and $S_p(T, p)$ is the p-percentile value of the peak wind speed over a period T, we have approximately:

$$S_p(\text{1-minute}, p) \qquad 1 \cdot 2 \, S(p)$$

$$S_p(\text{1-day}, p) \qquad 1 \cdot 2 \, S(p) \cdot 6 \, \text{m/s}$$

$$S_p(\text{1-year}, p) \qquad 2 \cdot 5 \, S(p) \cdot 18 \, \text{m/s}$$

A variation in averaging time makes very little difference to the probability distribution of winds below about 6 m/s, as may be seen in Figures 59 and 60. At slightly higher wind speeds, up to about 10 m/s, averaging time makes quite a considerable difference, but at still higher wind speeds (where however the sample size is too small to exclude the possibility of random fluctuations) the effect of averaging time decreases markedly. A possible explanation for this is that there are two types of flow present. Velocities up to 10 m/s may occur predominately under, say, extensive pressure systems which give rise to turbulent flow with moderate velocities over long fetches. Under these conditions the turbulent length scale is short, of the order of the height, say 10 m, and the higher velocity peaks are short duration gusts. Many such gusts are markedly reduced by increases in the averaging time. On the other hand velocities over 12 m/s may occur predominately in ordered structures (such as cold air outflows) associated with thunderstorms, and in these ordered structures the length scale is of the order of the transverse dimension (500 m to 2000 m) and velocities may remain fairly constant over periods of 30 seconds, or even 300 seconds. Some support for this hypothesis can be obtained by finding those occasions when the wind speed, measured with a 30 second averaging period, exceeds 12 m/s. These occasions are listed in Table 8.1, and all of them occurred during type 1 incidents, when a thunderstorm occurred with a cold outflow causing a temperature drop of 2°C or more. The last column of Table 8.1 gives the ratio of the time for which the 30-second average speed is greater than 12 m/s to the time the 6-second average speed is greater than 12 m/s. The fact that the numbers are all close to unity supports the suggestion that the choice of averaging time is not very critical in this type of incident. Moreover all the values of this ratio are greater than 0·62, the value of the same ratio for the 10 m/s exceedances, and this suggests that statistical scatter alone is not sufficient to explain the rise in the curve of Figure 59 beyond 10 m/s. If the hypothesis is correct, that the averaging time does not greatly affect the probability of exceeding large wind speeds in thunderstorm incidents, then there are implications for building designers. Some wind load codes allow a reduction in the design speed for large frontal areas which, it is supposed, cannot be completely enveloped by the 3-second design gust. This supposition may not be supported in regions where the design wind occurs predominately in thunderstorm type incidents.
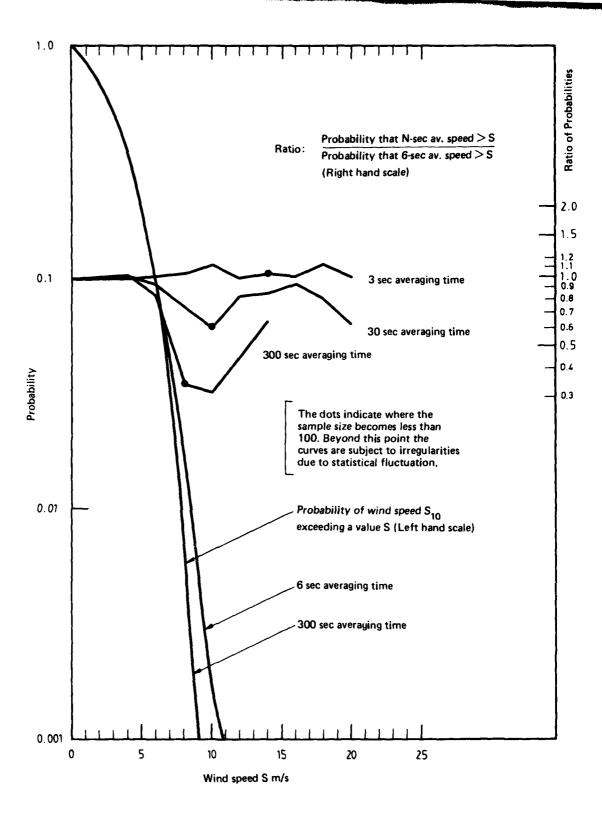
Fig. 59   Effect of averaging time on probability distribution of wind speed measured at the 10 metre level.
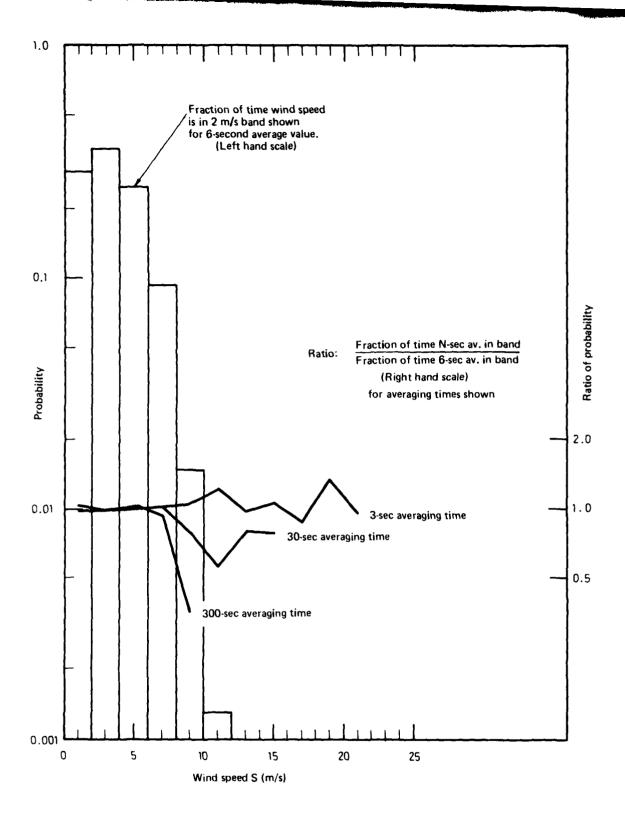
Fig. 60   Effect of averaging time on histogram of wind speed measured at the 10 metre level.
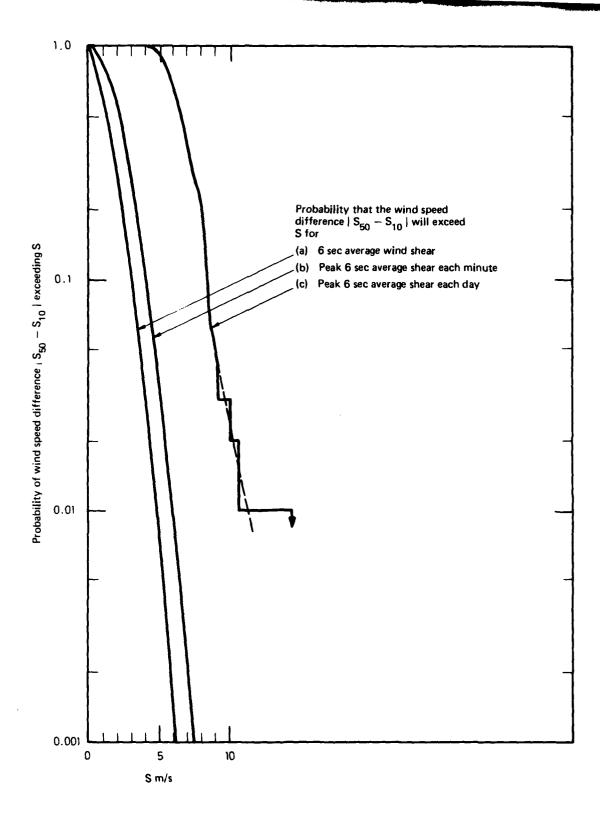
Fig. 61   Comparison of shear probability distribution and various extreme value distributions.
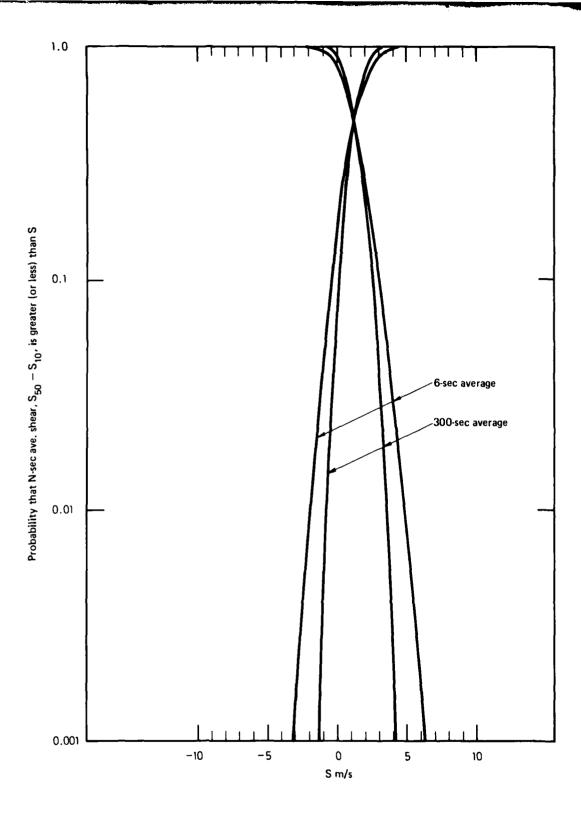
Fig. 62   Probability distribution of wind shear for two different averaging times.
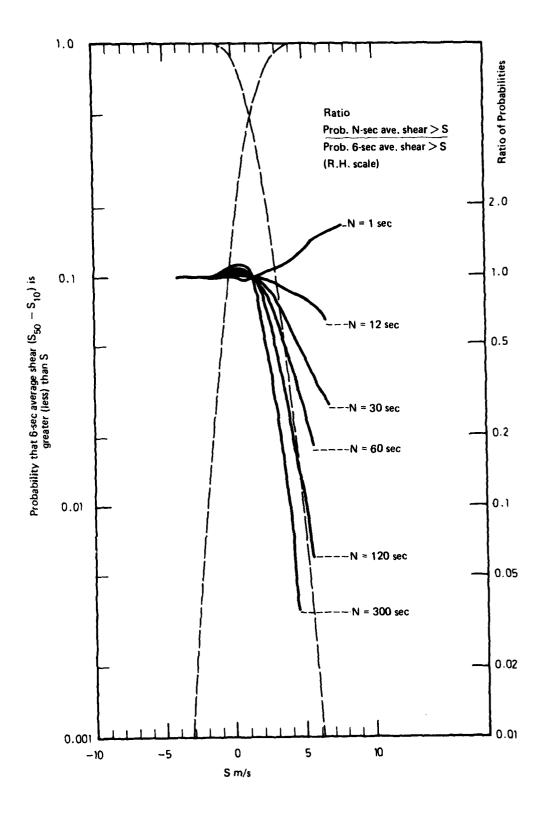
Fig. 63   Effect of averaging time on probability distribution of wind shear.
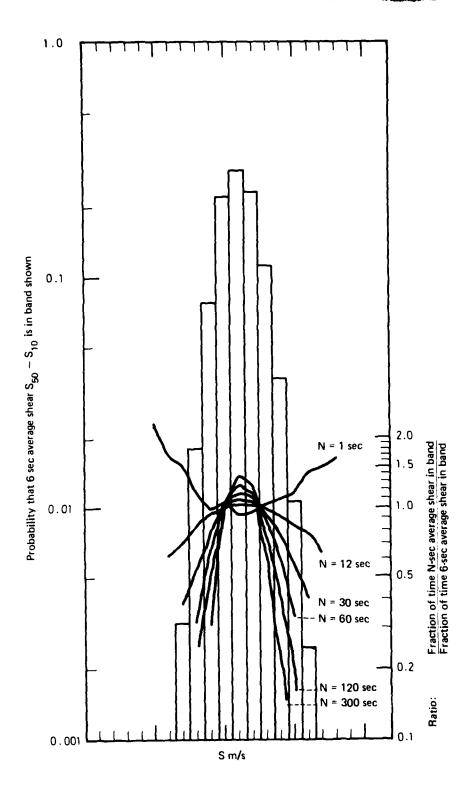
Fig. 64   Effect of averaging time on histograms of shear in the lowest 50 m.

For wind shear, Figure 61 compares the probability distribution of the 6-second average wind speed difference between anemometers at the 50 m and 10 m levels with the peak 6-second average value each day. For a given probability level the peak value each minute is about 20% greater than the corresponding percentile value, and the peak value each day is greater by a further 5 m/s. The effect of averaging time is much greater with wind shear than with wind speed. Figure 62 shows cumulative probability curves for averaging times of 6 seconds and 300 seconds. Because the shear distribution tails off in both positive and negative directions, and because the plots use logarithmic probability scales, it is desirable to plot both the probability of a shear exceeding a given value, and the probability of it being less than a given value. This has been done in Figure 62. Figure 63 repeats the curves of Figure 62 for the 6-second average shear, and also shows how averaging time affects the probability of exceeding a given shear. For a 30 second averaging time, a moderate shear of 5 m/s is only exceeded 0·45 times as often as with a 6-second averaging time, and a severe shear is (by extrapolation) only exceeded one tenth as often as with a 6-second averaging time. Figure 64 gives a similar set of curves for the probability density (or histogram). Increasing the averaging time increases the occurrence of shears around the mean value of 1 m/s and decreases the occurrence of extreme shears.

TABLE 8.1

Occasions on which wind speeds, S_{10}, having 30-second average values in excess of 12 m/s were recorded

Date 1976	Time	Tape	File Number	Period (sec) during which N-sec average speed is greater than 12 m/s		Ratio A/B
				$N = 30$ A	$N = 6$ B	
13 November	0916–0929*	203	3	270	312	0·865
13 November	2149–2157	204	1	120	132	0·909
26 November	1802–1810*	217	2	120	174	0·690
30 November	1609–1623*	221	1, 2	750	702	1·068†
4 December	1713–1802*	225	1	390	534	0·730
All other files of data in sample of 81 tapes				0	144	
Totals				1650	1998	0·826

Notes:

* An asterisk denotes that this time period occurred during a TAST watch period.

† A number greater than unity may occur in the last column because average speeds were calculated in non-overlapping blocks. A 30-second period during which the average speed is over 12 m/s may consist of a short time well over 12 m/s and the rest of the time below 12 m/s.

TABLE 8.2

Occasions when the 30-second average shear between 50 m and 10 m was "strong" or "severe".

Date	Type of incident	Time	Peak 30-sec average shear	No. of seconds shear $> 6·5$ m/s	Rank of severity
12 November	3	2150	7·32	18	4
		2207	8·22	30	
13 November	1	0917	6·73	6	5
		0922	7·99	36	
		0928	6·70	18	

TABLE 8.2 (*Continued*)

Date	Type of incident	Time	Peak 30-sec average shear	No. of seconds shear $> 6 \cdot 5$ m/s	Rank of severity
13 November	1	2153	7·48	24	3
		2202	9·01	60	
30 November	1	1611	8·47	36	1
		1613	10·95	36	
		1618	10·91	30	
		1620	11·26	102	
		1623	8·78	54	
		1624	6·88	18	
		1626	6·61	6	
4 December	1	1732	6·64	12	16
12 December	3	2027	6·92	18	11
		2049	6·95	24	
15 December	4	1602	6·91	18	13
4 January	4	1346	7·00	36	10
5 January	n.c.	1135	6·85	18	14
		1757	6·50	12	
23 January	4	1437	6·59	12	12
		1505	6·92	30	
		1718	6·61	6	
24 January	(3)	2035	7·04	18	9
25 January	5	1220	7·44	18	6
		1232	7·88	48	
		1308	6·94	18	
		1449	7·03	24	
2 February	4	1218	7·20	24	8
2 February	3	1949	9·22	42	2
		2011	7·56	24	
		2012	6·53	6	
26 February	1	1507	6·55	12	15
		1508	6·64	12	
		1508	6·52	6	
27 February	4	1526	6·56	6	7
		1535	7·32	24	
		1600	6·66	12	

Note: n.c. = not a classified incident.

For aeronautical purposes it is important to know what type of meteorological conditions are associated with the most severe occurrences of wind shear. Table 8.2 lists the occasions when a 30-second average value of wind shear (between the 50 m level and the 10 m level) exceeded 6·5 m/s, i.e. those occasions when the shear was classified as "strong" or "severe". It is not surprising to find that the most severe shear is associated with the thunderstorm and gust front on 30 November. That particular storm was unusually severe. The peak gust of 28·5 m/s corresponded to a 5 year return period for Brisbane. It is more surprising to find that two of the five severest shear occurrences were during type 3 incidents, which although probably associated with storms, did not have any large temperature drops recorded, and so could not have been associated with any but weak or old gust fronts. It is of interest to note that the second most severe shear occurrence (which occurred on 2 February) did not occur on a thunder day and was not a declared TAST, although it was associated with heavy rain and "partial squalls" at most levels. The situation on 25 January was the sixth most severe shear occurrence, and was not related to storms or rain at all. The temperature was very high, the wind was strong and disturbed by convective activity. It was one of the type 5 situations described in Section 6.6.

9. DURATION OF SHEAR BURSTS

The effect of a high shear occurrence will depend in part on how long the high shear is maintained. Figure 65 shows how often a shear of 3·5 m/s is exceeded for various durations. Of those shears which last for at least 12 seconds only 1% last for longer than 120 seconds. The shear limit of 3·5 m/s is fairly low but was chosen so that statistically significant numbers were available.

The increasing number of exceedances with increasing averaging time is to be expected, for if a wind speed time history fluctuates above and below a threshold then averaging will smooth the time history and whilst this will remove short excursions above the threshold, it will also remove short excursions below the threshold, thus amalgamating what were two short excursions of the threshold into one long exceedance. However the effect shown in Figure 65 may have been exaggerated as an artifact of the method of calculation by non-overlapping blocks. For if, say, the 3-second average shear is continuously above a given threshold for 12 seconds, then the 12-second average over that same time must necessarily be above the threshold.* However there will also be cases when the 3-second average shear is only above the threshold for, say, 9 seconds, but if the next 3-second value is only slightly below the threshold, the 12-second average may be large enough to exceed the threshold. With the method of non-overlapping blocks, this would be counted as an exceedance of the 12-second average value for a 12-second duration. It would be better to calculate the 12-second average shear at closely spaced points, using overlapping data blocks, but this was not done because of the increased computational effort involved.

Figure 66 shows the effect of varying the shear level for the case of 30 second average shear. It can be shown that for every 1000 cases when the shear in the lower 50 metres exceeded the 3·5 m/s threshold used in Figure 65, there are 9 cases when the shear exceeded the threshold of strong shears (6·5 m/s in 50 m).

10. WIND SHEAR MONITORING AS A LANDING AID

Many of the graphs of wind shear, such as Figures 17d and 23, show great variation with time. In consequence, it seems that many of the proposed methods of measuring wind shear are not likely to be very useful for any quantitative application to landings in the Brisbane area.

---

* The situation is quite complex. The 12-second block used for averaging may not coincide with the 12 seconds during which the 3 second average is above the threshold. In general the 12-second period above the threshold will be split between two blocks. Often, one of these blocks will have more than half the 3-second average data exceeding the threshold, so that there will be a high probability that the 12-second average for that block will also be above the threshold. Even when the two 12-second blocks each have half of the data above the threshold, there is a 50% chance for each block that the 12-second average will be above the threshold.
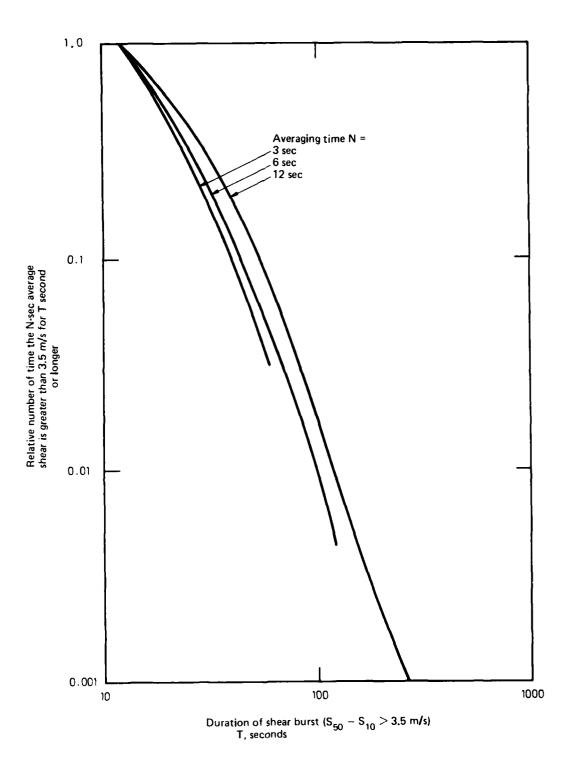
Fig. 65   Relative durations of shear bursts above 0.07/sec.
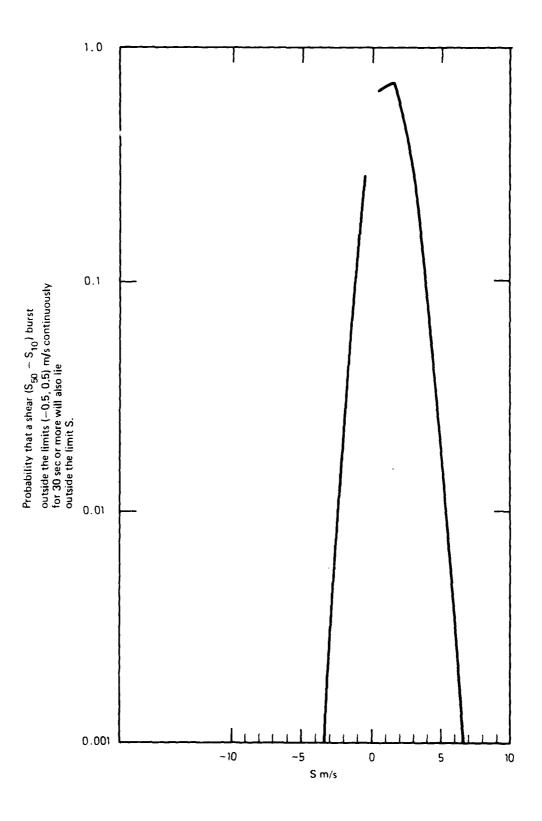
Fig. 66   Probability distribution of magnitudes of prolonged shear bursts.

An aircraft can pass through the last 100 m of its descent in something less than 30 seconds. On this sort of time scale the shear may appear fairly steady. But two minutes later when the next aircraft lands, the shear may easily have doubled, have dropped to zero, or in some cases have even undergone a complete reversal in sign. There are, of course, situations in which the mean shear (using, say, a 6-minute averaging time) is fairly steady for long periods of time. However the cases observed in this category generally had a fairly low mean wind shear, around 3 meter per second in 50 metre, or 0.06/sec. The danger in these situations was more related to the occasional peaks and troughs when for a minute or two at a time the shear might take large positive or negative values. It should be stressed that these comments apply not only to transient situations such as occur in thunderstorms and particularly in thunderstorm gust fronts, although they may be more pronounced in such situations. They were also observed to apply to shears measured in steady situations such as arise during strong winds. If measurements are made with a time lag (e.g. reports from a previous aircraft) or a spatial separation (e.g. an echo sounder to one side of the runway) the shear extremes encountered by a landing aircraft will almost certainly be different from the measured value. The only type of sensor which appears effective for this purpose is a laser or similar sensor looking along the glide slope during the actual landing.

II. HORIZONTAL STRUCTURE OF THE WIND

Figure 67 shows the autocorrelation structure of the wind speed measurements plotted as a function of the separation $d = Vt'$, where

$$R(d) = \langle S(t) S(t + t') \rangle / \langle S^2(t) \rangle$$

and in this case S denotes the deviation of the wind speed from its mean value, V, and the triangular brackets denote an expected value. The data used to compute these autocorrelations were selected from the incidents in Table 6.1 so as to be in fairly stationary turbulent records. Specifically, 8-minute records were chosen and divided into four 2-minute segments. The mean, standard deviation, skewness and kurtosis of each segment, and of the whole record were calculated. A record was accepted for analysis if:

(a) the standard deviation of each segment exceeded 0.45 m/s,

(b) the coefficient of variation of each segment was not less than 0.1,

(c) the kurtosis of each segment was less than 6,

(d) the mean of each 2-minute segment did not differ from the mean of the entire record by more than

$$3 * \text{standard deviation of record}/\sqrt{120},$$

and

(e) the kurtosis of each 2-minute segment did not differ from the kurtosis of the entire record by more than $3\sqrt{24}/\sqrt{120}$.

An important consequence of the selection process is that some significant cases involving ordered structures were eliminated from consideration. Such ordered structures, which may involve correlations over large distances, need to be studied individually. For the normal turbulent cases, the main feature of the autocorrelation in the present context is that beyond separations of 100 m, the wind speed at two points is virtually uncorrelated. This has relevance to the interpretation of the wind shear. It was not desirable to mount anemometers at the 10 m level on the tower, because the adjacent tuning hut would have had an uncertain shielding effect. Furthermore the horizontal array of masts could not be placed closer to the tower because of the buried earth mat associated with the transmitter. This means that the shear between the 50 metre level and the 10 metre level involves not only a vertical separation, but also a horizontal separation of 270 m or greater, depending on which 10 m mast is used. In a stationary turbulent situation the mean shear is not affected by the horizontal separation, but the variance is increased. Because the horizontal separation is greater than 100 m it does not matter which of the horizontal array anemometers is used to measure S_{10}. Although the statistics of the observed velocity differences

78
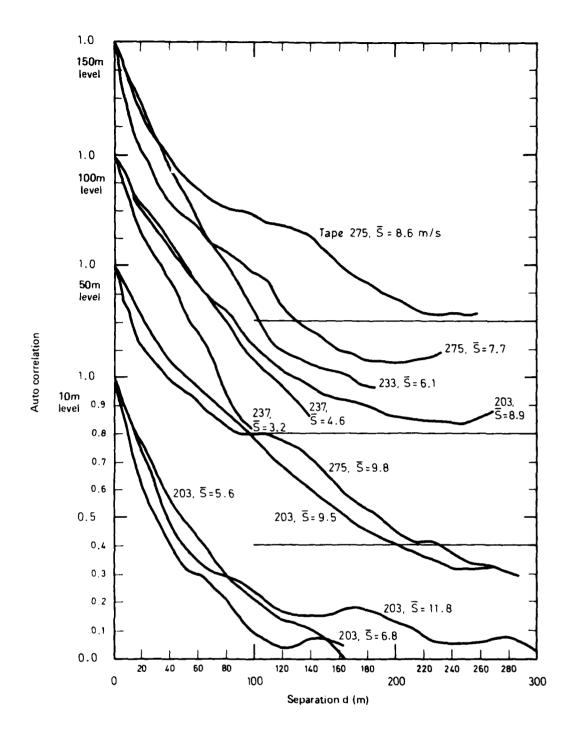
Fig. 67   Sample auto correlations of wind speed measured at various altitudes.

differ from those of the true vertical shear, they are representative of the differences an aircraft will encounter when coming in to land on a glide slope. They are therefore of direct significance to the aeronautical application.

The differences in airspeed encountered in a horizontal plane may not be directly applicable to a landing aircraft, but they are of some significance during the ground roll part of the take off. Figure 68 shows a selection of wind speed time histories measured at the top of some of the 10 m poles. S_{p10} for example denotes the wind speed at the top of pole 10. The location of the various poles is shown in Figure 1, and the distances of the poles from the centre (pole 11) is shown in Table 11.1.

The instantaneous differences between some of these wind speeds is shown in Figure 69. The horizontal separation between the relevant poles is shown in Table 11.2.

TABLE 11.1

Pole Number	Distance from Pole 11 (metres)
1	+ 210
2	+ 150
3	+ 90
4	+ 30
5	- 30
6	- 90
7	- 30
8	+ 30
9	- 150
10	- 150

TABLE 11.2

Poles	Separation (metres)
10-9	300
9-7	120
7-4	42
4-1	180

The only pair with a separation much less than 100 m is (pole 7, pole 4) and Figure 69 shows that the general level of velocity differences for this pair is somewhat less than for the other pairs, and the frequency of return to zero is somewhat greater, as would be expected. The general level of the horizontal differences may be compared with the differences in the vertical plane shown for the same incident in Figure 23.
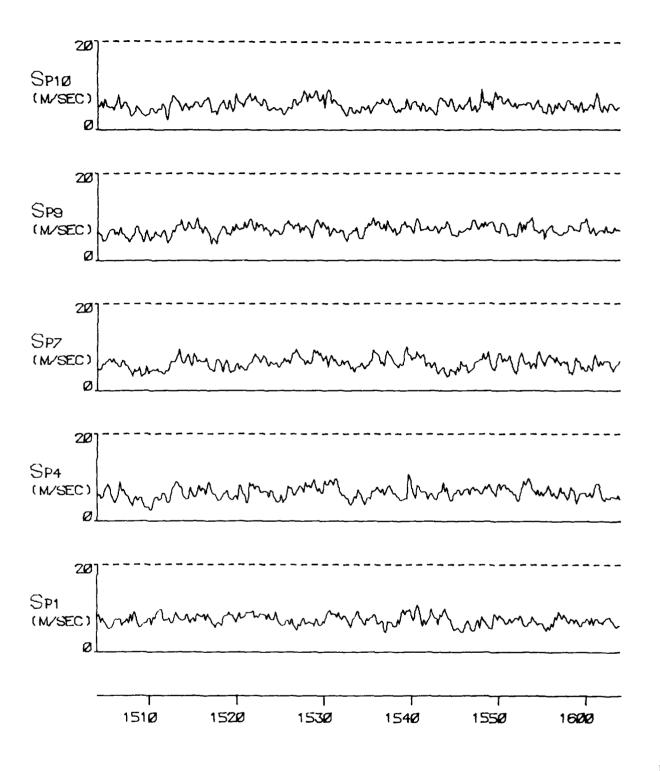
Fig. 68   Wind speed time histories measured simultaneously at several different 10 metre poles during the type 4 incident on 27 Feb 1977
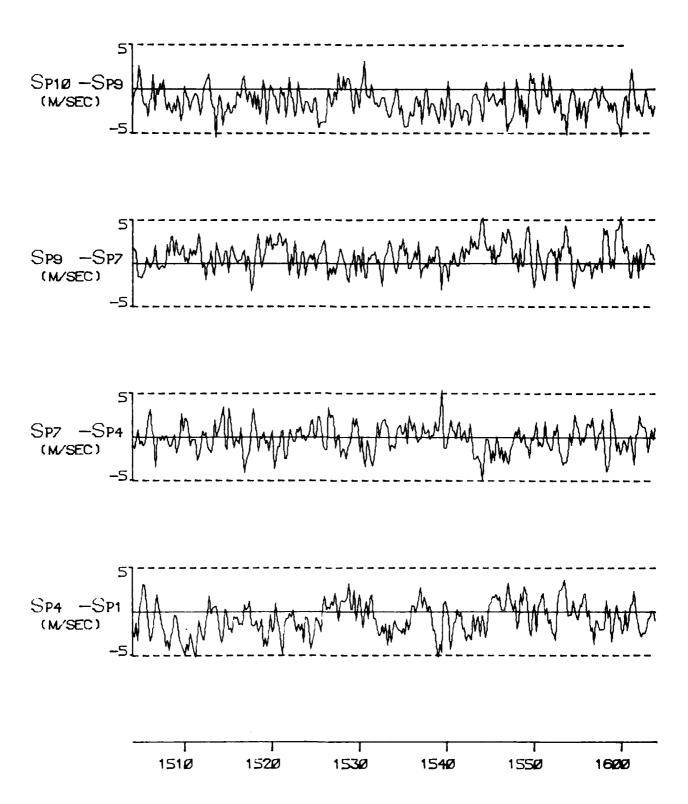
Fig. 69   Differences in wind speed between simultaneous measurements at various points
at the 10 metre level during the type 4 incident on 27 Feb. 1977.

CONCLUSIONS AND RECOMMENDATIONS

1. The strongest winds were found to occur in thunderstorm gust front situations. The five severest incidents (during which the 30-second average wind speed exceeded 12 m/s) were in this category.

2. Some of the strongest wind shears were also found to occur in association with thunderstorms, but unlike the wind speed case, there were some strong shears which were not associated with gust fronts. Of the five severest incidents (in which 30 second average wind speed differences in excess of $7 \cdot 9$ m/s were measured in the lowest 50 m), two incidents were not associated with gust fronts. There were further incidents of only slightly lower severity which were not even associated with thunderstorms. It is recommended that further study be made of the situations giving rise to these non-gust front, high shear occurrences.

3. In a small sample of five storms for which some sort of radar coverage was available, the gust front was found to occur at various distances up to 16 km from the centre of the storm. It is recommended therefore that conservative operational practices based on American experiences be continued. (Charba and Sasaki observed a case in which the gust front of an Oklahoma storm was 30 km ahead of the centre of the radar echo.)

4. Wind speed profiles described by the power law, $S/S_0 = (z/z_0)^m$ appear to have the same value for the exponent, m, in the thunderstorm situation as in other types of situations. However it can be inferred from the study, reported in Section 8, of the effect of averaging times on the wind speed histograms that the length scales of wind speed fluctuations in thunderstorm situations tend to be very much greater than in normal turbulence. It is recommended that further study be made to determine whether this observation invalidates the commonly applied reduction of design wind loads for buildings with large frontal areas if the building is in a geographic region where winds of the design value occur principally in thunderstorms.

5. An important characteristic of almost all the observed time histories of wind shear was their variability. It is recommended that the operational effects of such variability be considered further because much of the discussion which has occurred to date on aeronautical effects of wind shear has been predicated on an implicitly assumed model of steady shear.

6. High shears generally occurred in short bursts well scattered throughout the period of the experiment. For example a moderate shear of $0 \cdot 1$/sec was exceeded for only $0 \cdot 7\%$ of the time. However this shear was exceeded in $2 \cdot 5\%$ of the minutes in which data were recorded, and on more than 90% of the days of the experiment. Similarly of all the shear bursts which exceeded $0 \cdot 07$/second for 12 seconds or longer, only 1% lasted longer than 120 seconds.

7. Because this experiment only covered one season of the year, it is not valid to extrapolate measured probability distributions of shear to a whole year basis. Moreover the sample on which these comments are based is unrepresentative in at least two ways. Firstly, it covered only summer conditions, and so there is a high probability of the occurrence of thermal convection which might break up flow patterns which would otherwise be steady. Secondly, there was almost no sampling during the early morning hours (midnight to 5 a.m.) and so there were no records of "low level jet streams" which had been observed under inversion conditions during some previous years when a few recordings were made on a 24 hour basis. It is recommended that a further period of sampling be made over a complete 12 month period, sampling 24 hours/day, so as to observe any other phenomena of possible aeronautical significance and to determine the annual probability distribution of wind shear at Brisbane. It is also recommended that similar tower measurements be made in a region typical of the Southern part of Australia so as to determine the wind shear probability distribution in a climatically different region of considerable aeronautical significance, and to better describe the weather conditions giving rise to aeronautically hazardous conditions.

REFERENCES

1. Allen, S. C., (1980)—Wind data from Black Mountain Tower.
   Bureau of Meteorology, Meteorological Note 110.

2. AUSTRALIA, (1954)—Bureau of Meteorology.—Australian meteorological observer's handbook.

3. Barclay, P. A., (1974)—Aircraft turbulence encounters during commercial operations in the vicinity of thunderstorms. Pre-prints, 6th conference on aerospace and aeronautical meteorology. El Paso, Texas, pp. 357–360. Published by American Meteorological Society.

4. Bedard, A. J. and Beran, D. W., (1977)—Detection of gust fronts using surface sensors. NOAA Tech. Memo. ERL WPL-20.

5. Bedard, A. J., Hooke, W. H. and Beran, D. W., (1977)—The Dulles airport pressure jump detector array for gust front detection. B.A.M.S., Vol. 58, No. 9, pp. 920–926. *See also* Hardesty *et al.* The Dulles airport acoustic-microwave radar wind and wind shear measuring system. B.A.M.S., Vol. 58, No. 9, pp. 910–918.

6. Bedard, J. R. and Meade, H. B., (1977)—The design and use of sensitive pressure-jump sensors to detect thunderstorm gust fronts. Part 1: Pressure jump detector design. Journal of Applied Meteorology, Vol. 16, pp. 1049–1055.

7. Benjamin, T. Brooke, (1968)—Gravity currents and related phenomena. Journal of Fluid Mechanics, Vol. 31, pp. 209–248.

8. Blackman, D. R., (1972)—Observations of the profile of the wind over suburban roughness. Monash University, Department of Mechanical Engineering, Report No. MMER 11.

9. Brancato, G. N., (1942)—The meteorological behaviour and characteristics of thunderstorms. United States Weather Bureau.

10. Brook, R. R. and Spillane, K. T., (1968)—Vertical shear in the boundary layer at Melbourne airport. Paper prepared for WMO Commission for Aeronautical Meteorology, Scientific and Technical Conference, London.

11. Brook, R. R., (1970)—Preliminary study of wind shear in the boundary layer at Melbourne airport (Tullamarine). Bureau of Meteorology, Australia Meteorological Study, No. 19.

12. Browning, K. A., (1968)—The organization of severe local storms. Weather, pp. 429–434.

13. Browning, K. A. *et al.*, (1976)—Structure of an evolving hailstorm. Part V.: Synthesis and implications for hail growth and hail suppression. Quarterly Journal, Royal Meteorological Society, Vol. 102, pp. 499–533.

14. Charba, J. and Sasaki, Y., (1971)—Gravity current model applied to analysis of squall-line gust front, pp. 277–283, pre-prints of papers presented at the Seventh conference on severe local storms. Published by American Meteorological Society.

15. Colmer, M. J., (1971)—On the character of thunderstorm gust fronts. Proceedings, Royal Aeronautical Society/CASI/AIAA. Conference on atmospheric turbulence, London.

16. Fawbush, E. J. and Miller, R. C., (1954)—A basis for forecasting peak wind gusts in non-frontal thunderstorms. B.A.M.S., Vol. 35, No. 1, pp. 14–19.

17. Fujita, T. T., (1976)—Spearhead echo and downburst near the approach end of John F. Kennedy airport runway, New York City. SMRP research paper 137. University of Chicago, Illinois. Also NASA CR-146561 (NTIS Accession No. N76-21841).

18. Fujita, T. T. and Caracena, F., (1977)—An analysis of three weather related accidents. B.A.M.S. Vol. 58, No. 11, pp. 1164-1181.

19. Goff, R. C., (1975)—Thunderstorm outflow kinematics and dynamics. NOAA Tech. Memo. ERL NSSL-75, (NTIS Accession, No. PB 250 808).

20. Goff, R. C., (1977)—Some observations of thunderstorm induced low level wind variations. Journal of Aircraft, Vol. 14, No. 5, pp. 423-427.

21. Hall, F. F., Neff, W. D. and Frazier, T. V., (1976)—Wind shear observations in thunderstorm density currents. Nature, Vol. 264, pp. 408-411.

22. Haurwitz, B., (1941)—Dynamic meteorology. McGraw-Hill.

23. Huschke, R. E., (1959)—Glossary of meteorology. American Meteorological Society, Boston, Mass.

24. Karman, von T., (1940)—The engineer grapples with non-linear problems. Bulletin, American Mathematical Society, Vol. 46, p. 615 (cited by Benjamin, 1968).

25. Keddie, Barbara, (1971)—Some aspects of wind information required in the landing of aircraft. The Meteorological Magazine, Vol. 100, No. 1186, p. 134.

26. Keulegan, G. H., (1958)—The motion of saline fronts in still water. National Bureau of Standards Report 5831 (cited by Benjamin, 1968).

27. McIntosh, D. H., (1972)—The meteorological glossary. Chemical Publishing Co. N.Y.

28. Meighen, P. J., Sherman, D. J. and Thomson, M. R., (1978)—Thunderstorm gust fronts from a radar viewpoint. Royal Meteorological Society—Australian branch. Proceedings, AIRMET conference, Canberra, 9-10 February 1978.

29. Mitchell, K. E. and Hovermale, J. B., (1977)—A numerical investigation of the severe thunderstorm gust front. Monthly Weather Review, Vol. 105, pp. 657-675.

30. Patterson, A. K., Sherman, D. J., Thomson, M. R. and Woodall, G., (1975)—Low level wind study—Bald Hills instrumentation system. ARL Structures Note 414.

31. Pearce, R. P., (1972)—Large wind shears near the earth's surface. ARC 33633.

32. Roberts, C. F., (1964)—A preliminary analysis of some observations of wind shear in the lowest 100 feet of the atmosphere, for application to the problem of the control of aircraft on approach. U.S. Weather Bureau.

33. Schrage, J. J., (1977)—Wind shear: A literature search, analysis and annotated bibliography. FAA RD-76-114 (NTIS Accession, No. AD-A037-310).

34. Scoggins, J. R., (1967)—Some properties of low altitude atmospheric turbulence at Cape Kennedy, Florida. Marshall Document TM X-53640.

35. Simpson, J. E., (1969)—A comparison between laboratory and atmospheric density currents. Quarterly Jornal, Royal Meteorological Society, Vol. 95, pp. 758-765.

36. Simpson, J. E., (1972)—Effects of the lower boundary on the head of a gravity current. Journal of Fluid Mechanics, Vol. 53, Part 4, pp. 759-768.

37. Sinclair, R. W., Anthes, R. A. and Panofsky, H. A., (1973)—Variation of the low level winds during the passage of a thunderstorm gust front. NASA CR-2289.

38. Singer, I. A. and Smith, M. E., (1953)—Relationship of gustiness to other meteorological parameters. Journal of Meteorology, Vol. 10, pp. 121-126.

39. Snyder, C. T., (1968)—Analog study of the longitudinal response of a swept-wing transport airplane to wind shear and sustained gusts during landing approach. NASA TN D-4477.

40. Thomson, M. R., (1975)—Low level wind study—Data acquisition program for the NOVA minicomputer at Bald Hills. ARL Structures Note 415.

41. Whittingham, H., (1964)—Extreme wind gusts in Australia. Bureau of Meteorology, Bulletin No. 46.

APPENDIX 1

Criteria for Choice of Significant Incidents

A period of the record was chosen for detailed study if any of the following occurred:

(a) A temperature drop in excess of 2°C.

(b) A 6-second average wind speed difference of 7·5 m/s between any two adjacent levels on the tower.

(c) A squall or "partial squall" (see later).

In addition it was necessary to define when a temperature rise in excess of 2°C occurred, in order to classify the various incidents into categories.

A *temperature drop* at time t was noted if the one minute mean temperature at some time, $t + 5$ minutes, was less than the mean temperature over the period $(t - 4, t)$ by at least 2°C, and less than the minimum 1-minute mean temperature in the period $(t - 15, t - 5)$ by at least 1°C, as illustrated in Figure 70. The actual time of onset of the temperature drop was defined as the time of the start of the greatest 4 minute drop, and the magnitude of the drop was obtained from the maximum temperature during the 15 minutes preceding the onset to the minimum temperature during the 10 minutes following the onset of the drop. A temperature rise was defined conversely.

A *squall* is conventionally defined (e.g. McIntosh, 1972) as a sudden increase in wind speed by at least 8 m/s, rising to at least 11 m/s and lasting at for least one minute. In the present analysis it was further required that:

(a) A rise in wind speed sufficient to signal a squall occurred within 9 minutes, and

(b) The wind speed rose to at least 1·5 times the maximum speed in the 10 minutes preceding the start of the rise. This second requirement was added in order to rule out short lulls in an otherwise high speed wind.

The time of onset of the squall was defined as the start of that two minute period during which the greatest increase in wind speed occurred. The minimum wind speed in the 15 minutes preceding onset and the maximum in the 15 minutes following onset were recorded.

A "*partial squall*" was defined similarly to a full squall except that a rise of at least 5 m/s to at least 7·5 m/s was required. The extra conditions (a) and (b) remained in force.

Time in minutes
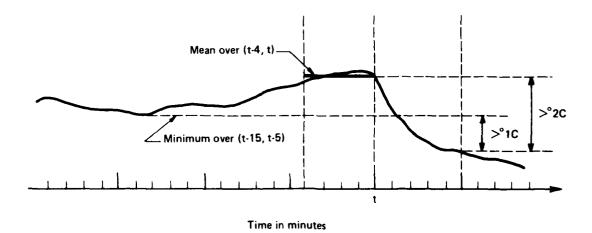
Fig. 70 Conditions defining a significant temperature drop.

APPENDIX 2

Data for Annual Maximum Wind Speeds

Whittingham (1964) lists the annual maximum wind speeds at various places in Australia from 1937 to 1962. Since then further data have accrued in Bureau of Meteorology records. The relevant data, extracted for the Brisbane area, follow, with parentheses denoting incomplete data, i.e. less than 360 days data for the relevant year.

Annual maximum wind speeds (in knots) in the Brisbane area

Station Ht anm. Year	Amberley 10 m	Archerfield Unknown	Eagle Farm 13 m	Brisbane 30 m
1938	—	—	—	43
1939	—	(46)	—	46
1940	—	49	—	58
1941	—	(55)	—	54
1942	—	(47)	—	46
1943	—	(66)	—	48
1944	(43)	(59)	—	44
1945	(47)	43	—	49
1946	—	77	—	69
1947	—	41	—	48
1948	—	52	—	49
1949	—	(51)	—	50
1950	—	—	—	56
1951	—	—	(53)	43
1952	—	—	51	44
1953	—	—	42	46
1954	—	—	58	58
1955	(50)	—	53	55
1956	44	—	49	56
1957	73	—	56	57
1958	68	—	58	51
1959	48	—	45	55
1960	41	—	45	39
1961	39	—	38	44
1962	82	—	49	60
1963	55	—	52	—
1964	(66)	—	46	—
1965	50	—	64	—
1966	76	—	49	—
1967	50	—	(42)	—
1968	45	—	48	—
1969	(48)	—	60	—
1970	52	—	75	—
1971	44	—	50	—
1972	(50)	—	49	—
1973	51	—	(57)	—
1974	(42)	—	49	—
1975	47	—	42	—
1976	51	—	54	—
1977	(37)	—	(42)	—

APPENDIX 3

Appendix 3 consists only of figures. There are six figures to describe each one-hour period of each incident. For the nth incident these figures are numbered $A.nA$, $A.nB$, . . ., $A.nF$, where:

$A.nA$ shows a selection of parameters,

$A.nB$ shows vertical velocity at various elevations,

$A.nC$ shows horizontal wind speed at various elevations,

$A.nD$ shows wind shear in the vertical,

$A nE$ shows wind speeds in the horizontal anemometer array, and

$A.nF$ shows wind shear in the horizontal direction.
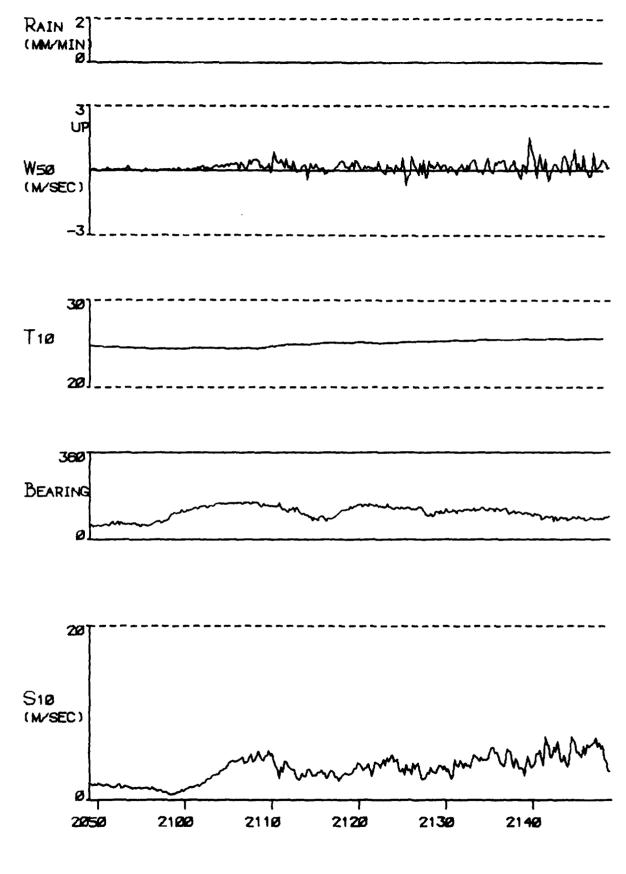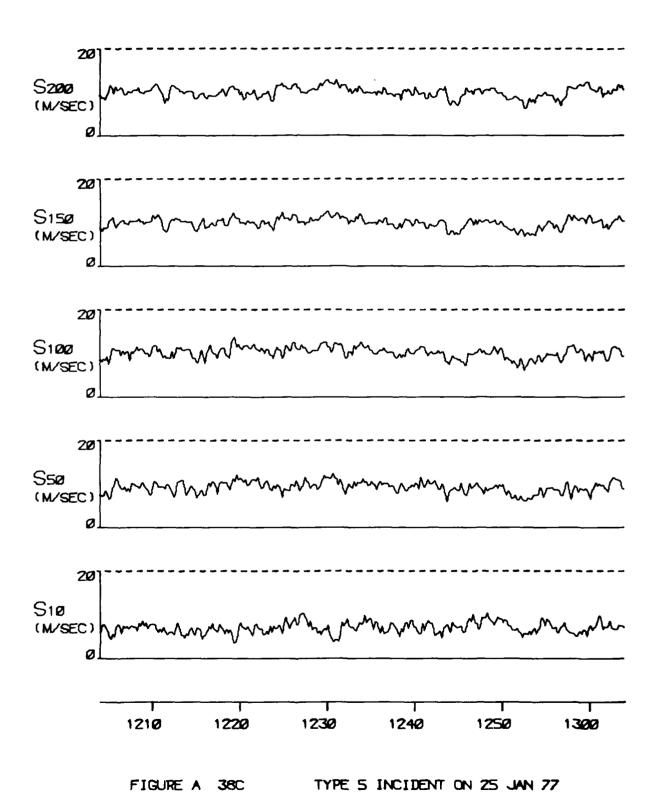
FIGURE A 1A   TYPE 3 INCIDENT ON 12 NOV 76
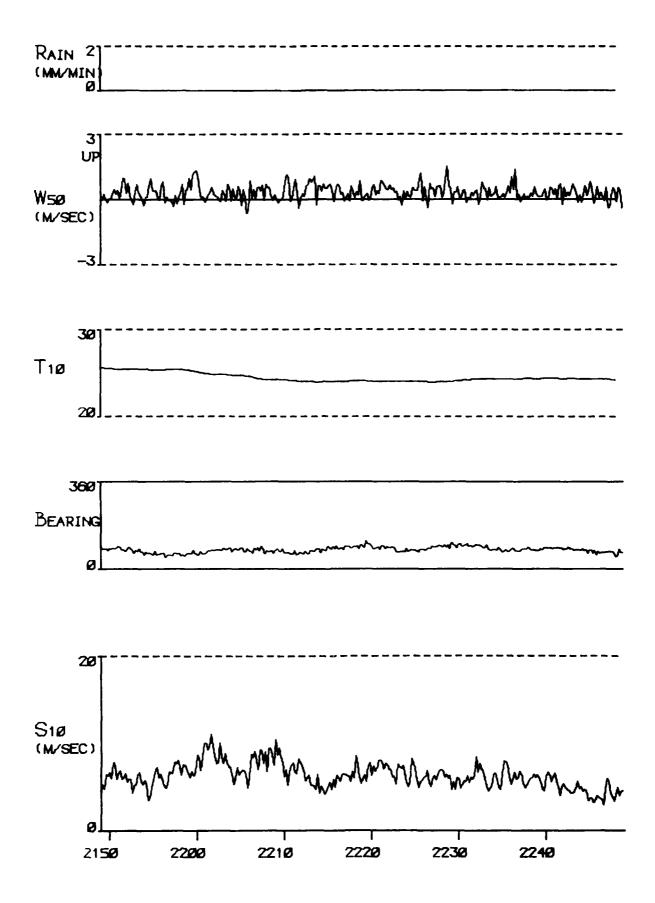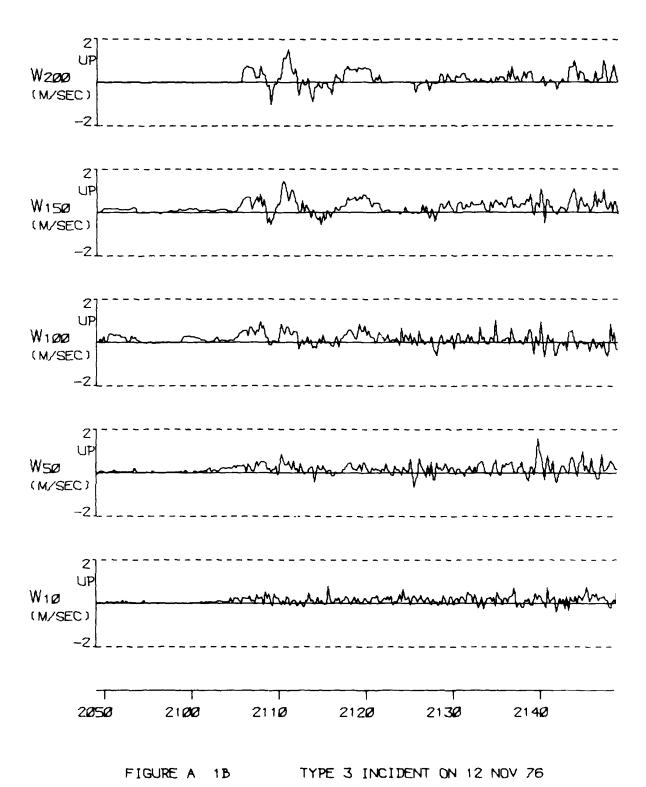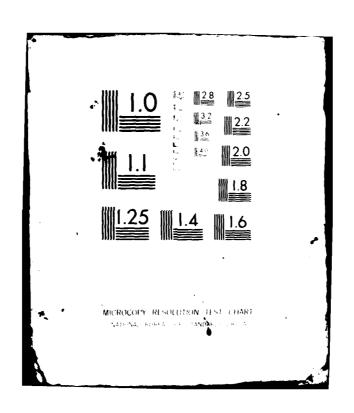
FIGURE A 1A (CONT) TYPE 3 INCIDENT ON 12 NOV 76

FIGURE A   1B   TYPE 3 INCIDENT ON 12 NOV 76

1.0

1.1

1.25 1.4 1.6

2.8 2.5
3.2 2.2
3.6
4.0 2.0

1.8

MICROCOPY RESOLUTION TEST CHART
NATIONAL BUREAU OF STANDARDS
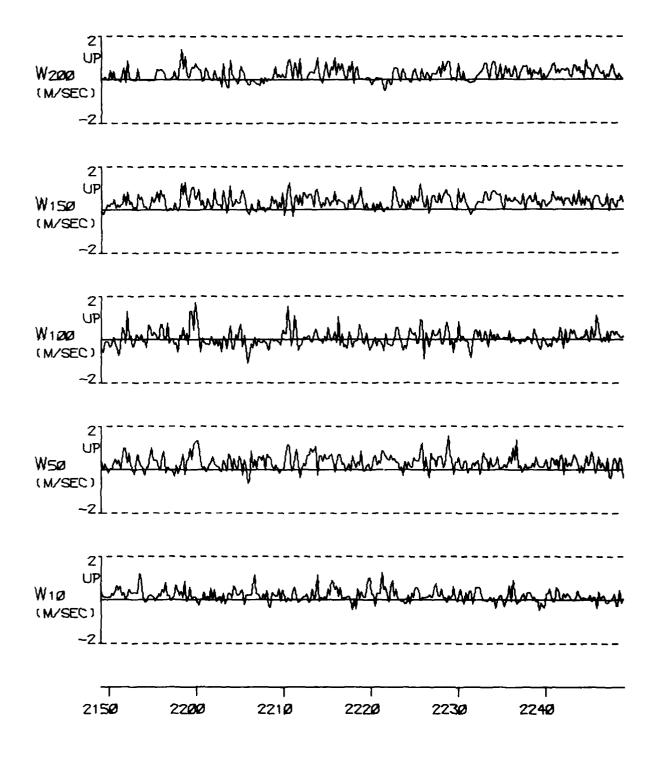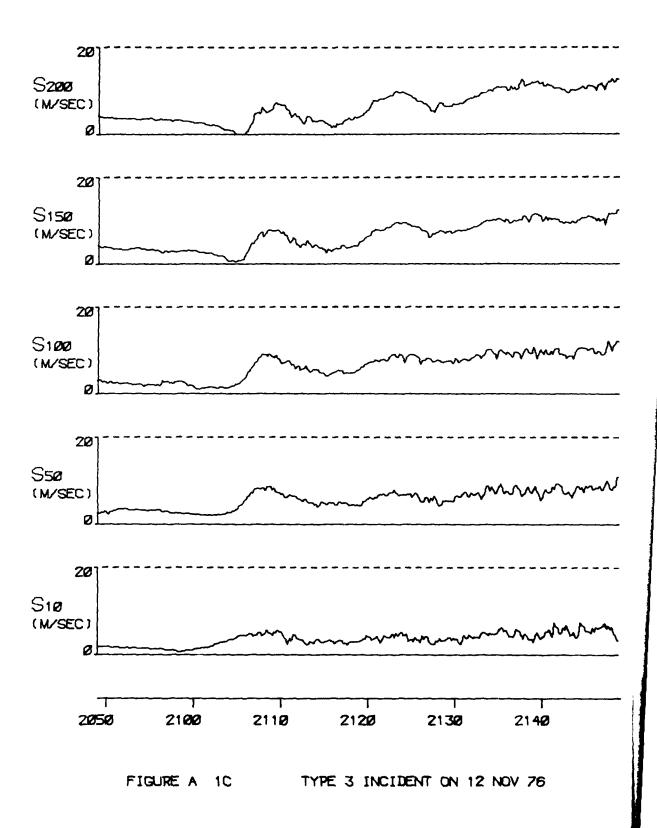
FIGURE A   1B (CONT) TYPE 3 INCIDENT ON 12 NOV 76

FIGURE A   1C   TYPE 3 INCIDENT ON 12 NOV 76
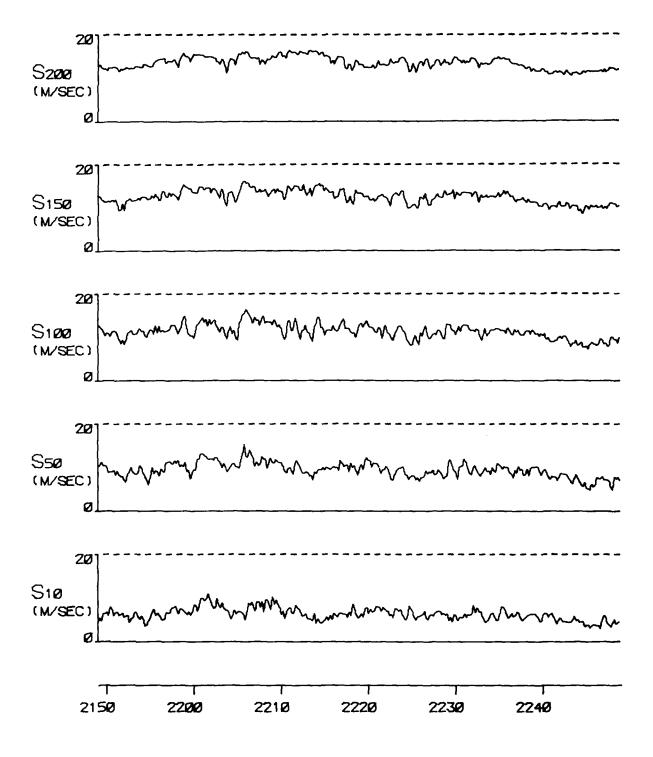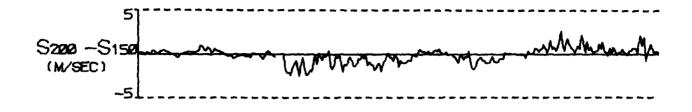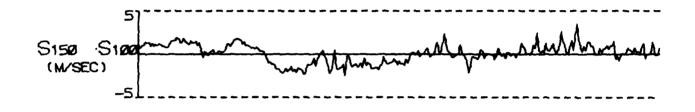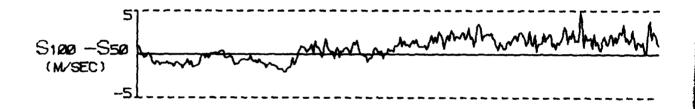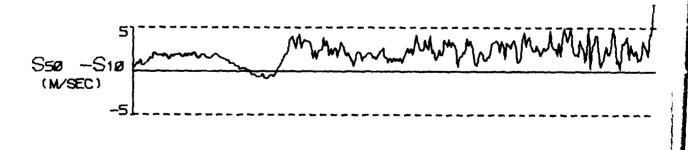
FIGURE A 1C (CONT) TYPE 3 INCIDENT ON 12 NOV 76
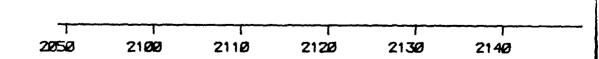
FIGURE A 1D   TYPE 3 INCIDENT ON 12 NOV 76
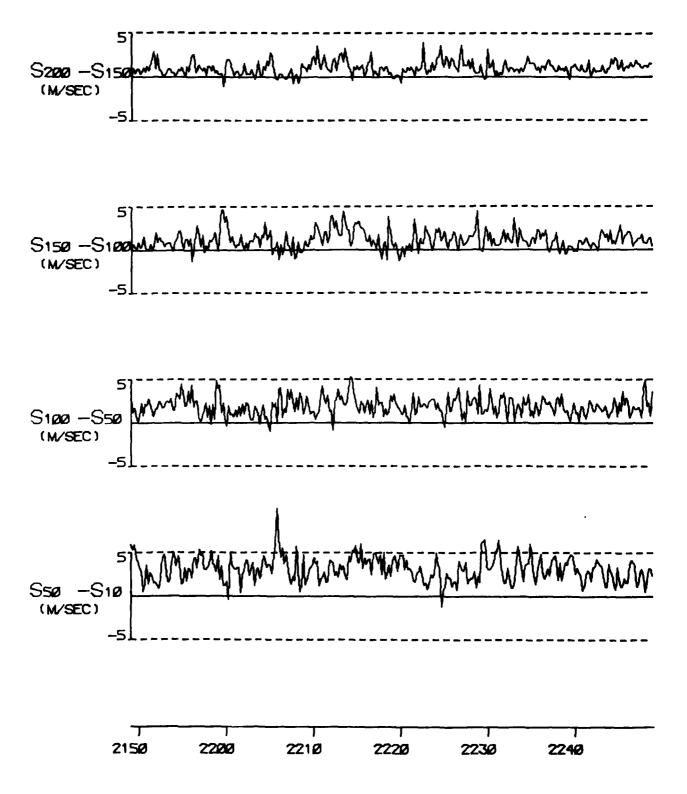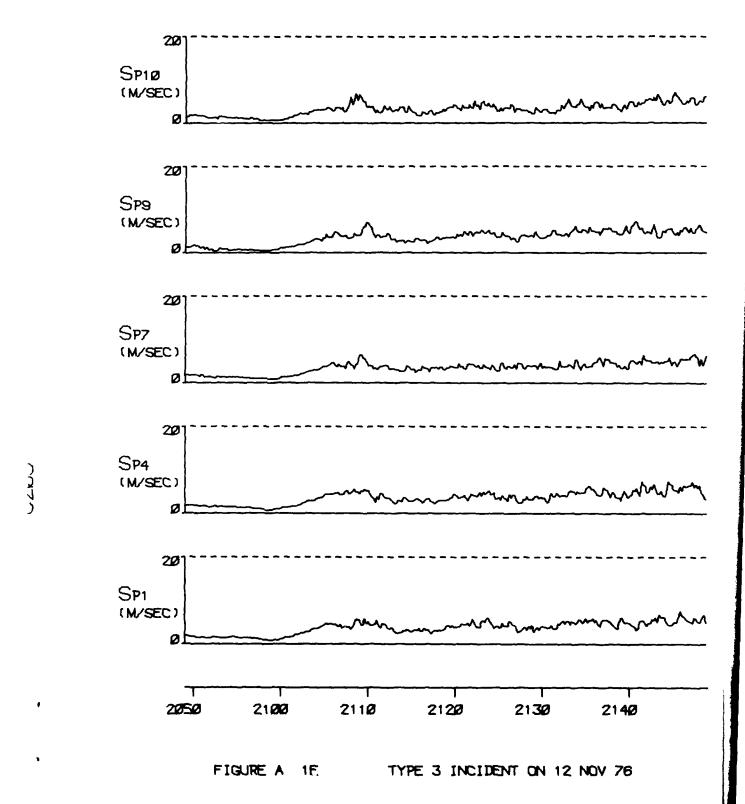
FIGURE A 1D (CONT) TYPE 3 INCIDENT ON 12 NOV 76

FIGURE A 1F. TYPE 3 INCIDENT ON 12 NOV 76
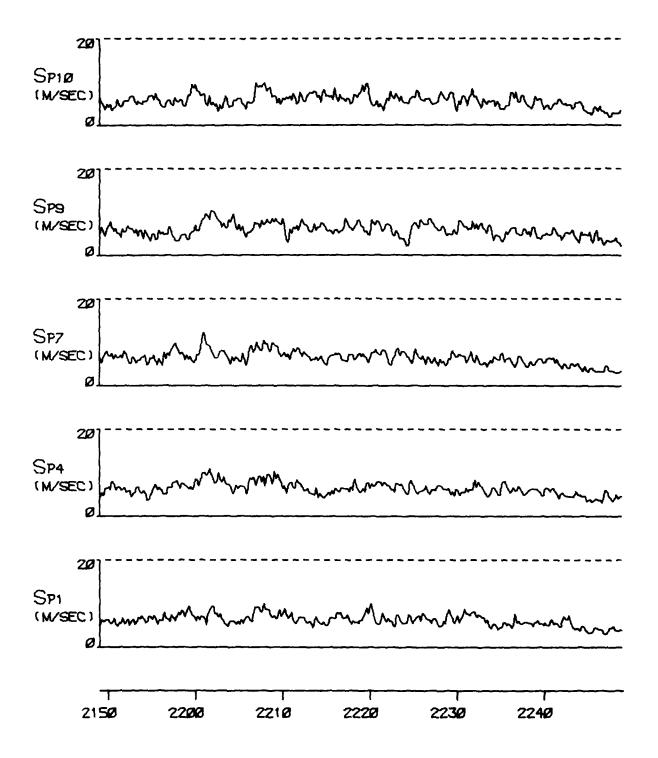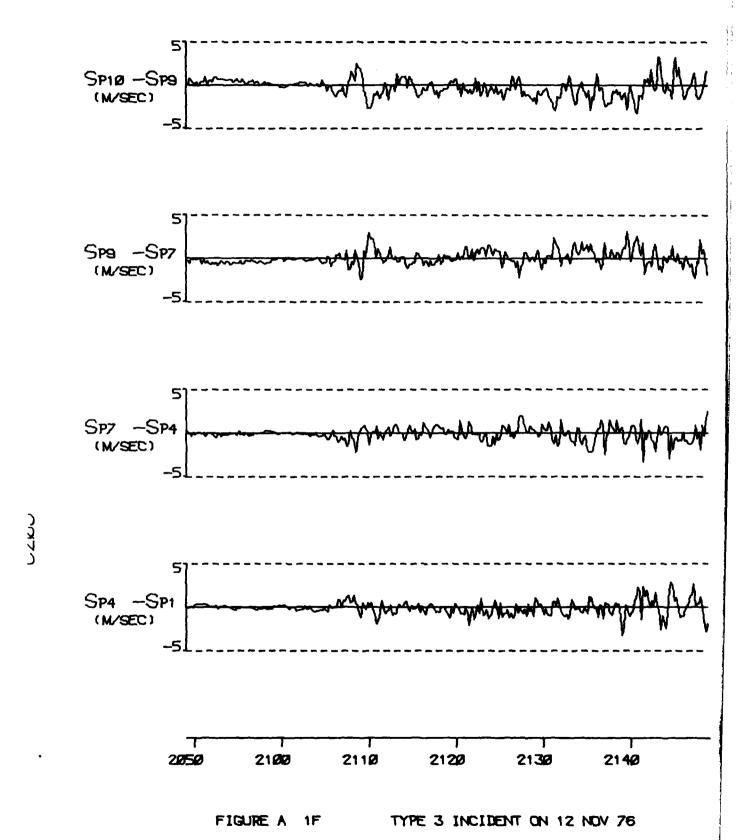
FIGURE A   1E (CONT) TYPE 3 INCIDENT ON 12 NOV 76

SP10 – SP9
(M/SEC)

SP9 – SP7
(M/SEC)

SP7 – SP4
(M/SEC)

SP4 – SP1
(M/SEC)

2050   2100   2110   2120   2130   2140
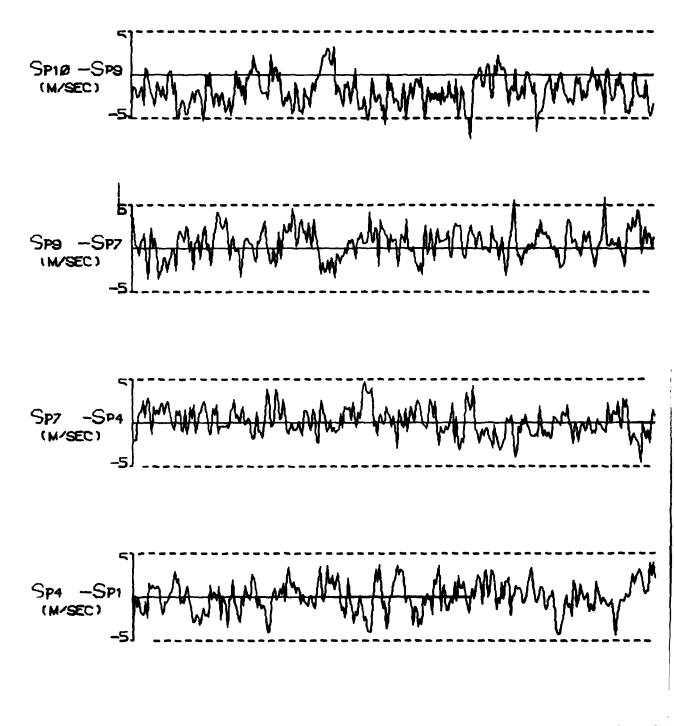
FIGURE A   1F   TYPE 3 INCIDENT ON 12 NOV 76
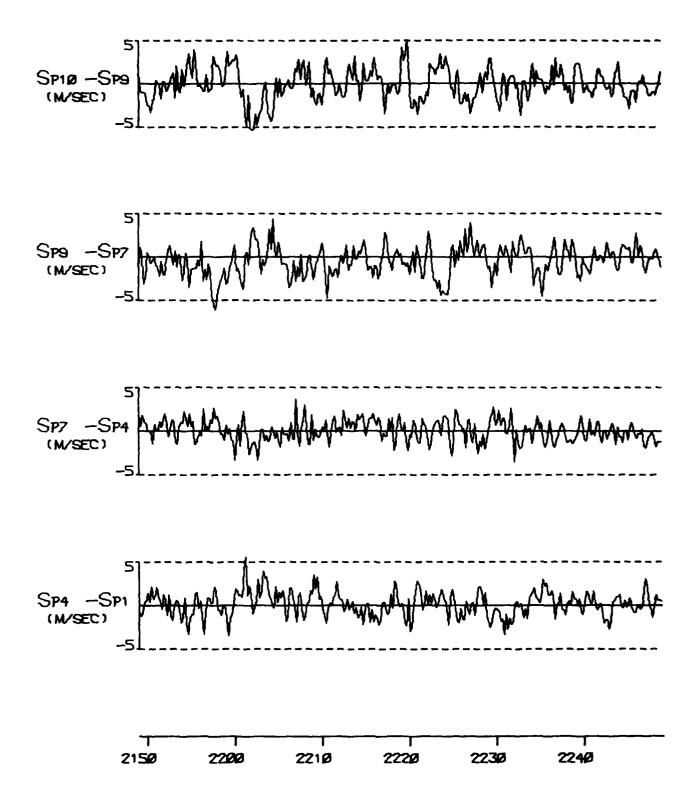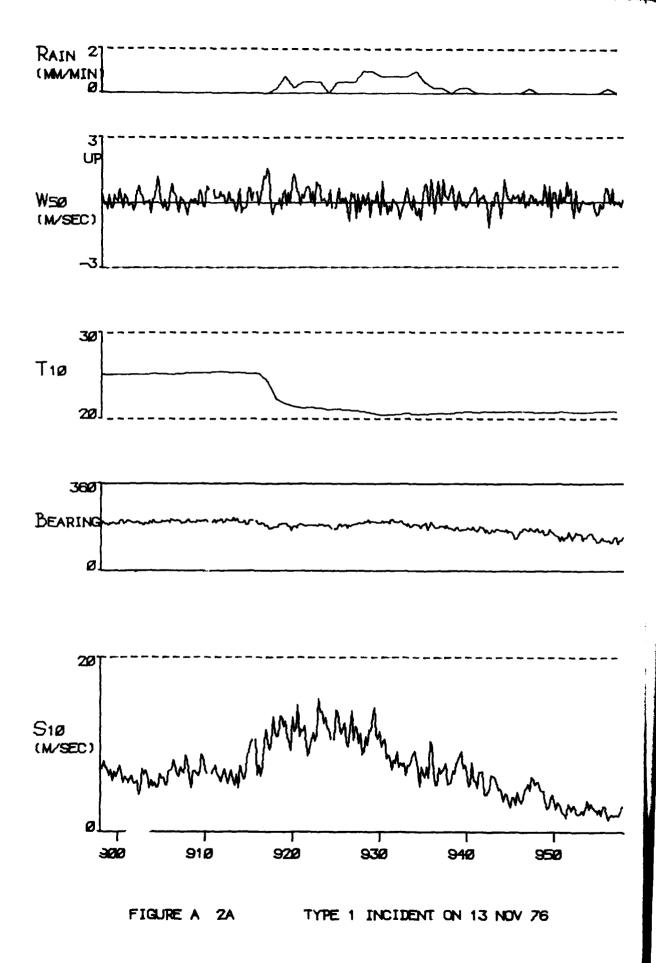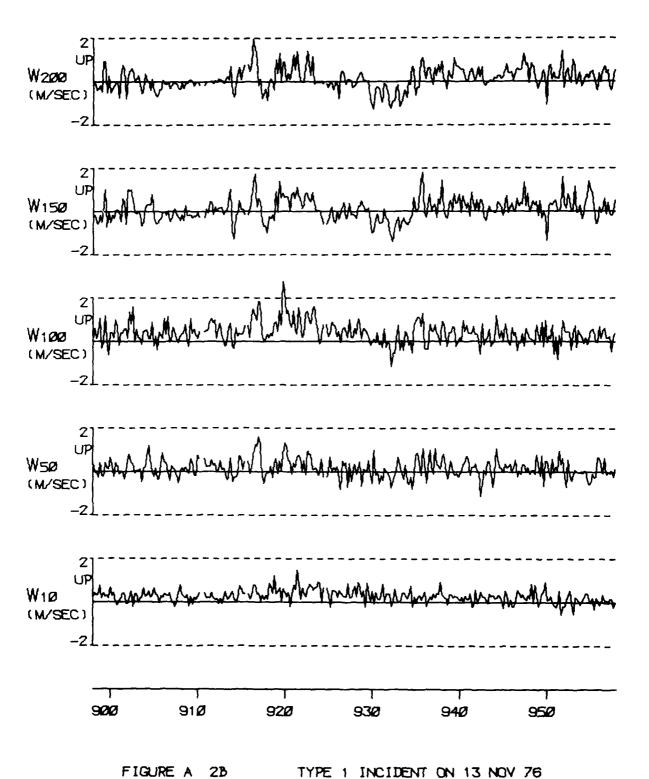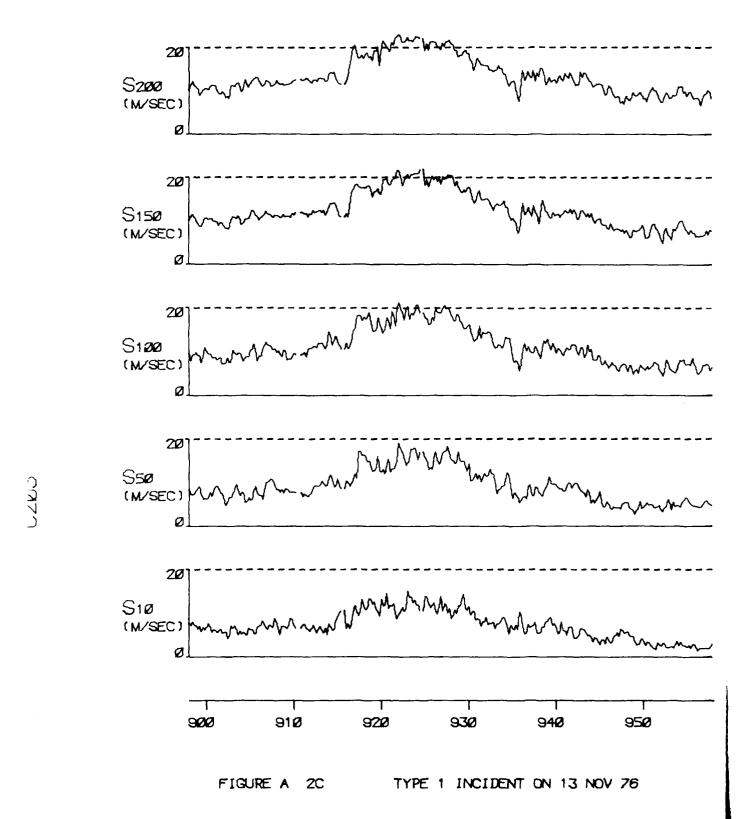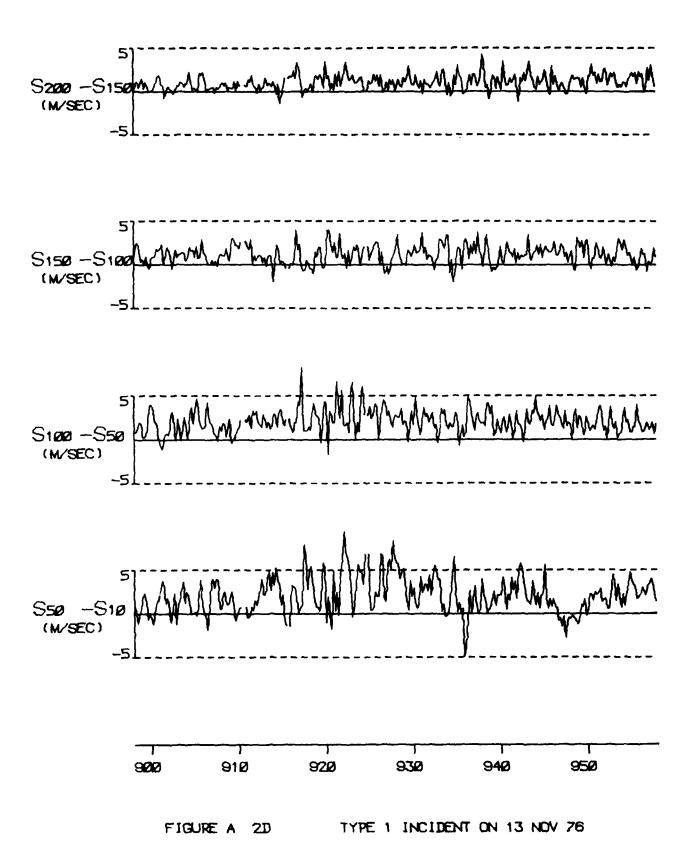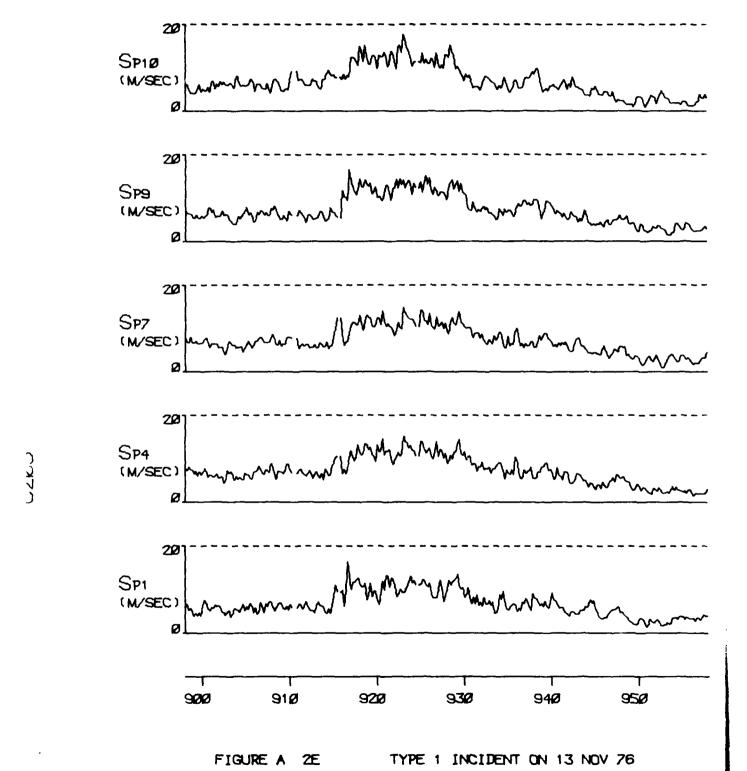
FIGURE A   1F (CONT) TYPE 3 INCIDENT ON 12 NOV 76

FIGURE A 2A   TYPE 1 INCIDENT ON 13 NOV 76

FIGURE A 2B   TYPE 1 INCIDENT ON 13 NOV 76

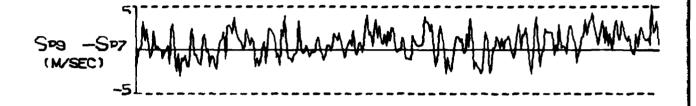FIGURE A 2C   TYPE 1 INCIDENT ON 13 NOV 76

S200 −S150
(M/SEC)

S150 −S100
(M/SEC)

S100 −S50
(M/SEC)

S50 −S10
(M/SEC)

900   910   920   930   940   950

FIGURE A 2D   TYPE 1 INCIDENT ON 13 NOV 76

FIGURE A 2E   TYPE 1 INCIDENT ON 13 NOV 76
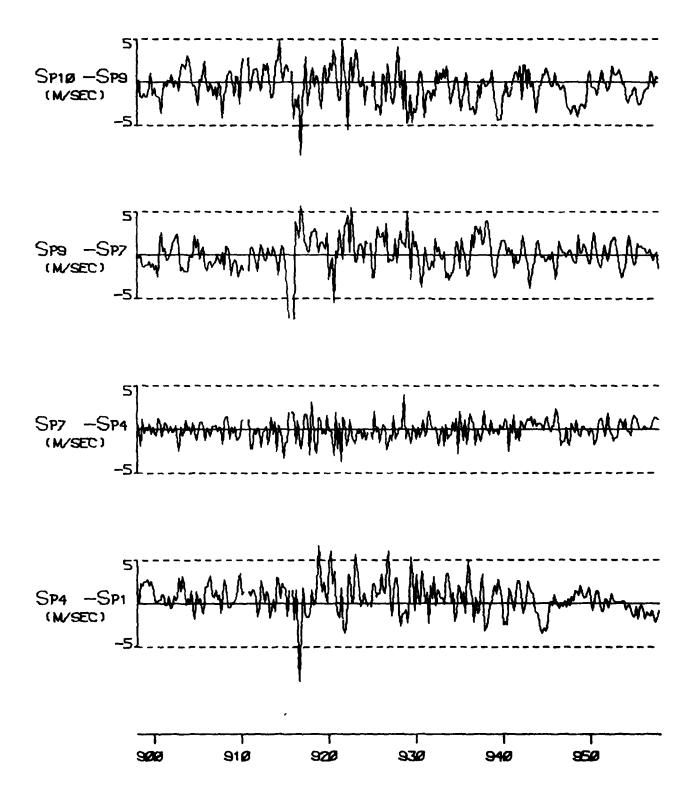
FIGURE A 2F   TYPE 1 INCIDENT ON 13 NOV 76
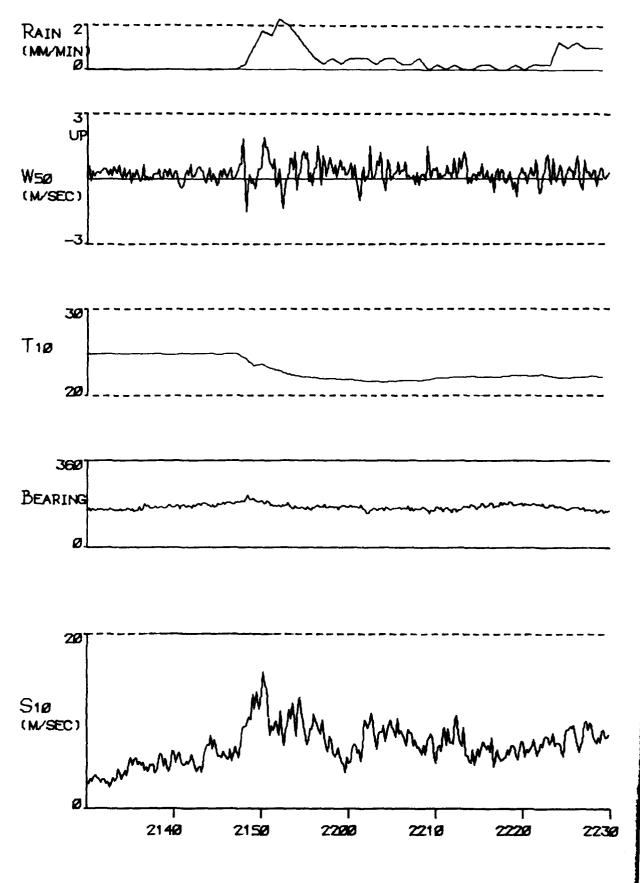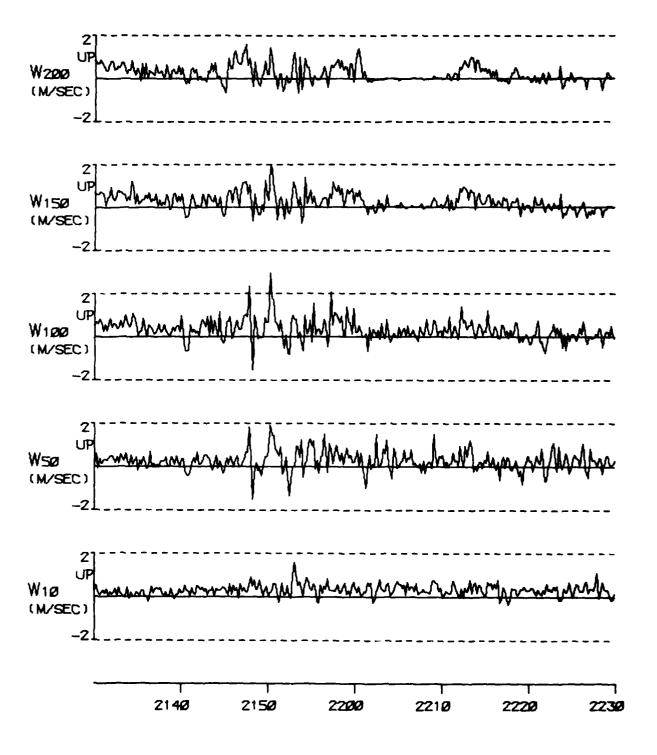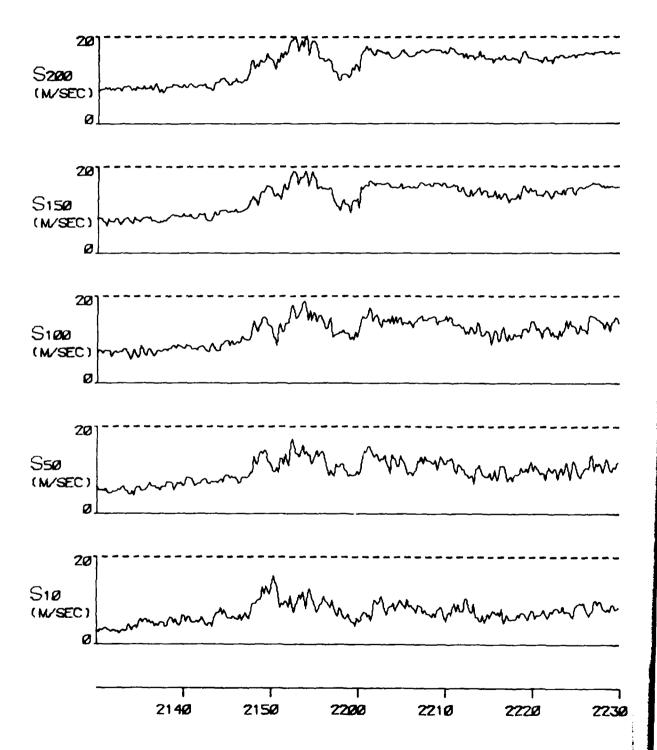
FIGURE A 3A   TYPE 1 INCIDENT ON 13 NOV 76

FIGURE A 3B   TYPE : INCIDENT ON 13 NOV 76
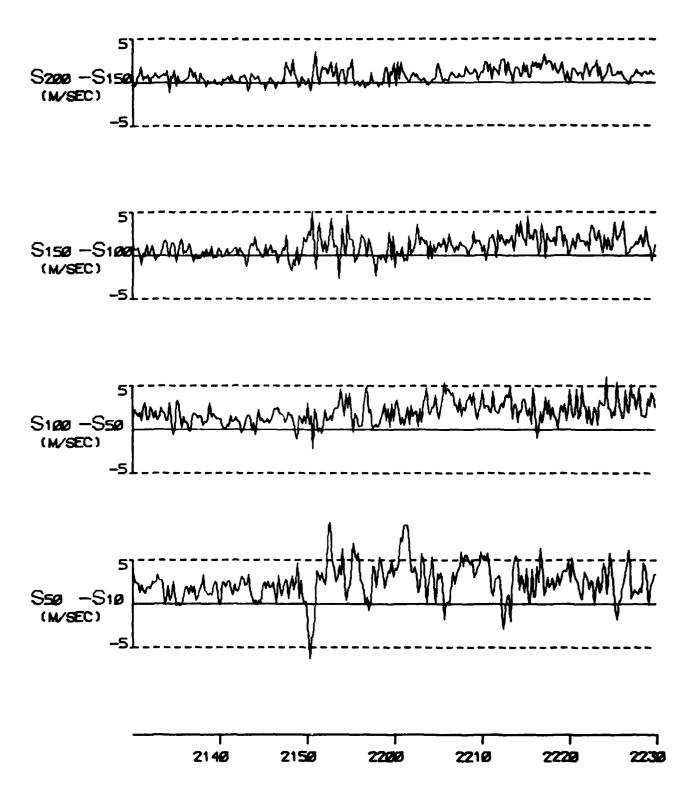
FIGURE A 3C   TYPE 1 INCIDENT ON 13 NOV 76

FIGURE A 3D   TYPE 1 INCIDENT ON 13 NOV 76

FIGURE A 3E   TYPE 1 INCIDENT ON 13 NOV 76

FIGURE A 3F   TYPE 1 INCIDENT ON 13 NOV 76

FIGURE A 4A   TYPE 3 INCIDENT ON 14 NOV 76

FIGURE A 4B   TYPE 3 INCIDENT ON 14 NOV 76

FIGURE A 4C   TYPE 3 INCIDENT ON 14 NOV 76

FIGURE A   4D   TYPE 3 INCIDENT ON 14 NOV 76
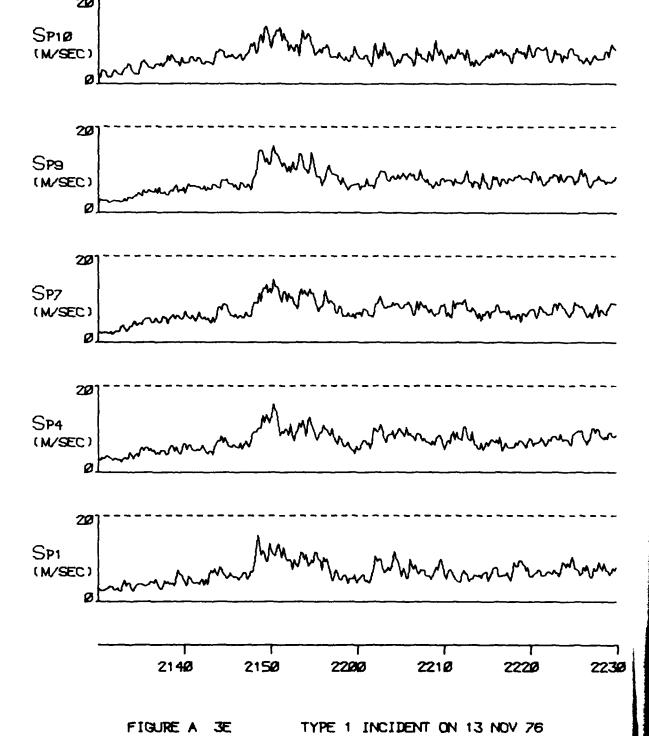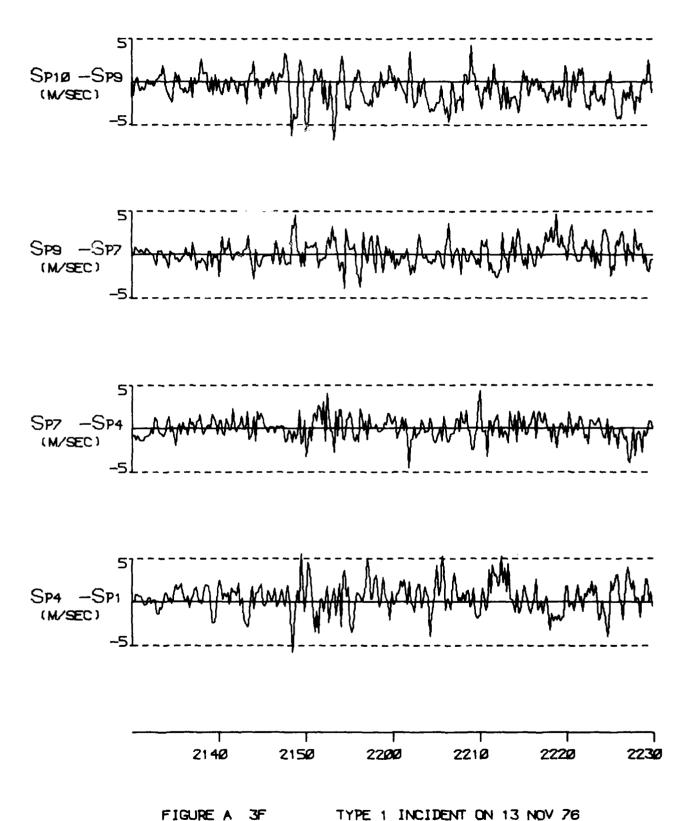
FIGURE A 4E   TYPE 3 INCIDENT ON 14 NOV 76
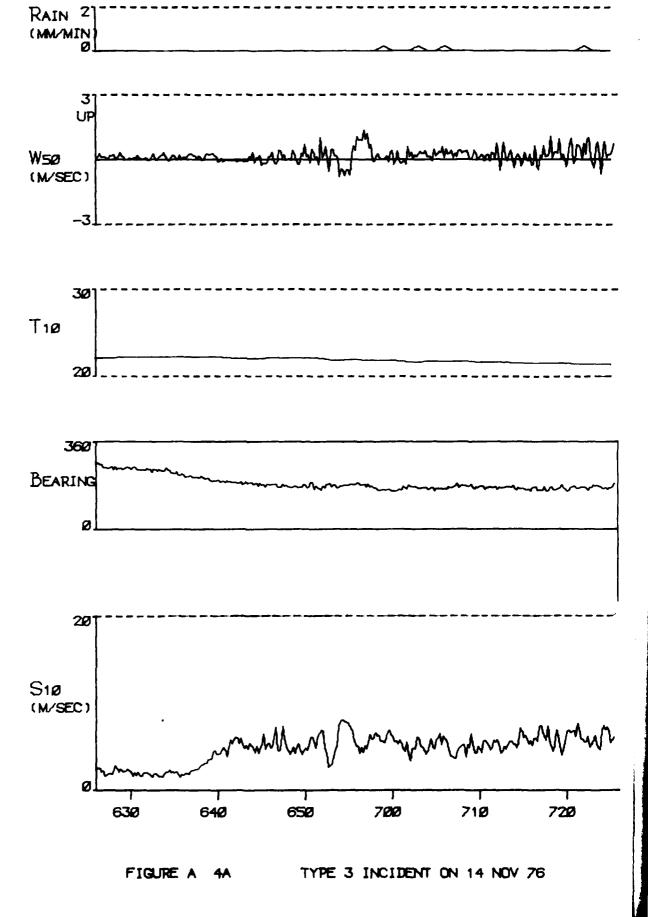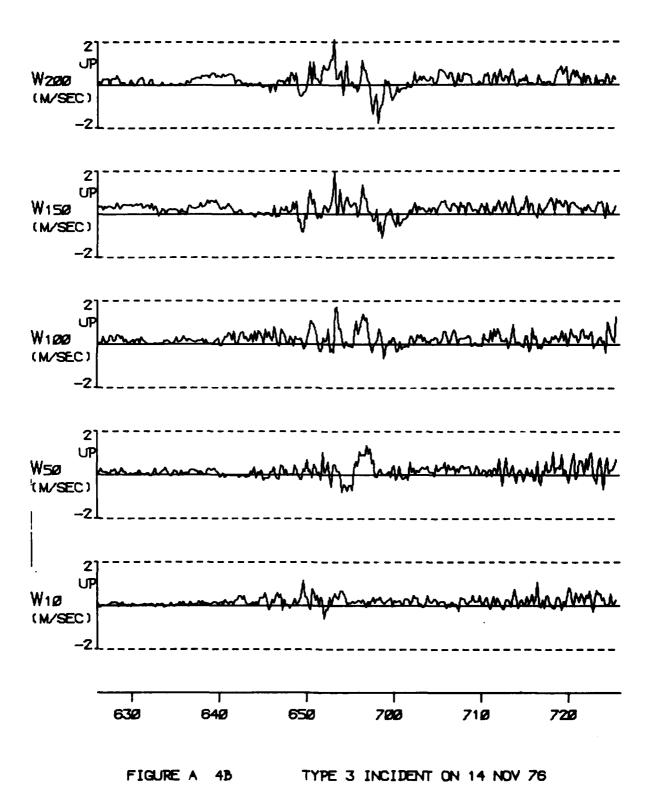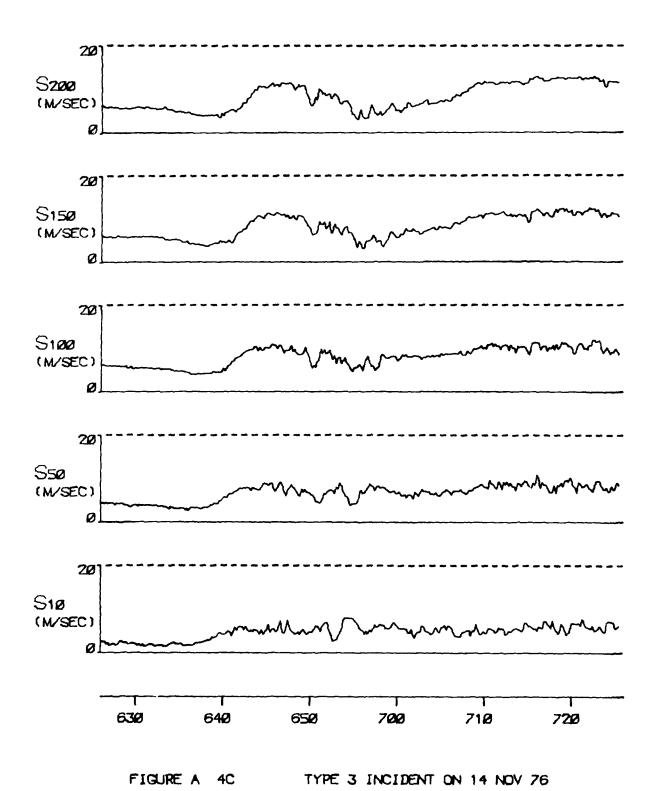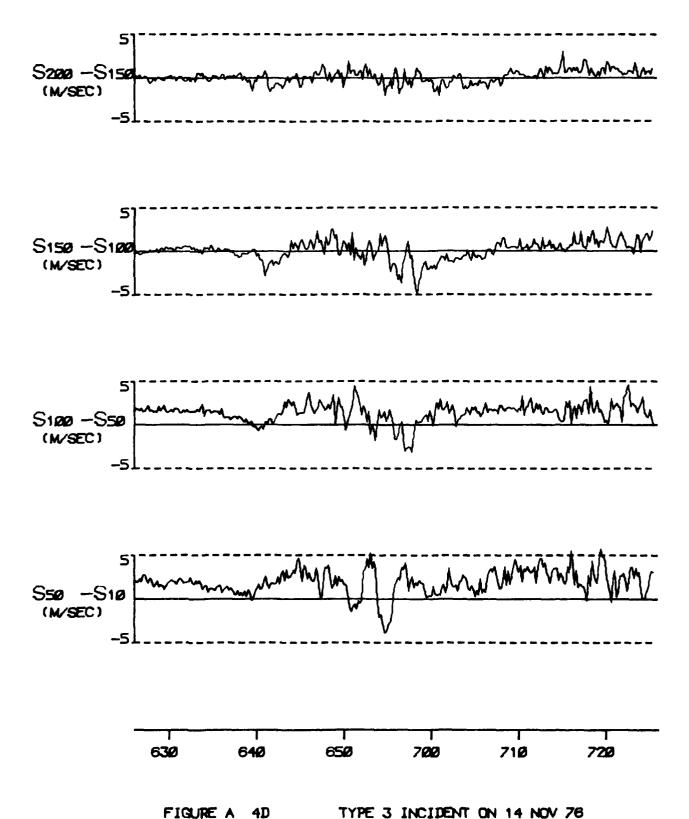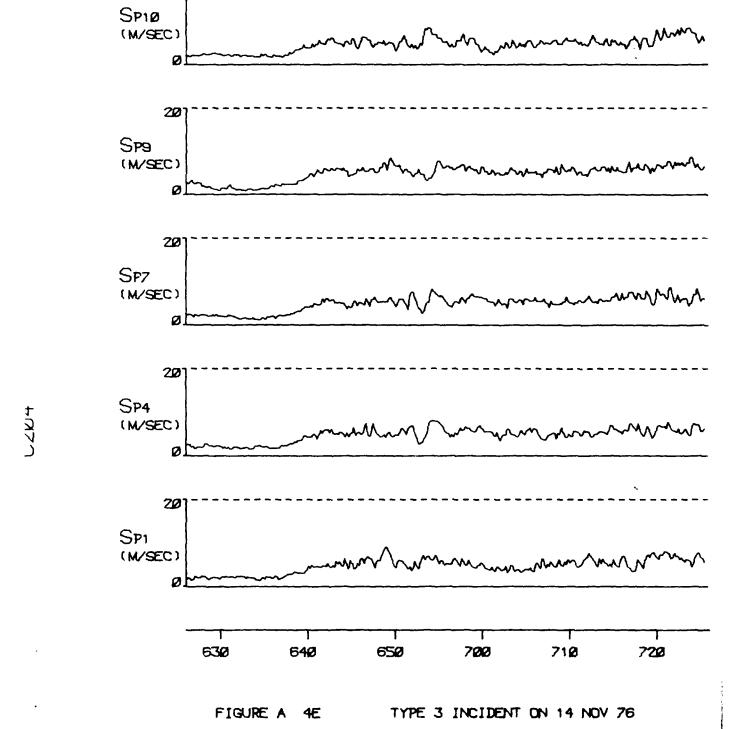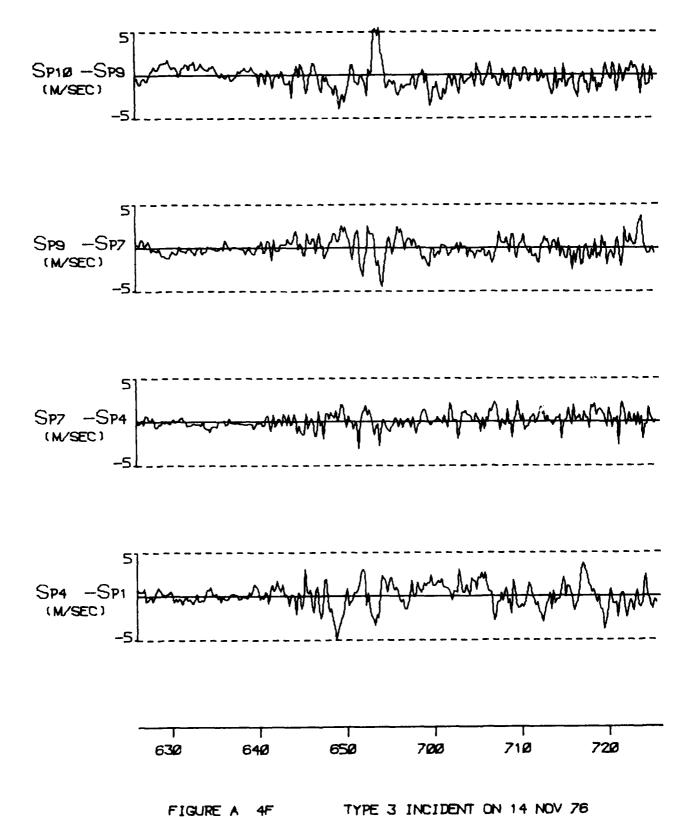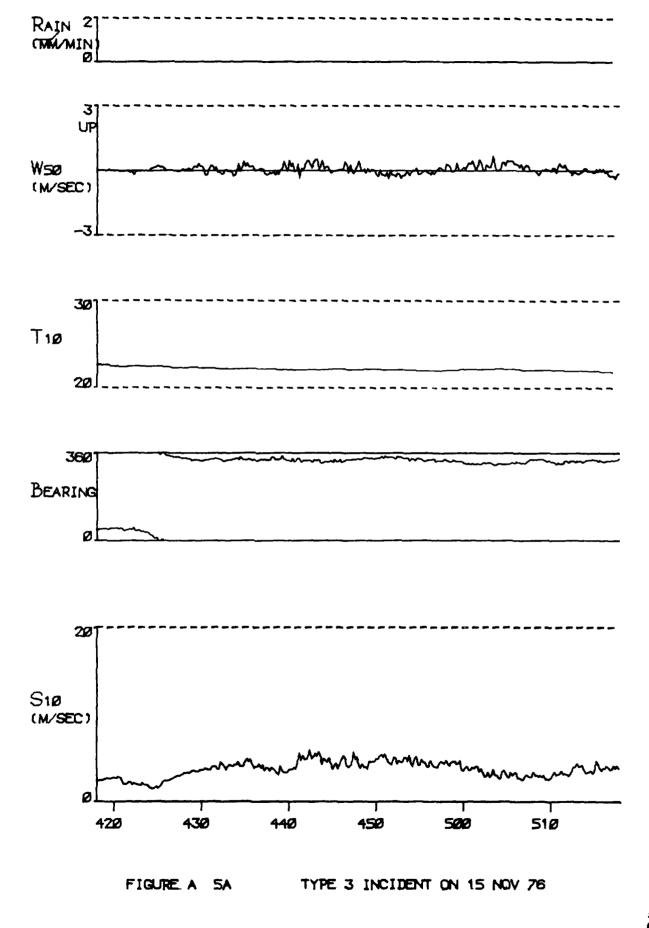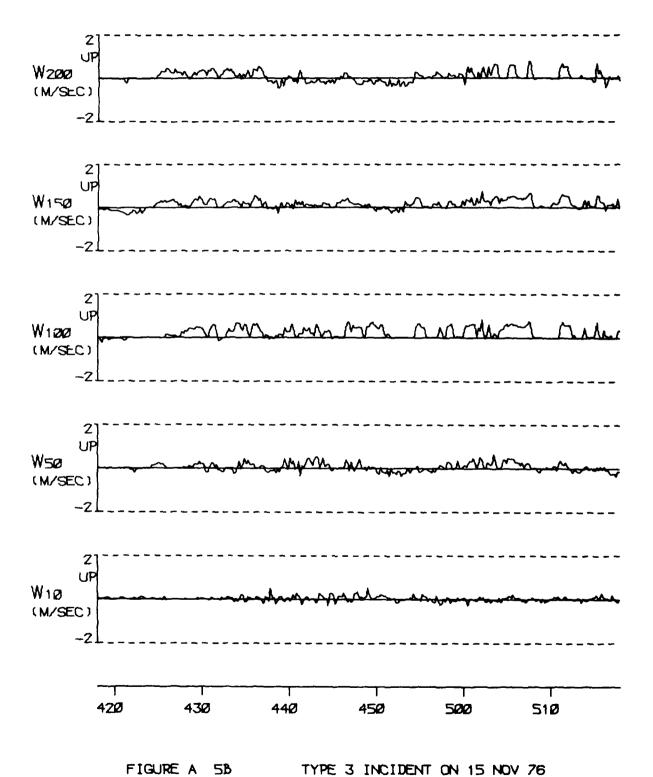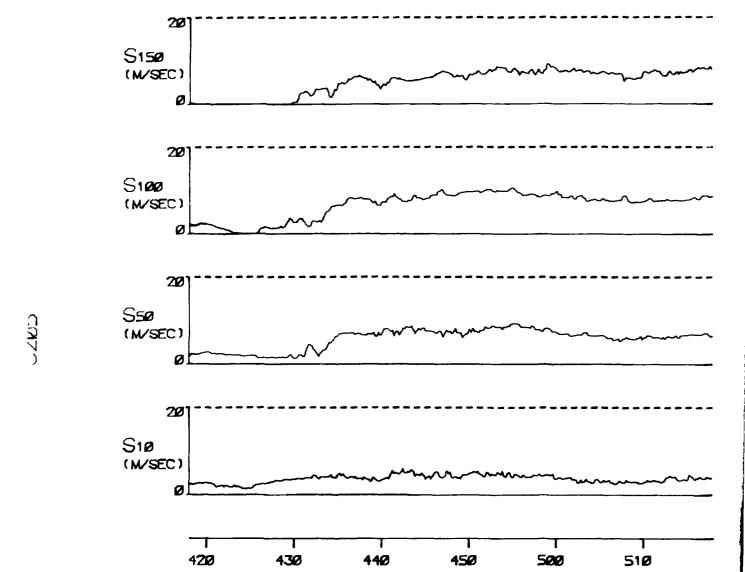
FIGURE A 4F   TYPE 3 INCIDENT ON 14 NOV 76

FIGURE A 5A   TYPE 3 INCIDENT ON 15 NOV 76

FIGURE A 5B   TYPE 3 INCIDENT ON 15 NOV 76

FIGURE A 5C   TYPE 3 INCIDENT ON 15 NOV 76

FIGURE A 5D   TYPE 3 INCIDENT ON 15 NOV 76

FIGURE A 5E   TYPE 3 INCIDENT ON 15 NOV 76
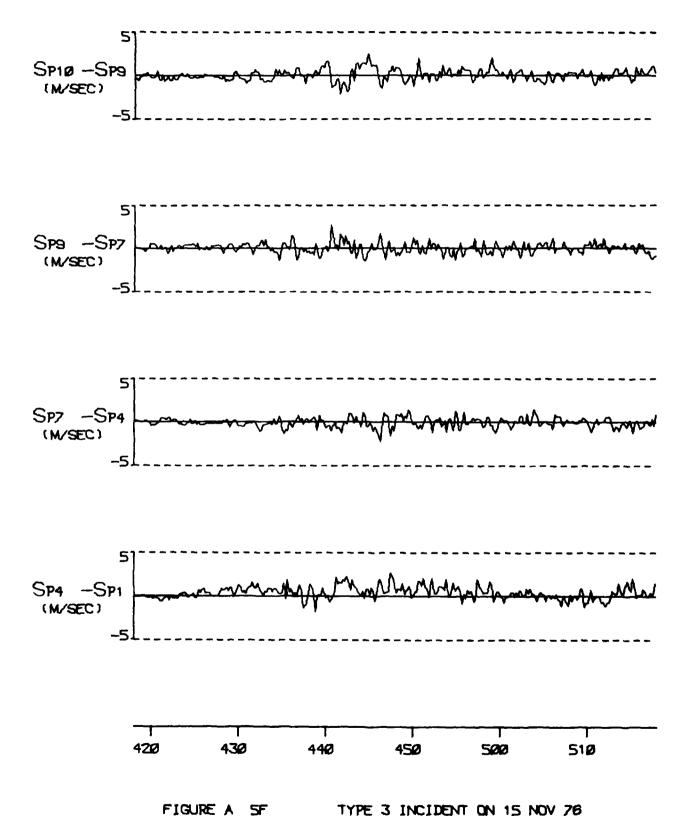
FIGURE A   SF   TYPE 3 INCIDENT ON 15 NOV 76
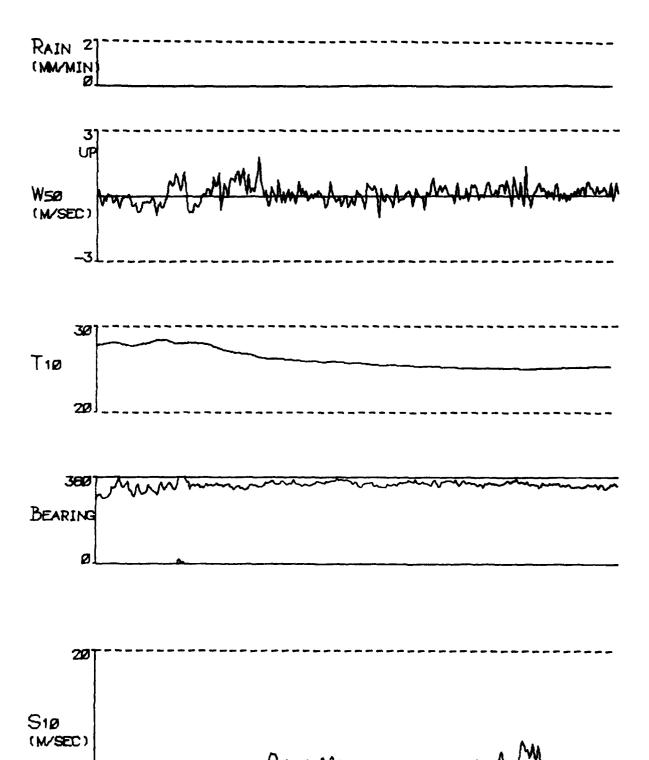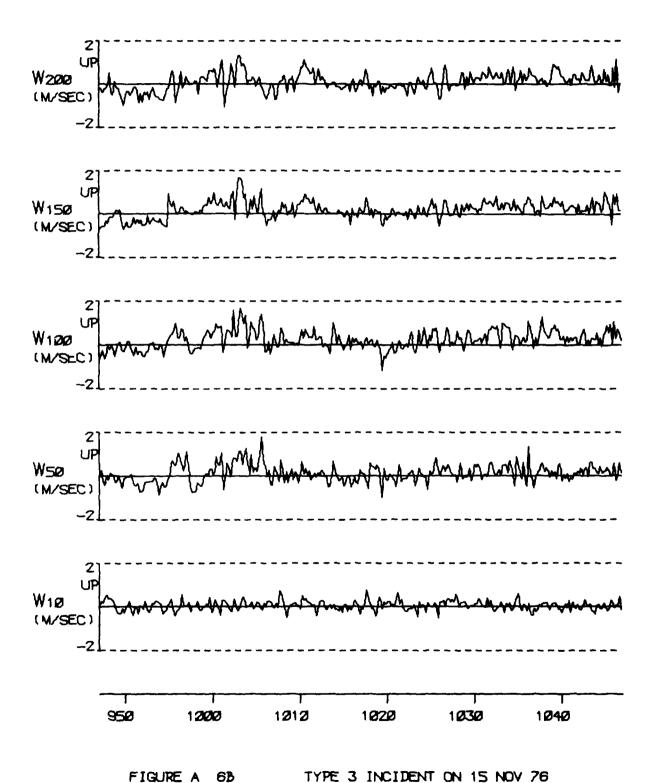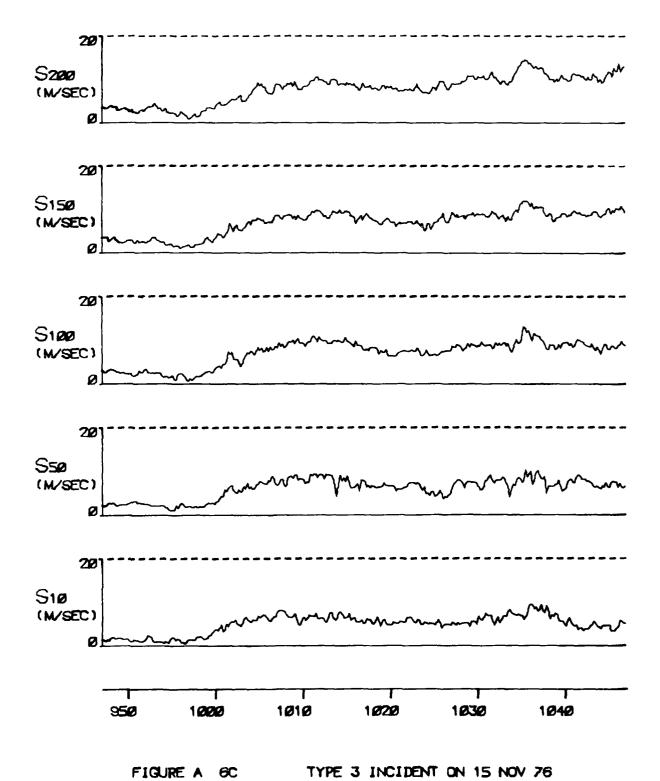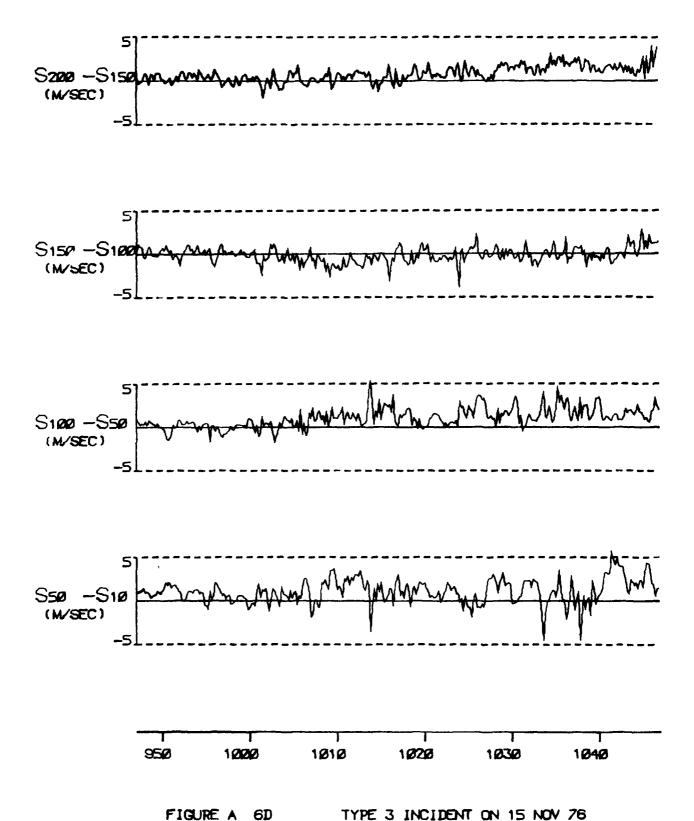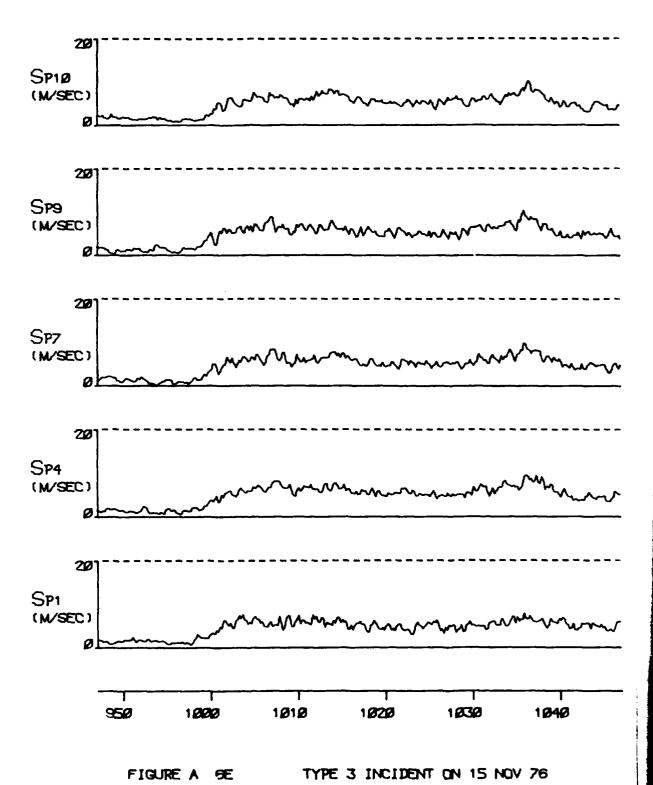
FIGURE A 6A   TYPE 3 INCIDENT ON 15 NOV 76

FIGURE A 6B   TYPE 3 INCIDENT ON 15 NOV 76

FIGURE A 6C   TYPE 3 INCIDENT ON 15 NOV 76

FIGURE A 6D   TYPE 3 INCIDENT ON 15 NOV 76

FIGURE A 6E   TYPE 3 INCIDENT ON 15 NOV 76

FIGURE A 6F   TYPE 3 INCIDENT ON 15 NOV 76

FIGURE A 7A   TYPE 3 INCIDENT ON 15 NOV 76

FIGURE A 7B   TYPE 3 INCIDENT ON 15 NOV 76

FIGURE A 7C   TYPE 3 INCIDENT ON 15 NOV 76

FIGURE A 7D   TYPE 3 INCIDENT ON 15 NOV 76

FIGURE A 7E   TYPE 3 INCIDENT ON 15 NOV 76

FIGURE A 7F   TYPE 3 INCIDENT ON 15 NOV 76

FIGURE A 8A   TYPE 4 INCIDENT ON 15 NOV 76

FIGURE A 8A (CONT) TYPE 4 INCIDENT ON 15 NOV 78

FIGURE A 8A (CONT) TYPE 4 INCIDENT ON 15 NOV 76

FIGURE A 8A (CONT) TYPE 4 INCIDENT ON 15 NOV 76

FIGURE A 8A (CONT) TYPE 4 INCIDENT ON 15 NOV 76

FIGURE A 6B   TYPE 4 INCIDENT ON 15 NOV 76

FIGURE A 6B (CONT) TYPE 4 INCIDENT ON 15 NOV 76

FIGURE A 6B (CONT) TYPE 4 INCIDENT ON 15 NOV 76

FIGURE A 6B (CONT) TYPE 4 INCIDENT ON 15 NOV 76

FIGURE A 8B (CONT) TYPE 4 INCIDENT ON 15 NOV 76

FIGURE A 8C   TYPE 4 INCIDENT ON 15 NOV 76

FIGURE A 8C (CONT) TYPE 4 INCIDENT ON 15 NOV 76

FIGURE A 6C (CONT) TYPE 4 INCIDENT ON 15 NOV 76

FIGURE A 8C (CONT) TYPE 4 INCIDENT ON 15 NOV 76

FIGURE A 6C (CONT) TYPE 4 INCIDENT ON 15 NOV 76

FIGURE A 8D   TYPE 4 INCIDENT ON 15 NOV 76
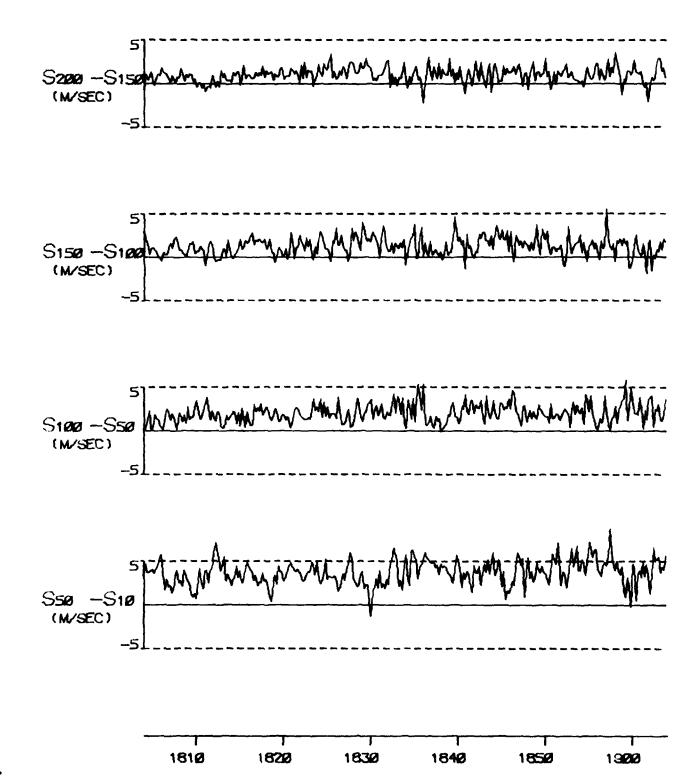
FIGURE A 8D (CONT) TYPE 4 INCIDENT ON 15 NOV 76
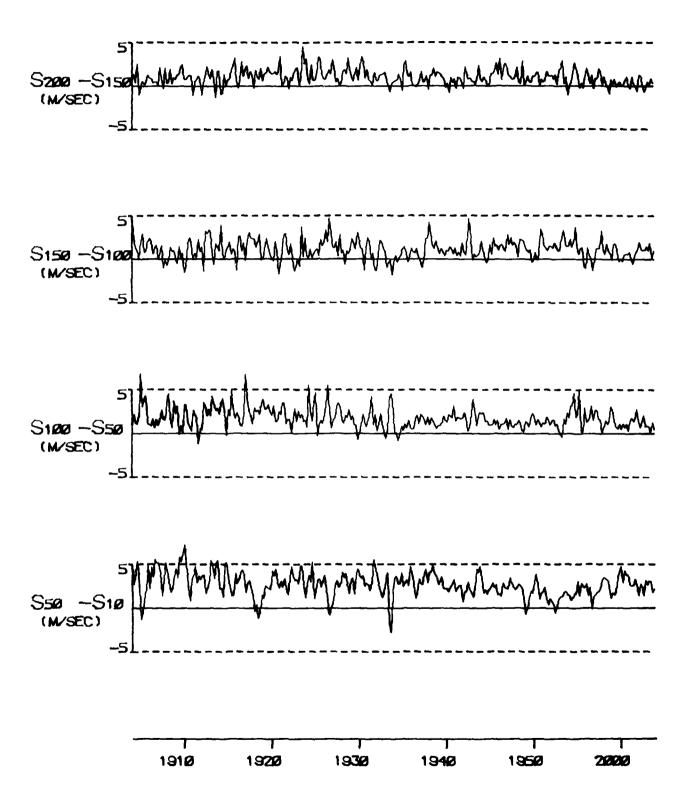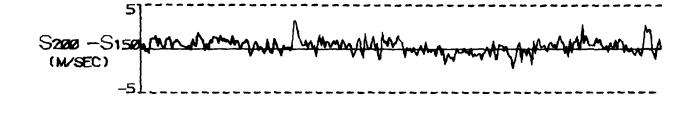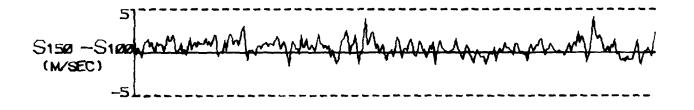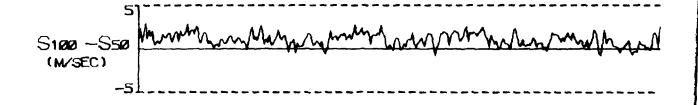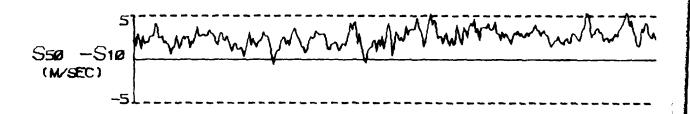
FIGURE A 8D (CONT) TYPE 4 INCIDENT ON 15 NOV 76

FIGURE A 8D (CONT) TYPE 4 INCIDENT ON 15 NOV 76

FIGURE A 6E   TYPE 4 INCIDENT ON 15 NOV 76

FIGURE A   6E (CONT) TYPE 4 INCIDENT ON 15 NOV 76

FIGURE A 6E (CONT) TYPE 4 INCIDENT ON 15 NOV 76

FIGURE A 6E (CONT) TYPE 4 INCIDENT ON 15 NOV 78

FIGURE A 6E (CONT) TYPE 4 INCIDENT ON 15 NOV 76

FIGURE A 6F   TYPE 4 INCIDENT ON 15 NOV 76

FIGURE A 8F (CONT) TYPE 4 INCIDENT ON 15 NOV 76

FIGURE A 6F (CONT) TYPE 4 INCIDENT ON 15 NOV 76

FIGURE A 6F (CONT) TYPE 4 INCIDENT ON 15 NOV 76

FIGURE A 6F (CONT) TYPE 4 INCIDENT ON 15 NOV 76

FIGURE A 9A   TYPE 4 INCIDENT ON 16 NOV 76

FIGURE A 9B   TYPE 4 INCIDENT ON 16 NOV 76

FIGURE A 9C   TYPE 4 INCIDENT ON 16 NOV 76

FIGURE A 9D   TYPE 4 INCIDENT ON 16 NOV 76
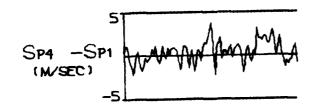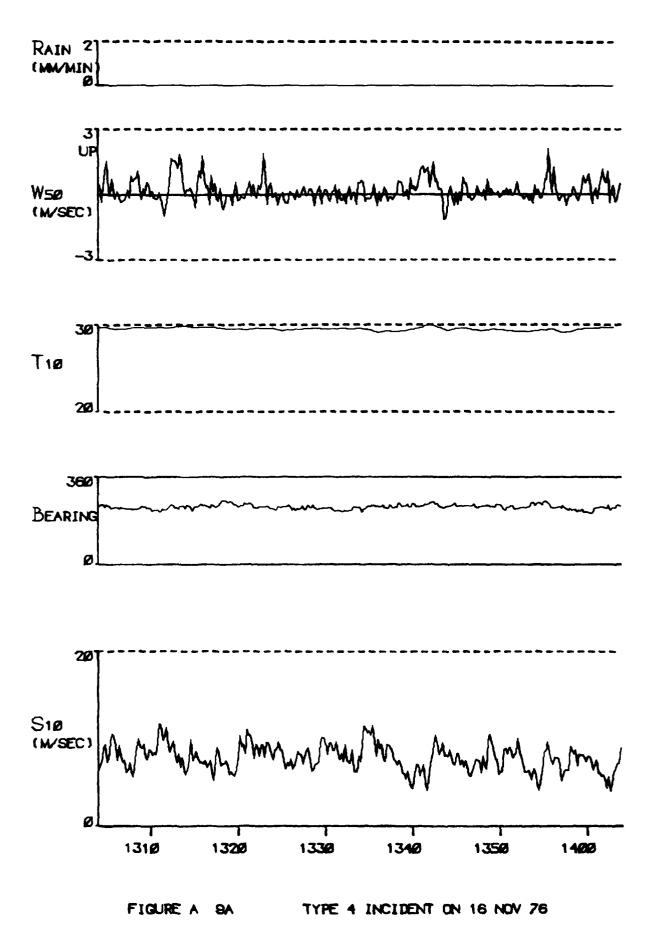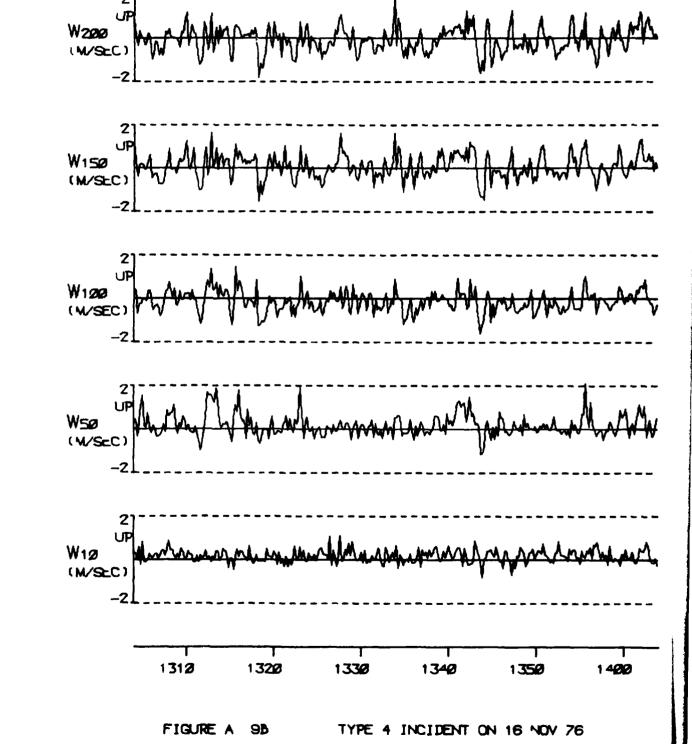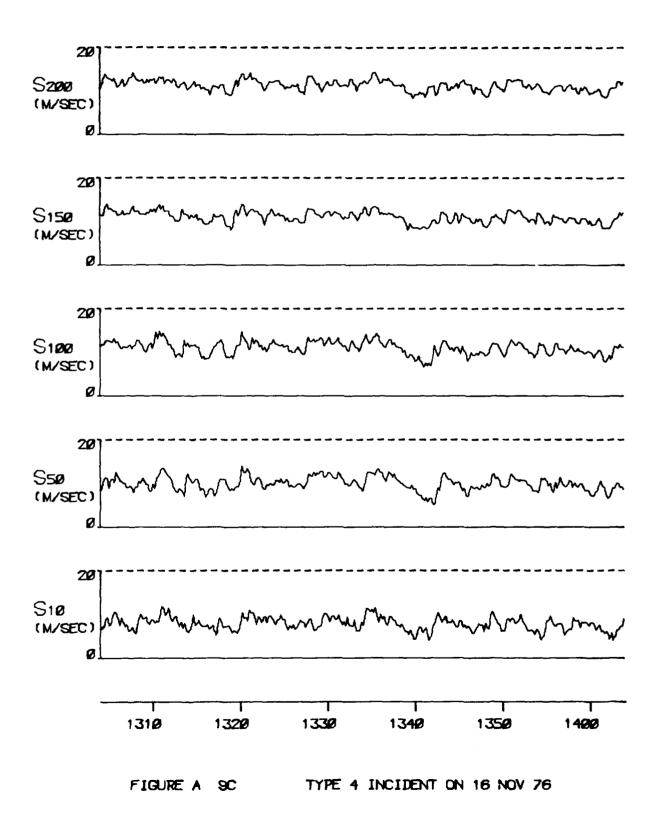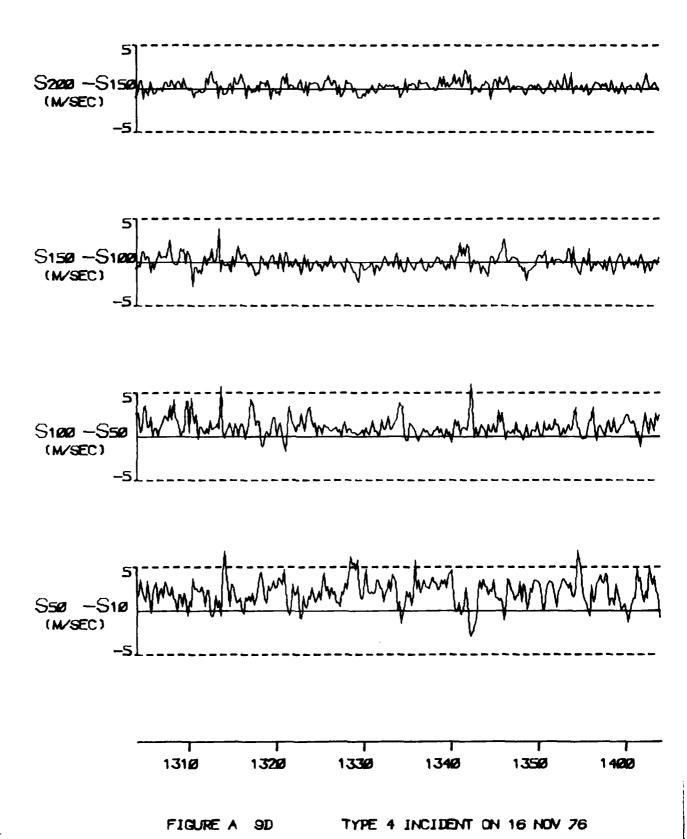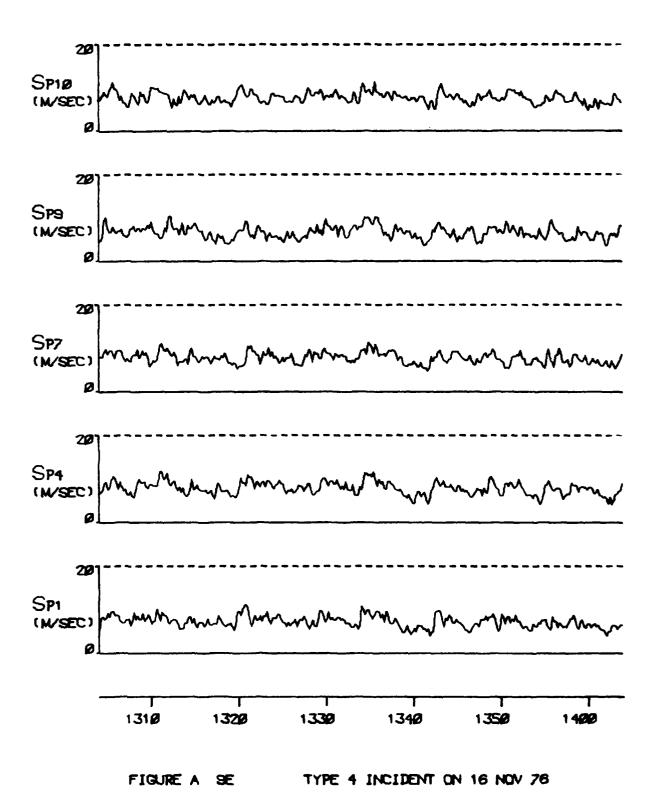
FIGURE A SE   TYPE 4 INCIDENT ON 16 NOV 76
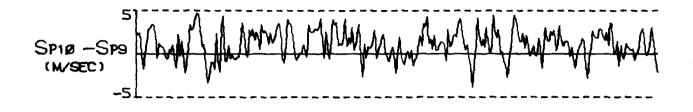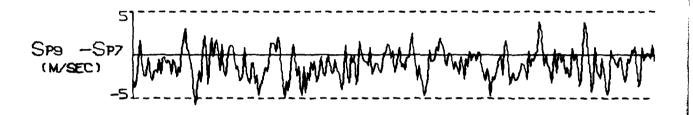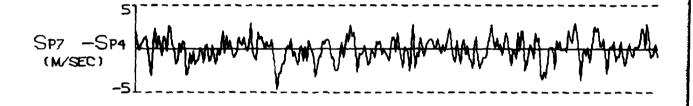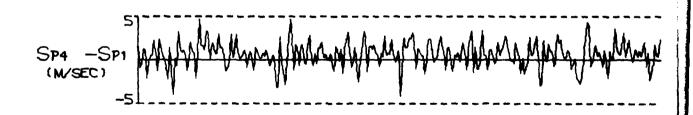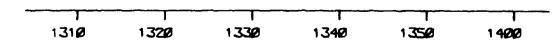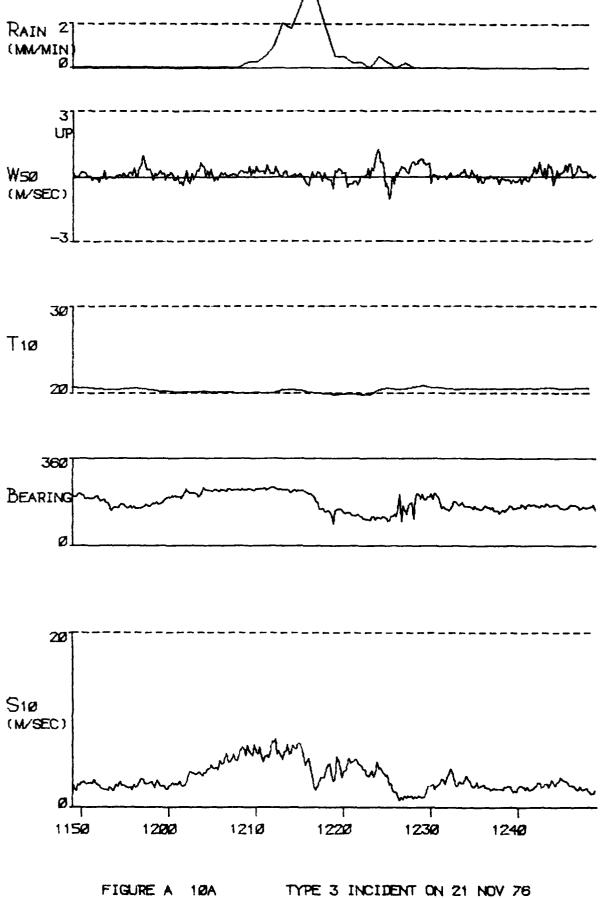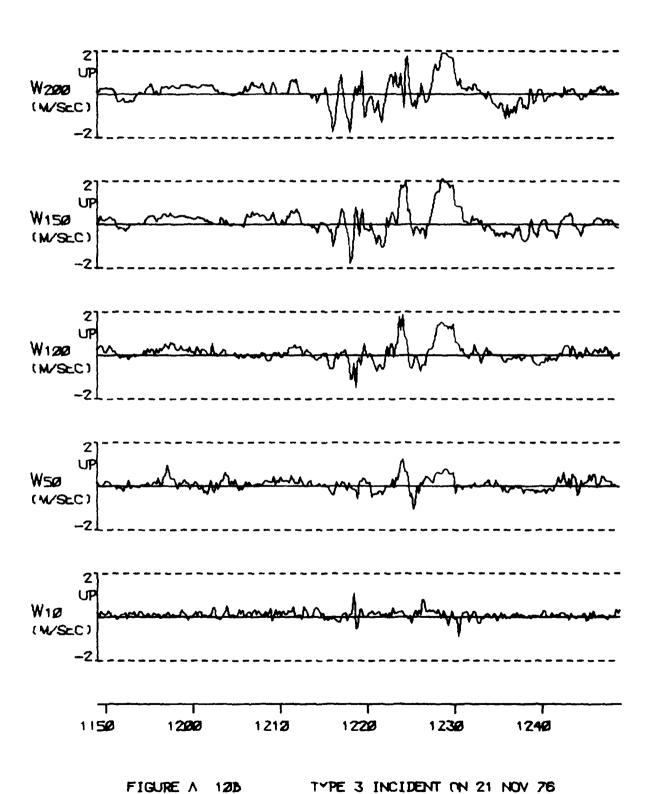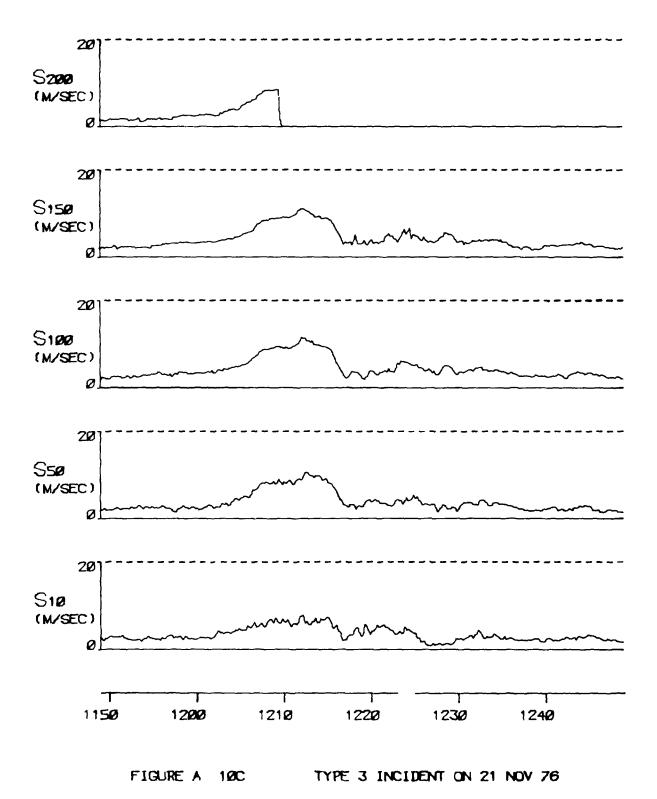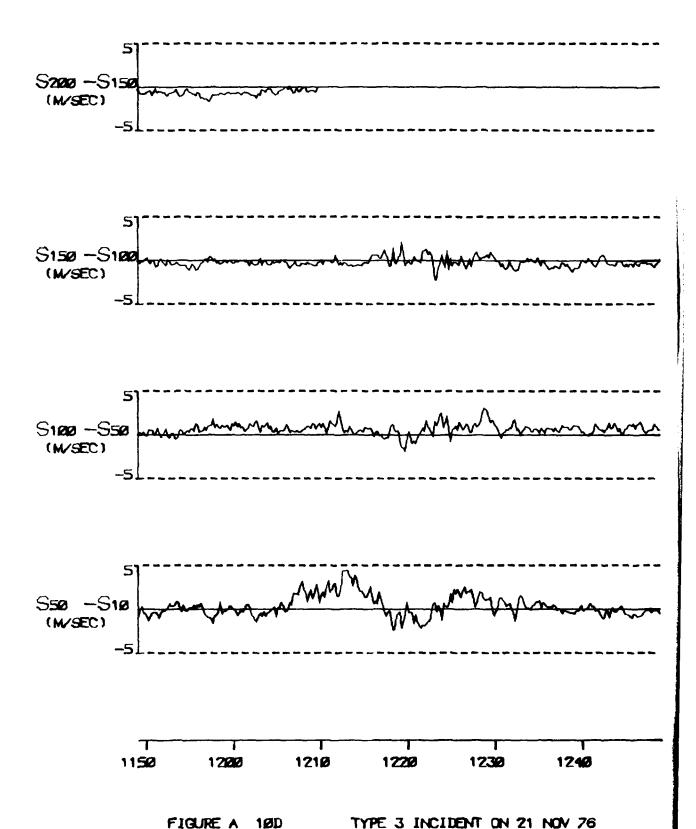
FIGURE A 9F   TYPE 4 INCIDENT ON 16 NOV 76

FIGURE A 10A   TYPE 3 INCIDENT ON 21 NOV 76

FIGURE A 12B   TYPE 3 INCIDENT ON 21 NOV 76

FIGURE A 10C   TYPE 3 INCIDENT ON 21 NOV 76

FIGURE A 10D   TYPE 3 INCIDENT ON 21 NOV 76

FIGURE A 10E   TYPE 3 INCIDENT ON 21 NOV 76

FIGURE A 10F   TYPE 3 INCIDENT ON 21 NOV 76

FIGURE A 11A   TYPE 3 INCIDENT ON 21 NOV 78

FIGURE A 11B   TYPE 3 INCIDENT ON 21 NOV 76

FIGURE A 11C   TYPE 3 INCIDENT ON 21 NOV 76
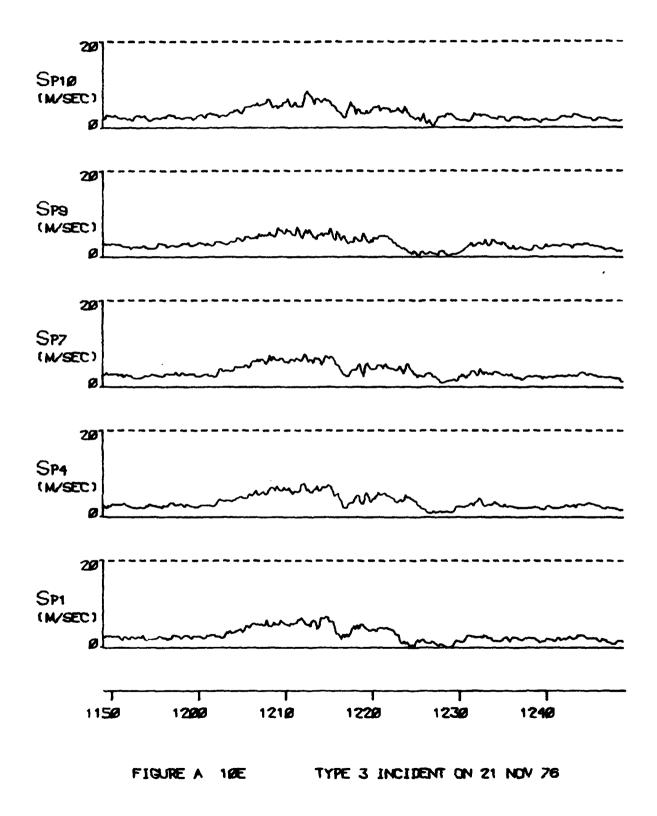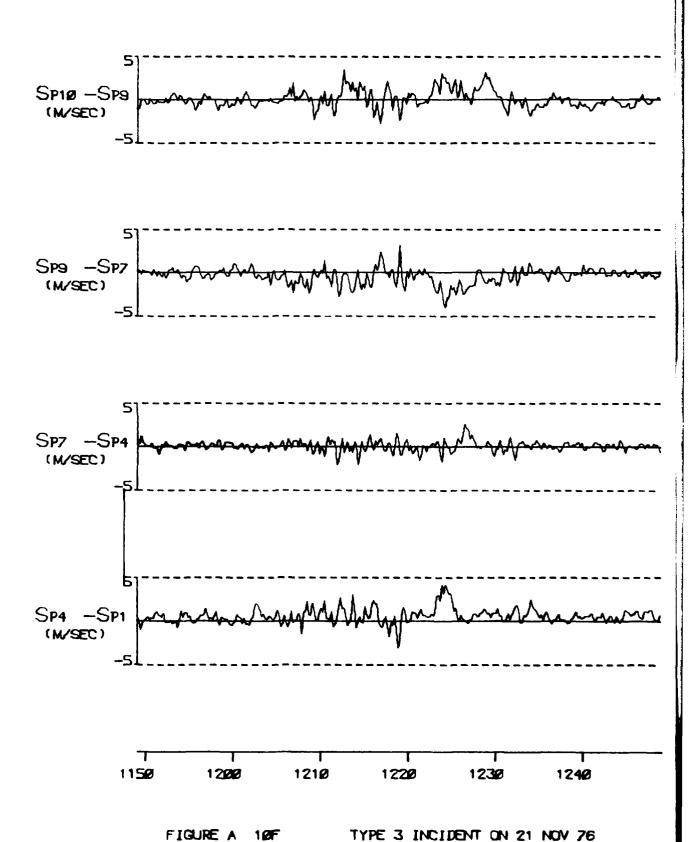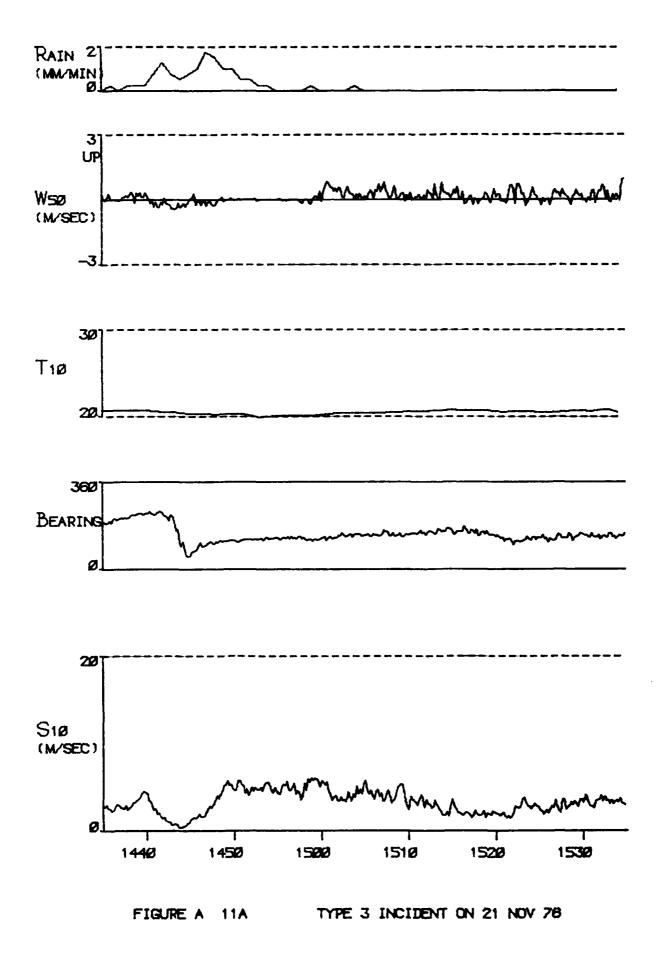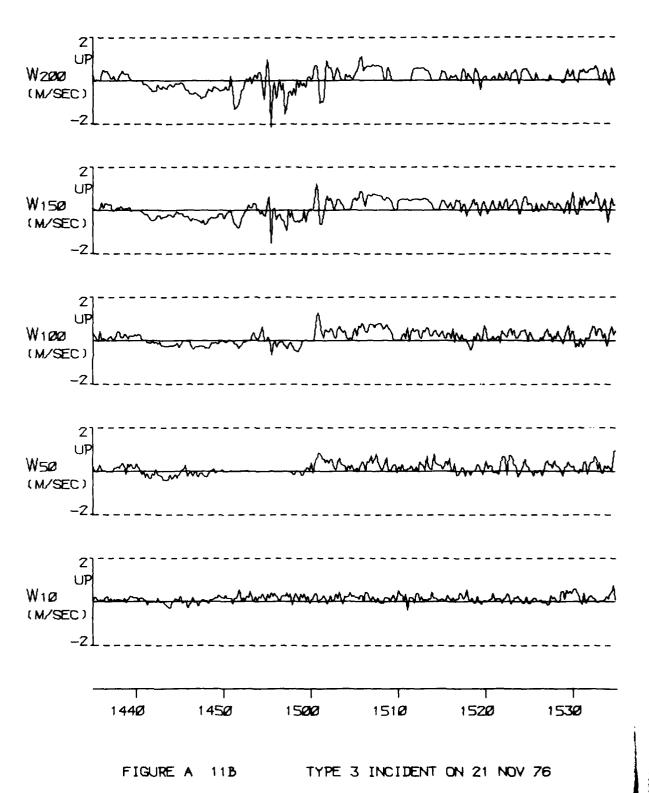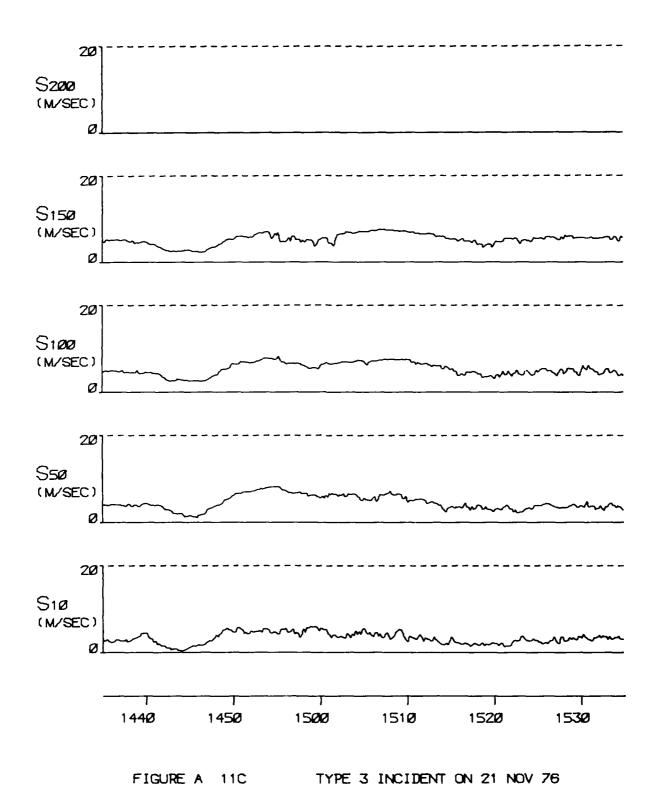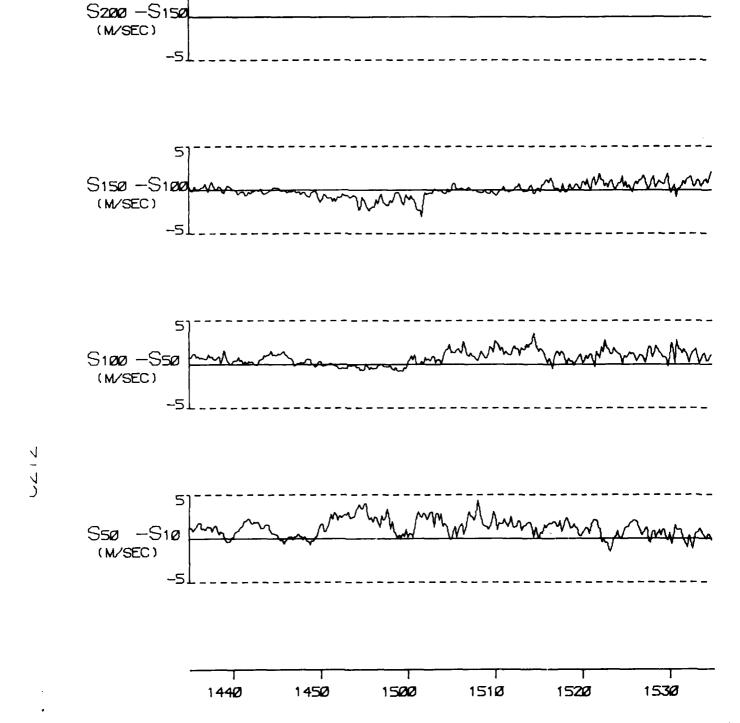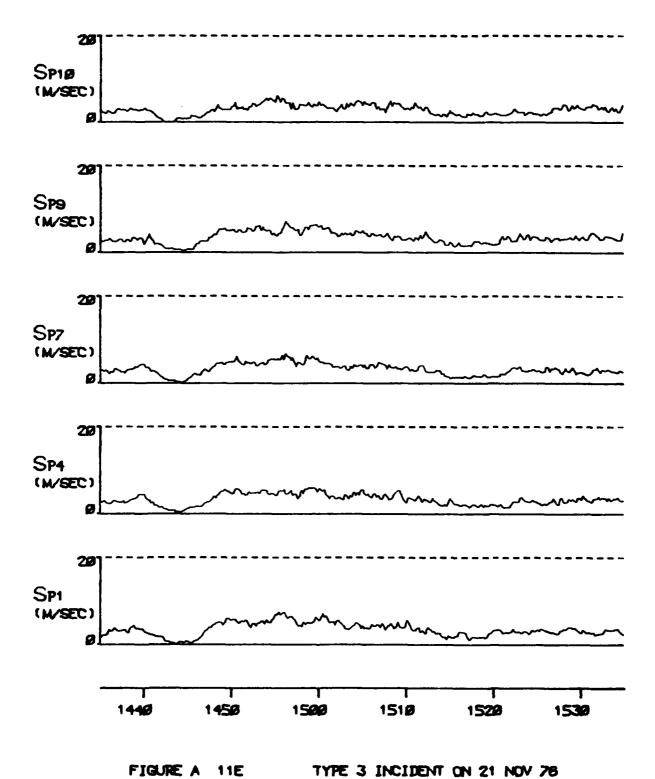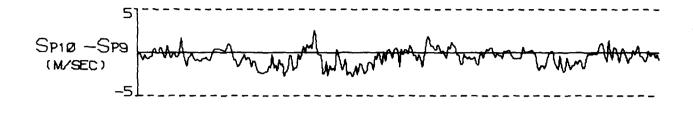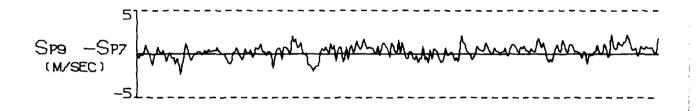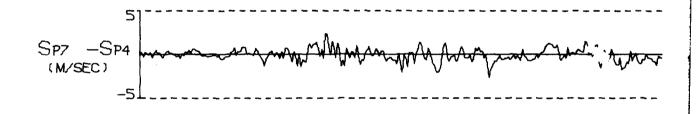
FIGURE A 11D   TYPE 3 INCIDENT ON 21 NOV 76
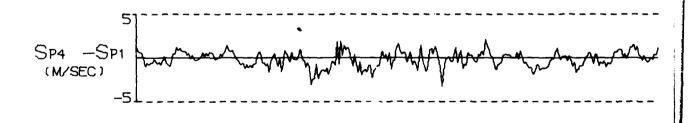
FIGURE A 11E   TYPE 3 INCIDENT ON 21 NOV 78
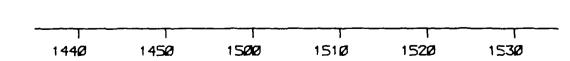
FIGURE A 11F   TYPE 3 INCIDENT ON 21 NOV 76
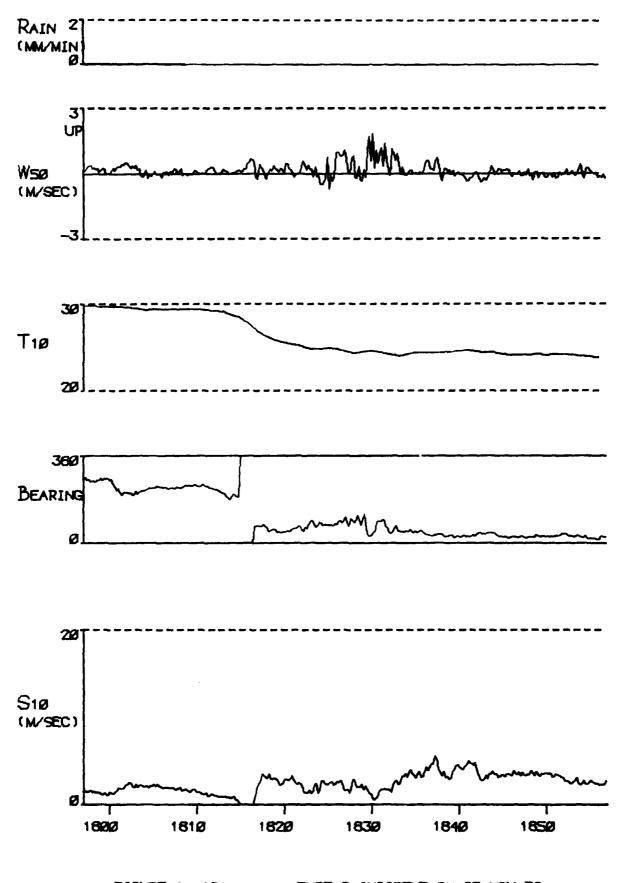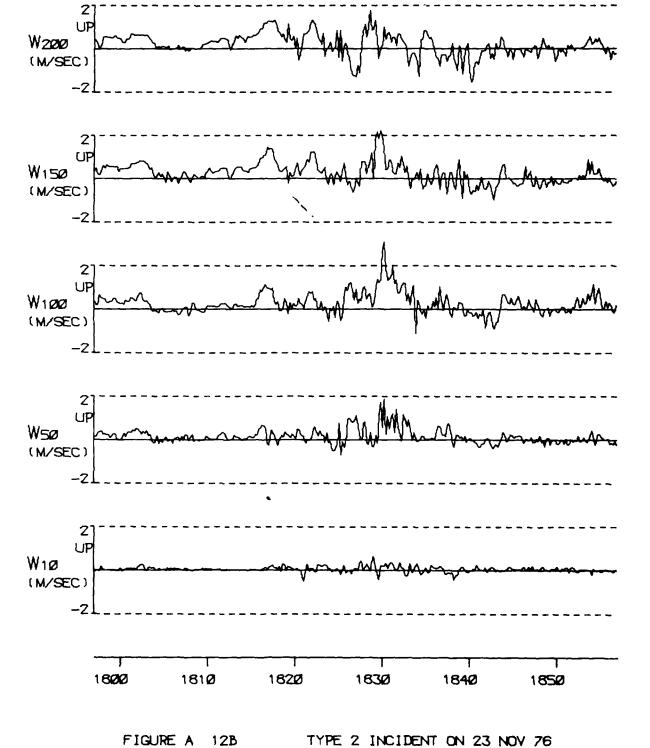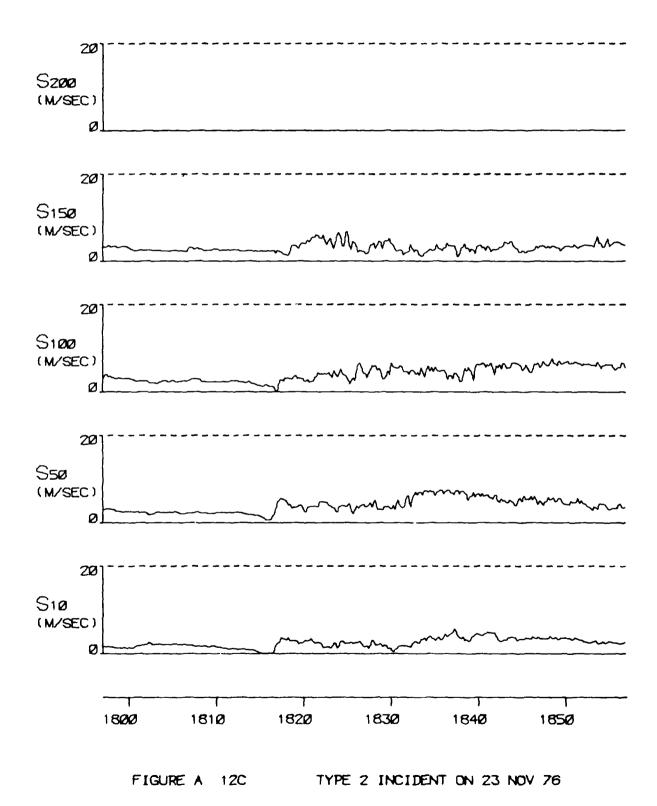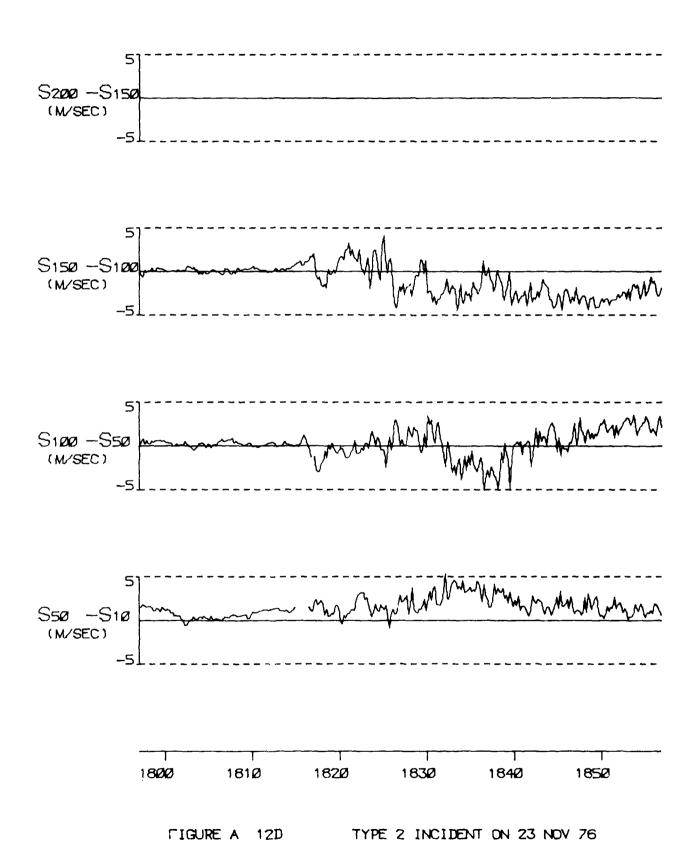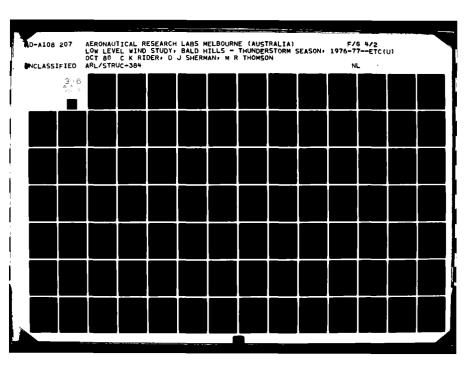
FIGURE A 12A   TYPE 2 INCIDENT ON 23 NOV 76

FIGURE A 12B   TYPE 2 INCIDENT ON 23 NOV 76

FIGURE A 12C   TYPE 2 INCIDENT ON 23 NOV 76

FIGURE A 12D   TYPE 2 INCIDENT ON 23 NOV 76

1.0

2.8 2.5
3.2 2.2
3.6

1.1 2.0

1.8

1.25 1.4 1.6
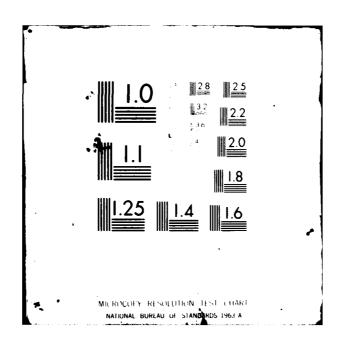
FIGURE A 12E   TYPE 2 INCIDENT ON 23 NOV 76
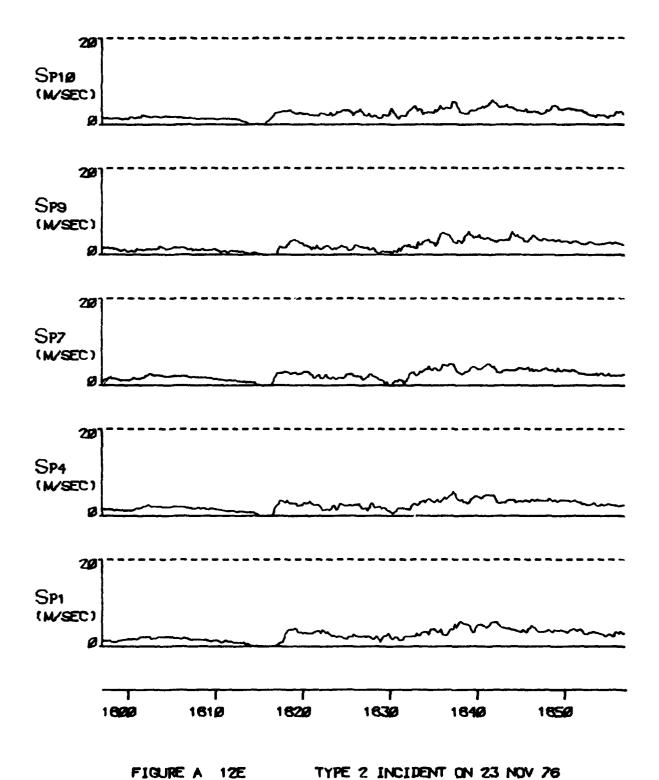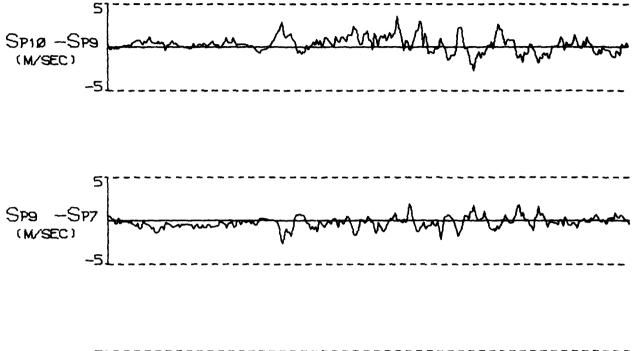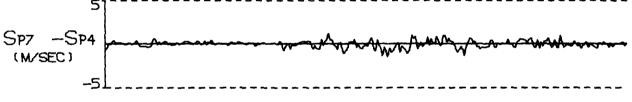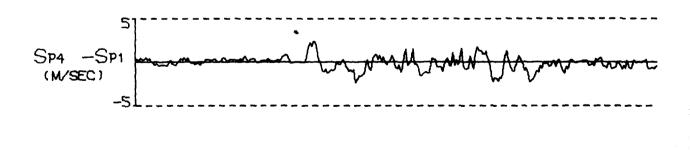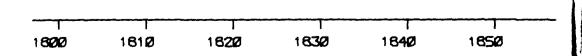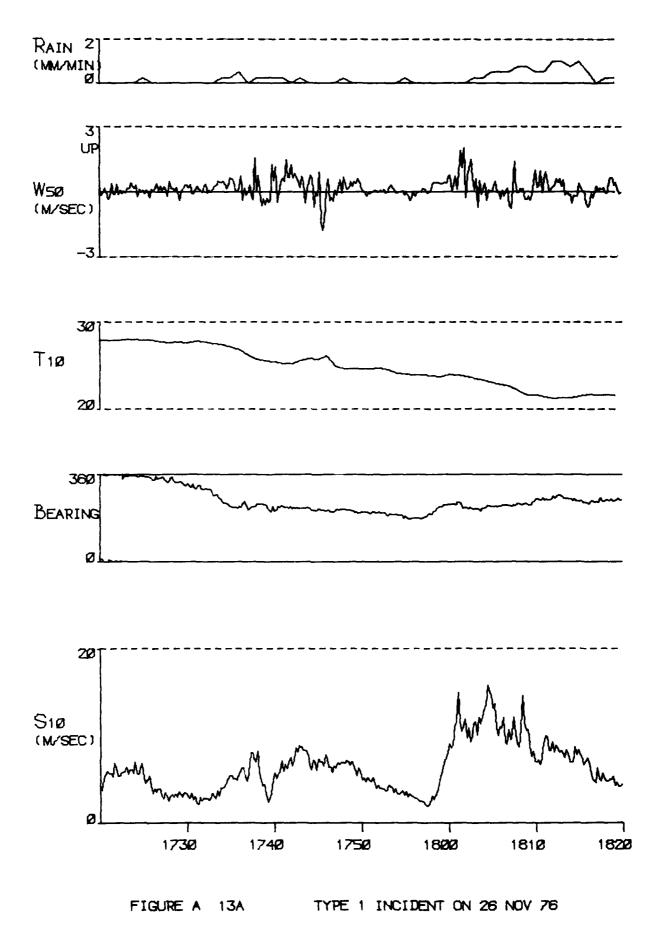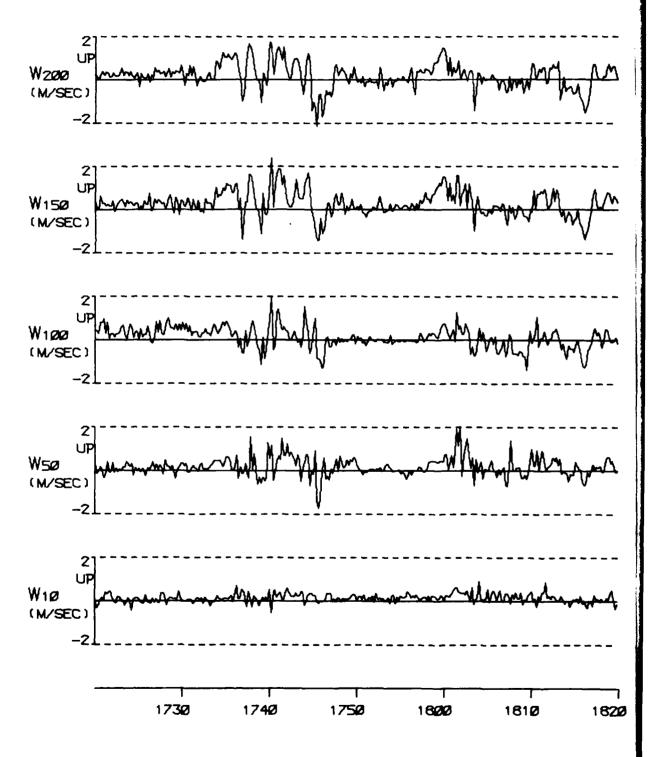
FIGURE A 12F   TYPE 2 INCIDENT ON 23 NOV 76

FIGURE A   13A   TYPE 1 INCIDENT ON 26 NOV 76

FIGURE A   13B   TYPE 1 INCIDENT ON 26 NOV 76
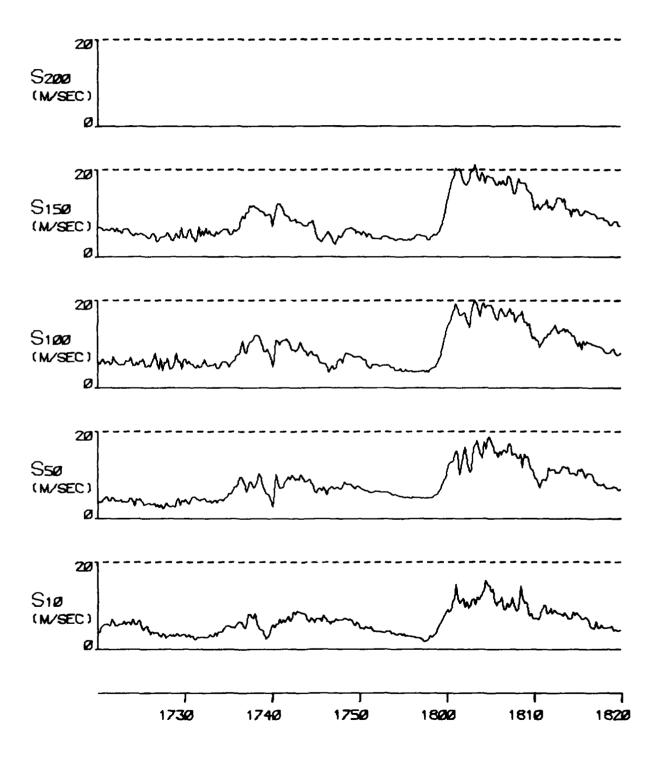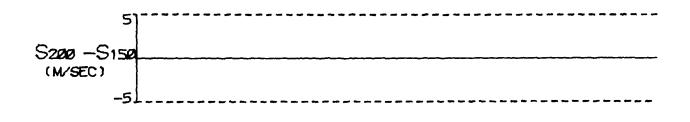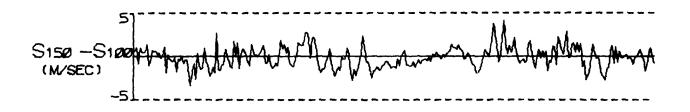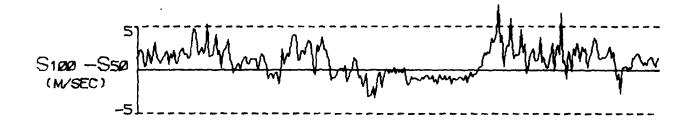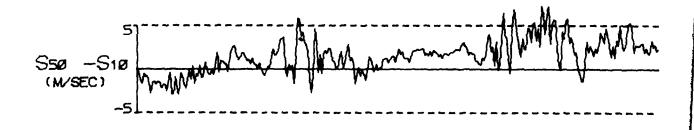
FIGURE A 13C   TYPE 1 INCIDENT ON 26 NOV 76
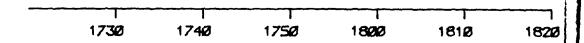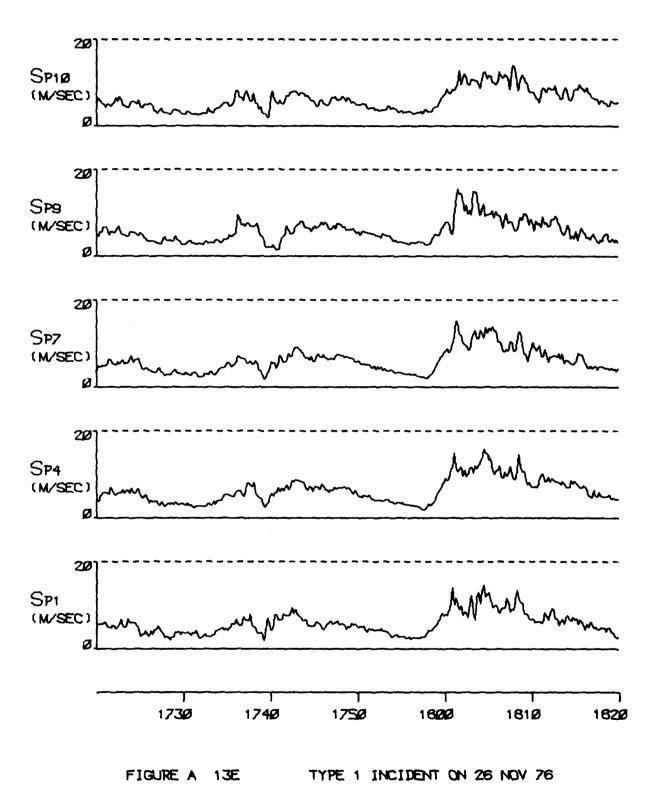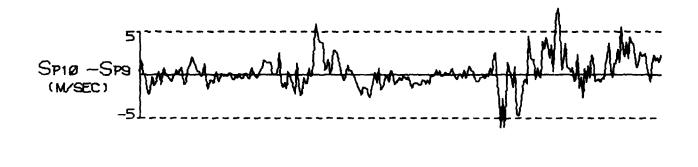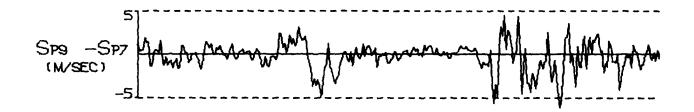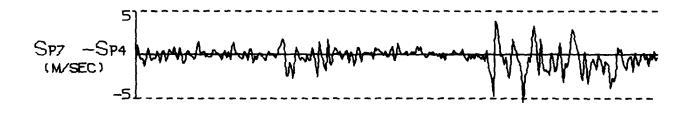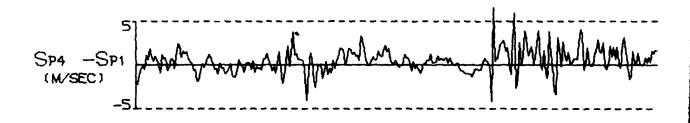
FIGURE A 13D   TYPE 1 INCIDENT ON 26 NOV 76

FIGURE A   13E   TYPE 1 INCIDENT ON 26 NOV 76
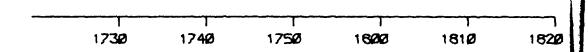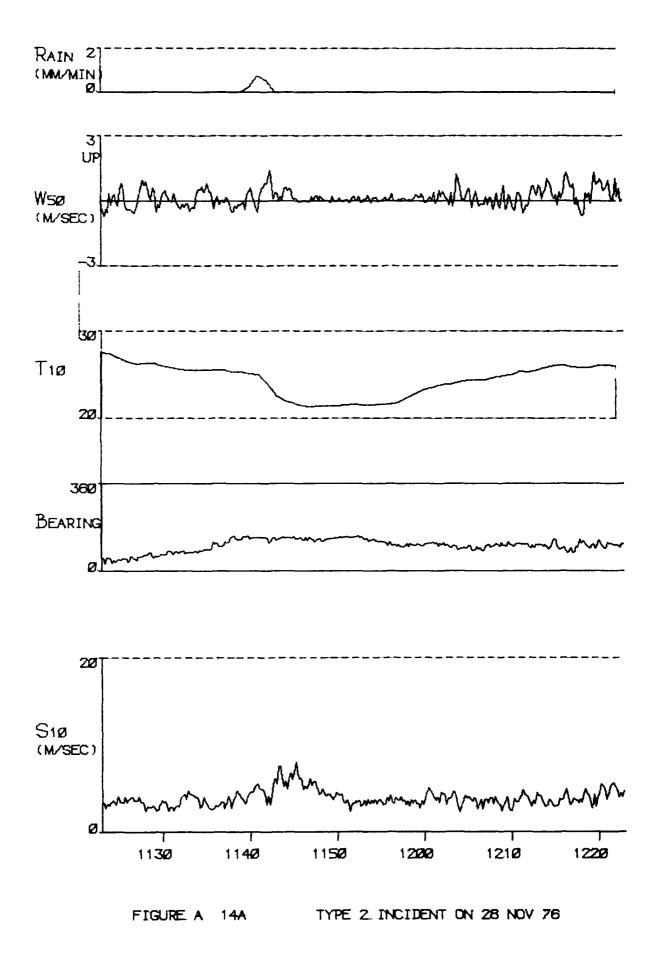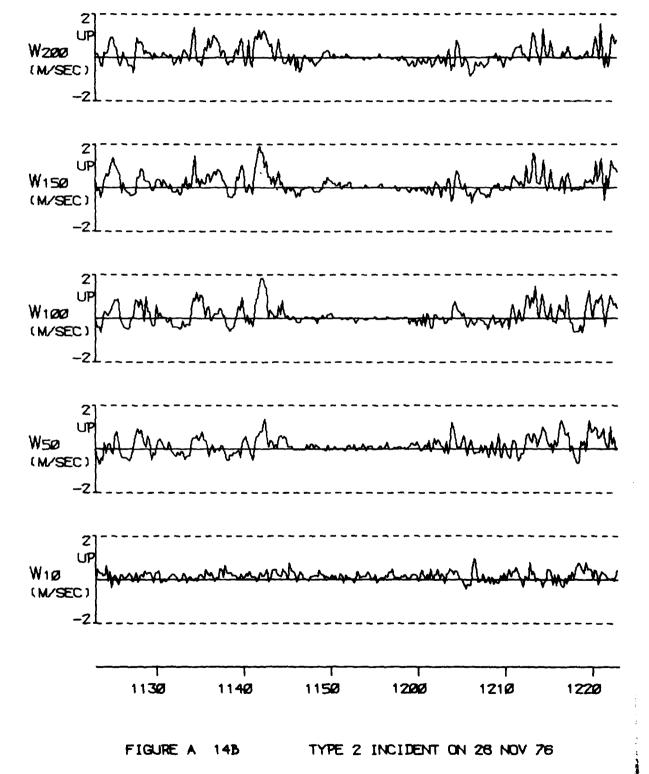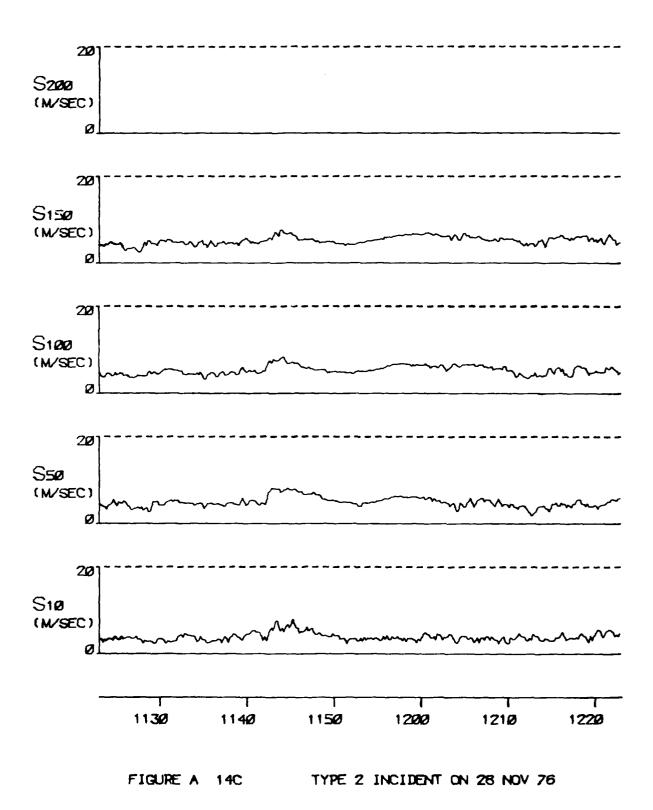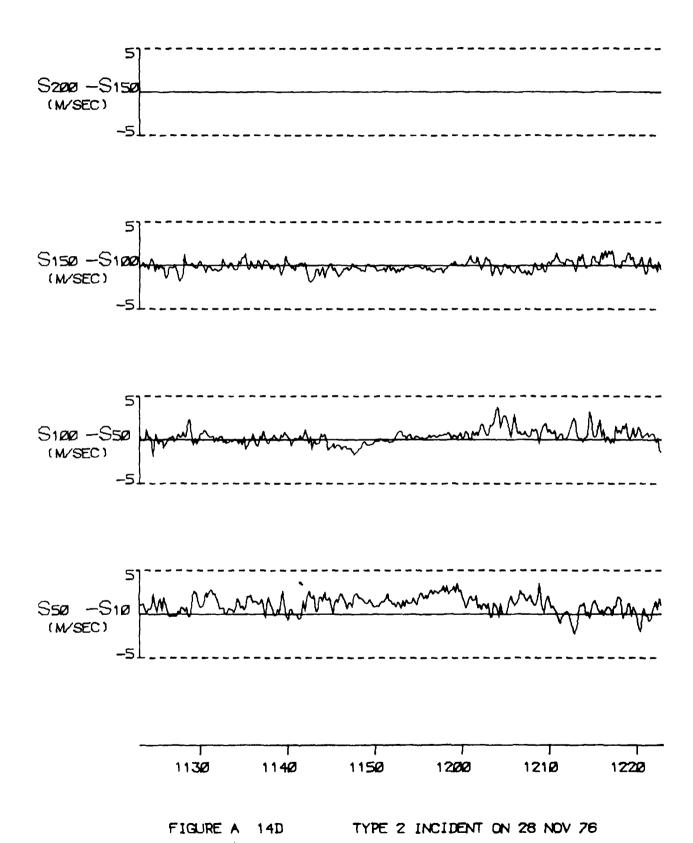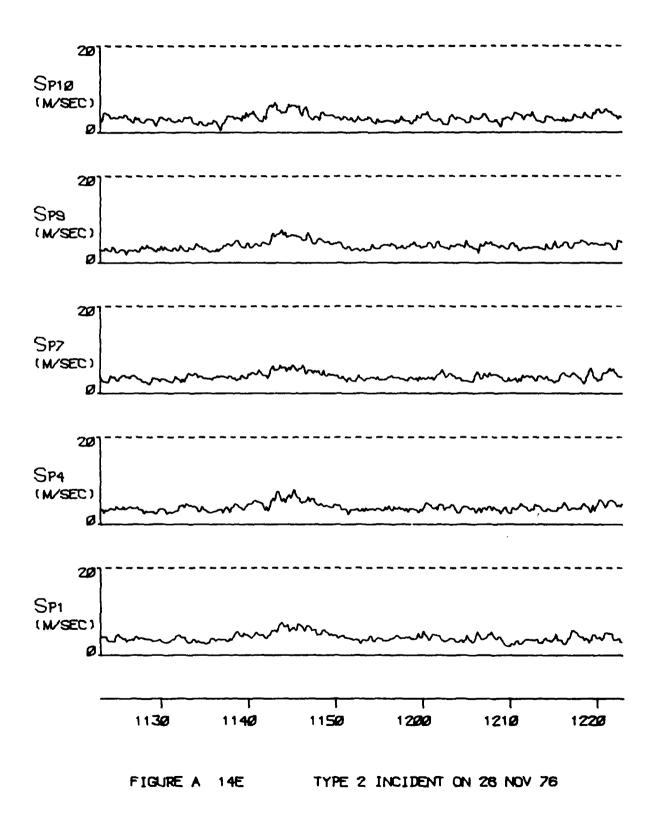
FIGURE A 13F   TYPE 1 INCIDENT ON 26 NOV 76

FIGURE A 14A   TYPE 2 INCIDENT ON 28 NOV 76

FIGURE A 14B   TYPE 2 INCIDENT ON 26 NOV 76

FIGURE A 14C   TYPE 2 INCIDENT ON 28 NOV 76

FIGURE A 14D   TYPE 2 INCIDENT ON 28 NOV 76

FIGURE A 14E   TYPE 2 INCIDENT ON 28 NOV 76
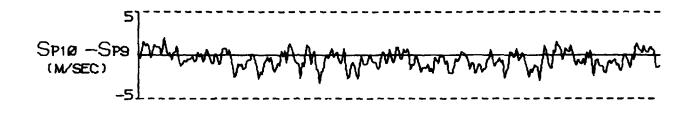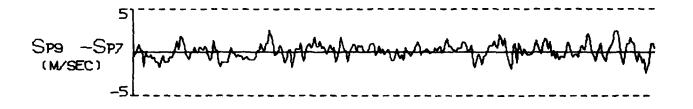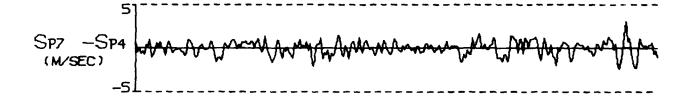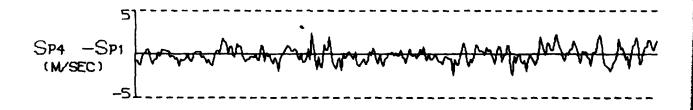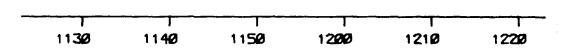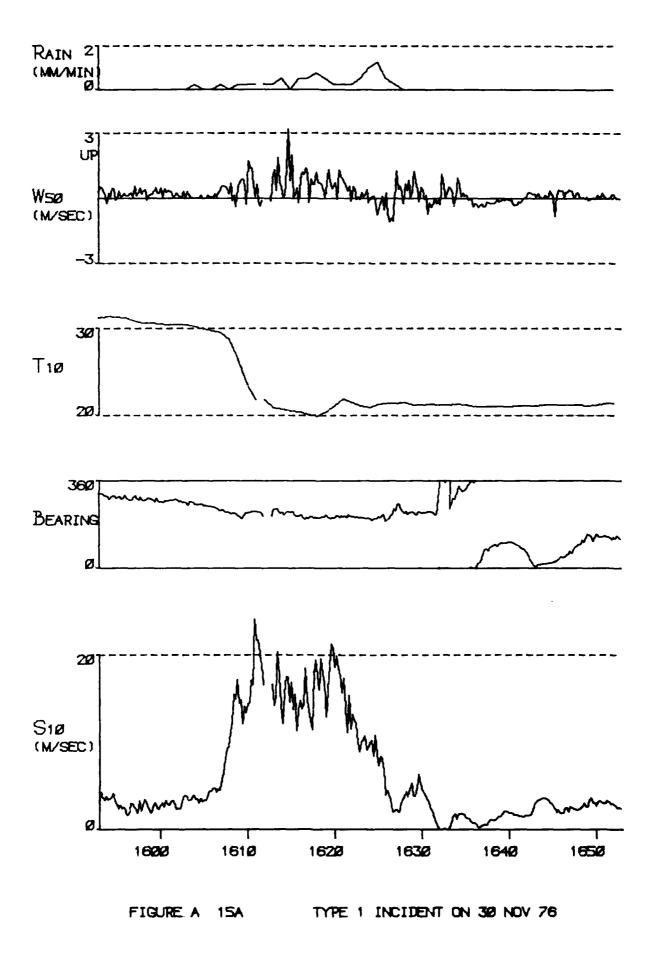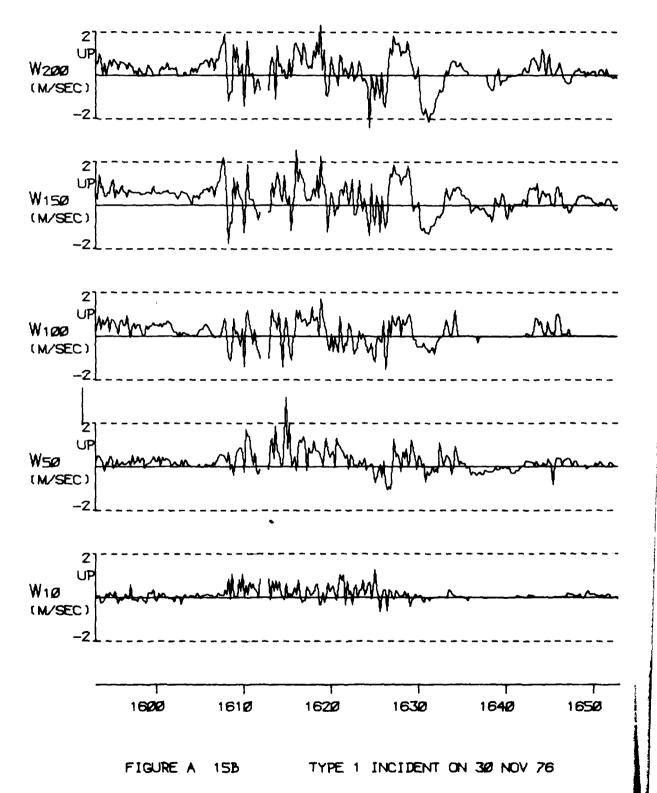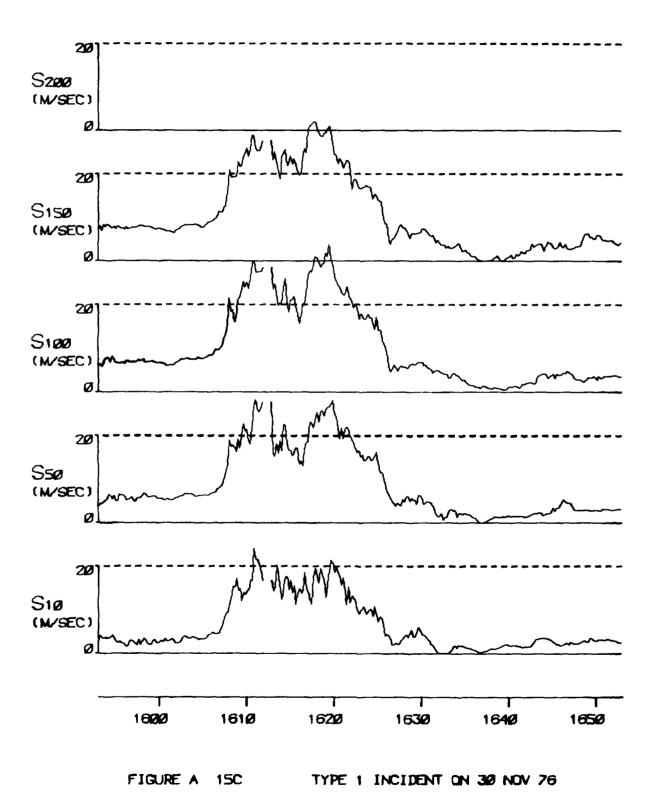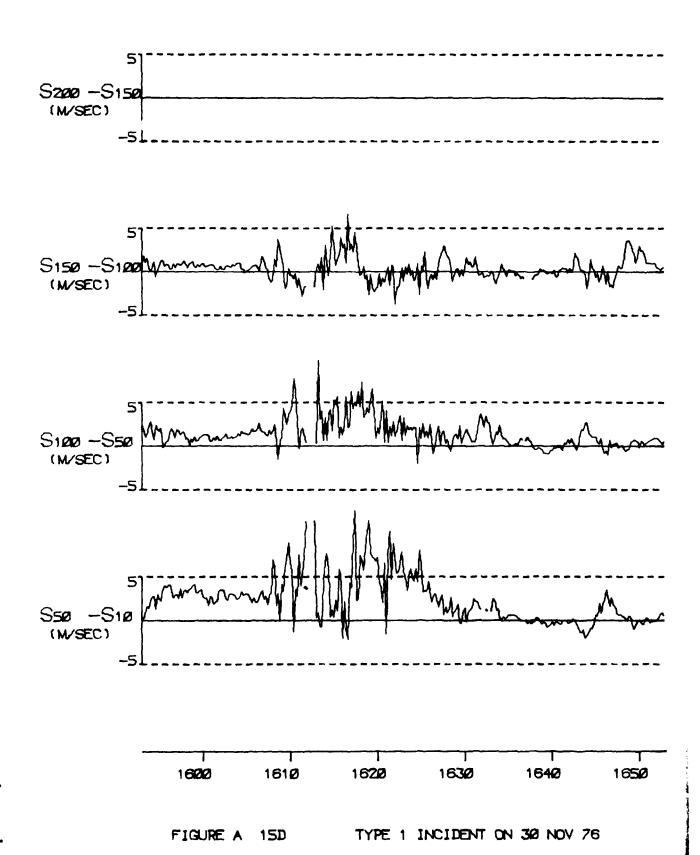
FIGURE A 14F   TYPE 2 INCIDENT ON 28 NOV 76

FIGURE A 15A   TYPE 1 INCIDENT ON 30 NOV 76

FIGURE A 15B   TYPE 1 INCIDENT ON 30 NOV 76

FIGURE A 15C   TYPE 1 INCIDENT ON 30 NOV 76

FIGURE A 15D   TYPE 1 INCIDENT ON 30 NOV 76
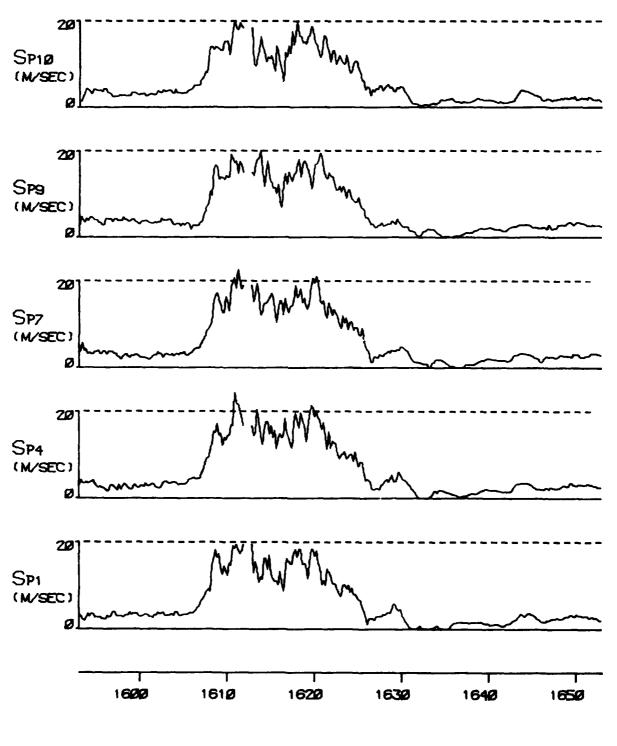
FIGURE A 15E   TYPE 1 INCIDENT ON 30 NOV 76
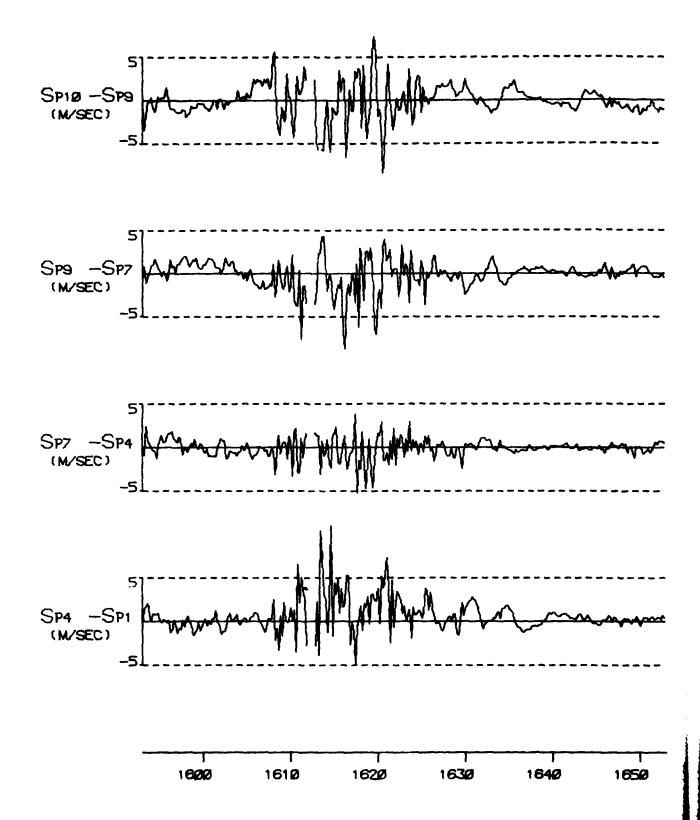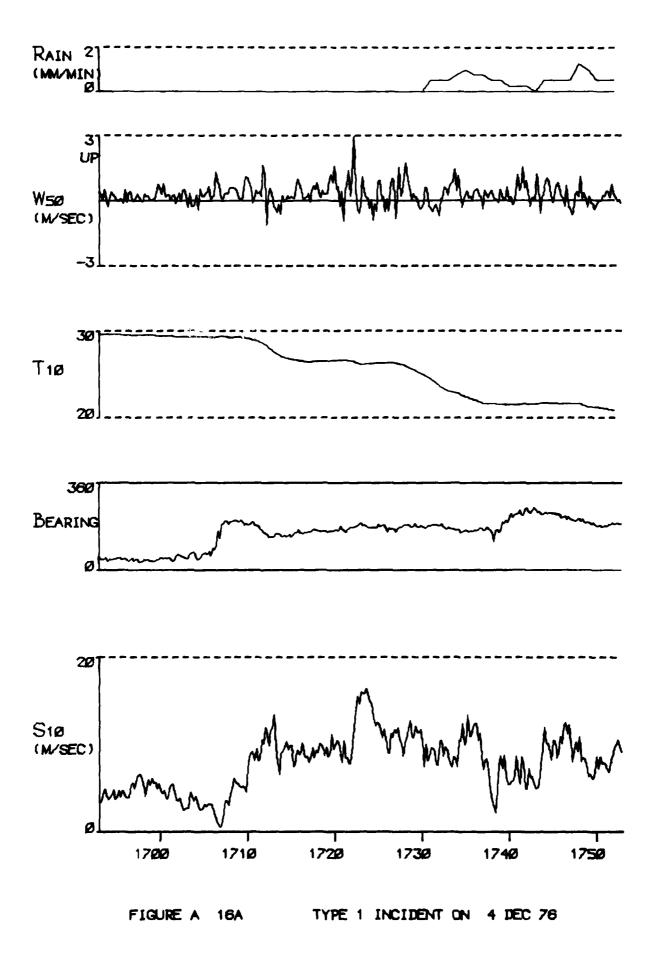
FIGURE A 15F   TYPE 1 INCIDENT ON 30 NOV 76

FIGURE A 16A   TYPE 1 INCIDENT ON 4 DEC 76
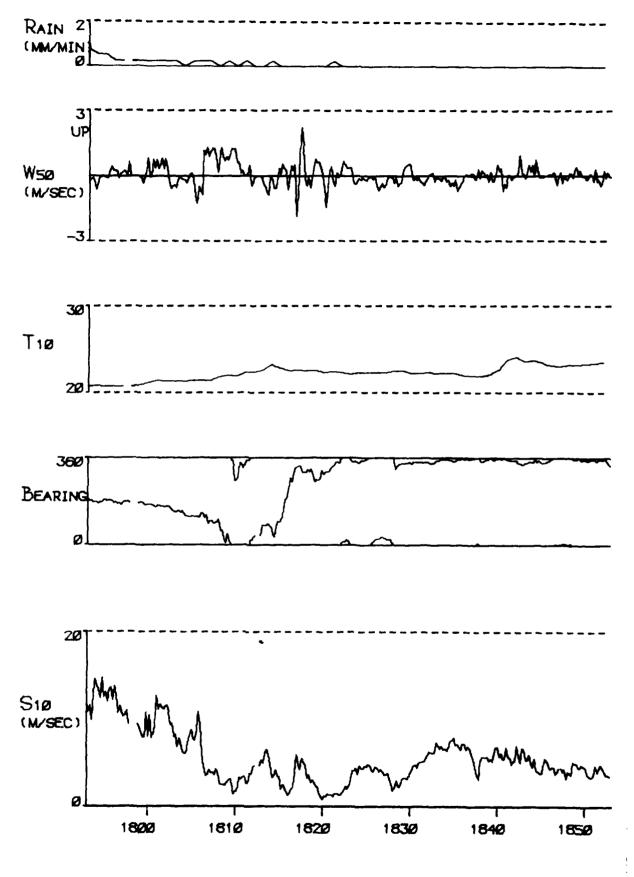
FIGURE A 16A (CONT) TYPE 1 INCIDENT ON 4 DEC 76

FIGURE A 16B   TYPE 1 INCIDENT ON 4 DEC 76
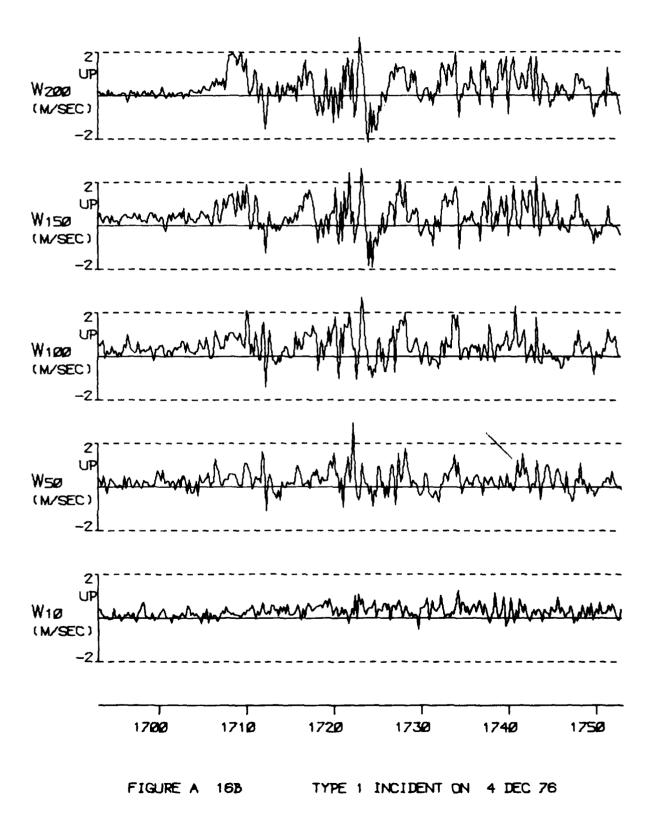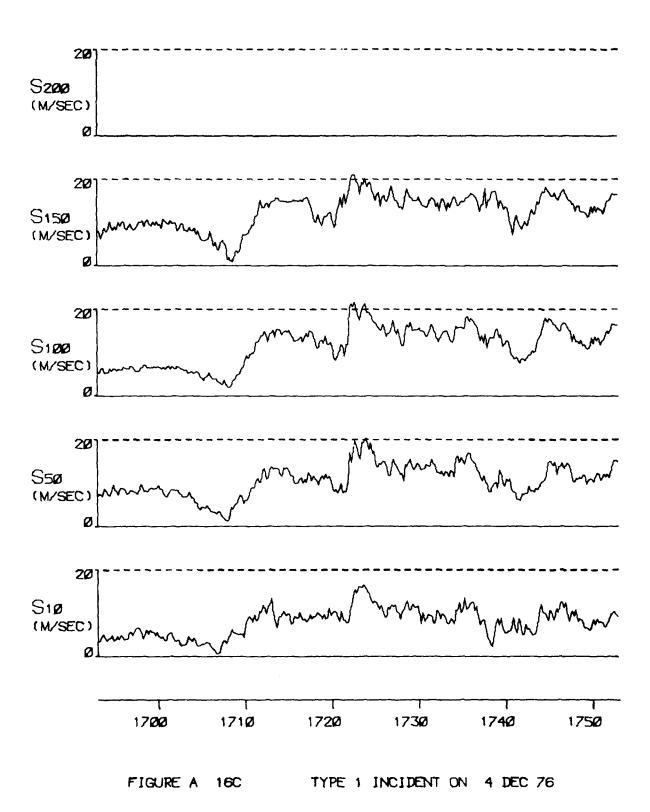
FIGURE A 16B (CONT) TYPE 1 INCIDENT ON 4 DEC 76

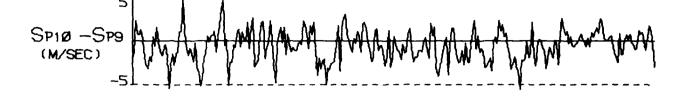FIGURE A 16C   TYPE 1 INCIDENT ON 4 DEC 76
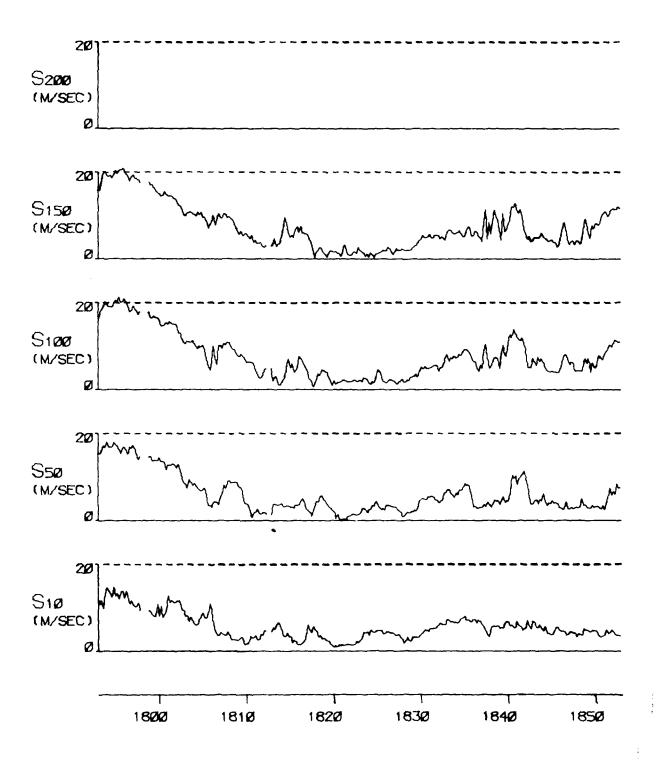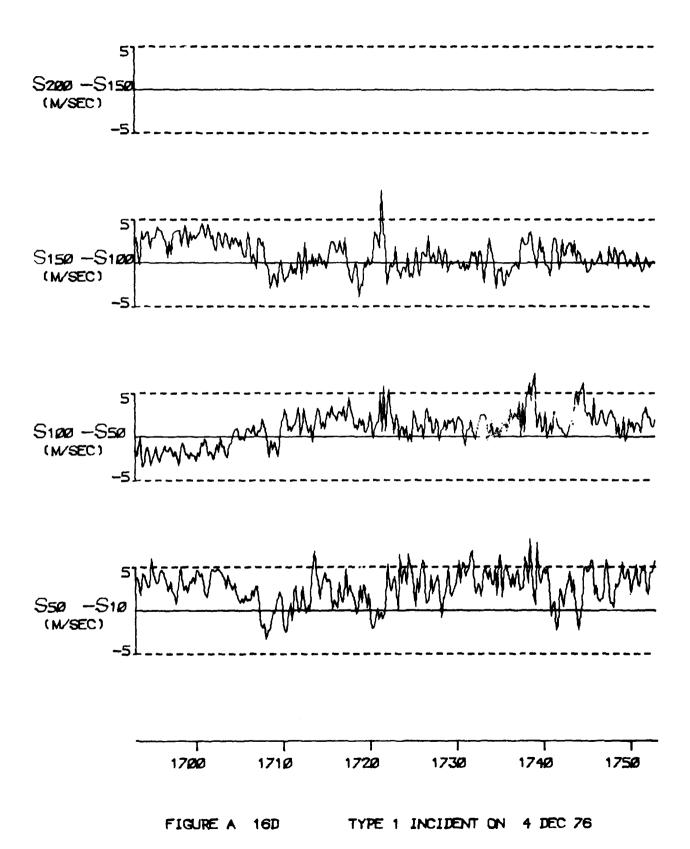
FIGURE A 16C (CONT) TYPE 1 INCIDENT ON 4 DEC 76

FIGURE A 16D   TYPE 1 INCIDENT ON 4 DEC 76
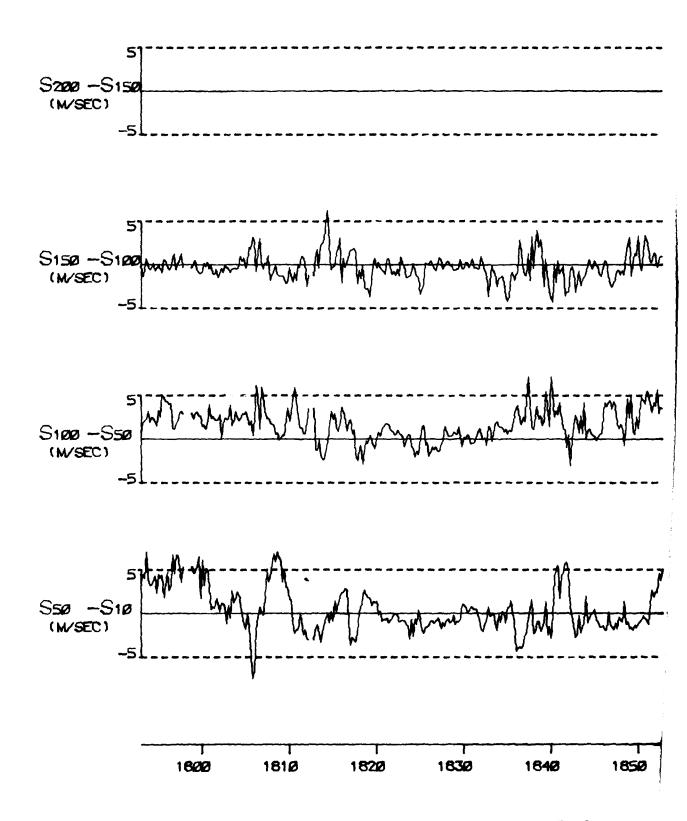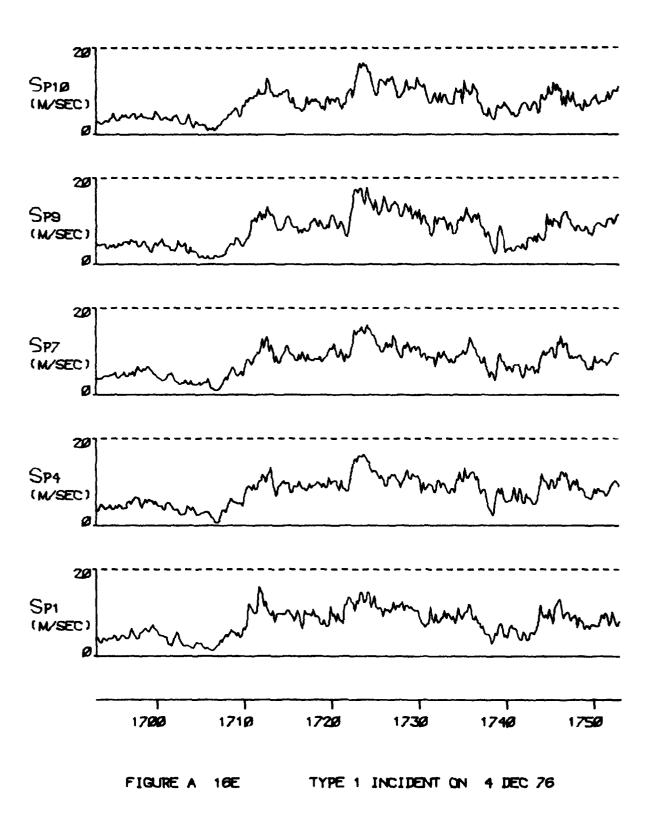
FIGURE A 16D (CONT) TYPE 1 INCIDENT ON 4 DEC 76

FIGURE A 16E   TYPE 1 INCIDENT ON 4 DEC 76
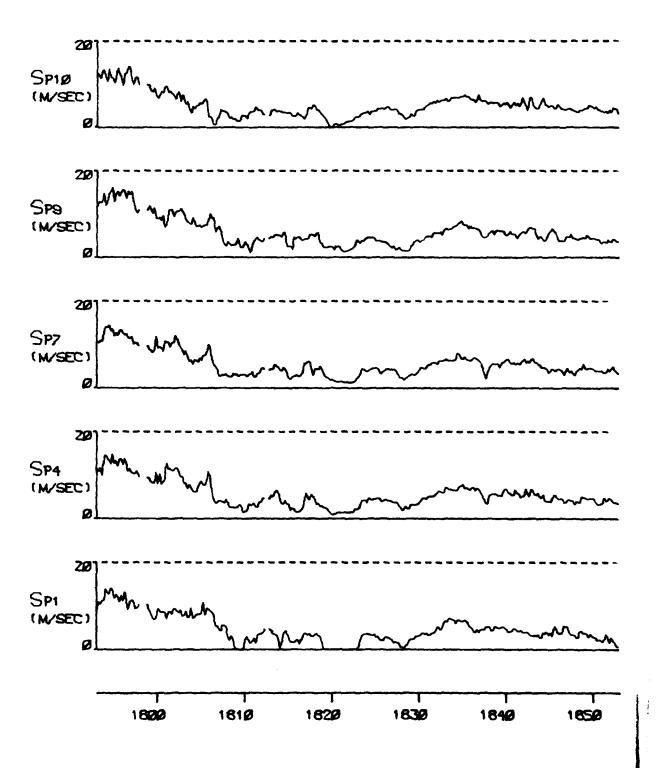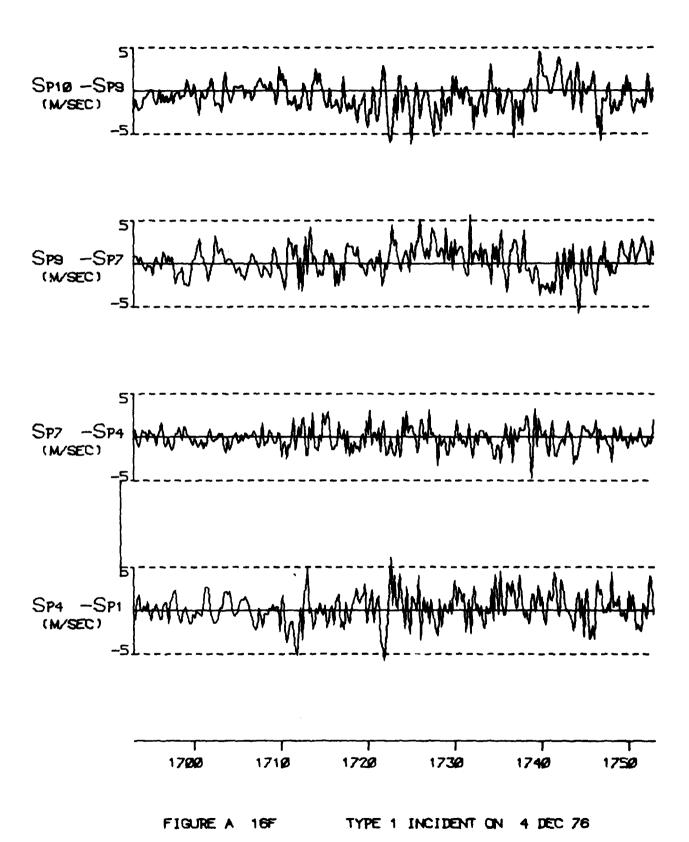
FIGURE A 16E (CONT) TYPE 1 INCIDENT ON 4 DEC 76

FIGURE A 16F   TYPE 1 INCIDENT ON 4 DEC 76
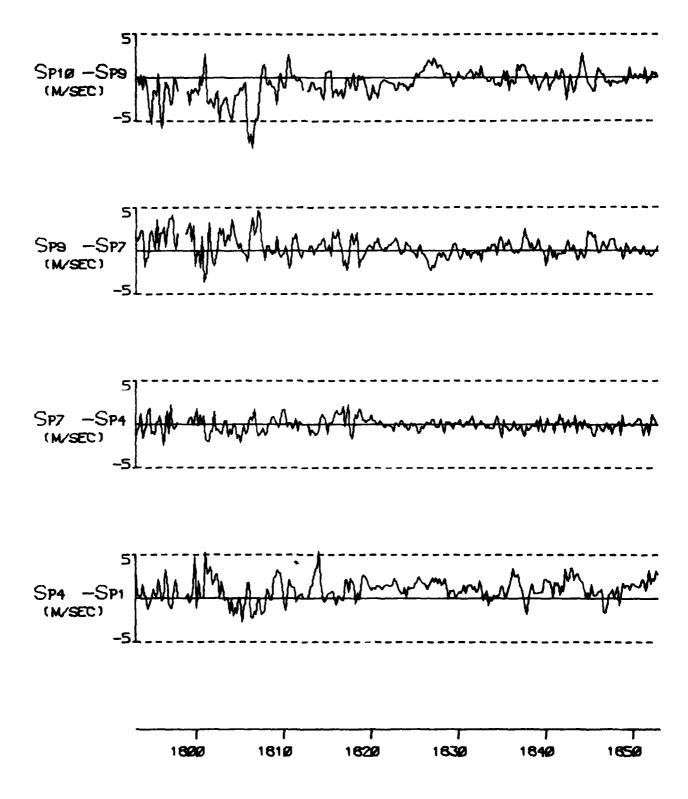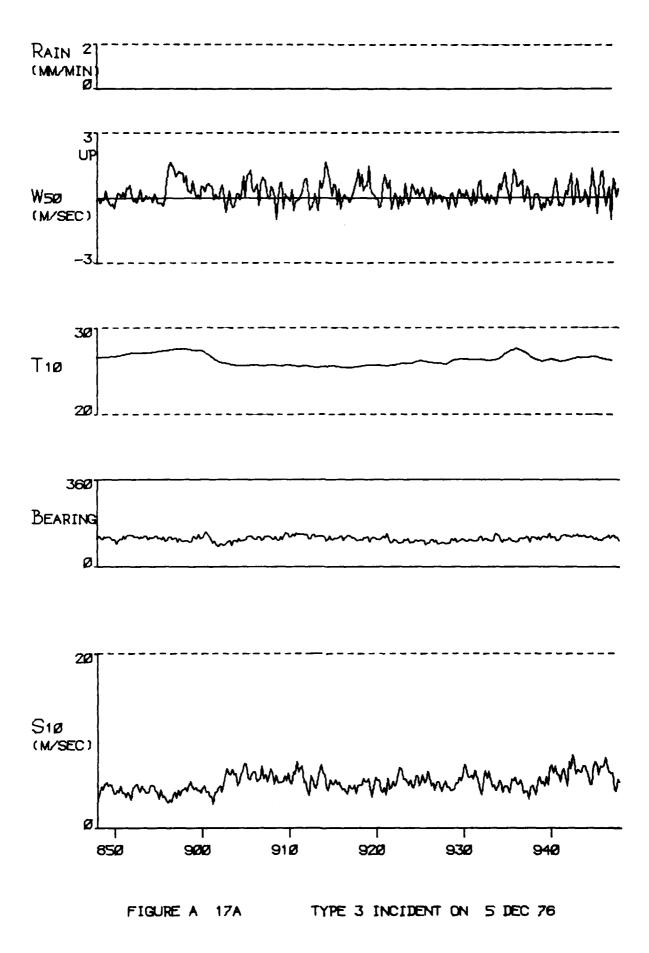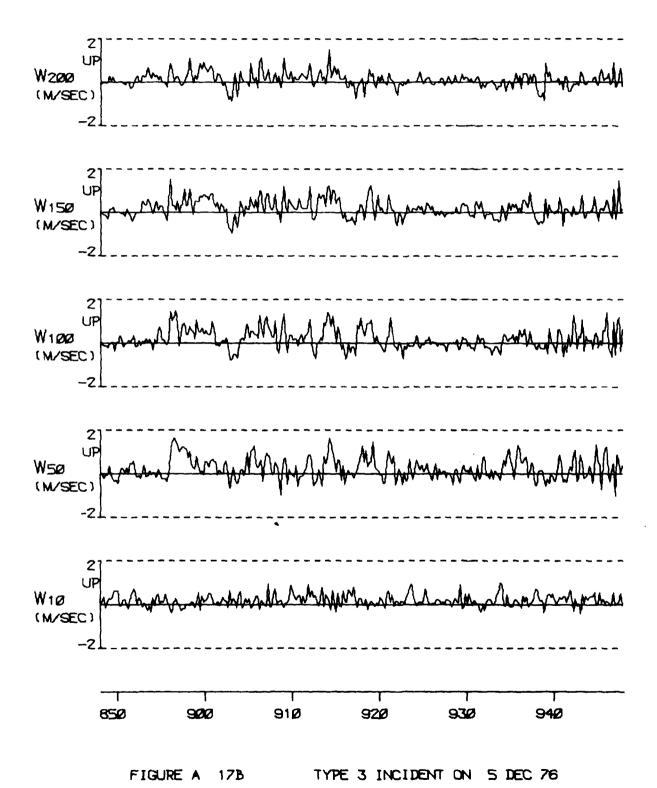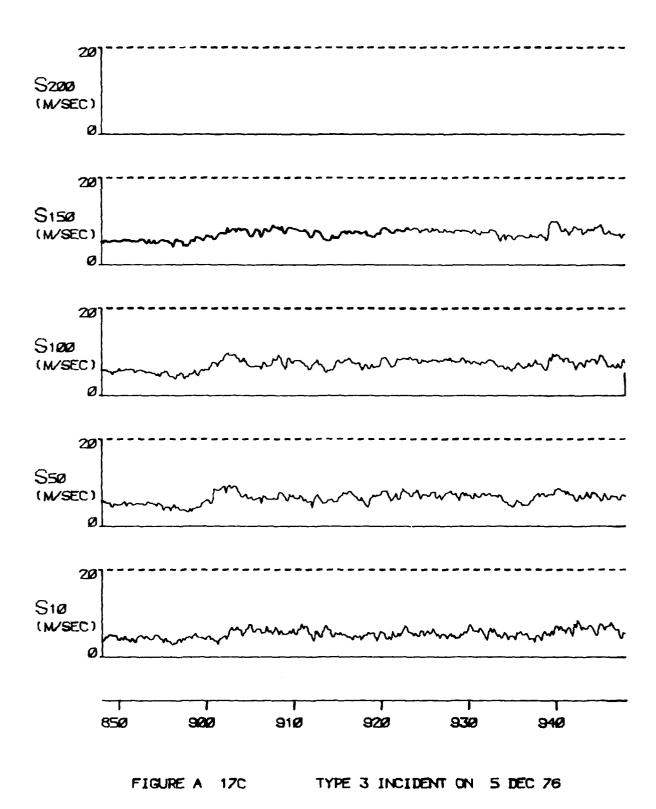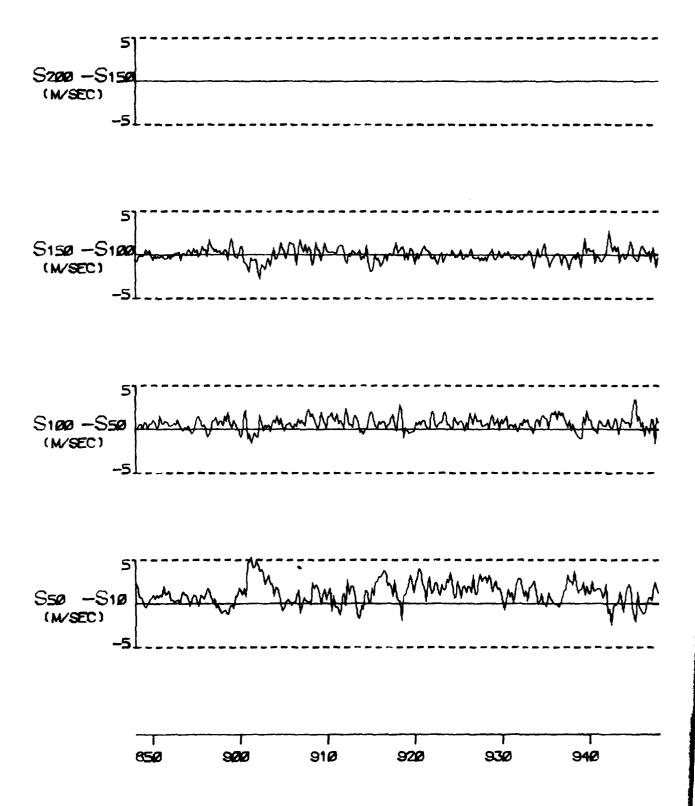
FIGURE A 16F (CONT) TYPE 1 INCIDENT ON 4 DEC 76

FIGURE A 17A   TYPE 3 INCIDENT ON 5 DEC 76

FIGURE A 17B   TYPE 3 INCIDENT ON 5 DEC 76

FIGURE A 17C   TYPE 3 INCIDENT ON 5 DEC 76

FIGURE A 17D   TYPE 3 INCIDENT ON 5 DEC 76
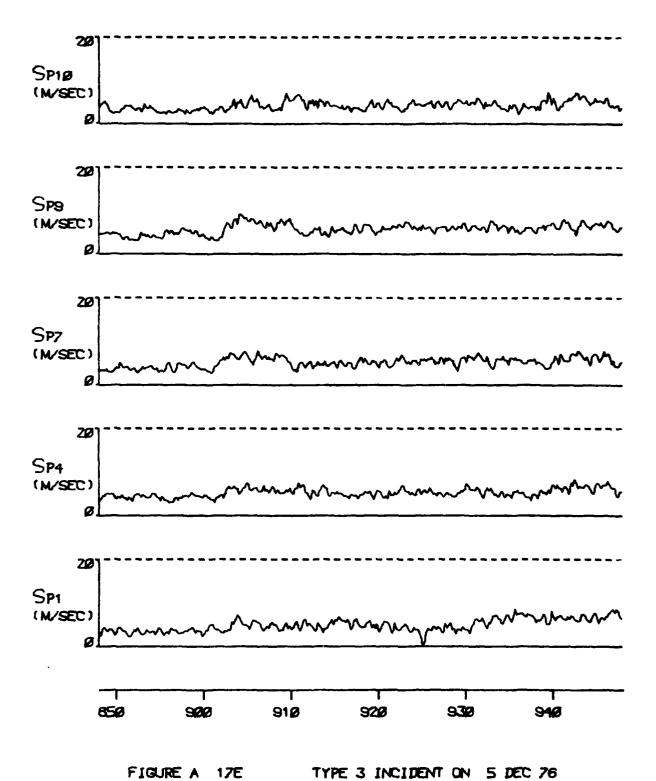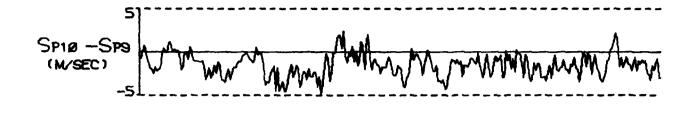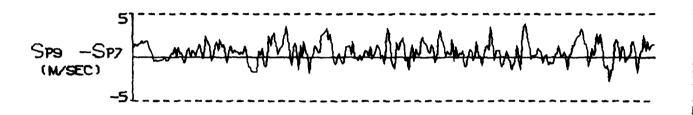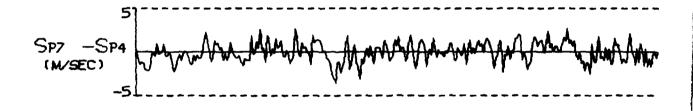
FIGURE A 17E   TYPE 3 INCIDENT ON 5 DEC 76
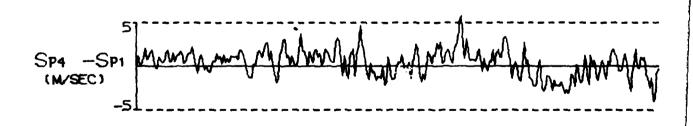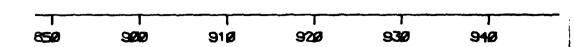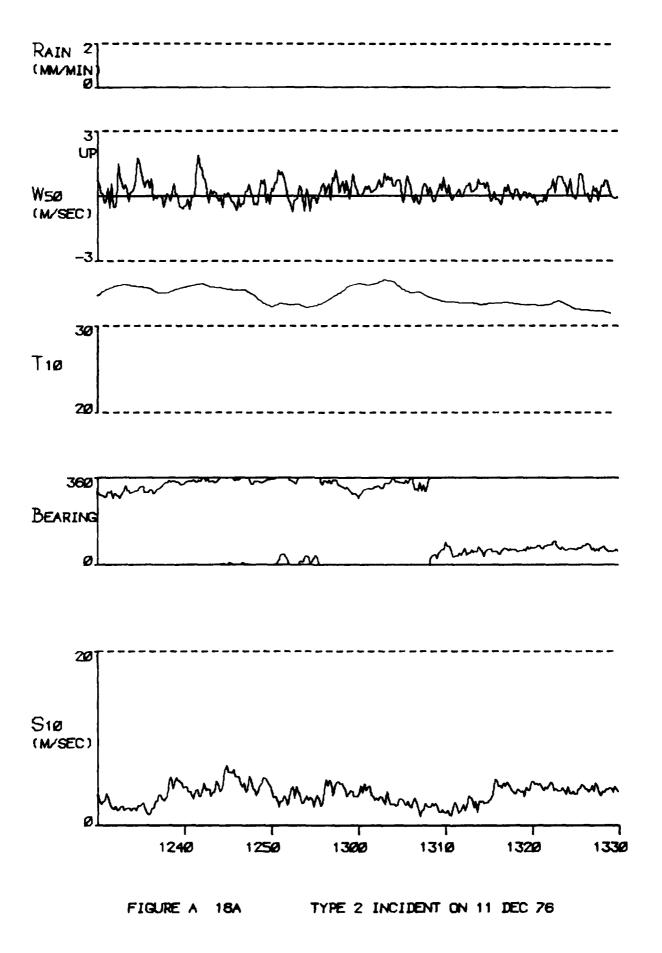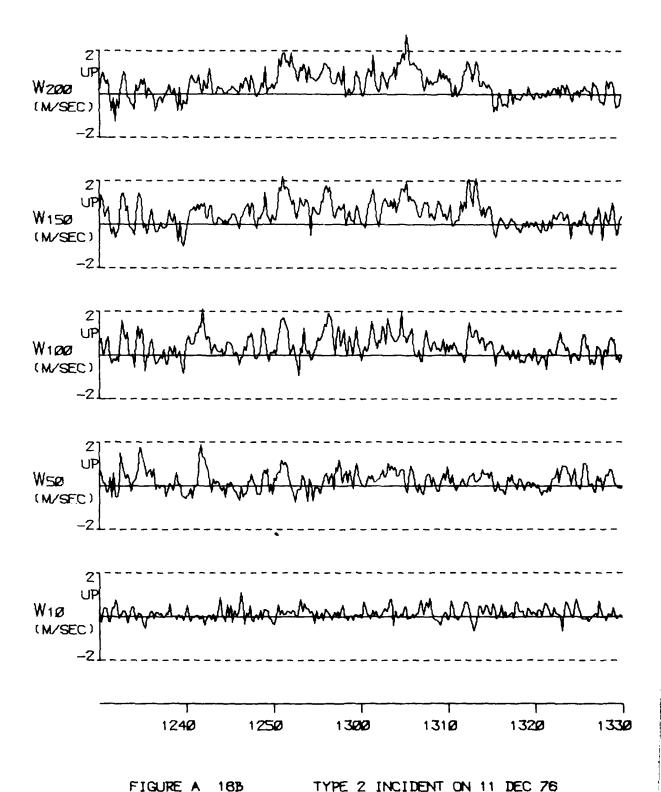
FIGURE A 17F   TYPE 3 INCIDENT ON 5 DEC 76

FIGURE A 18A   TYPE 2 INCIDENT ON 11 DEC 76

FIGURE A 18B   TYPE 2 INCIDENT ON 11 DEC 76
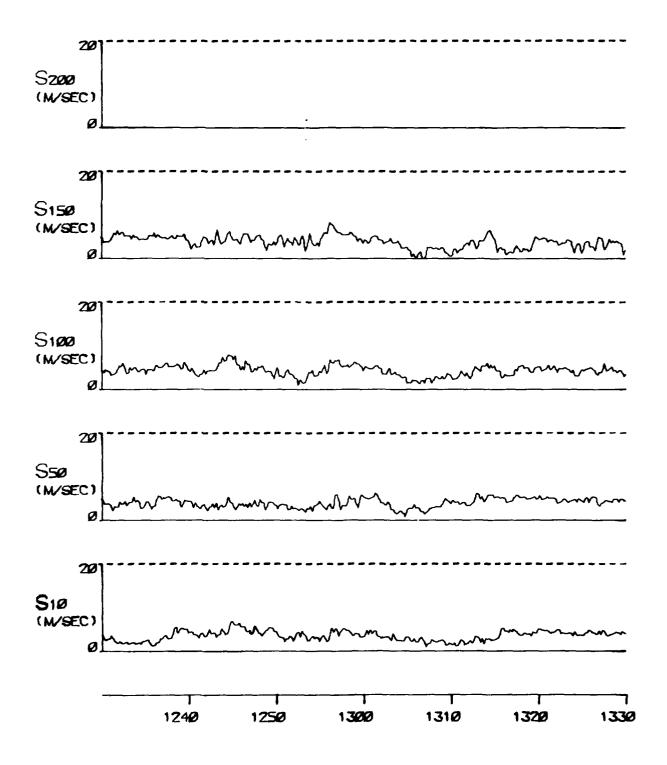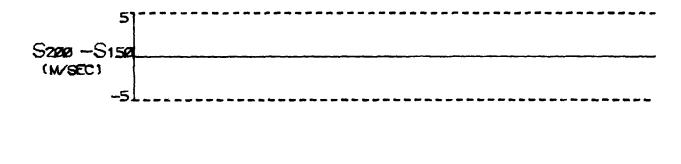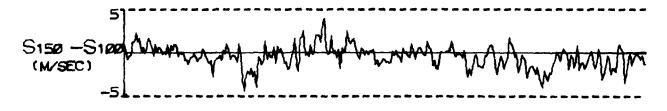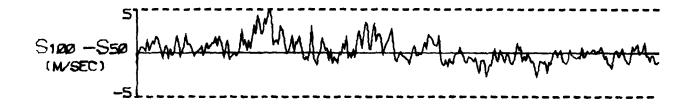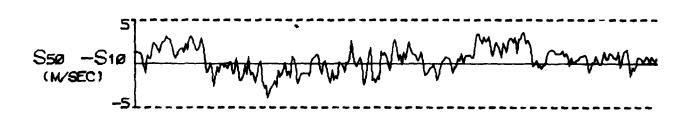
FIGURE A 16C   TYPE 2 INCIDENT ON 11 DEC 76
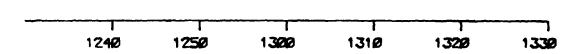
FIGURE A 18D   TYPE 2 INCIDENT ON 11 DEC 76
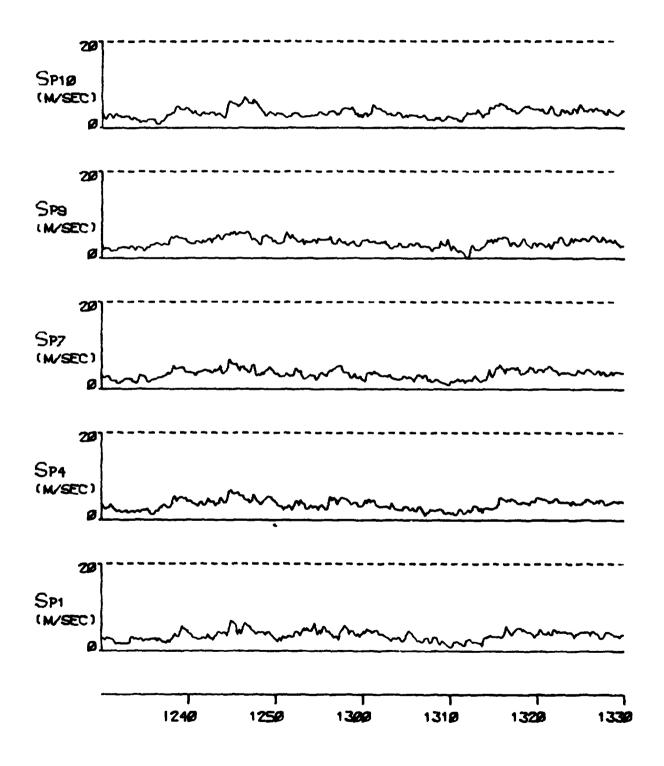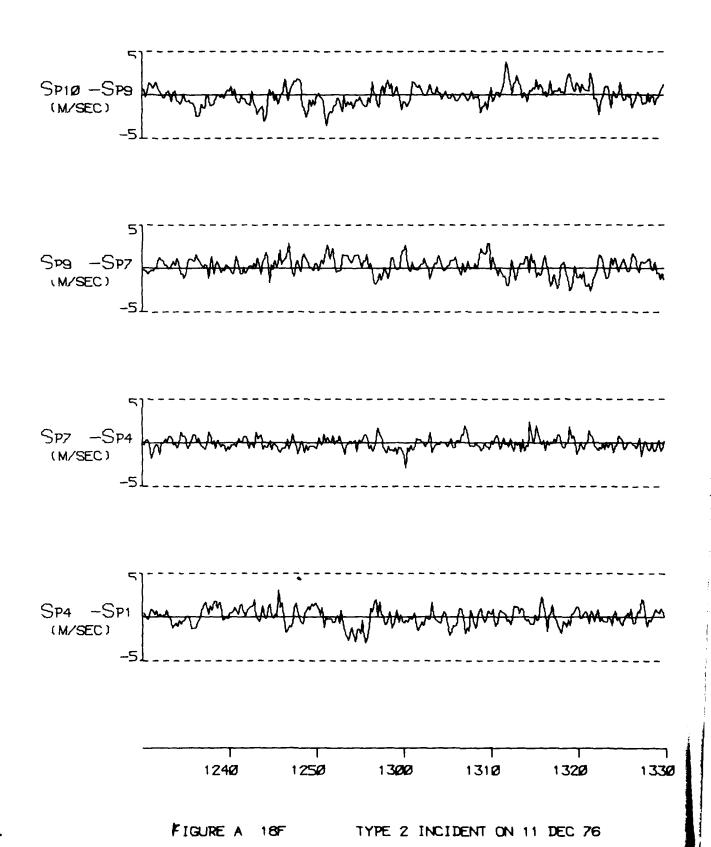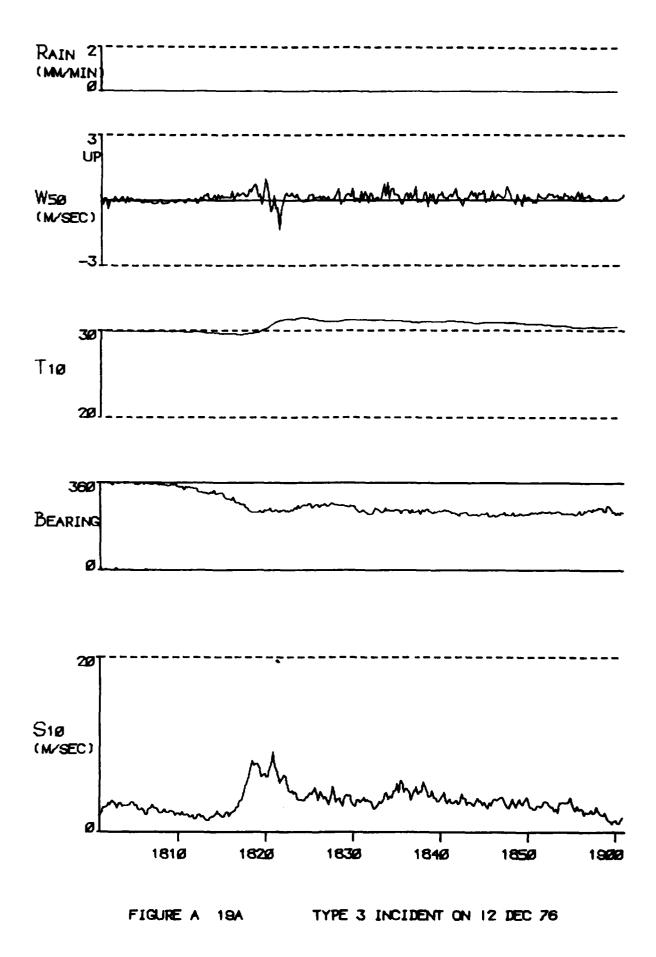
FIGURE A 16E   TYPE 2 INCIDENT ON 11 DEC 76
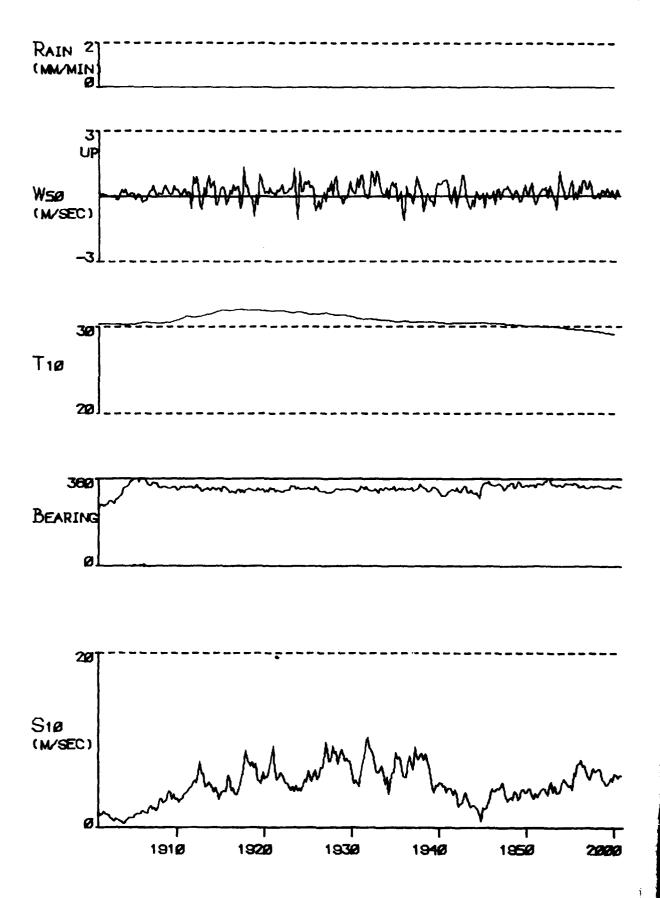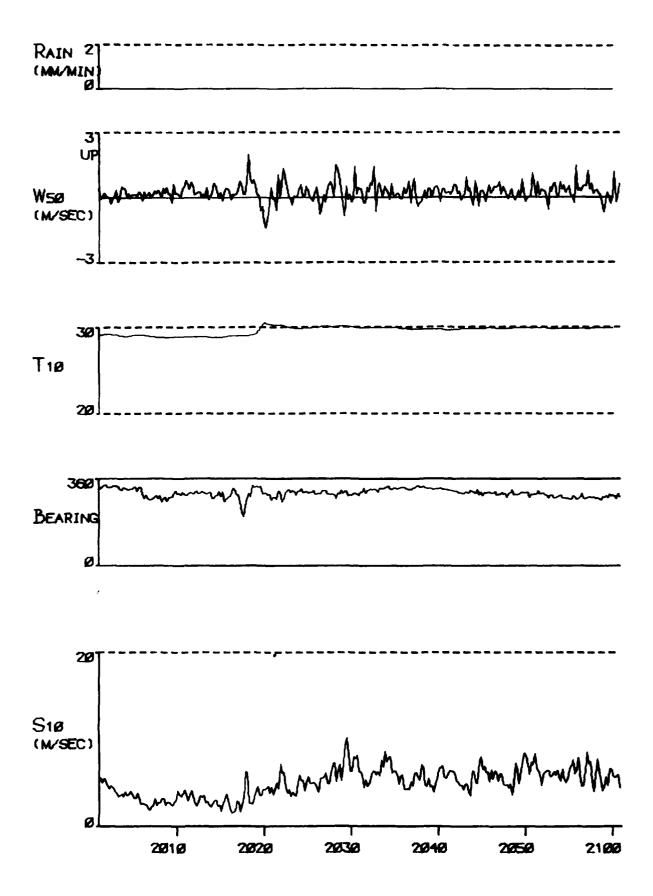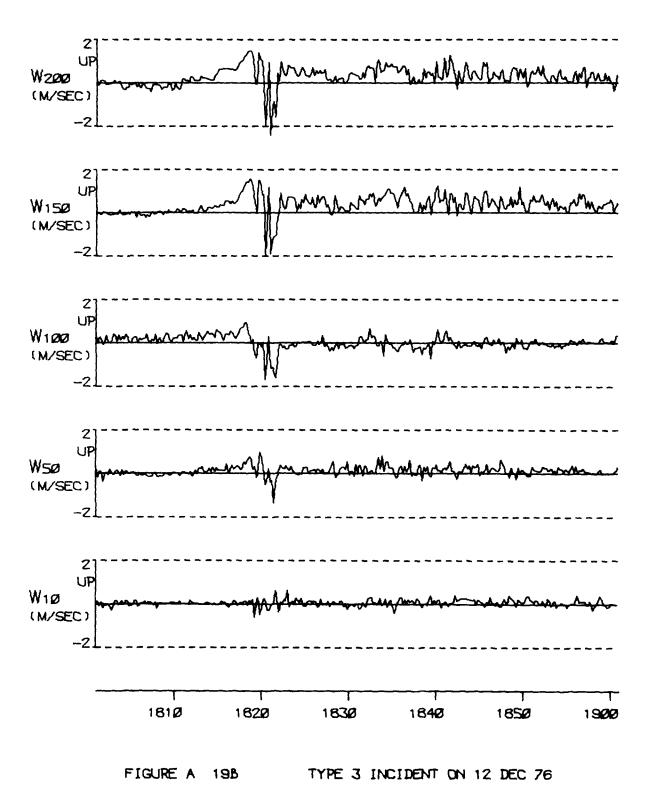
FIGURE A 18F   TYPE 2 INCIDENT ON 11 DEC 76

FIGURE A 19A   TYPE 3 INCIDENT ON 12 DEC 76

FIGURE A 19A (CONT) TYPE 3 INCIDENT ON 12 DEC 76

FIGURE A 19A (CONT) TYPE 3 INCIDENT ON 12 DEC 76

FIGURE A   19B   TYPE 3 INCIDENT ON 12 DEC 76

FIGURE A 19B (CONT) TYPE 3 INCIDENT ON 12 DEC 76

FIGURE A 19B (CONT) TYPE 3 INCIDENT ON 12 DEC 76
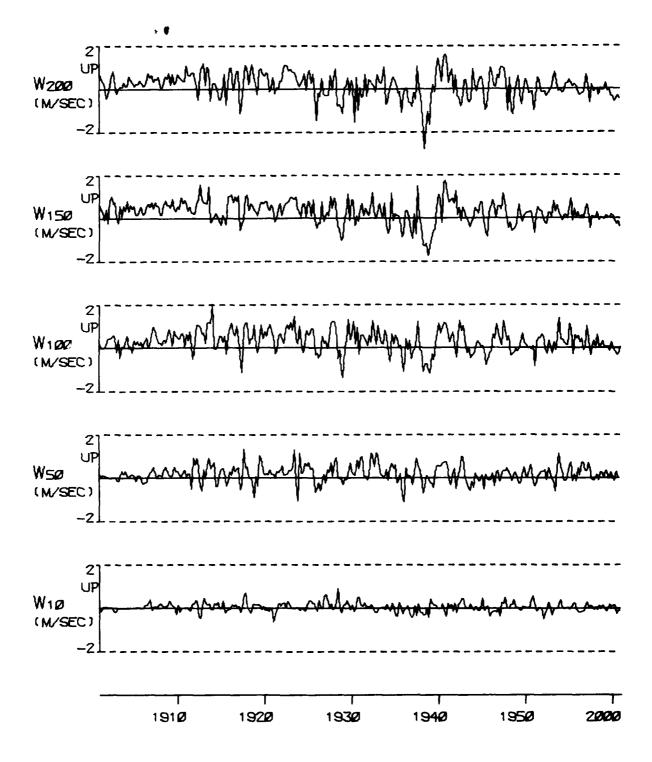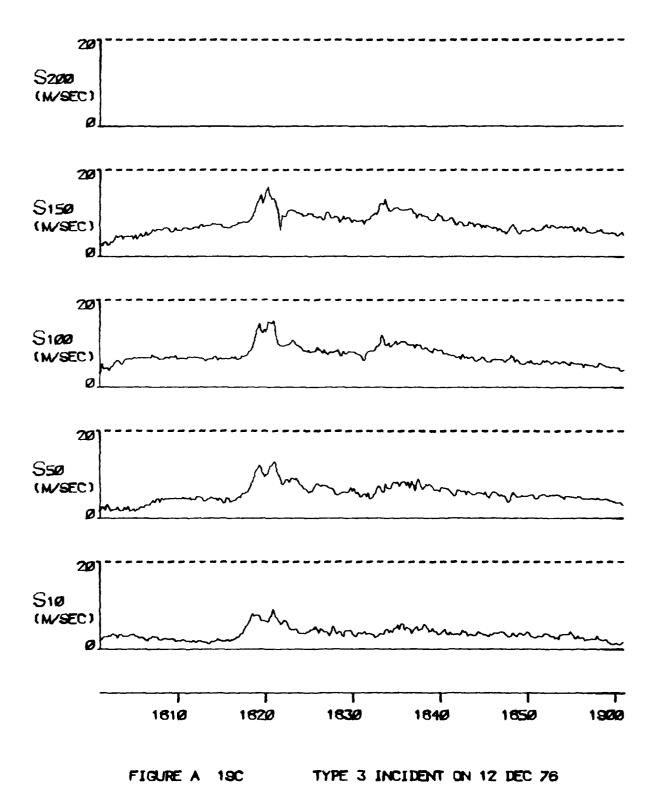
FIGURE A 19C   TYPE 3 INCIDENT ON 12 DEC 76

FIGURE A 19C (CONT) TYPE 3 INCIDENT ON 12 DEC 76
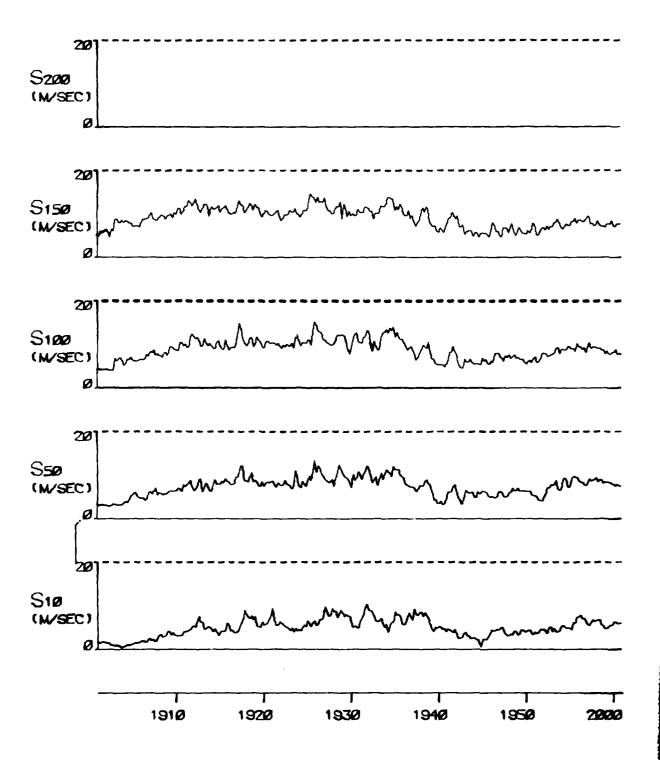
FIGURE A   19C (CONT) TYPE 3 INCIDENT ON 12 DEC 76
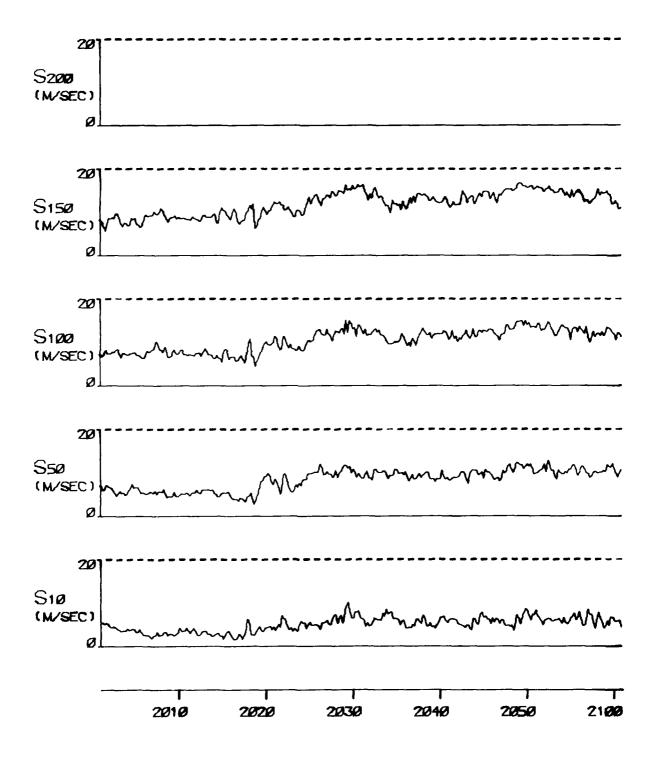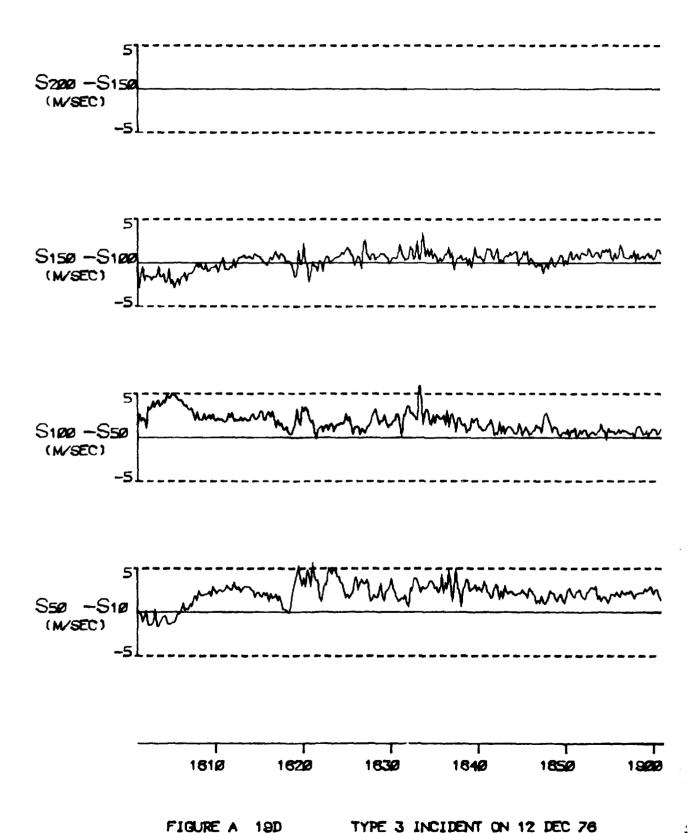
FIGURE A 19D   TYPE 3 INCIDENT ON 12 DEC 76
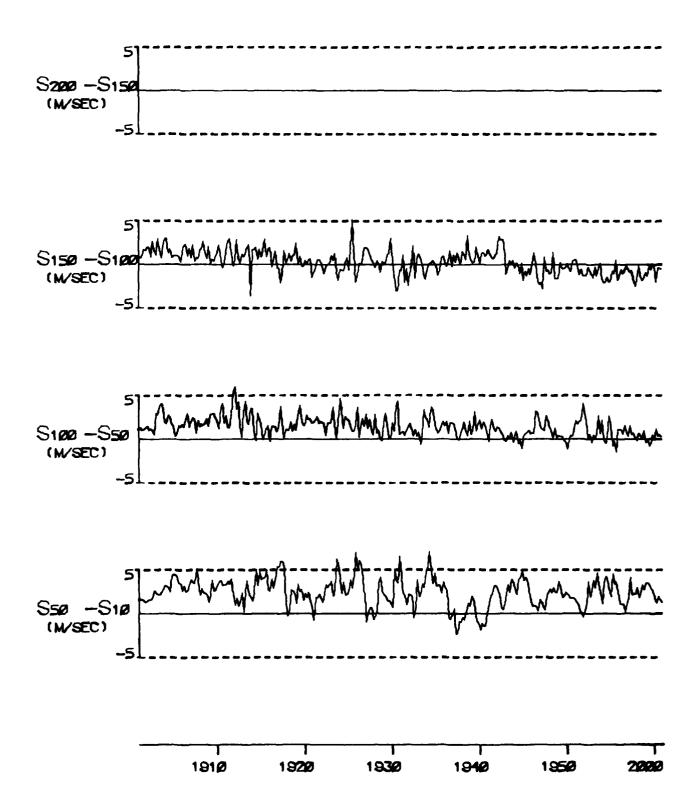
FIGURE A 19D (CONT) TYPE 3 INCIDENT ON 12 DEC 76
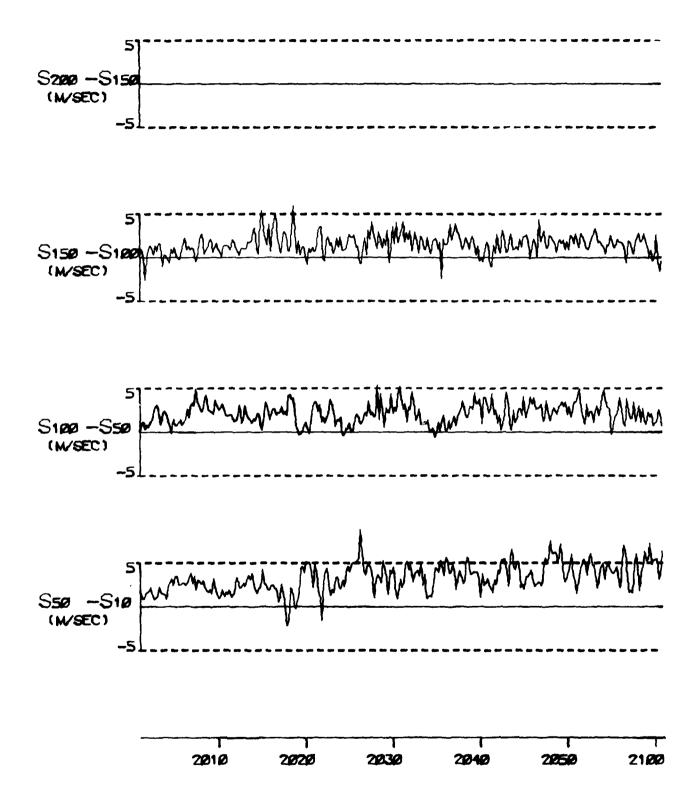
FIGURE A 19D (CONT) TYPE 3 INCIDENT ON 12 DEC 76
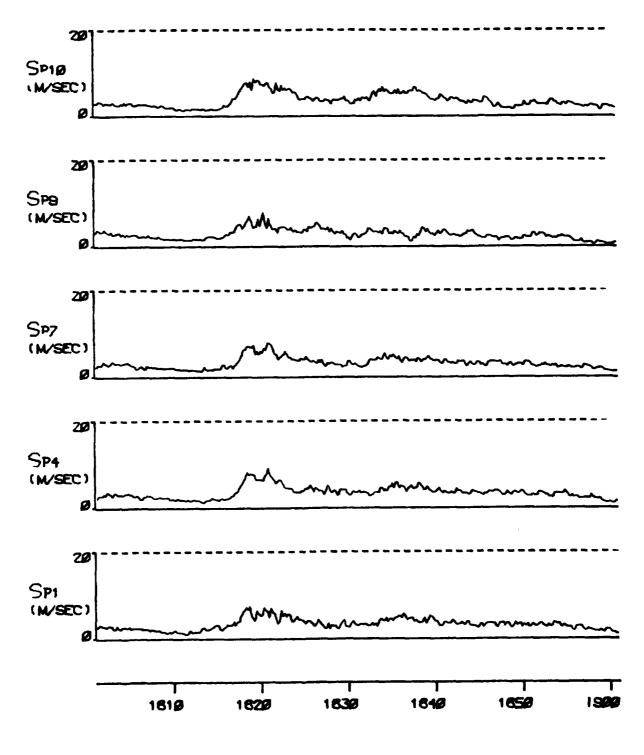
FIGURE A 1SE   TYPE 3 INCIDENT ON 12 DEC 78

FIGURE A 1SE (CONT) TYPE 3 INCIDENT ON 12 DEC 76
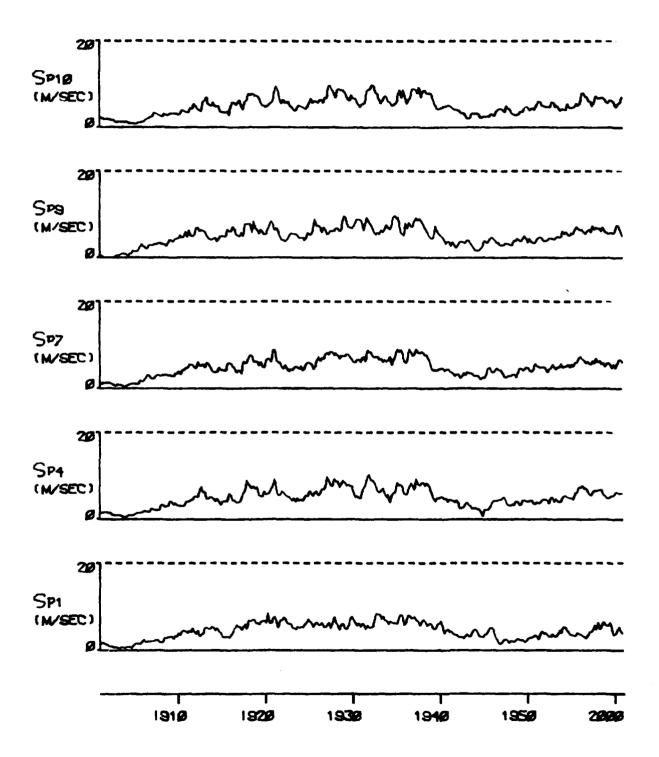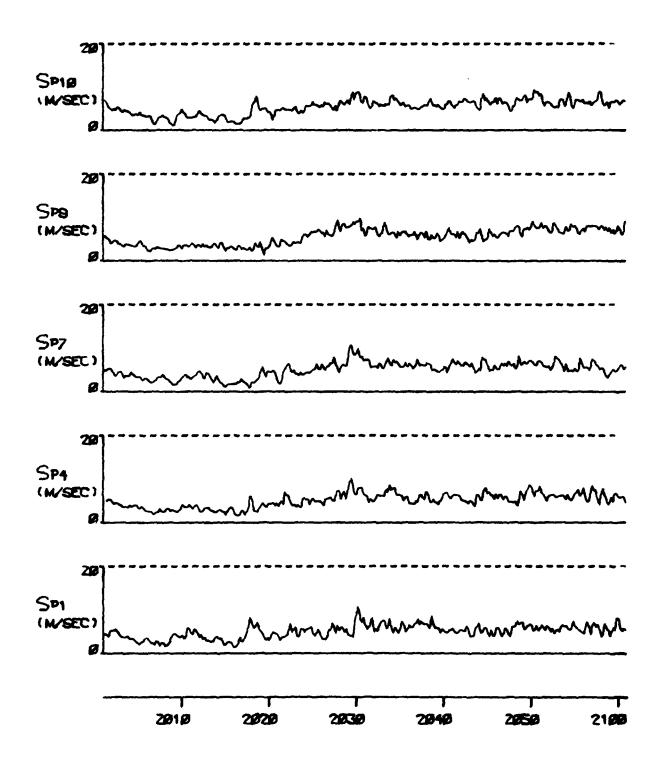
FIGURE A 18E (CONT) TYPE 3 INCIDENT ON 12 DEC 76

C235
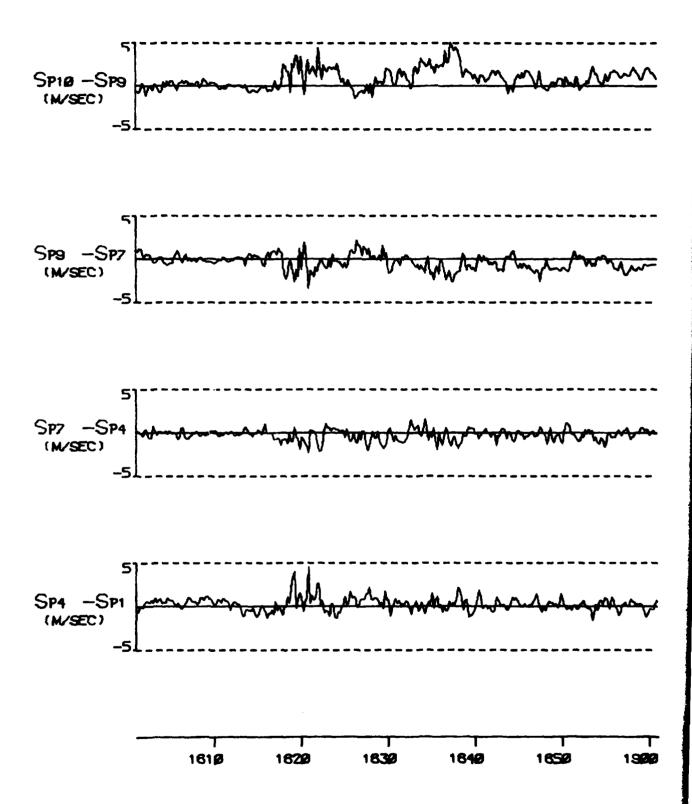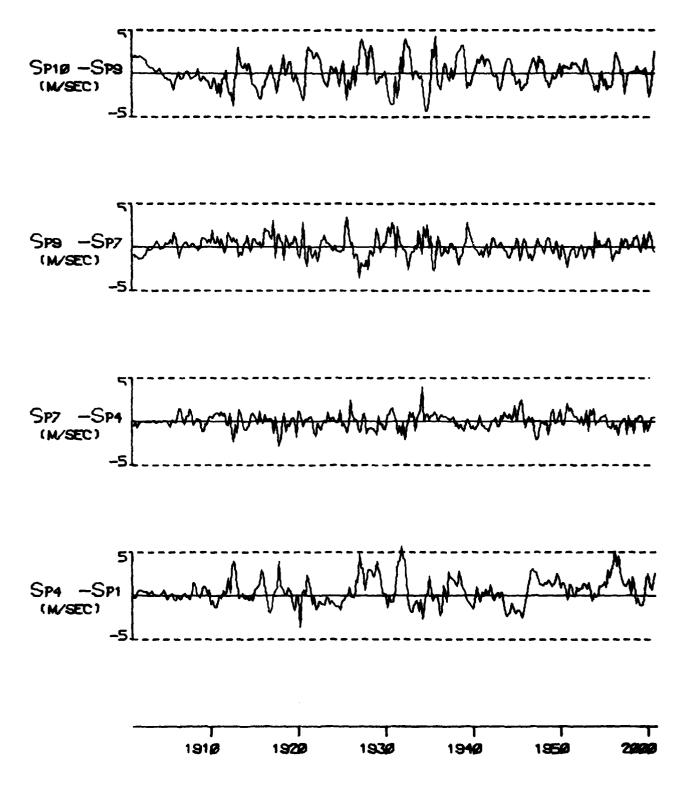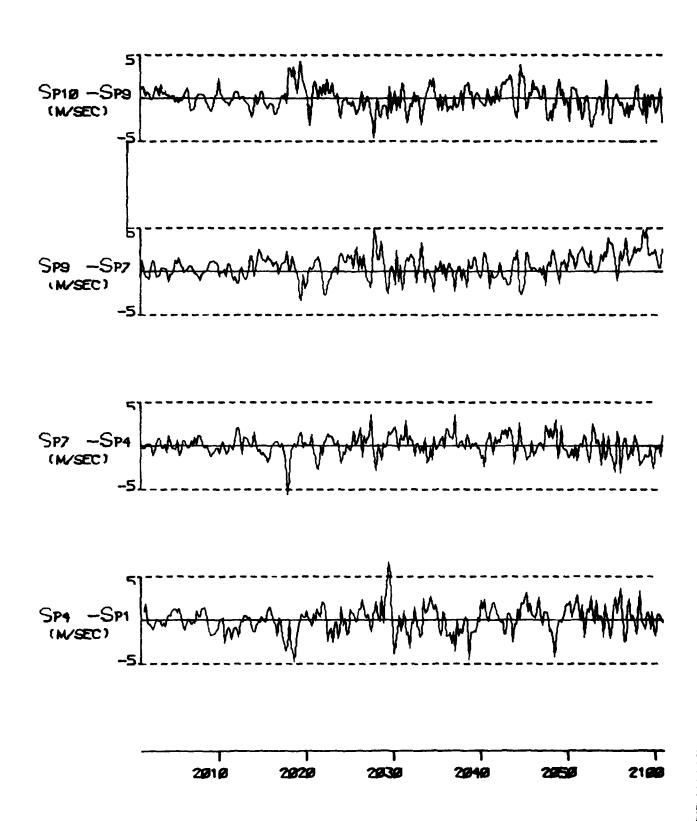
FIGURE A 19F   TYPE 3 INCIDENT ON 12 DEC 76

FIGURE A 19F (CONT) TYPE 3 INCIDENT ON 12 DEC 76
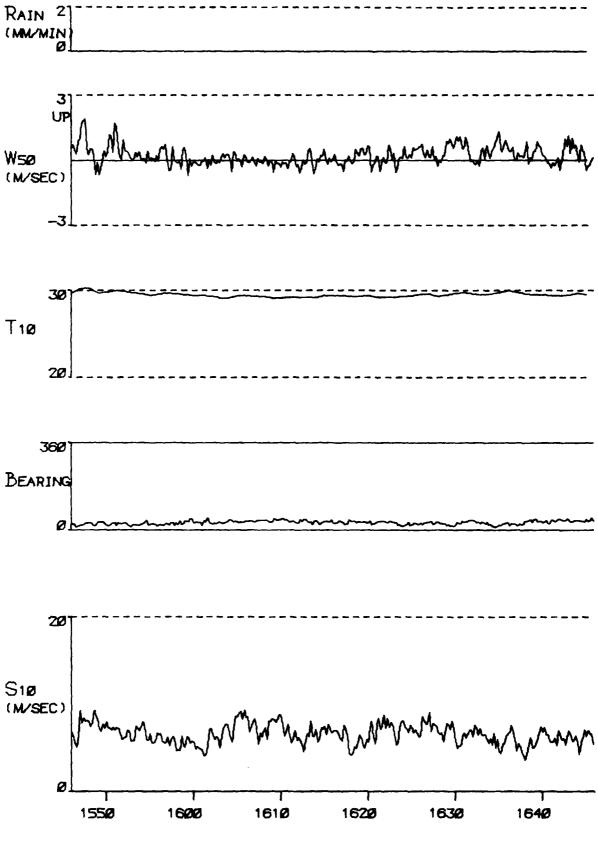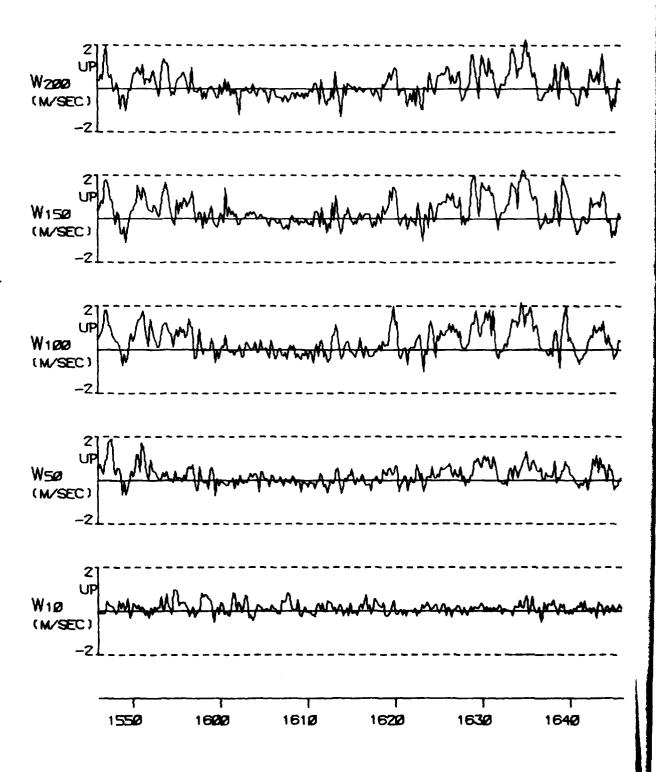
C233

FIGURE A 1SF (CONT) TYPE 3 INCIDENT ON 12 DEC 76

FIGURE A 20A   TYPE 4 INCIDENT ON 15 DEC 78
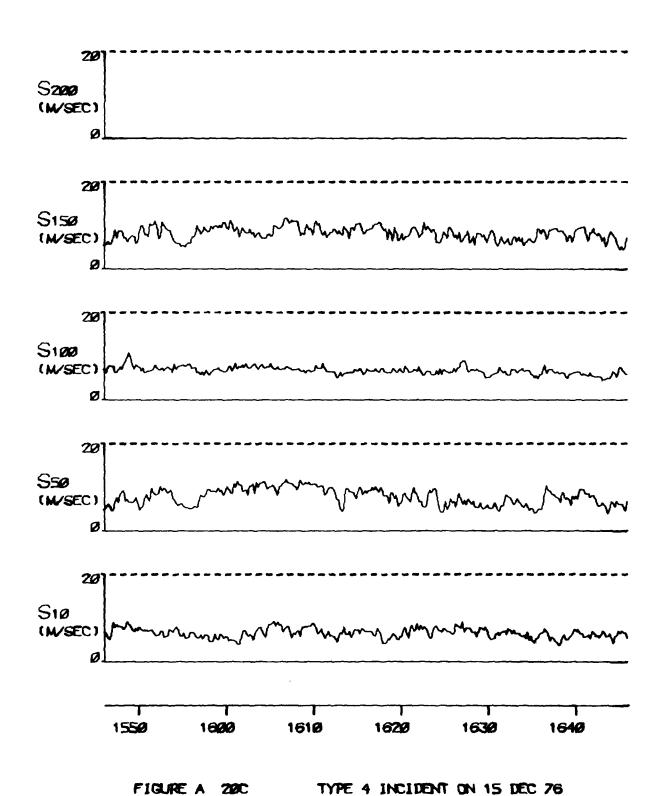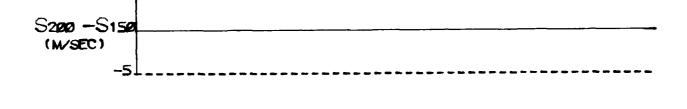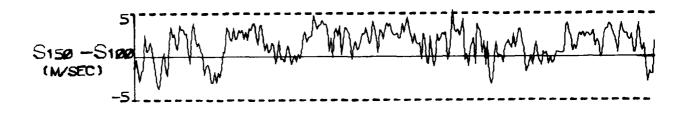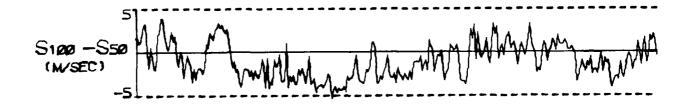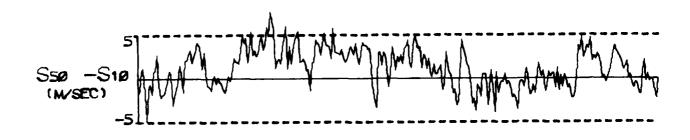
C236

FIGURE A 20B   TYPE 4 INCIDENT ON 15 DEC 76
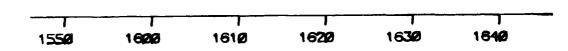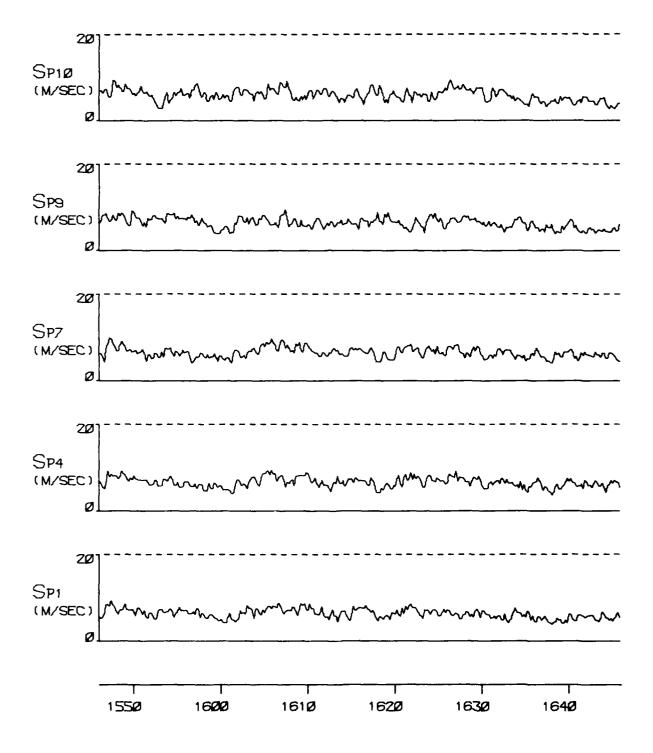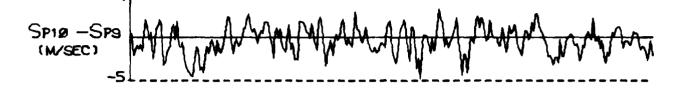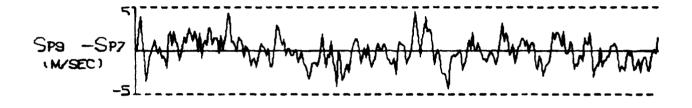
FIGURE A 20C   TYPE 4 INCIDENT ON 15 DEC 76
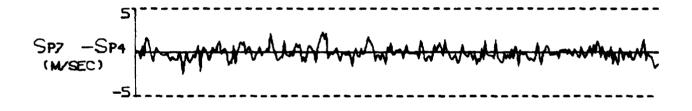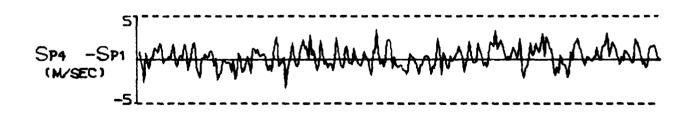
FIGURE A 20D   TYPE 4 INCIDENT ON 15 DEC 76

FIGURE A 20E   TYPE 4 INCIDENT ON 15 DEC 76
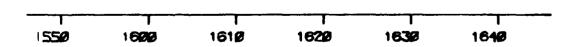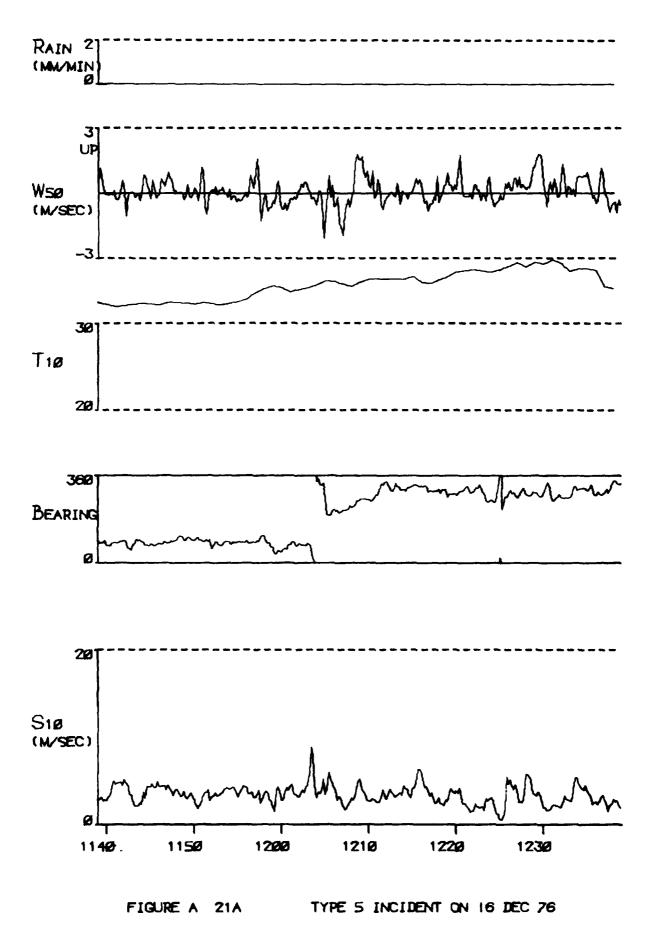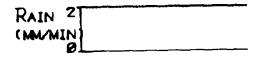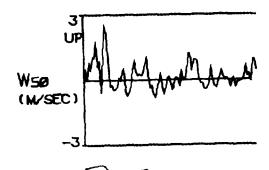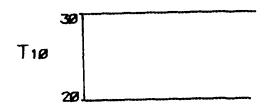
FIGURE A 20F   TYPE 4 INCIDENT ON 15 DEC 76

FIGURE A 21A   TYPE 5 INCIDENT ON 16 DEC 76
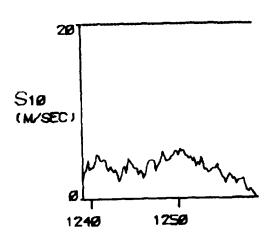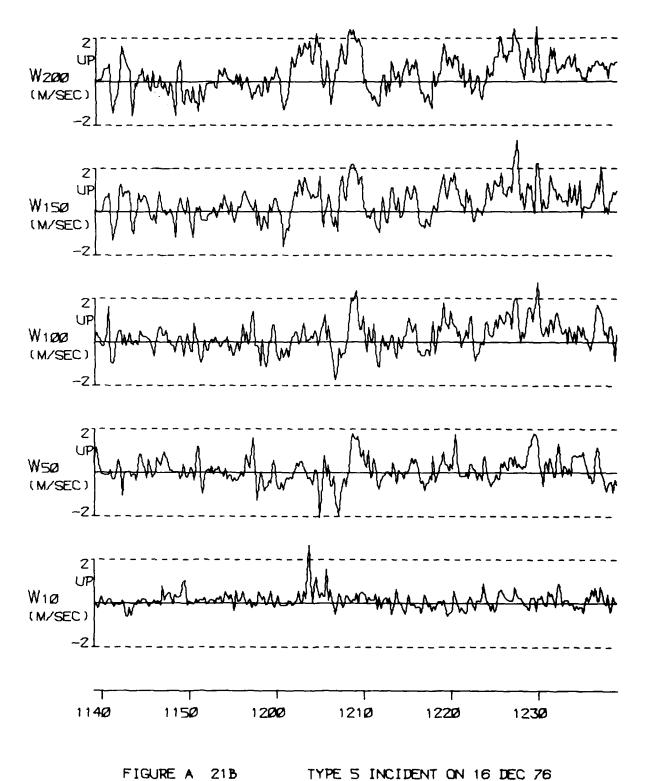
FIGURE A 21A (CONT) TYPE 5 INCIDENT ON 16 DEC 76

FIGURE A 21B   TYPE 5 INCIDENT ON 16 DEC 76
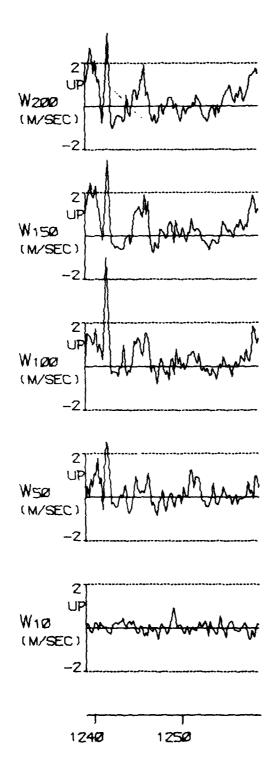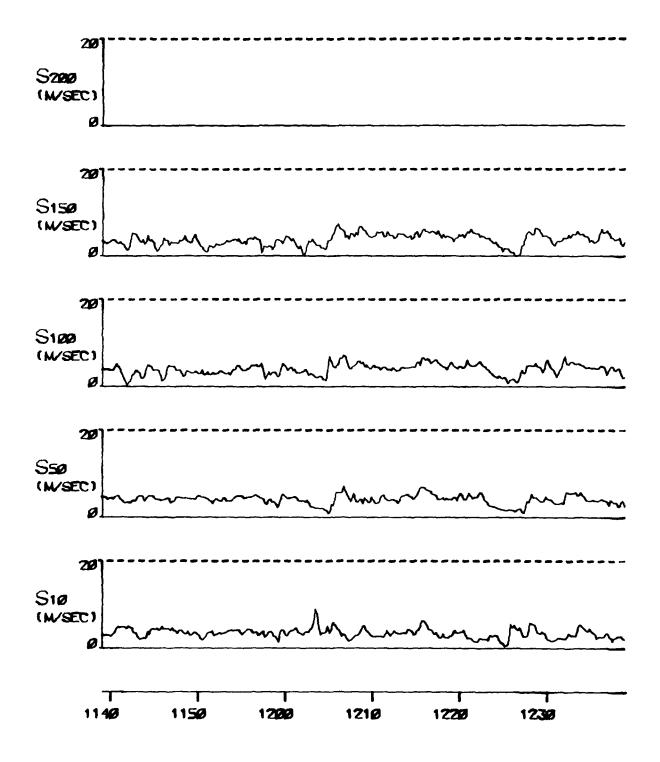
FIGURE A 21B (CONT) TYPE 5 INCIDENT ON 16 DEC 76

FIGURE A 21C   TYPE 5 INCIDENT ON 16 DEC 76

C23/
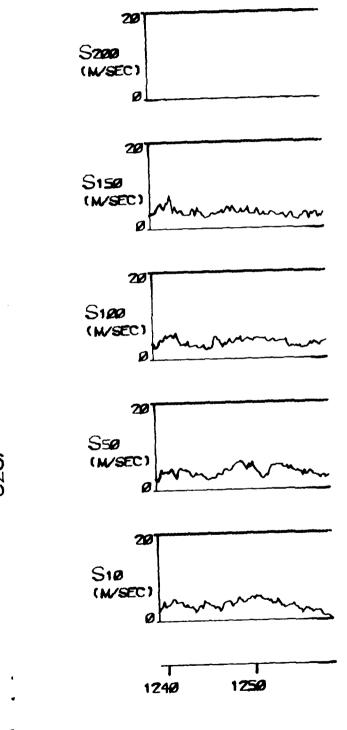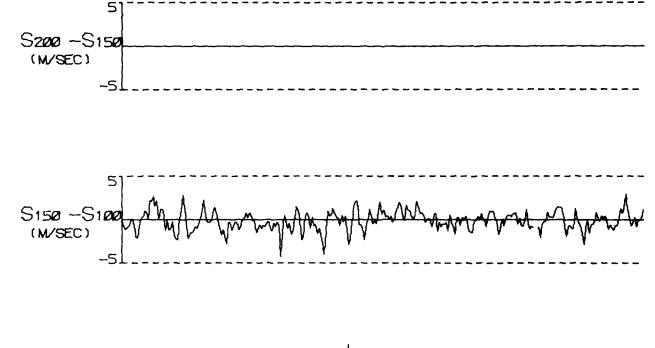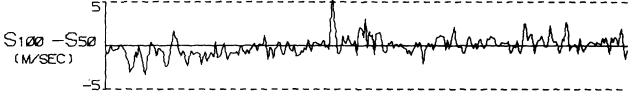
FIGURE A 21C (CONT) TYPE 5 INCIDENT ON 16 DEC 76
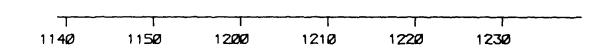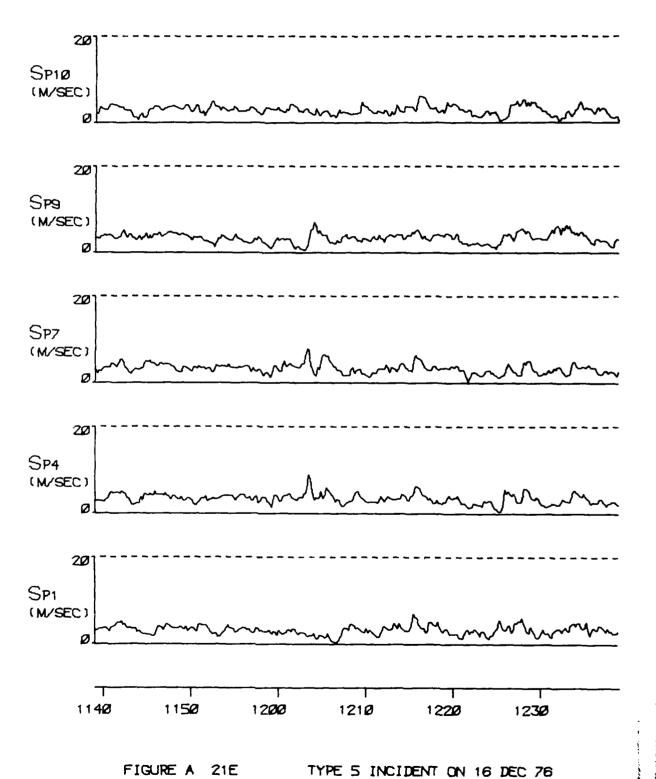
FIGURE A 21D   TYPE 5 INCIDENT ON 16 DEC 76

FIGURE A 21E   TYPE 5 INCIDENT ON 16 DEC 76
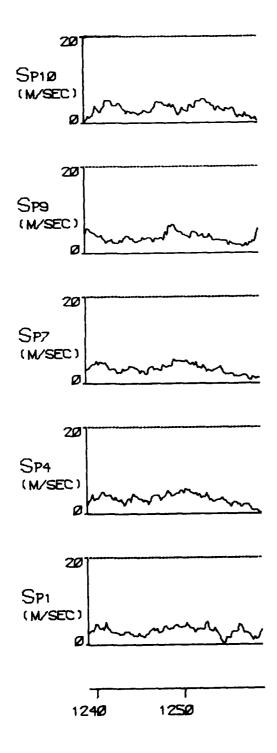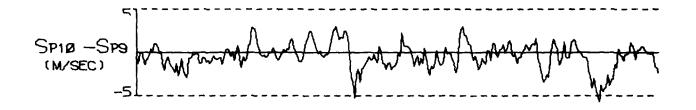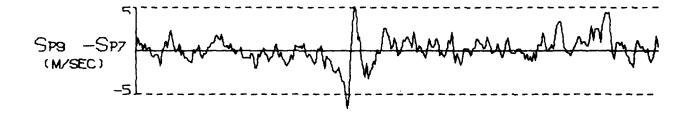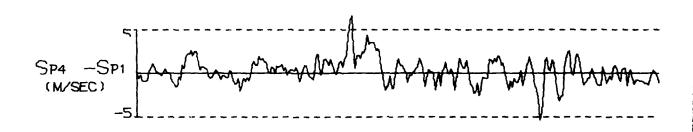
FIGURE A 21E (CONT) TYPE 5 INCIDENT ON 16 DEC 76
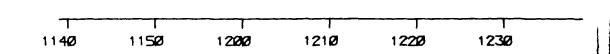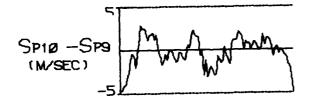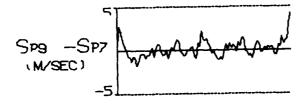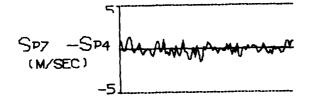
FIGURE A 21F   TYPE 5 INCIDENT ON 16 DEC 76
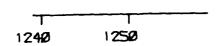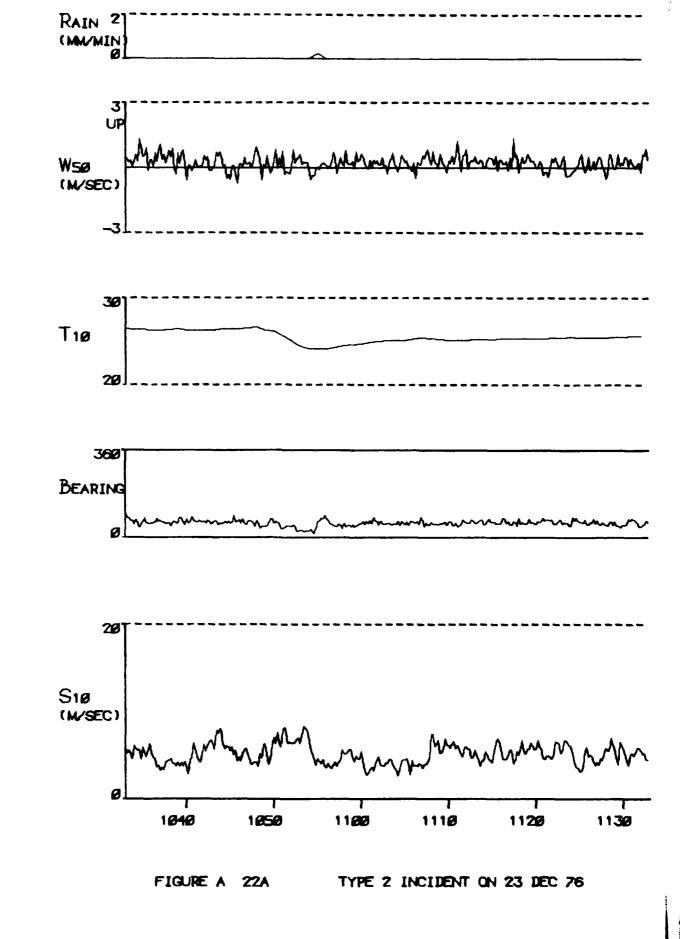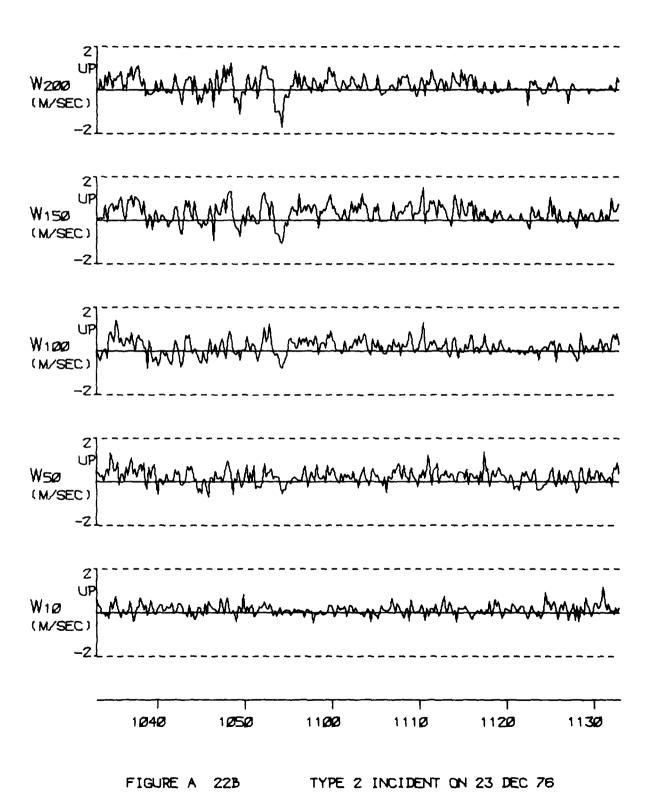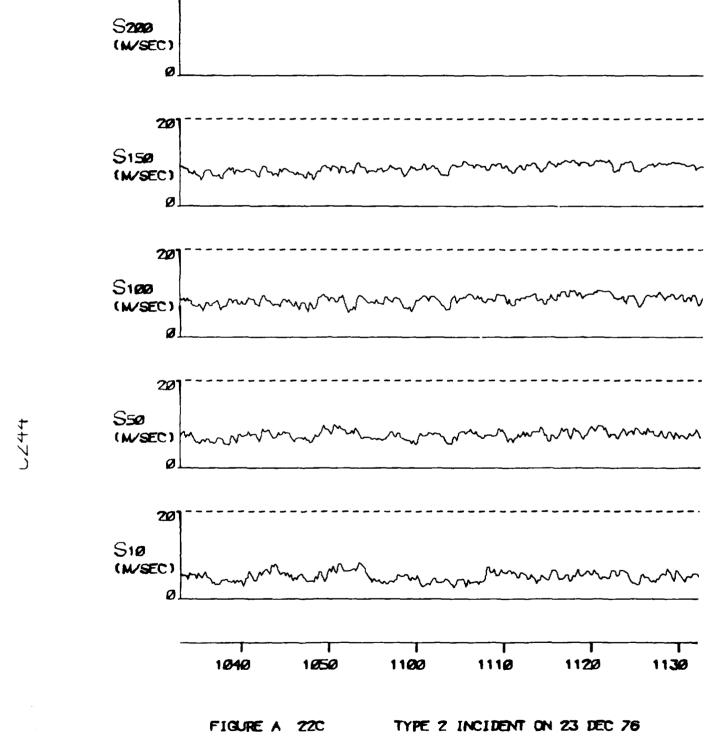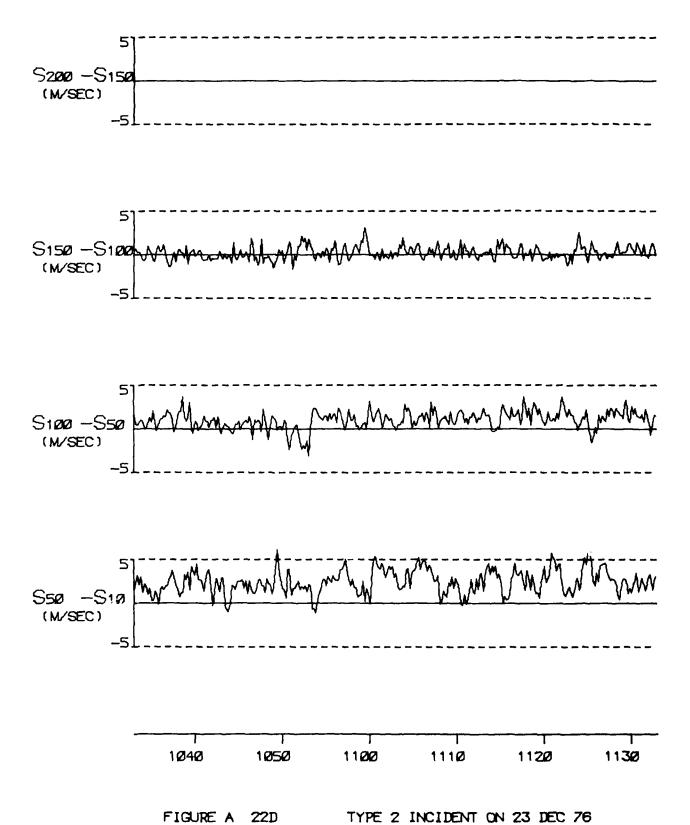
FIGURE A 21F (CONT) TYPE 5 INCIDENT ON 16 DEC 76

RAIN 2
(MM/MIN) 0

3
UP
W50
(M/SEC)
-3

30
T10
20

360
BEARING
0

20
S10
(M/SEC)
0

1040   1050   1100   1110   1120   1130

FIGURE A 22A   TYPE 2 INCIDENT ON 23 DEC 76

FIGURE A 22B   TYPE 2 INCIDENT ON 23 DEC 76

FIGURE A 22C   TYPE 2 INCIDENT ON 23 DEC 76

FIGURE A 22D   TYPE 2 INCIDENT ON 23 DEC 76
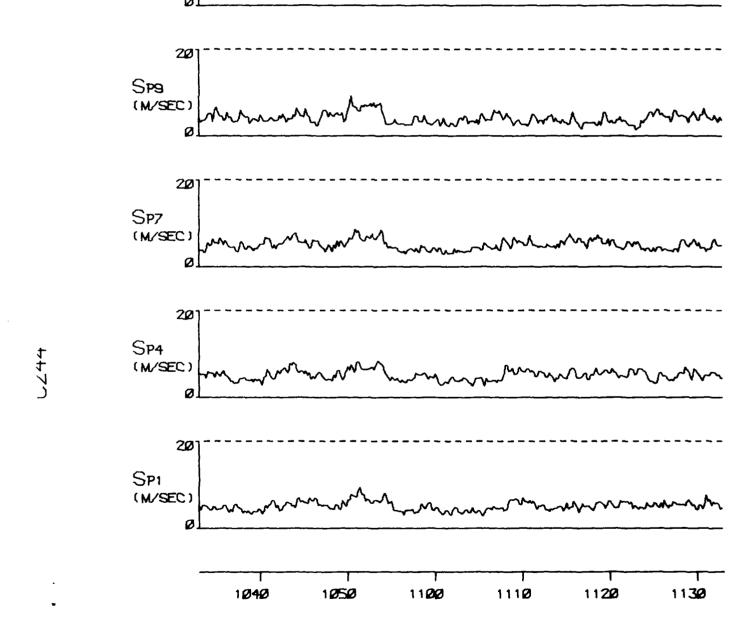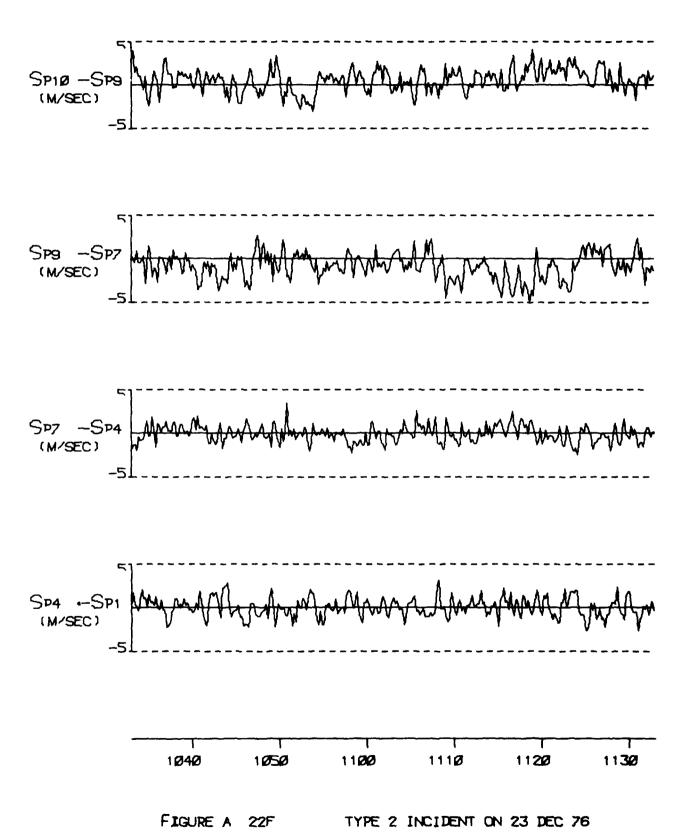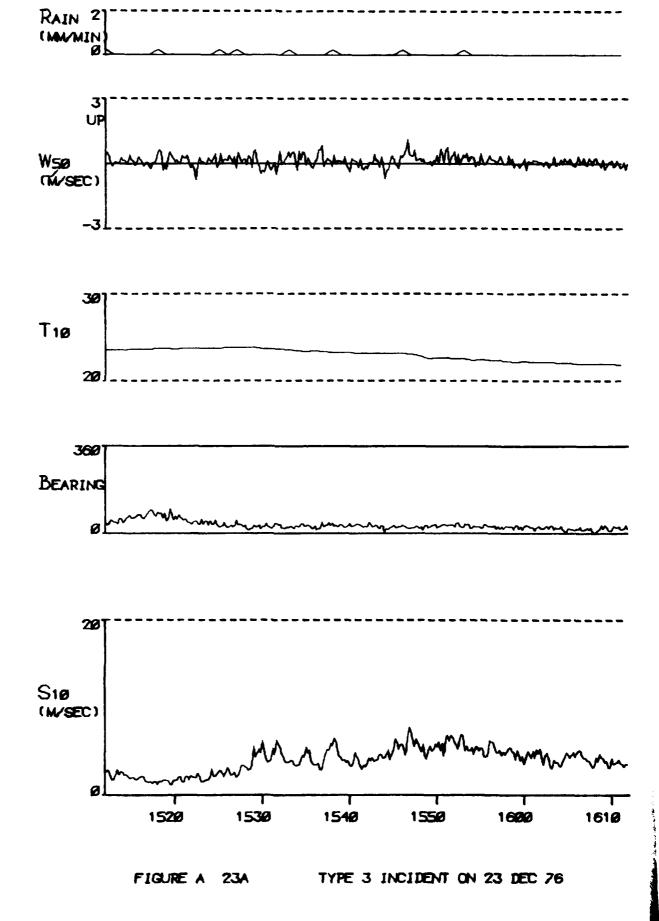
FIGURE A 22E   TYPE 2 INCIDENT ON 23 DEC 76

FIGURE A 22F   TYPE 2 INCIDENT ON 23 DEC 76

FIGURE A 23A   TYPE 3 INCIDENT ON 23 DEC 76
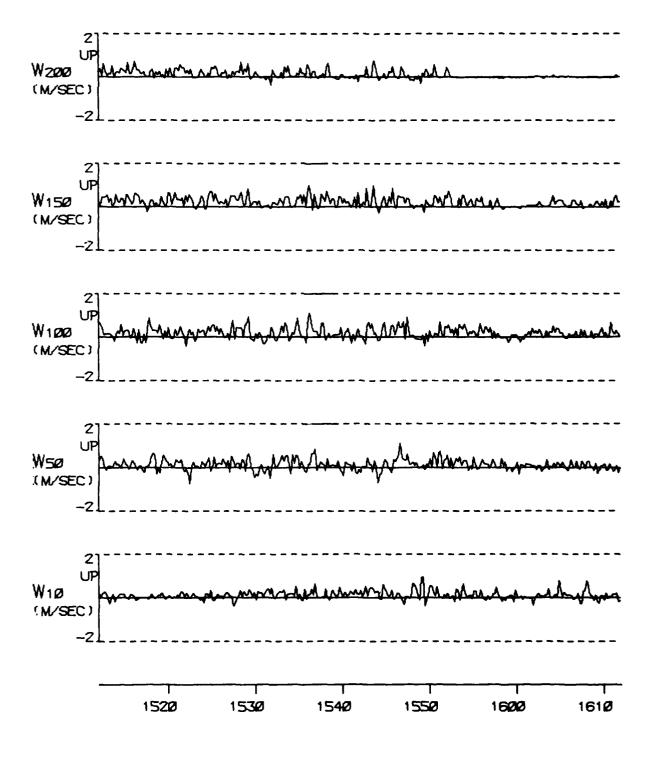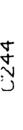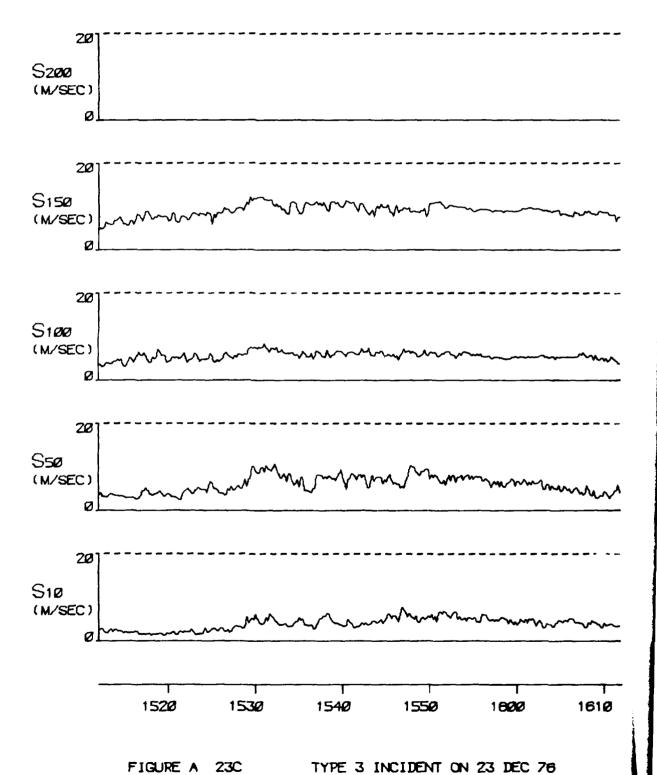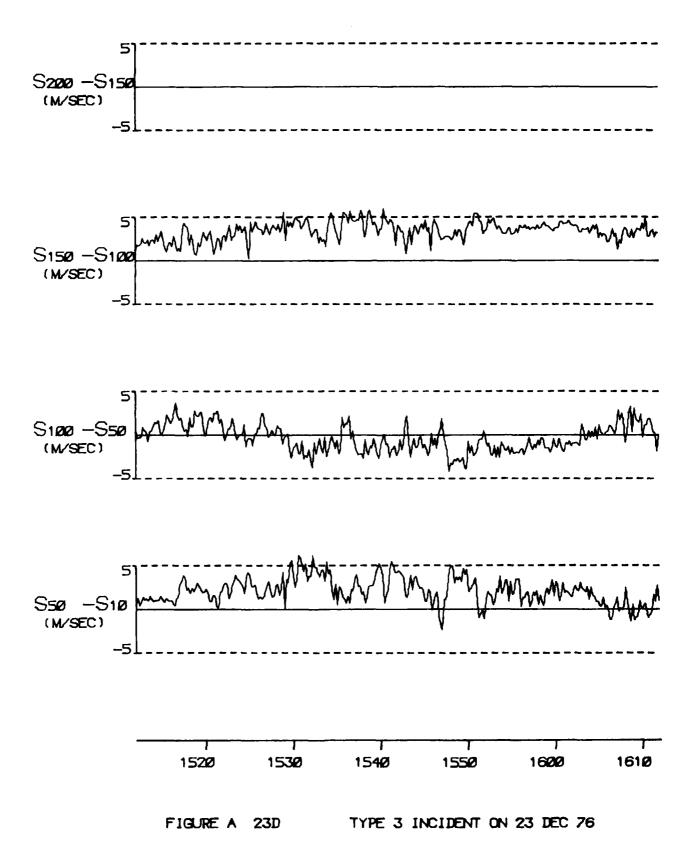
FIGURE A 23B   TYPE 3 INCIDENT ON 23 DEC 76

C244

FIGURE A 23C   TYPE 3 INCIDENT ON 23 DEC 76

FIGURE A 23D   TYPE 3 INCIDENT ON 23 DEC 76

C244

FIGURE A 23E   TYPE 3 INCIDENT ON 23 DEC 76

FIGURE A 23F   TYPE 3 INCIDENT ON 23 DEC 76

FIGURE A 24A   TYPE 3 INCIDENT ON 24 DEC 76

FIGURE A 24B   TYPE 3 INCIDENT ON 24 DEC 76
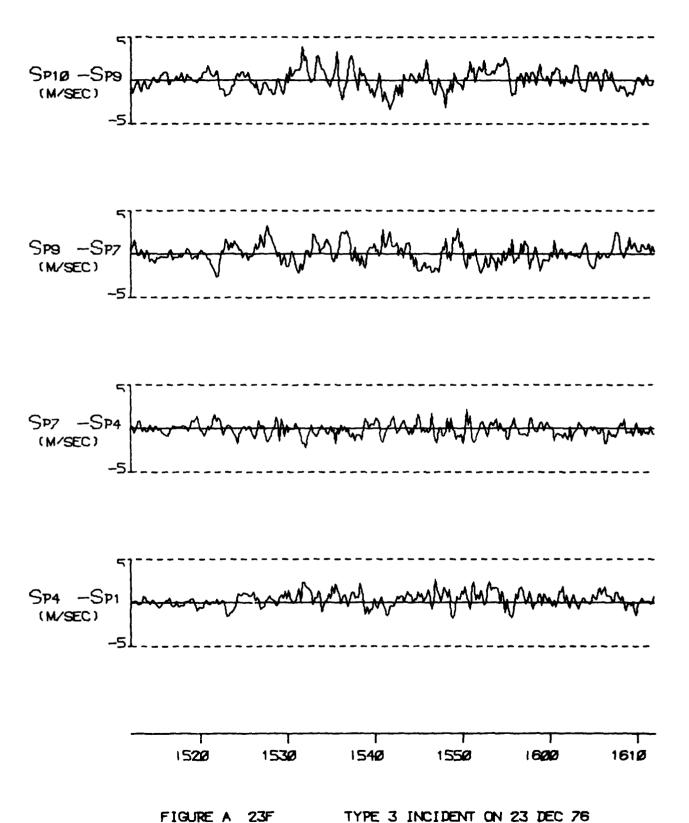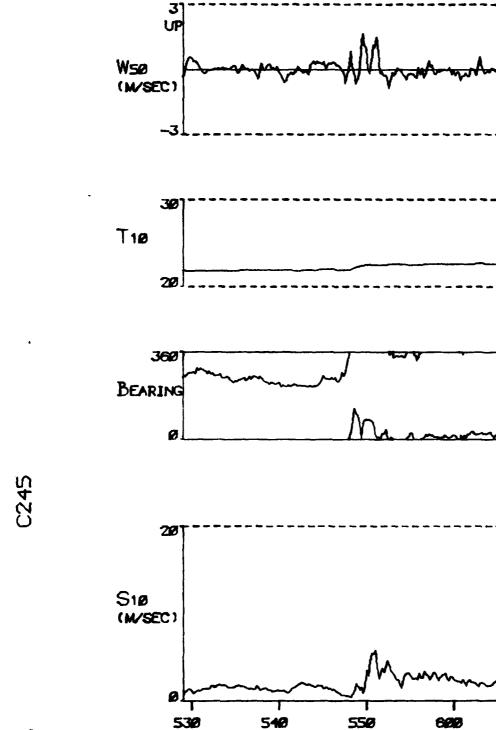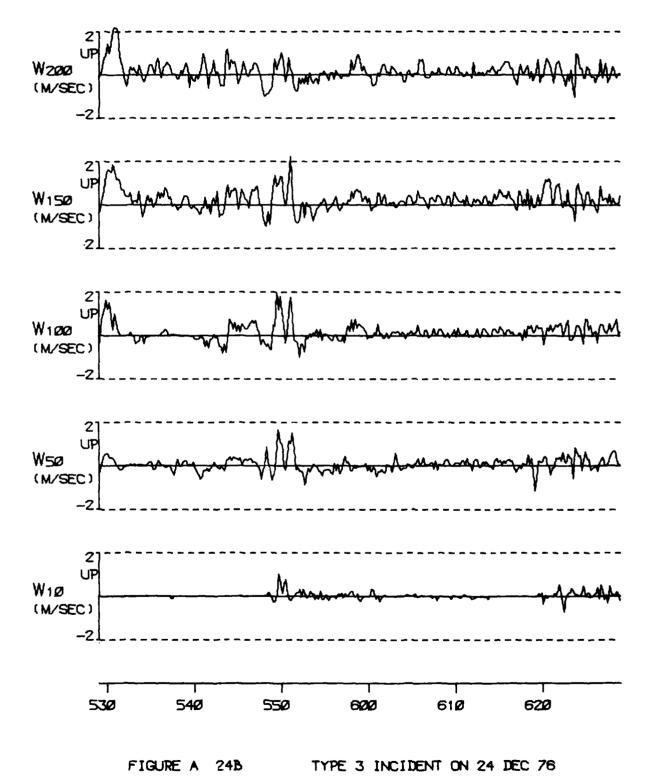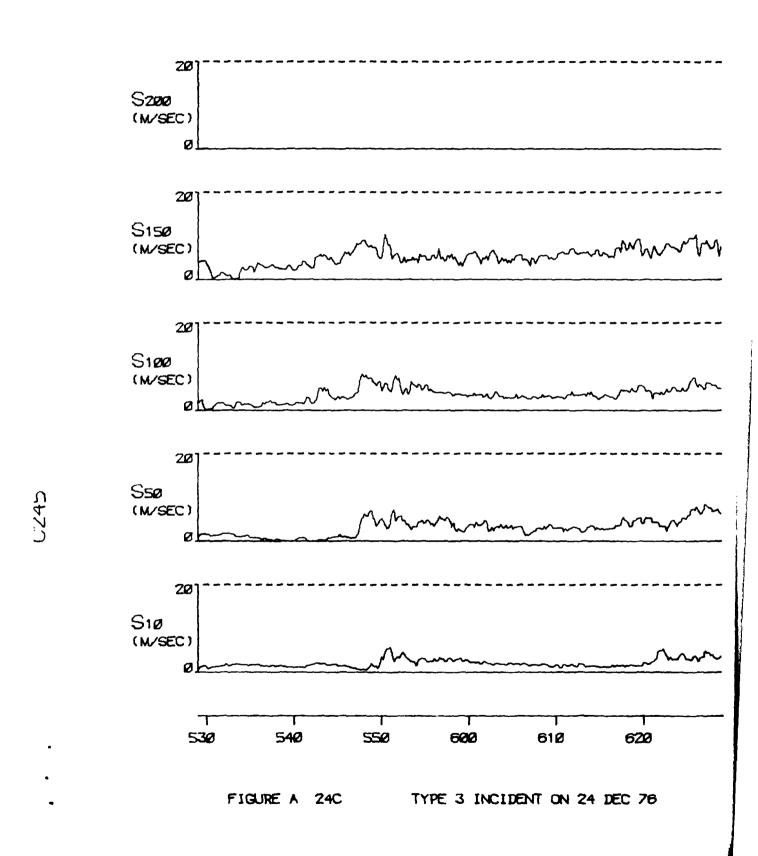
FIGURE A 24C   TYPE 3 INCIDENT ON 24 DEC 78
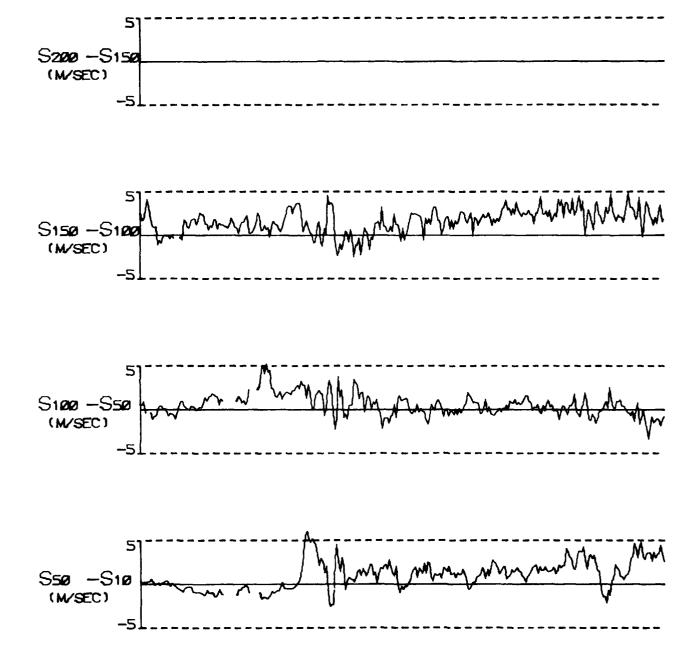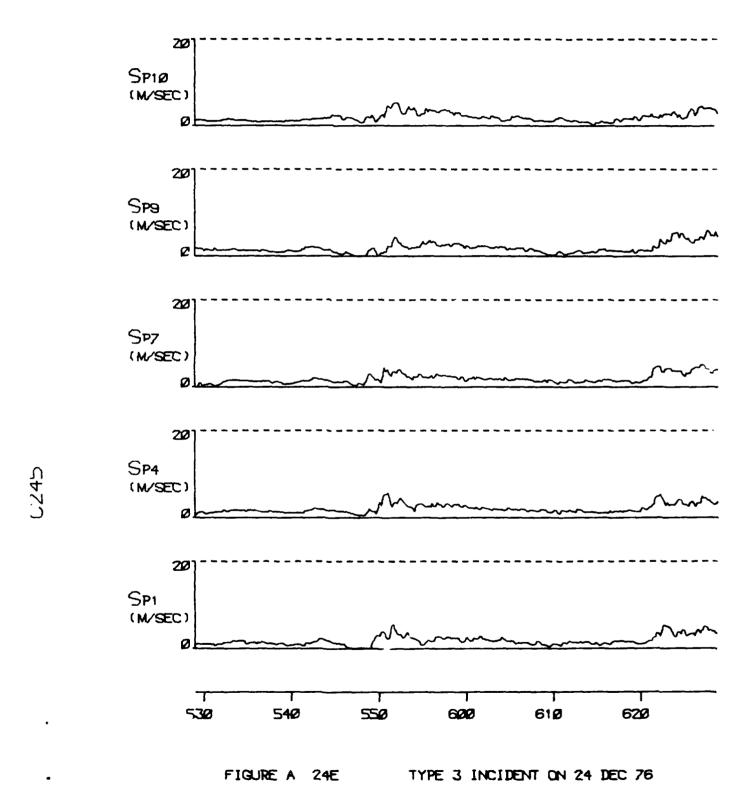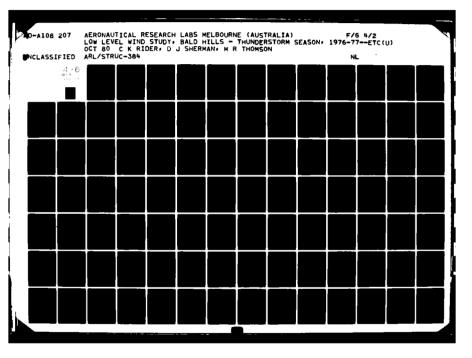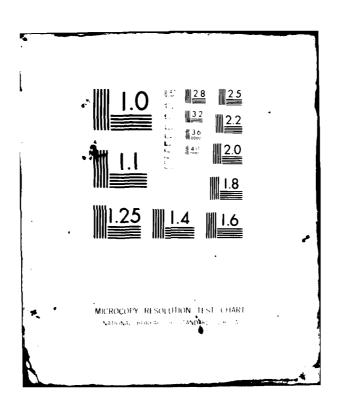
FIGURE A 24D   TYPE 3 INCIDENT ON 24 DEC 76

FIGURE A 24E   TYPE 3 INCIDENT ON 24 DEC 76

1.0

2 8 | 2 5

3 2 | 2.2

3 6

1.1 | 4 0 | 2.0

1.8

1.25 | 1.4 | 1.6

MICROCOPY RESOLUTION TEST CHART

NATIONAL BUREAU OF STANDARDS
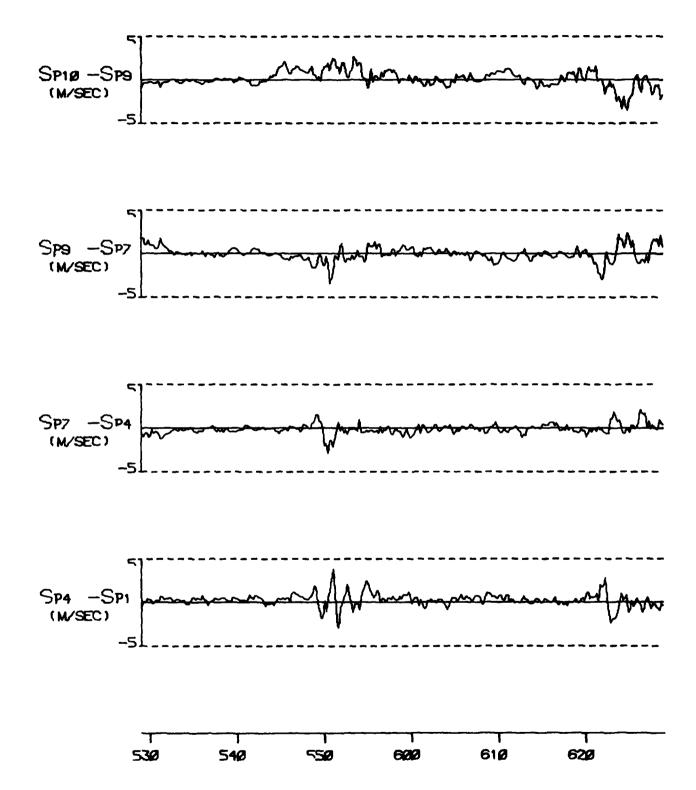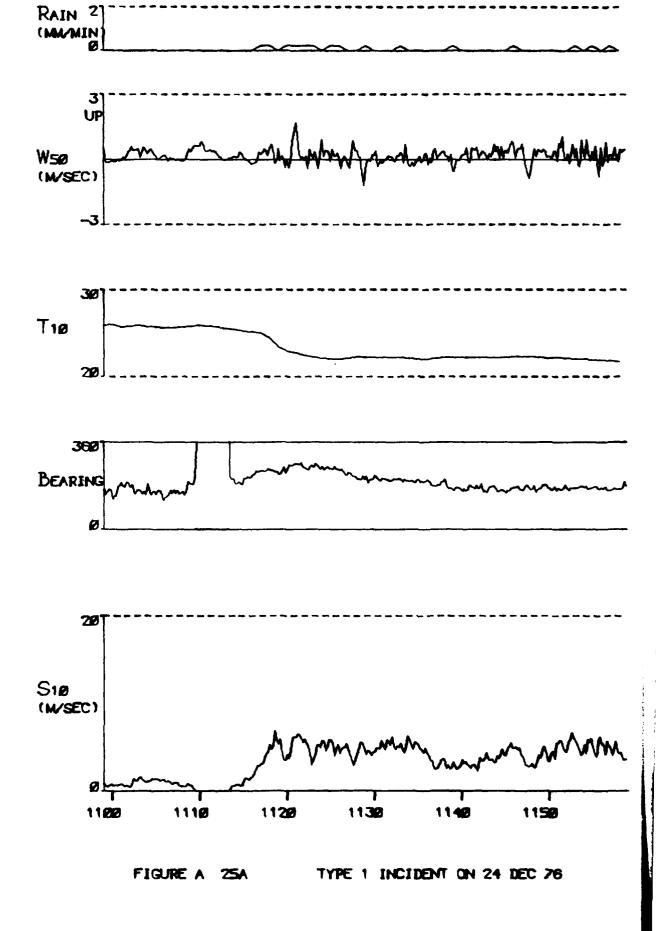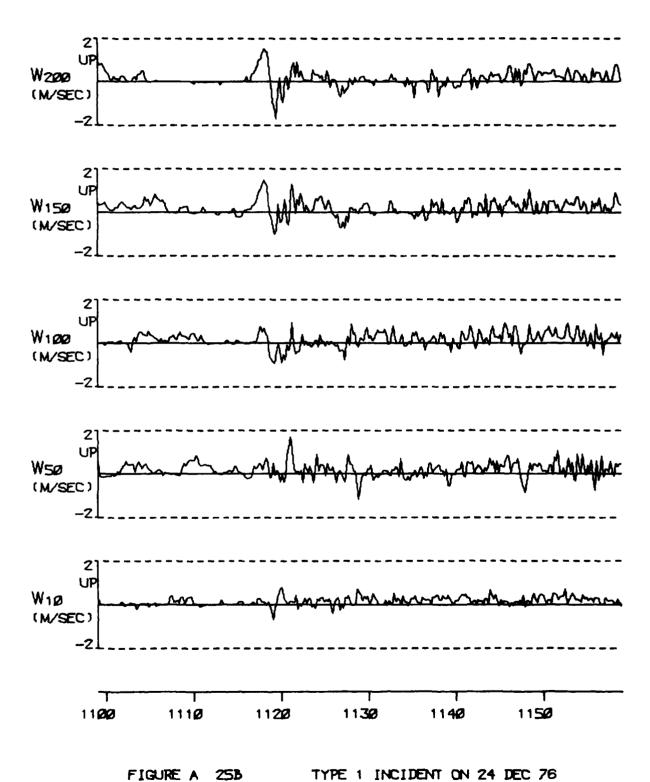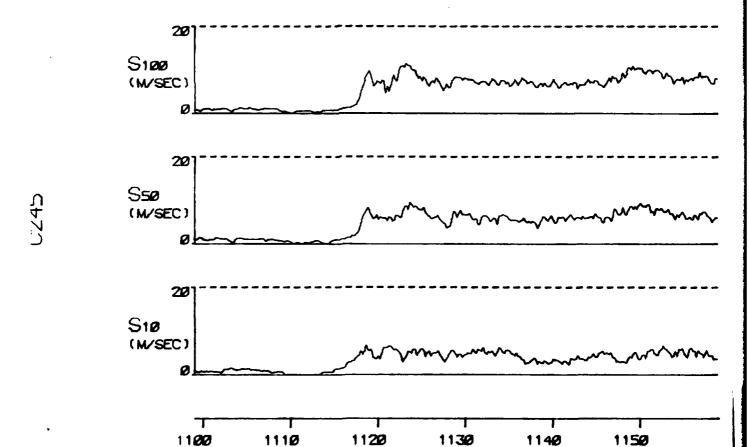
FIGURE A 24F   TYPE 3 INCIDENT ON 24 DEC 76
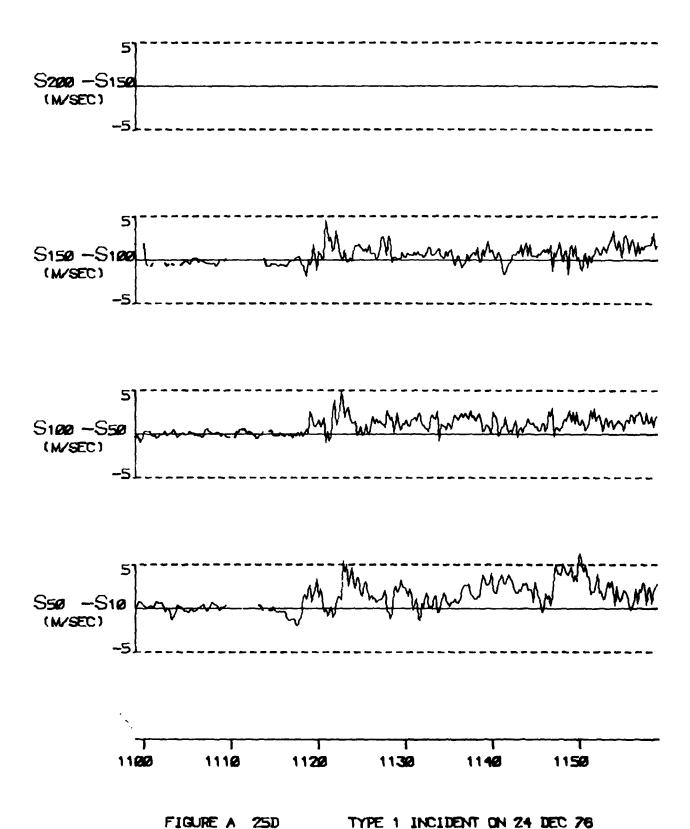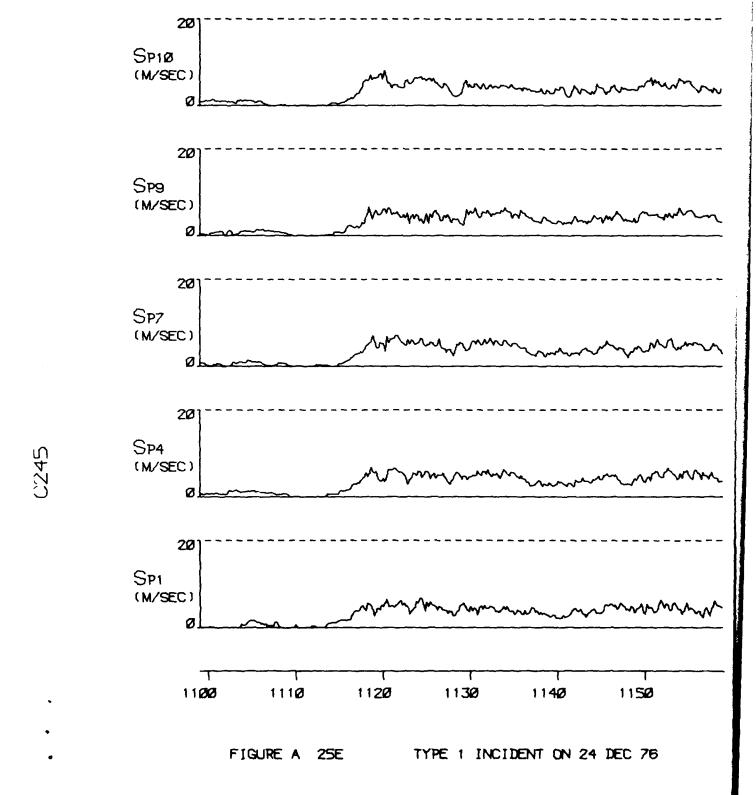
FIGURE A 25A   TYPE 1 INCIDENT ON 24 DEC 76

FIGURE A 25B   TYPE 1 INCIDENT ON 24 DEC 76

FIGURE A 2SC   TYPE 1 INCIDENT ON 24 DEC 76

FIGURE A 25D   TYPE 1 INCIDENT ON 24 DEC 76

FIGURE A 25E   TYPE 1 INCIDENT ON 24 DEC 76
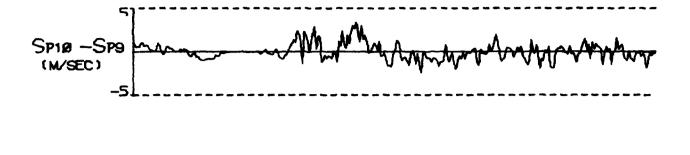
FIGURE A 2SF   TYPE 1 INCIDENT ON 24 DEC 76
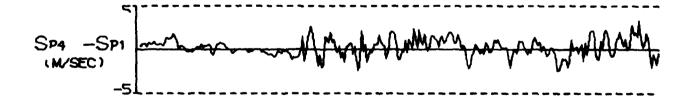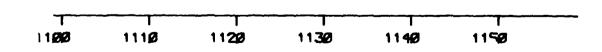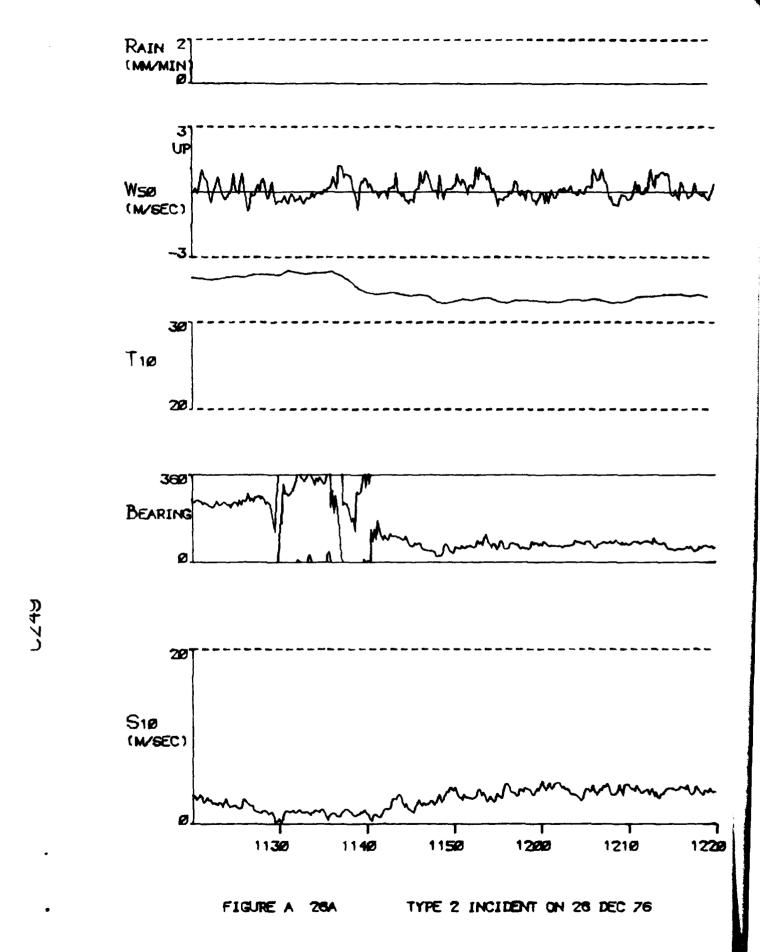
FIGURE A 28A   TYPE 2 INCIDENT ON 28 DEC 76
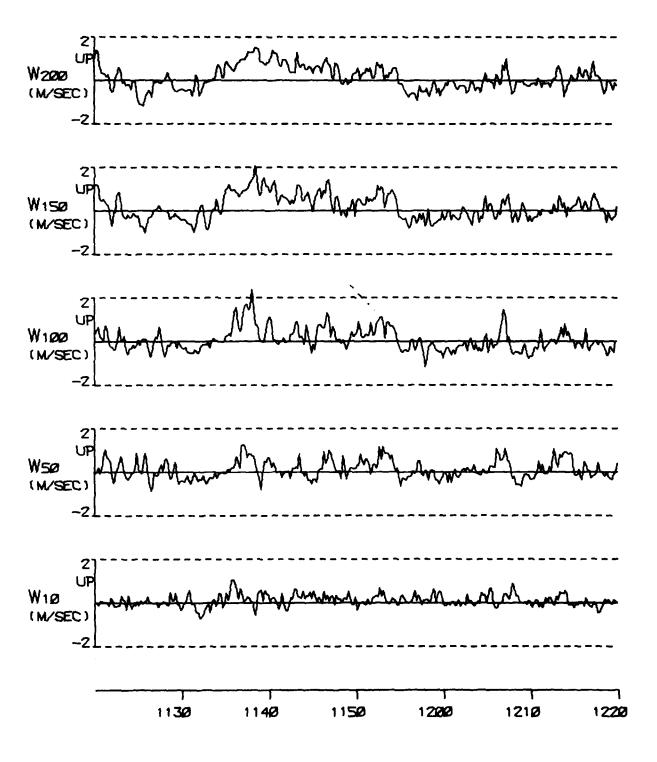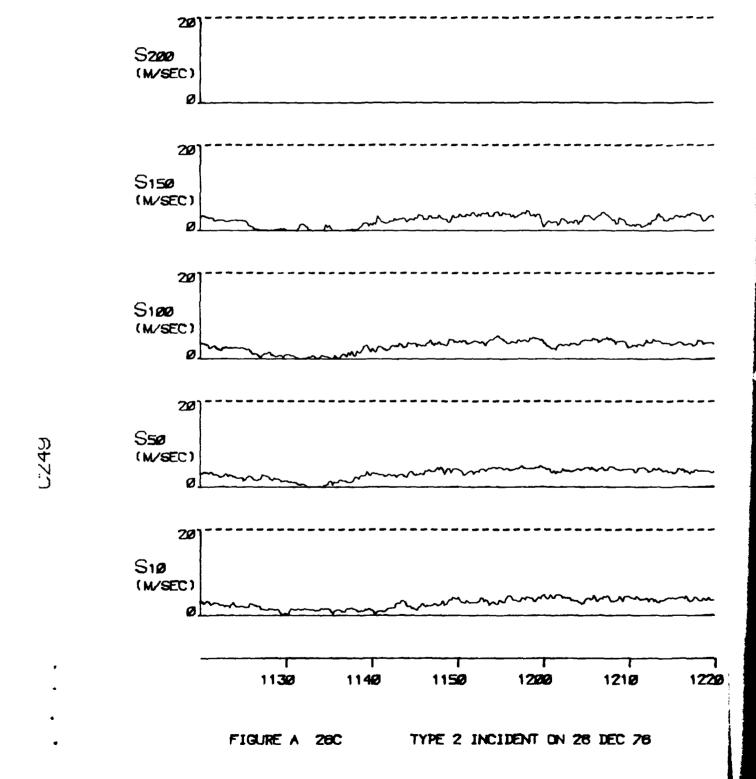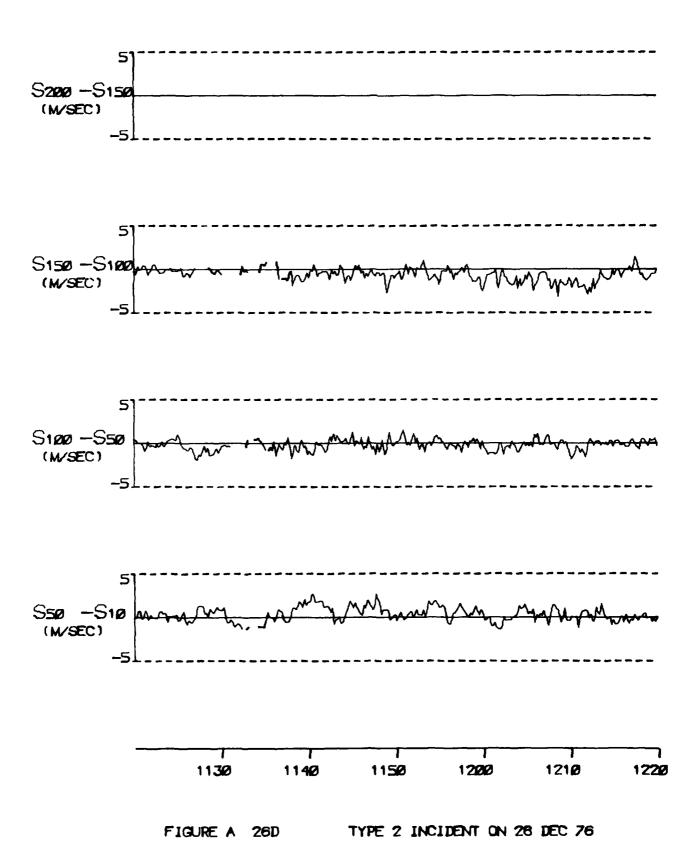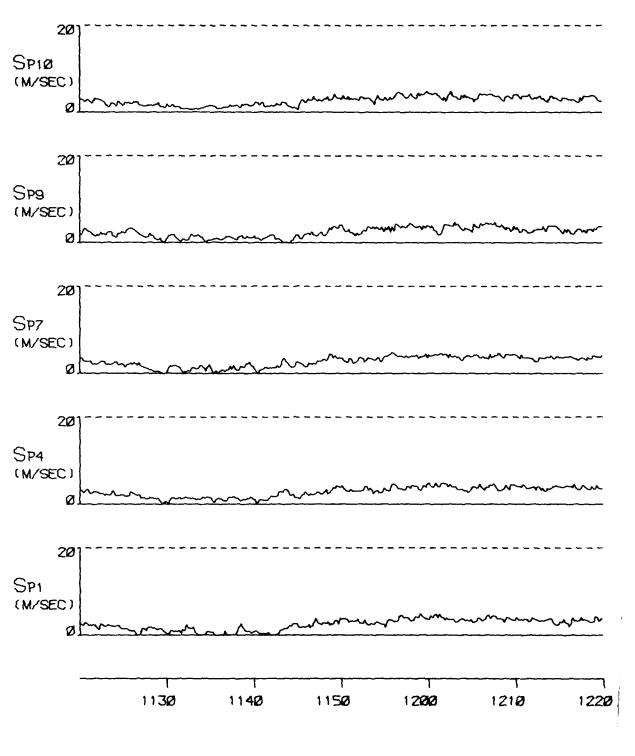
FIGURE A .26B   TYPE 2 INCIDENT ON 28 DEC 76

FIGURE A 26C   TYPE 2 INCIDENT ON 26 DEC 76

FIGURE A 26D   TYPE 2 INCIDENT ON 26 DEC 76

SP10
(M/SEC)

SP9
(M/SEC)

SP7
(M/SEC)

SP4
(M/SEC)

SP1
(M/SEC)

1130   1140   1150   1200   1210   1220
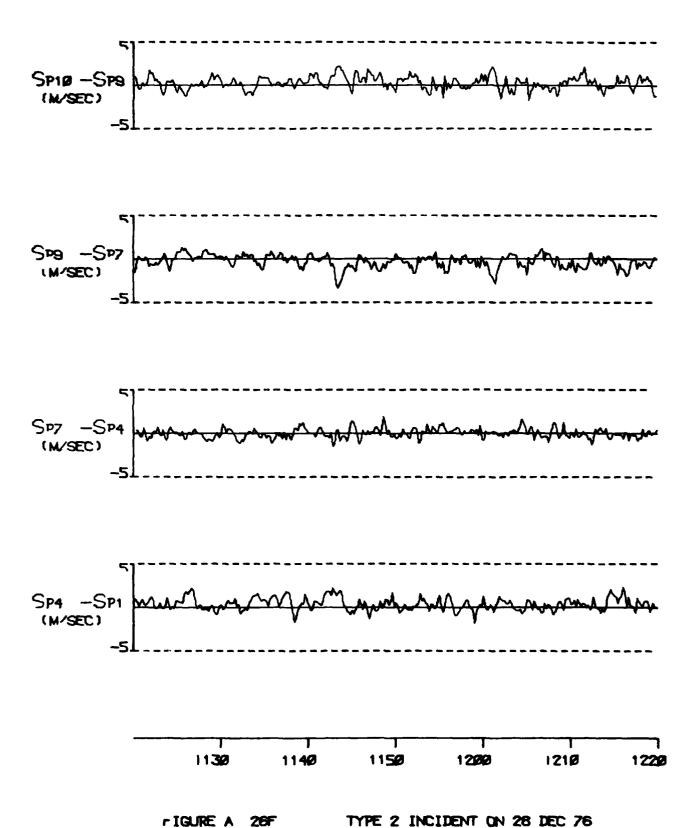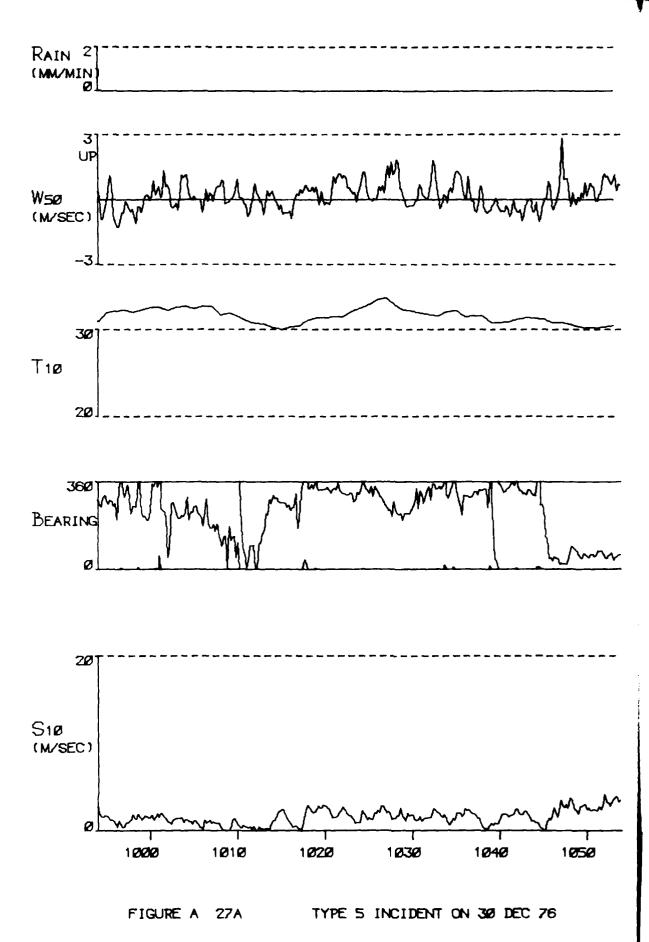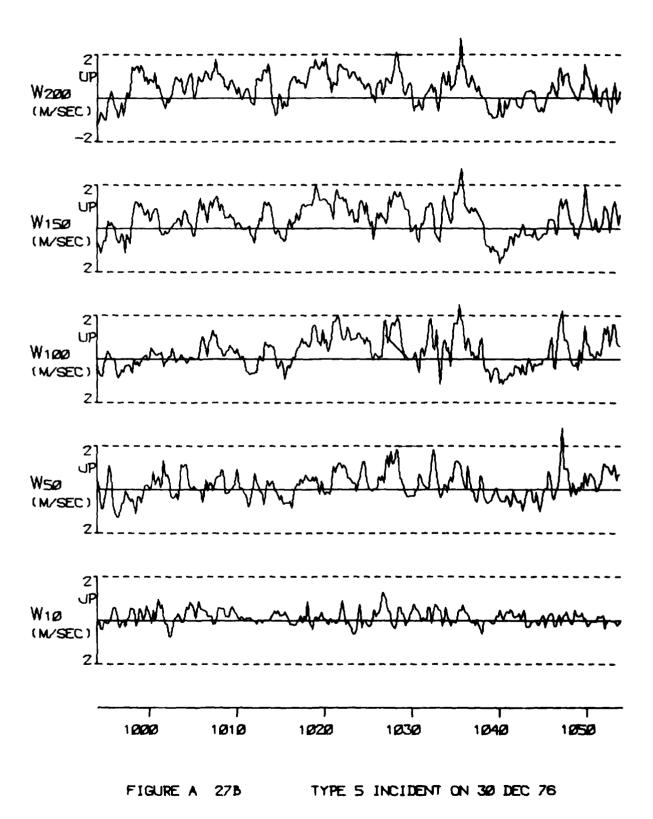
FIGURE A 26E   TYPE 2 INCIDENT ON 28 DEC 76

FIGURE A 26F   TYPE 2 INCIDENT ON 28 DEC 76

RAIN 2
(MM/MIN)
0

3
UP
W50
(M/SEC)
-3

30
T10
20

360
BEARING
0

20
S10
(M/SEC)
0

1000   1010   1020   1030   1040   1050

FIGURE A 27A   TYPE 5 INCIDENT ON 30 DEC 76

FIGURE A 27B   TYPE 5 INCIDENT ON 30 DEC 76

FIGURE A 27C   TYPE S INCIDENT ON 30 DEC 76

FIGURE A 27D   TYPE 5 INCIDENT ON 30 DEC 76

FIGURE A 27E   TYPE 5 INCIDENT ON 30 DEC 76

FIGURE A 27F   TYPE 5 INCIDENT ON 30 DEC 76
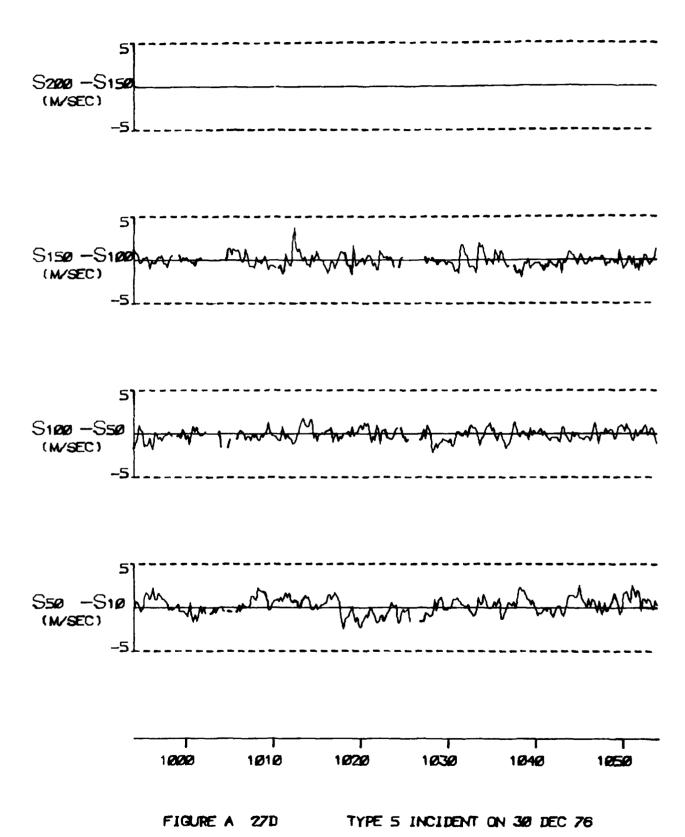
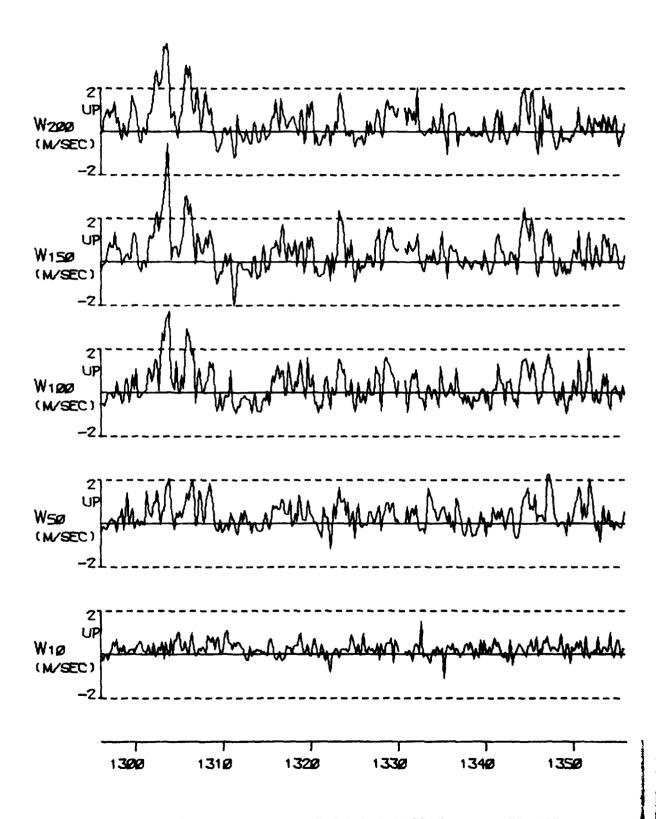FIGURE A 28A   TYPE 3 INCIDENT ON 2 JAN 77
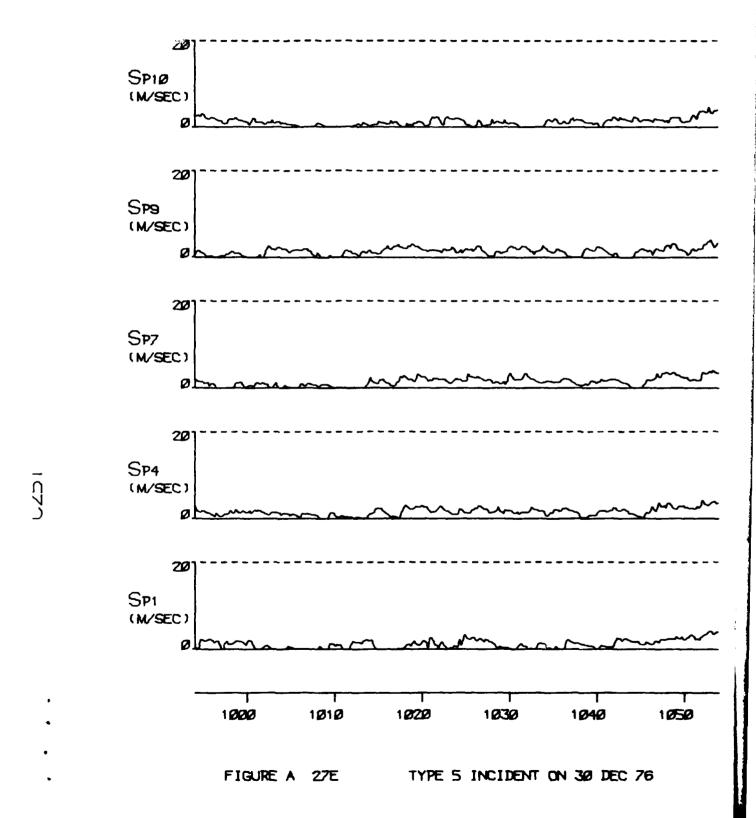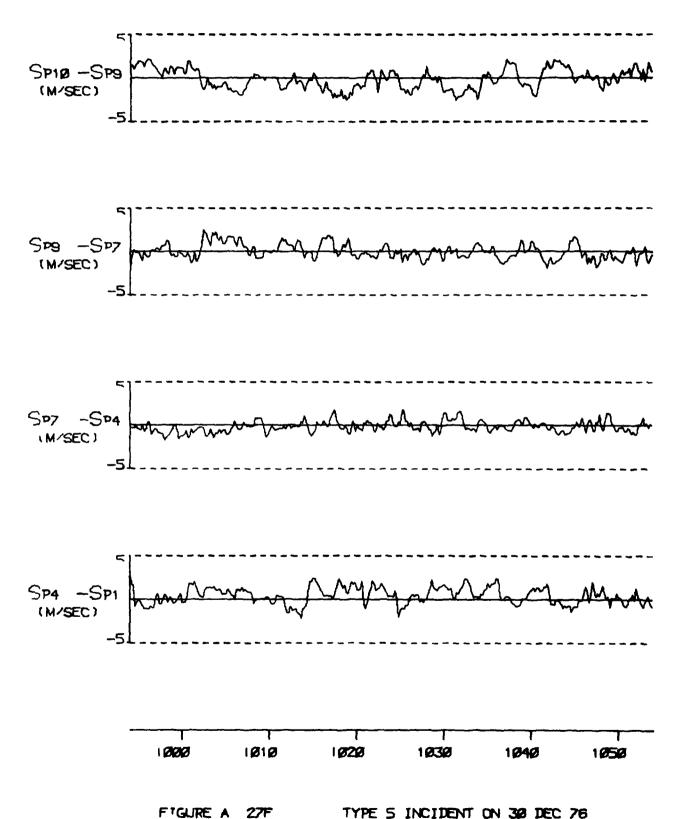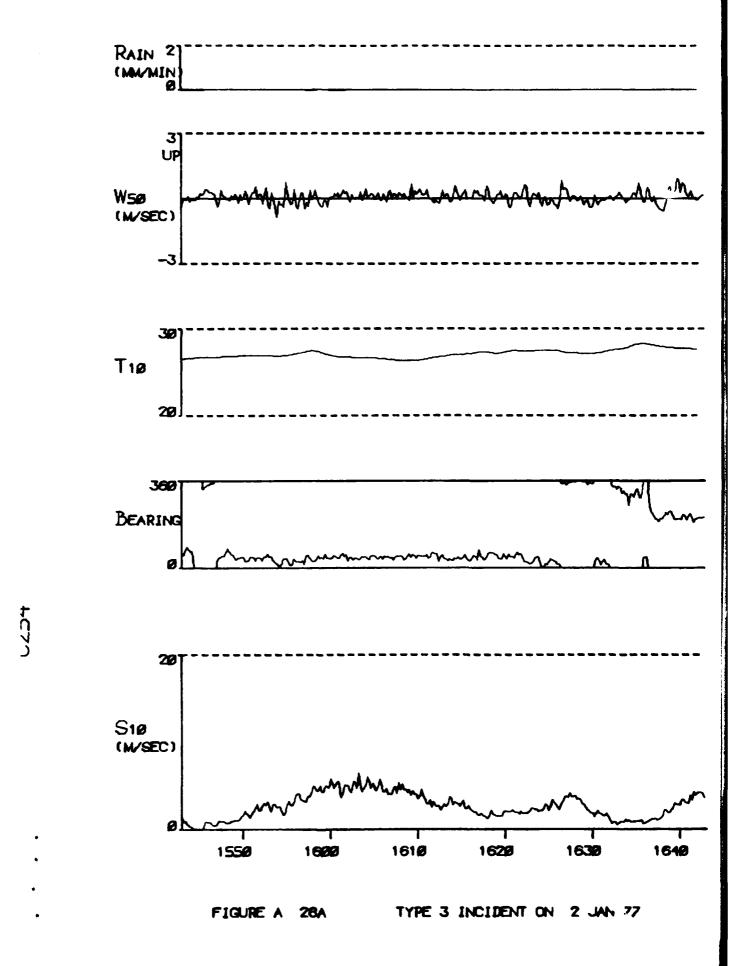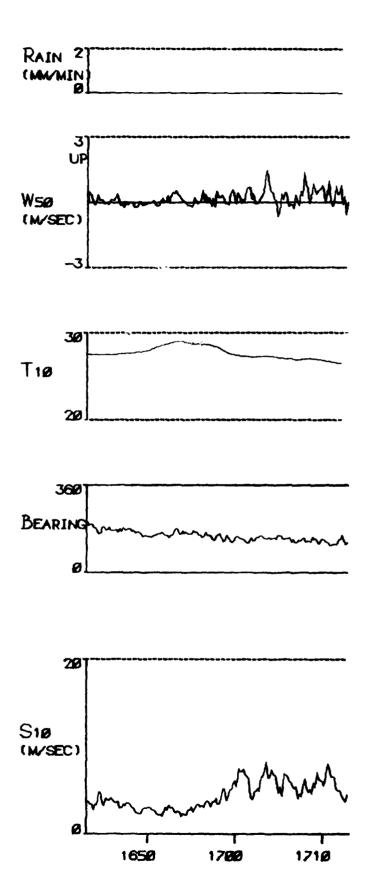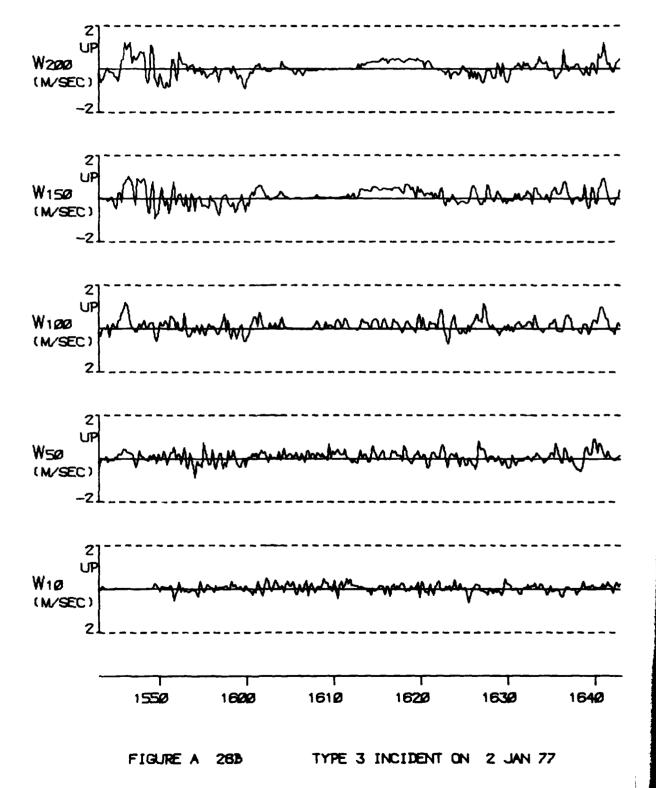
FIGURE A 28A (CONT) TYPE 3 INCIDENT ON 2 JAN 77

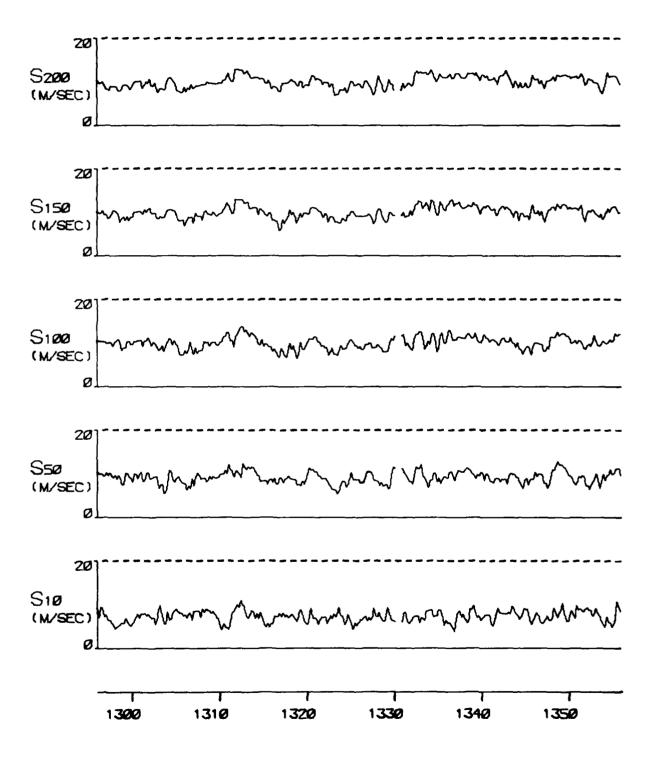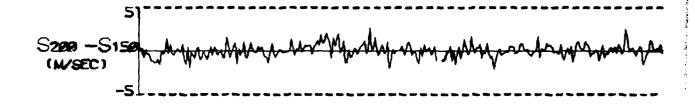FIGURE A 28B   TYPE 3 INCIDENT ON 2 JAN 77
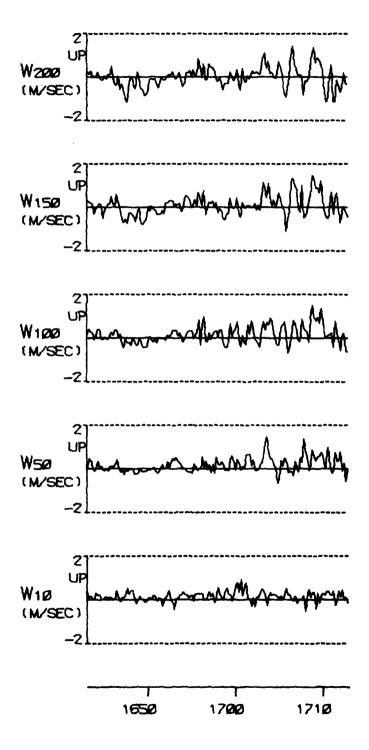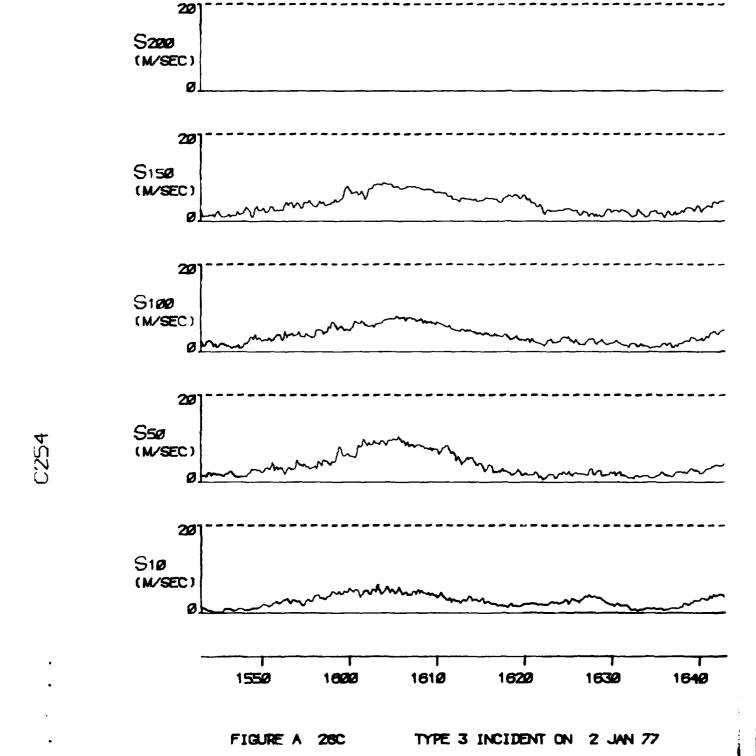
FIGURE A 28B (CONT) TYPE 3 INCIDENT ON 2 JAN 77

C254

FIGURE A 28C   TYPE 3 INCIDENT ON 2 JAN 77
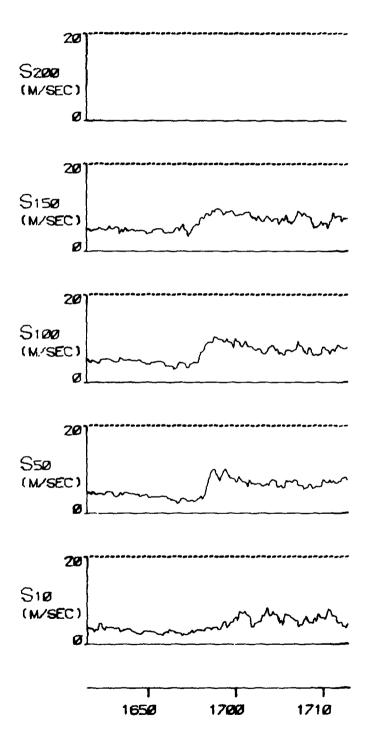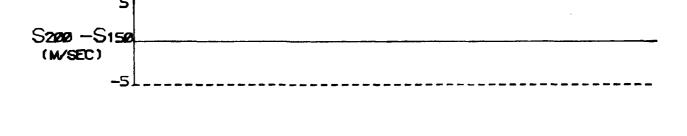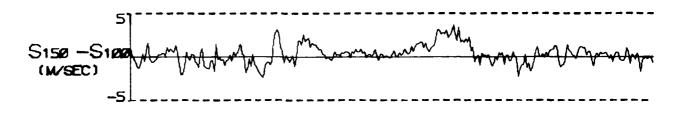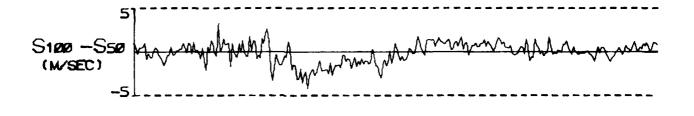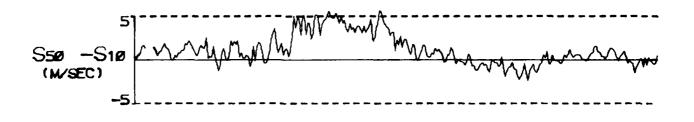
FIGURE A 26C (CONT) TYPE 3 INCIDENT ON 2 JAN 77
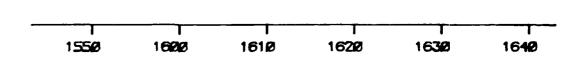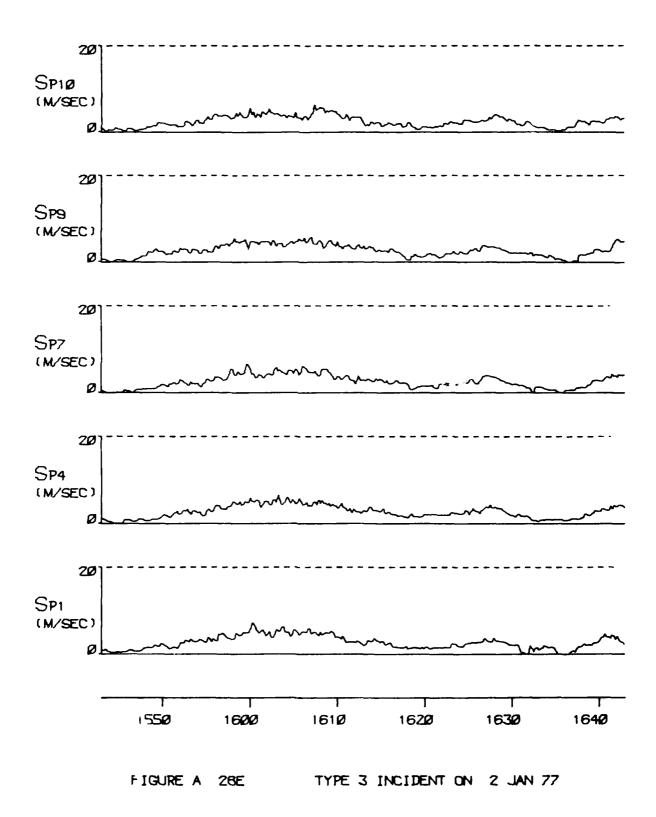
FIGURE A 28D   TYPE 3 INCIDENT ON 2 JAN 77

FIGURE A 26E   TYPE 3 INCIDENT ON 2 JAN 77

FIGURE A   26E (CONT) TYPE 3 INCIDENT ON   2 JAN 77

FIGURE A 28F   TYPE 3 INCIDENT ON 2 JAN 77
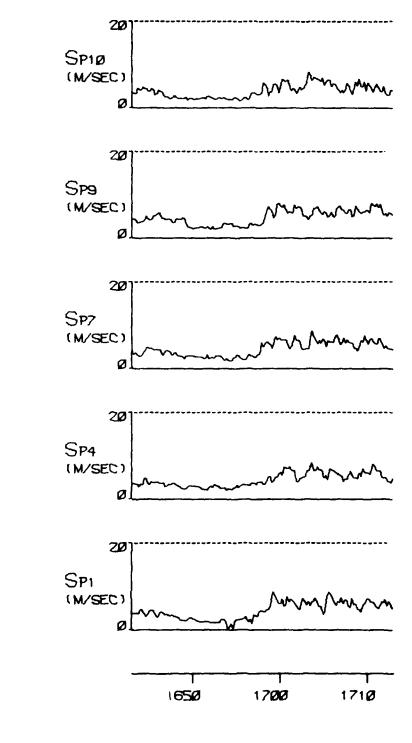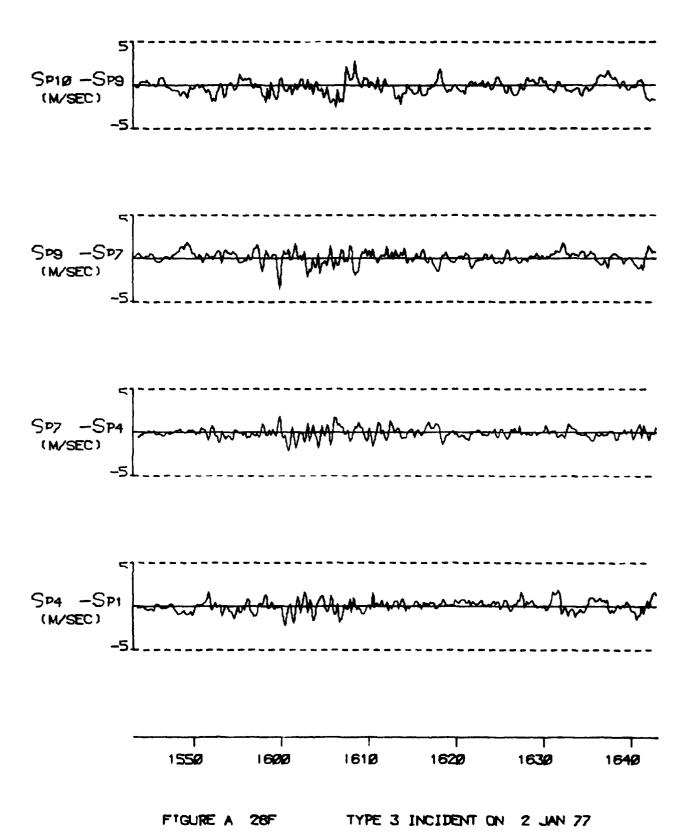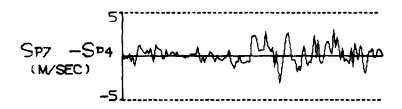
FIGURE A 28F (CONT) TYPE 3 INCIDENT ON 2 JAN 77
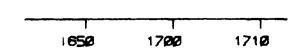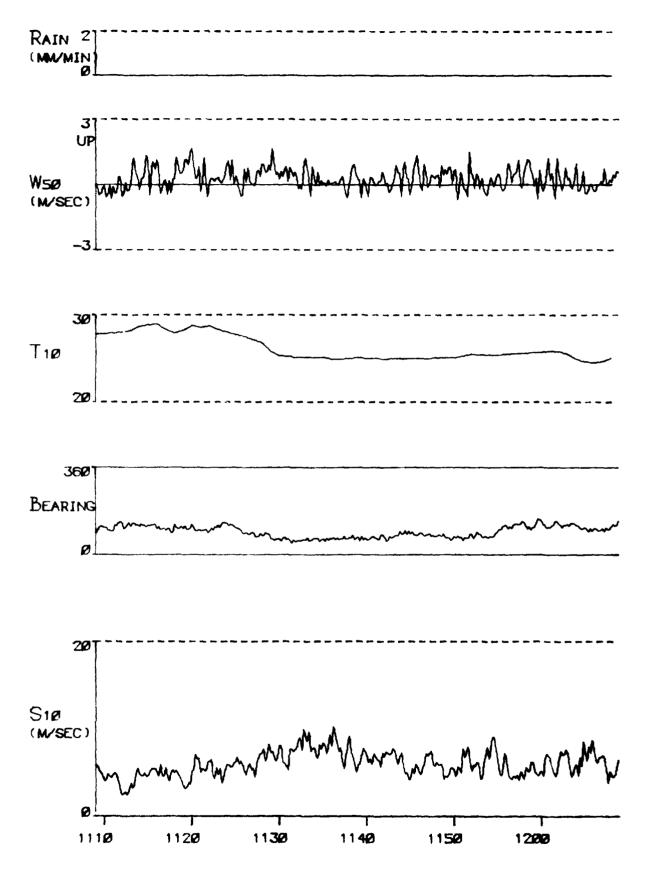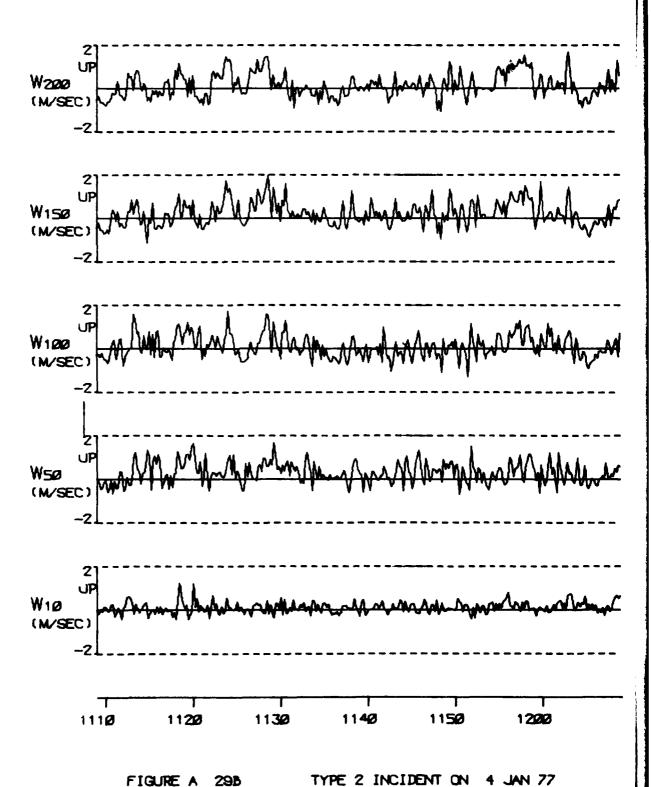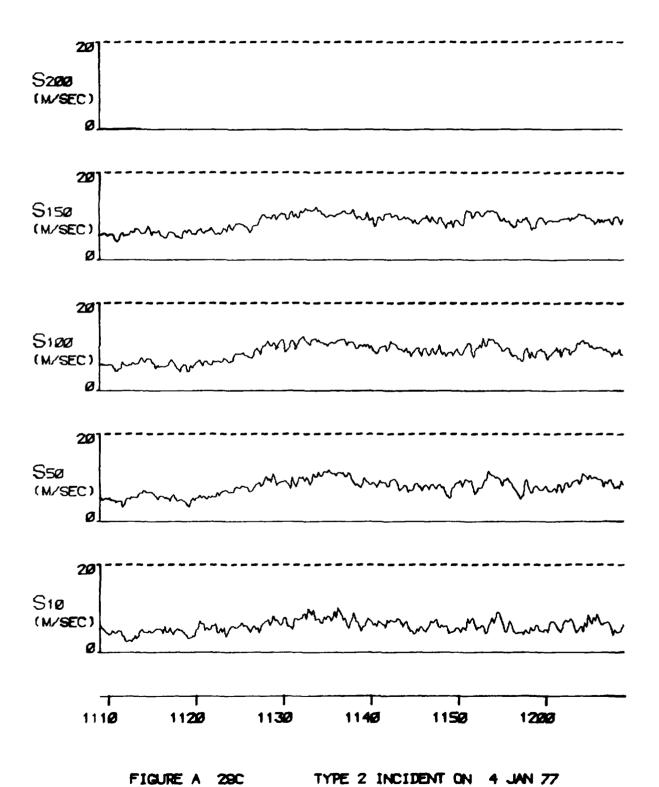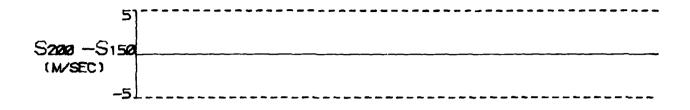
FIGURE A 29A   TYPE 2 INCIDENT ON 4 JAN 77

FIGURE A 29B   TYPE 2 INCIDENT ON 4 JAN 77
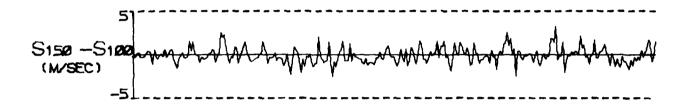
FIGURE A 29C   TYPE 2 INCIDENT ON 4 JAN 77
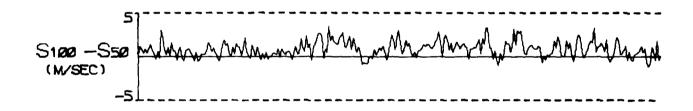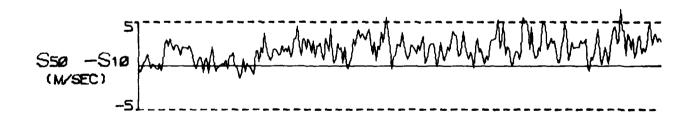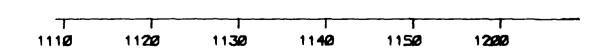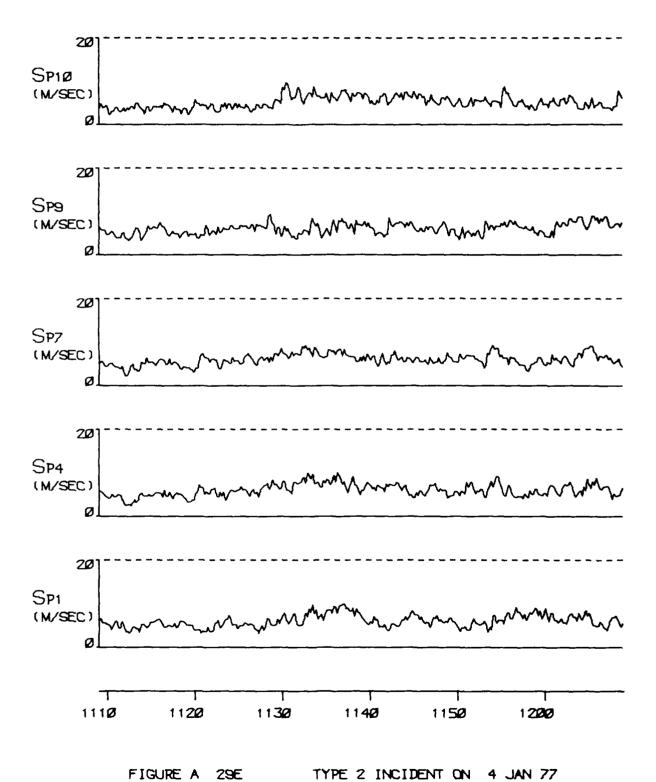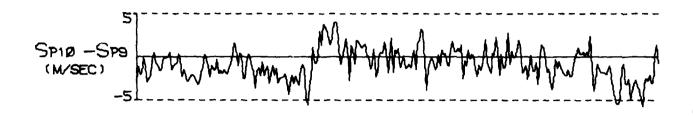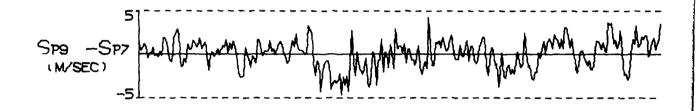
FIGURE A 29D   TYPE 2 INCIDENT ON 4 JAN 77
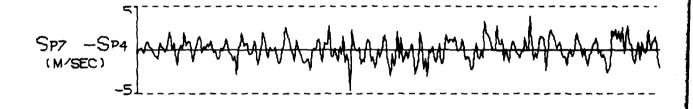
FIGURE A 29E   TYPE 2 INCIDENT ON 4 JAN 77
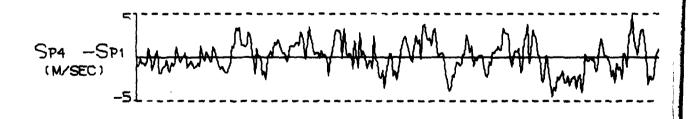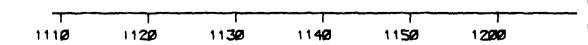
FIGURE A 29F   TYPE 2 INCIDENT ON 4 JAN 77
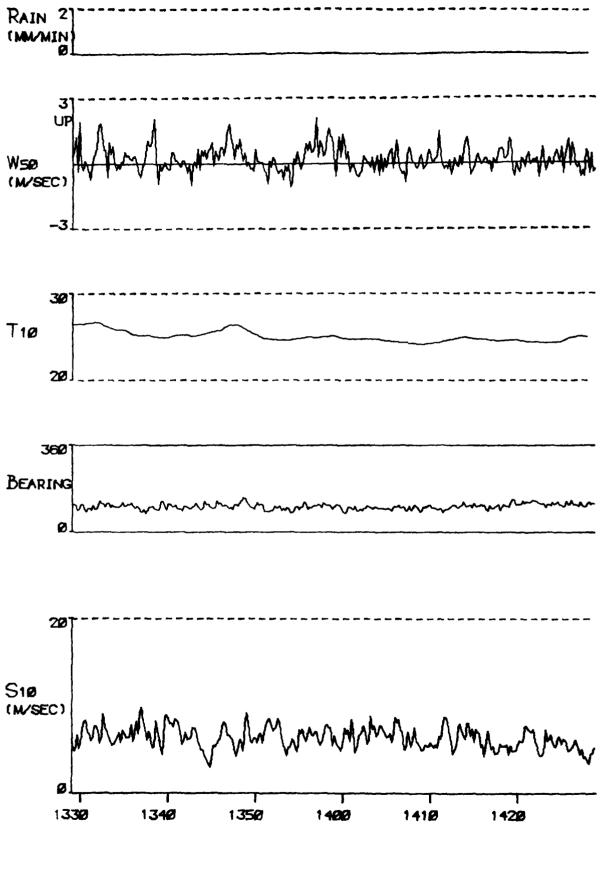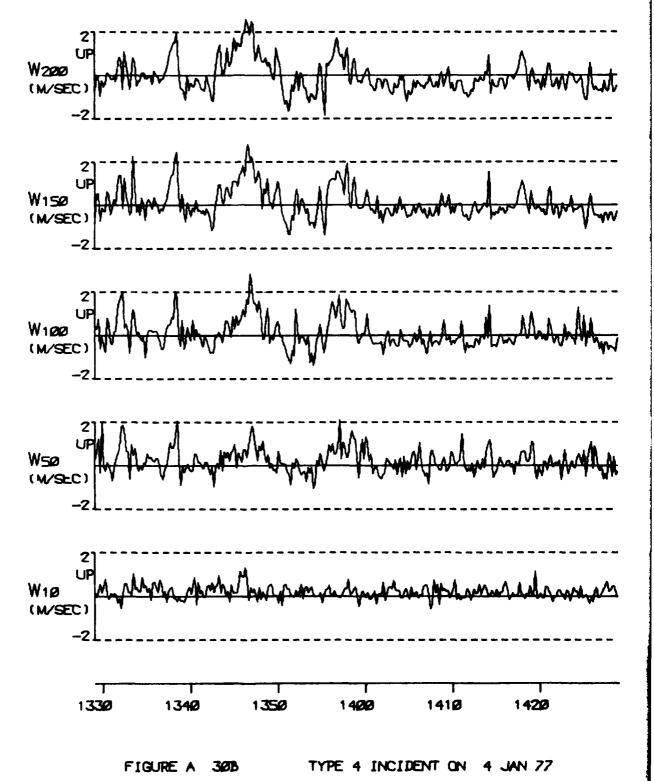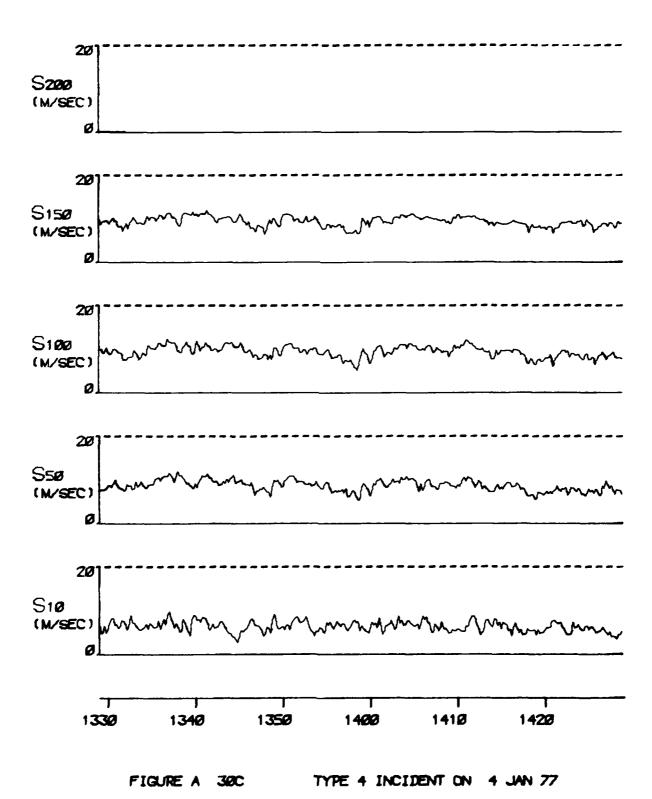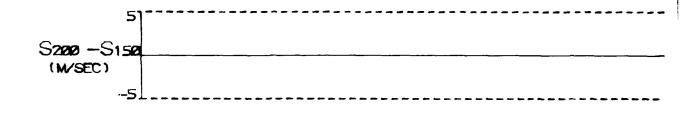
FIGURE A 30A   TYPE 4 INCIDENT ON 4 JAN 77

FIGURE A 30B   TYPE 4 INCIDENT ON 4 JAN 77
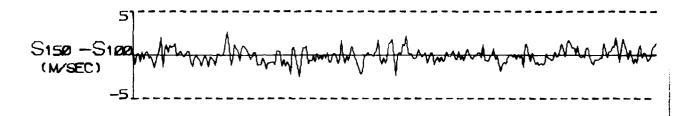
C256

FIGURE A 30C   TYPE 4 INCIDENT ON 4 JAN 77
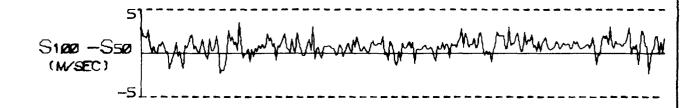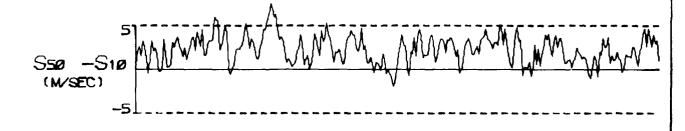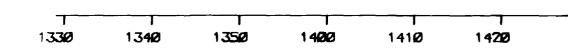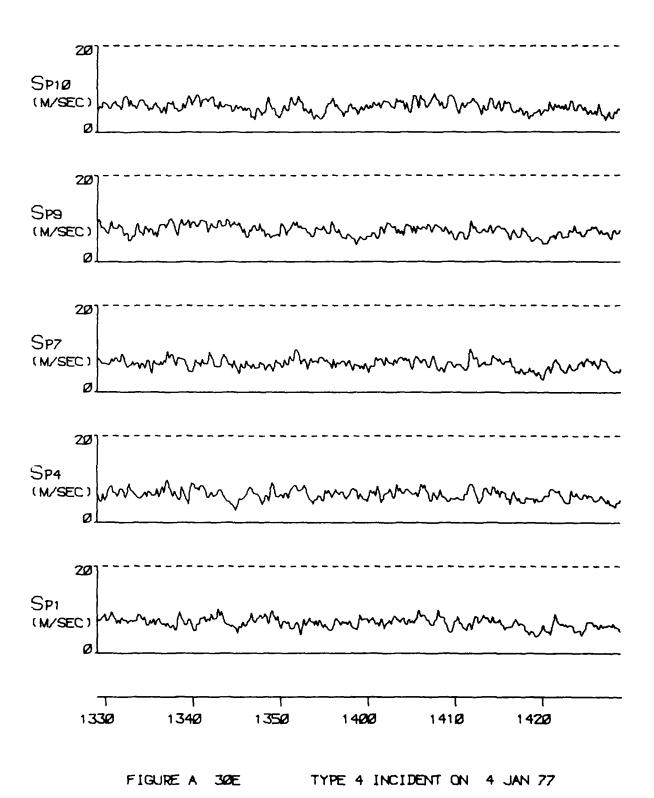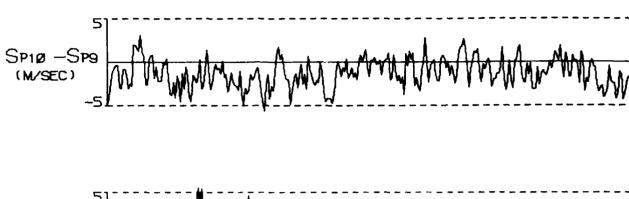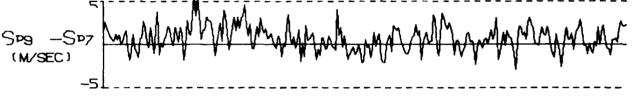
FIGURE A 30D   TYPE 4 INCIDENT ON 4 JAN 77

FIGURE A 30E   TYPE 4 INCIDENT ON 4 JAN 77
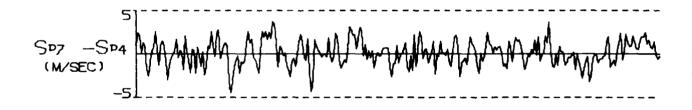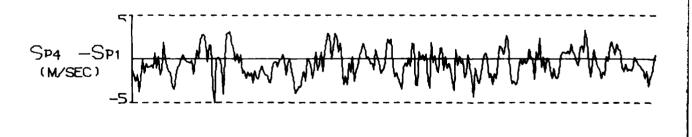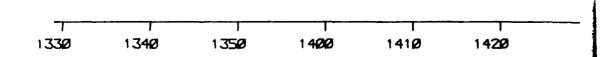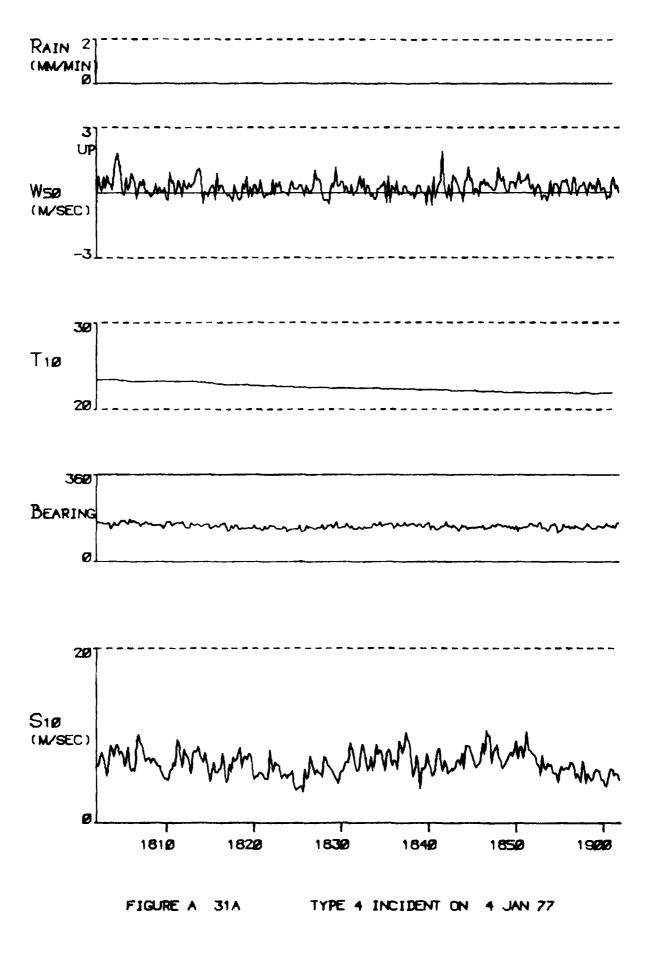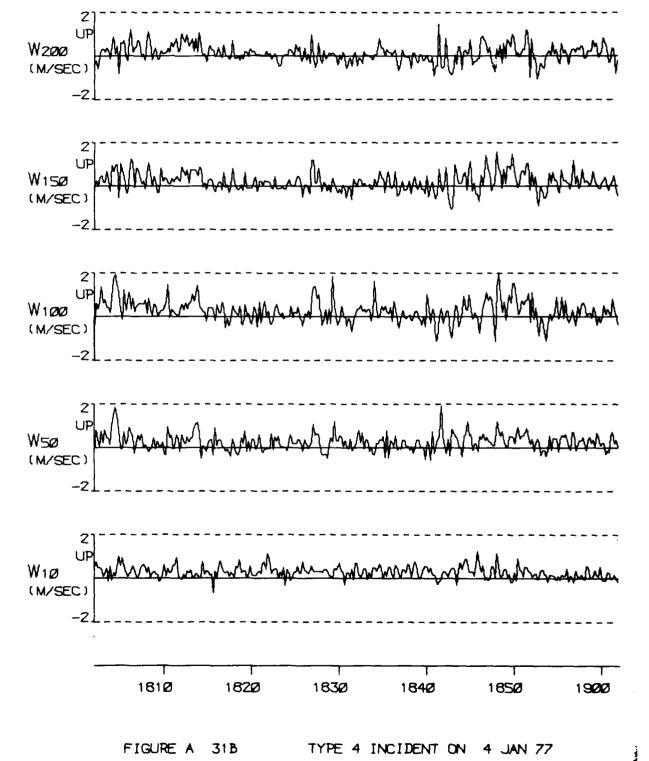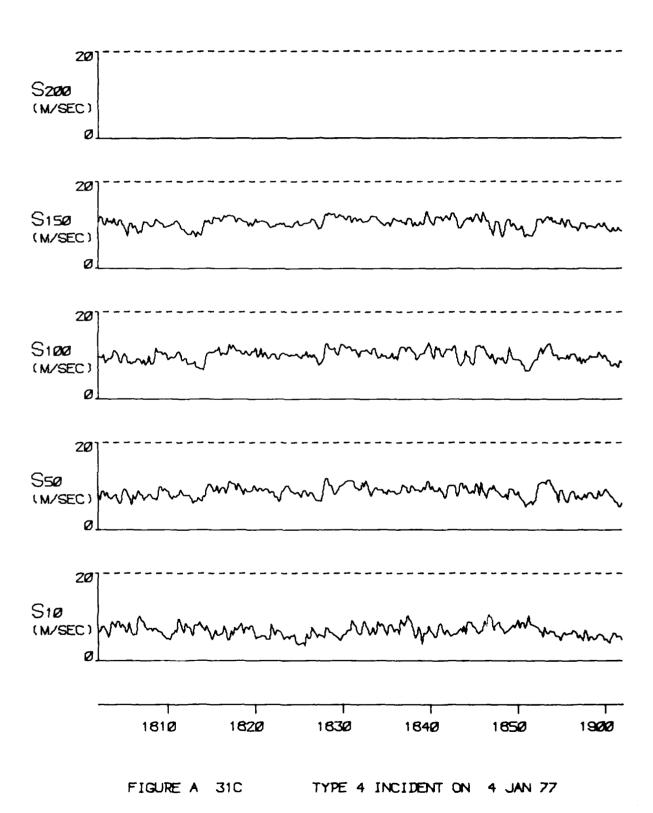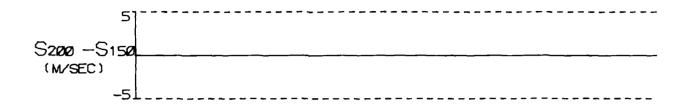
FIGURE A 30F   TYPE 4 INCIDENT ON 4 JAN 77

FIGURE A 31A   TYPE 4 INCIDENT ON 4 JAN 77

FIGURE A 31B   TYPE 4 INCIDENT ON 4 JAN 77
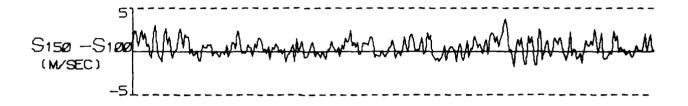
FIGURE A 31C   TYPE 4 INCIDENT ON 4 JAN 77
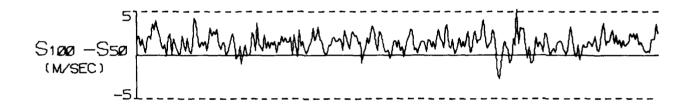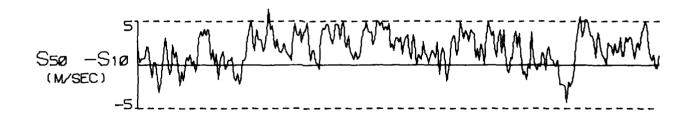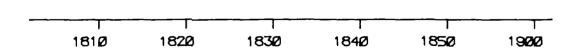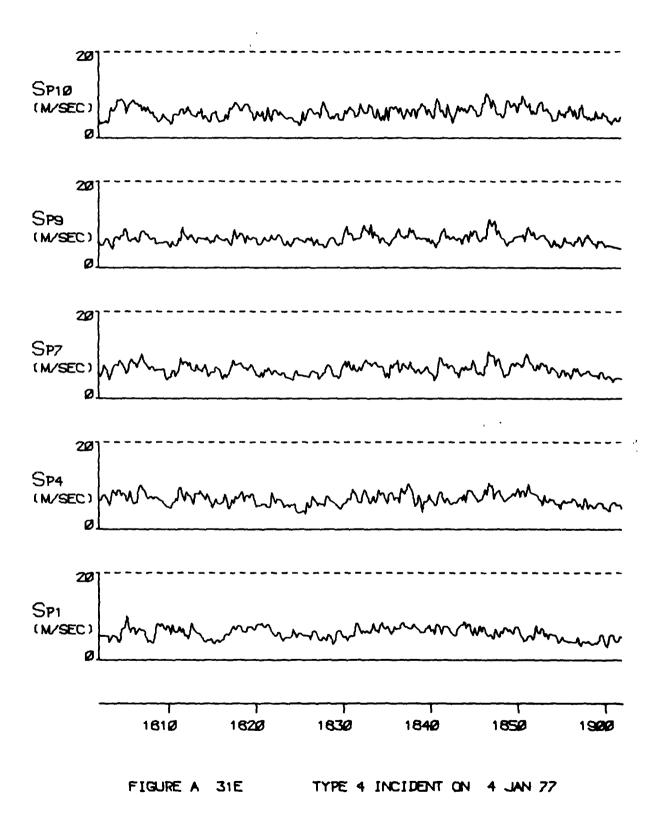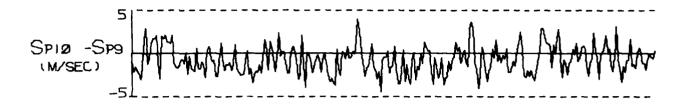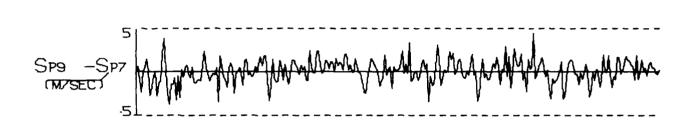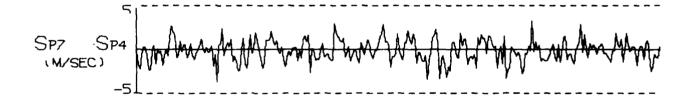
FIGURE A 31D   TYPE 4 INCIDENT ON 4 JAN 77
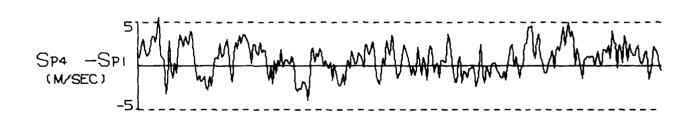
FIGURE A 31E   TYPE 4 INCIDENT ON 4 JAN 77
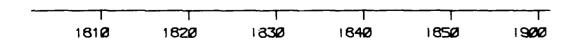
FIGURE A 31F   TYPE 4 INCIDENT ON 4 JAN 77
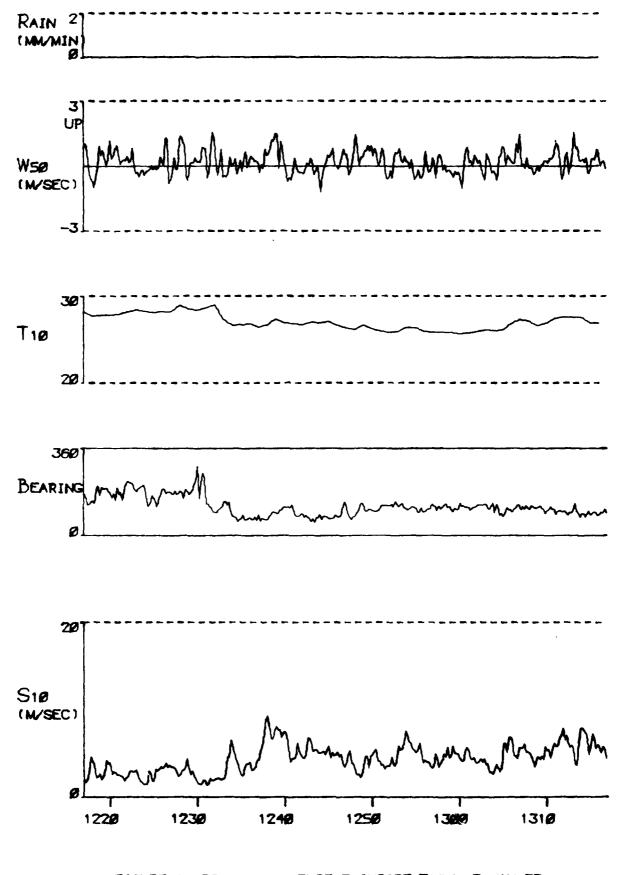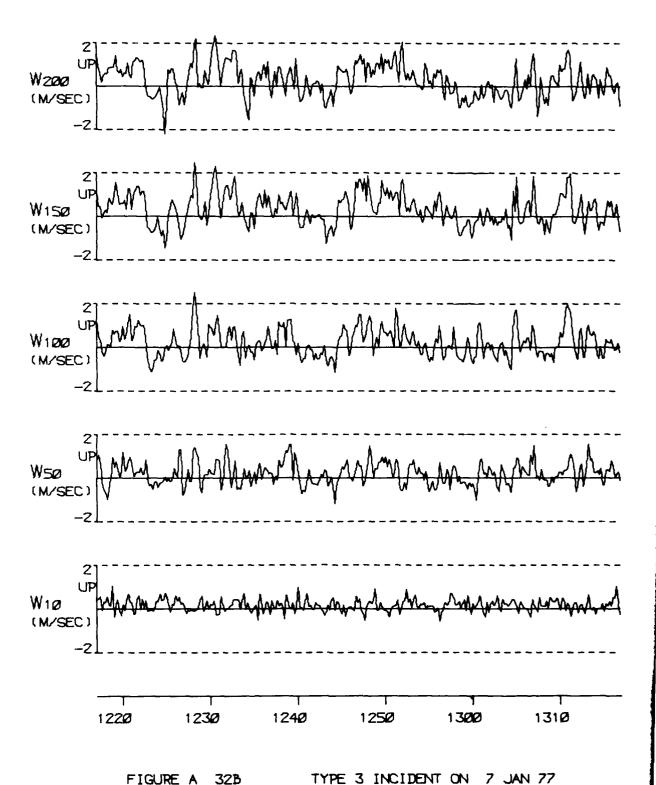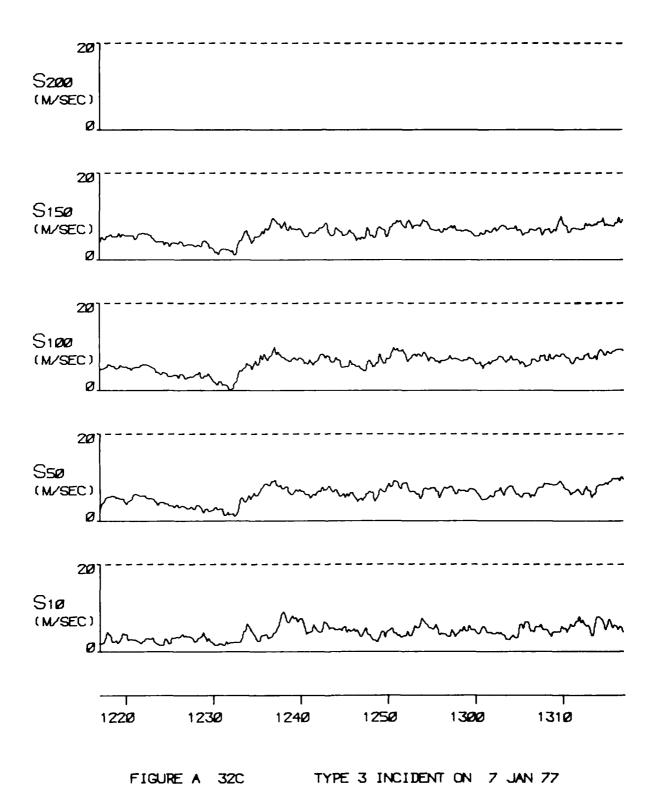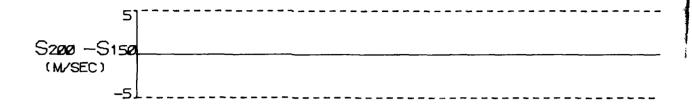
FIGURE A 32A   TYPE 3 INCIDENT ON 7 JAN 77

FIGURE A 32B   TYPE 3 INCIDENT ON 7 JAN 77

FIGURE A 32C   TYPE 3 INCIDENT ON 7 JAN 77

FIGURE A 32D   TYPE 3 INCIDENT ON 7 JAN 77

FIGURE A 32E   TYPE 3 INCIDENT ON 7 JAN 77
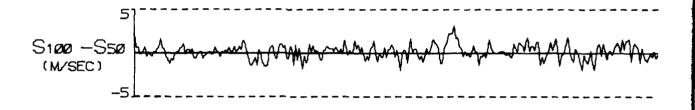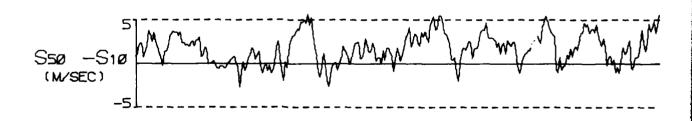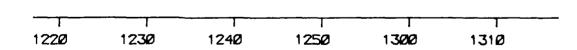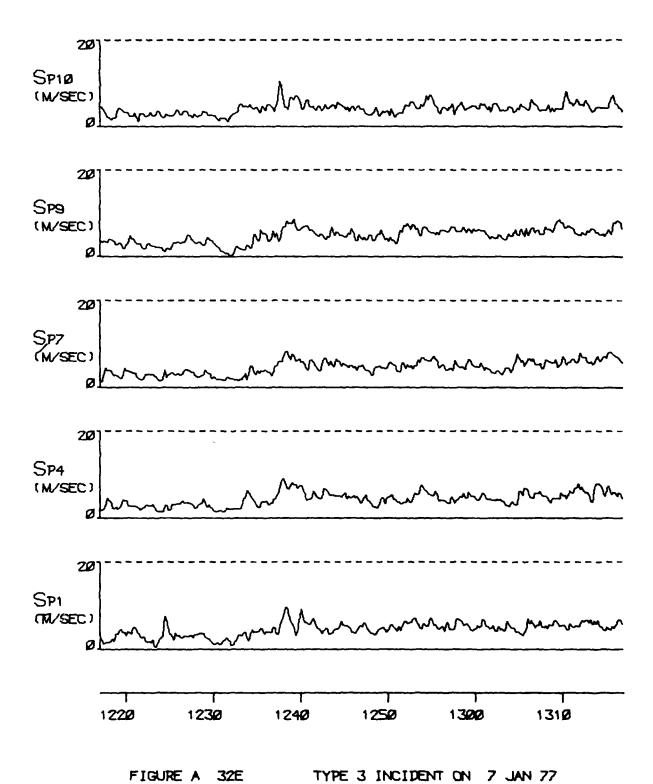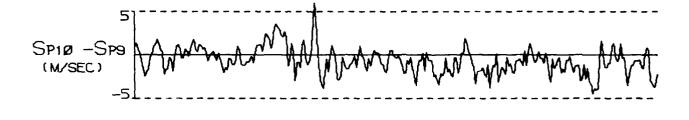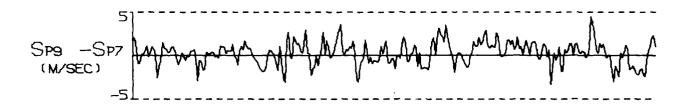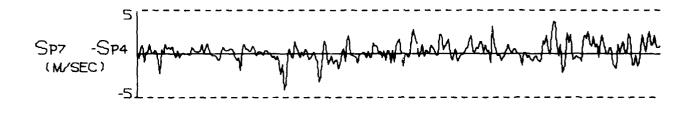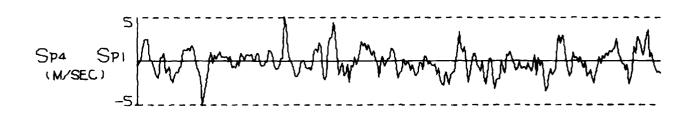
FIGURE A 32F   TYPE 3 INCIDENT ON 7 JAN 77
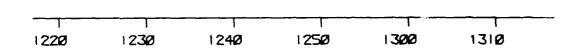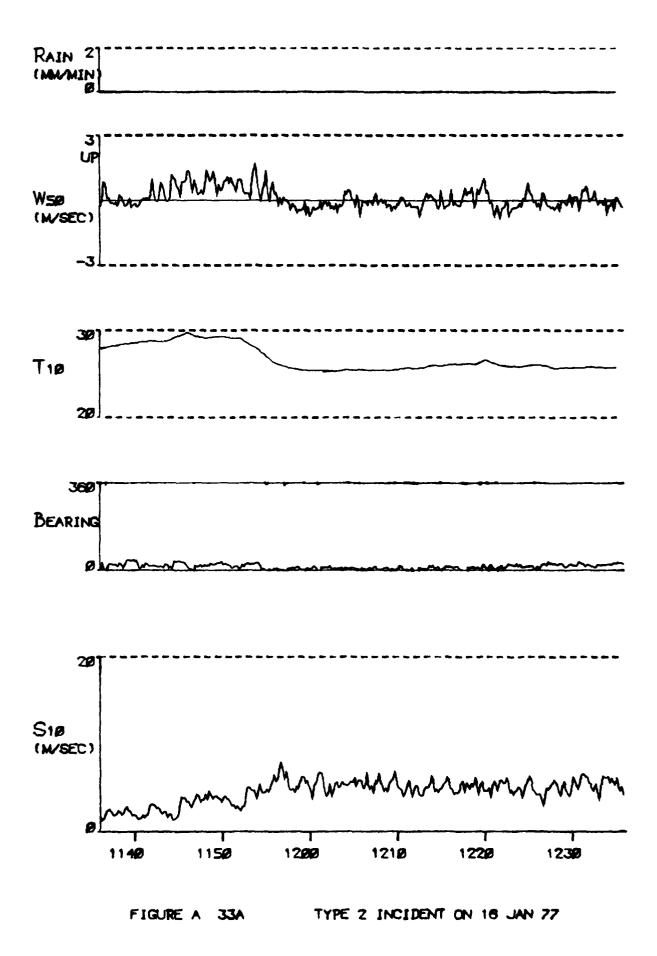
FIGURE A 33A   TYPE 2 INCIDENT ON 16 JAN 77
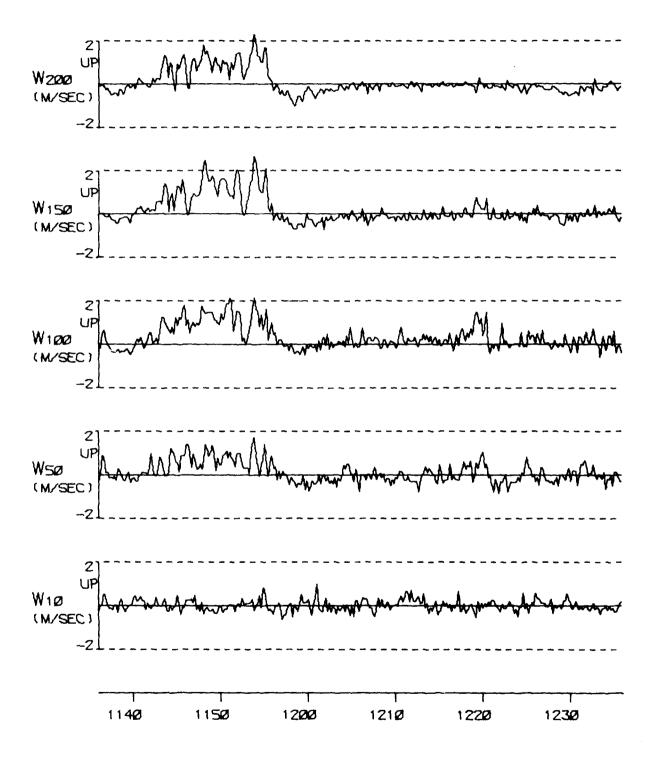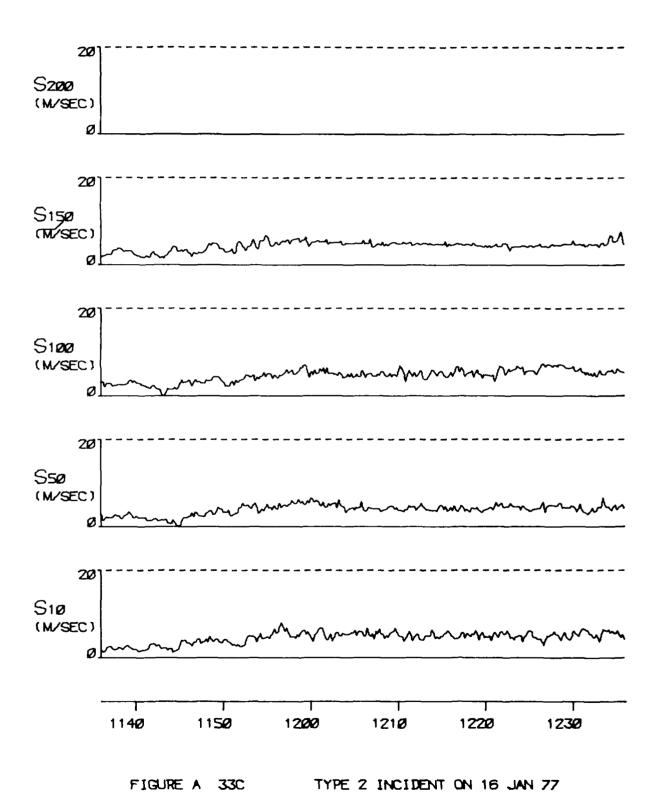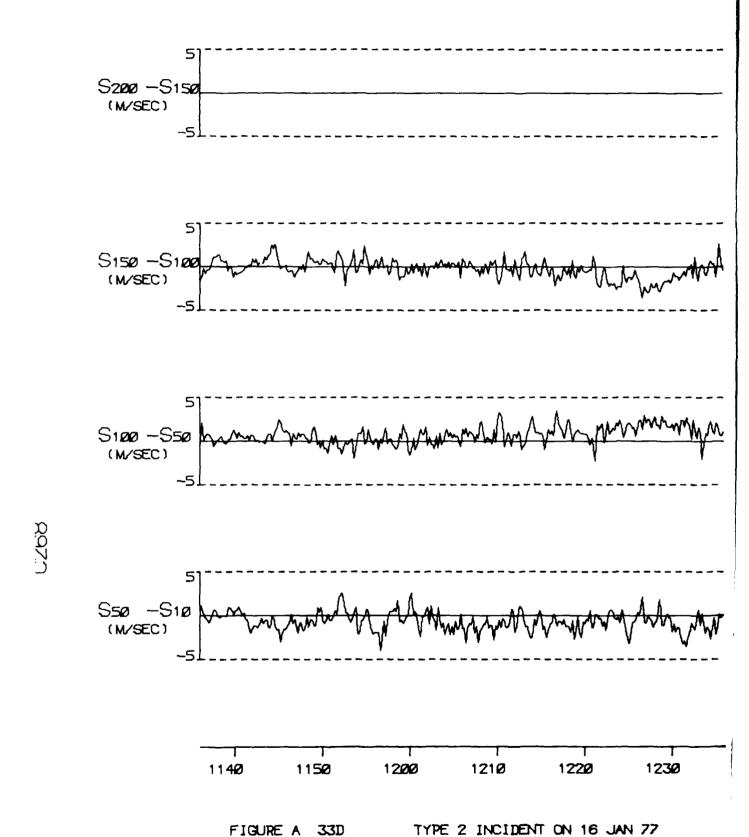
FIGURE A 33B   TYPE 2 INCIDENT ON 16 JAN 77

FIGURE A 33C   TYPE 2 INCIDENT ON 16 JAN 77

FIGURE A 33D   TYPE 2 INCIDENT ON 16 JAN 77
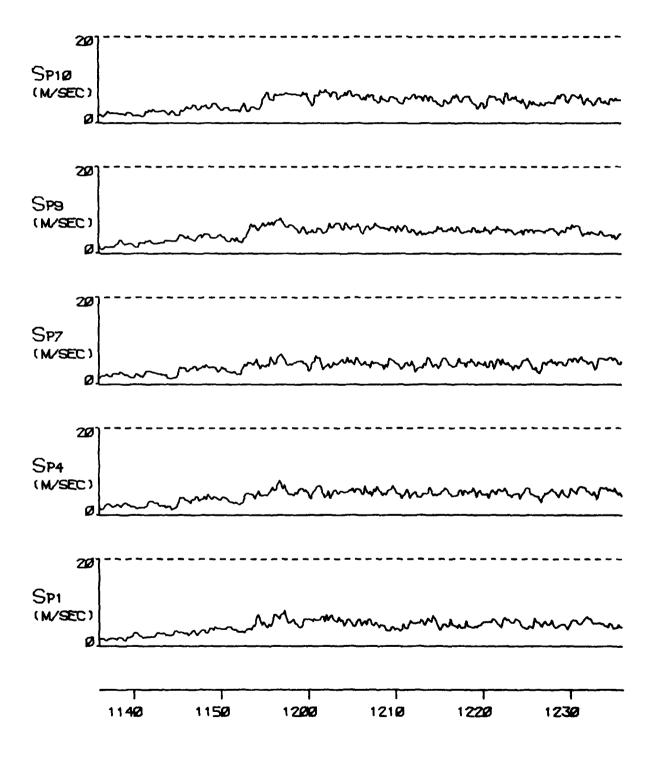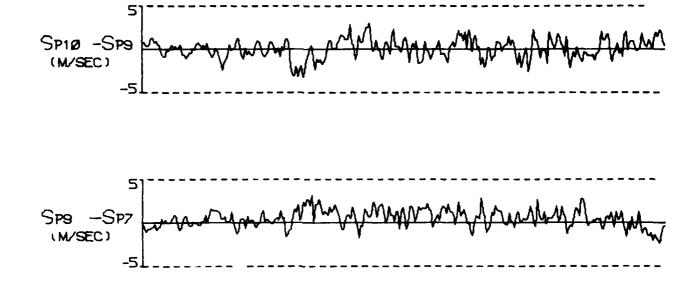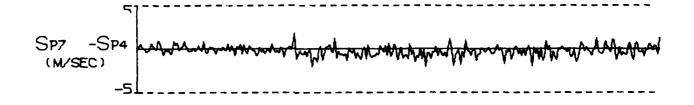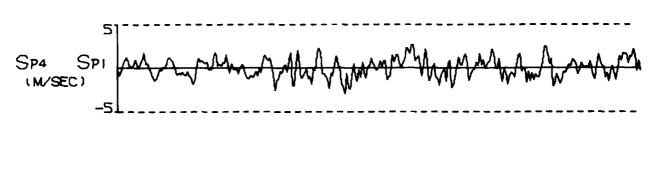
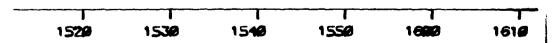FIGURE A 33E   TYPE 2 INCIDENT ON 16 JAN 77
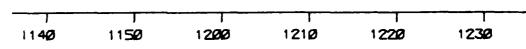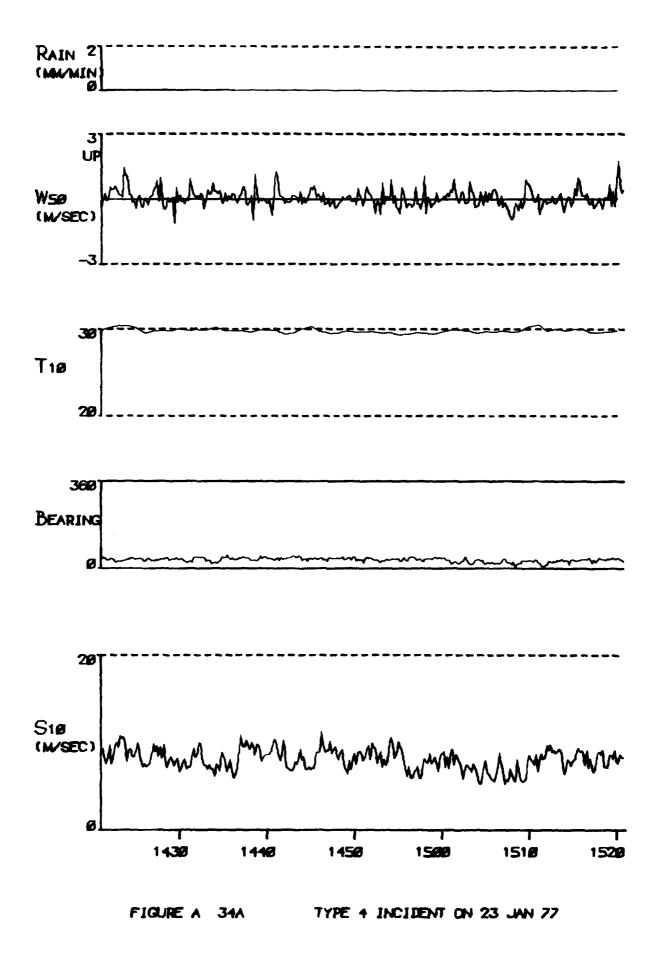
FIGURE A 33F   TYPE 2 INCIDENT ON 16 JAN 77
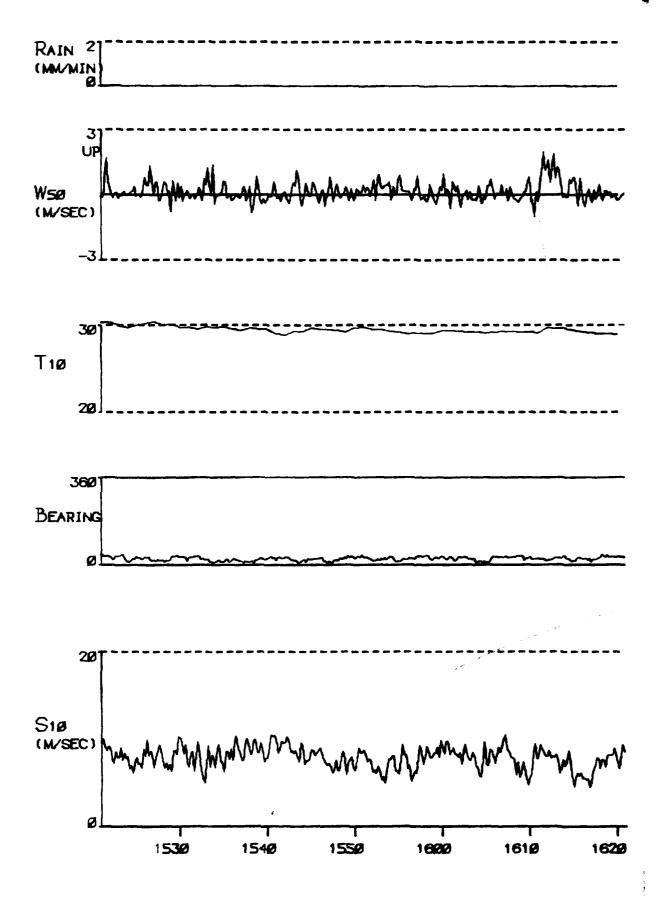
FIGURE A 34A   TYPE 4 INCIDENT ON 23 JAN 77
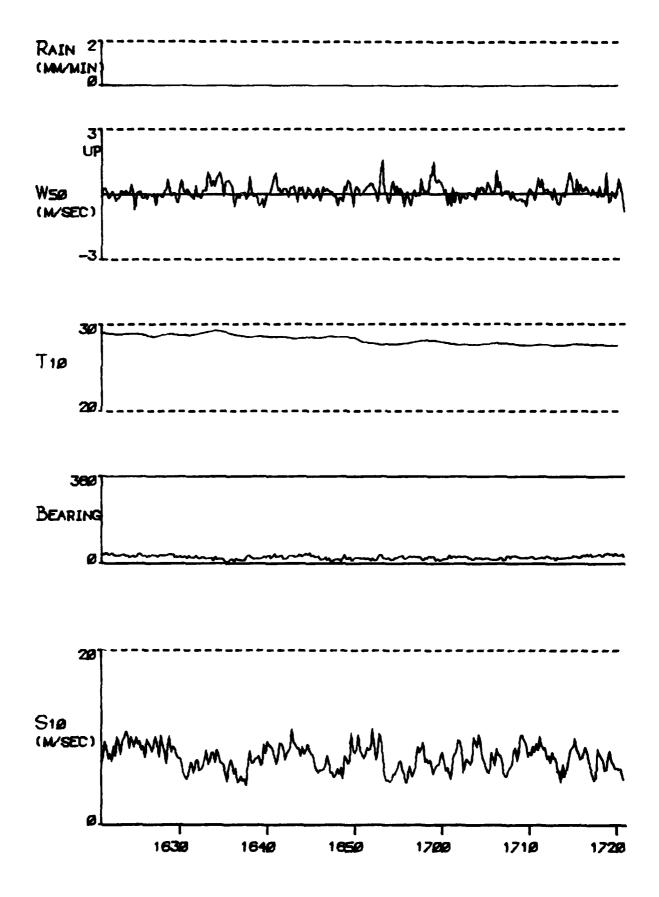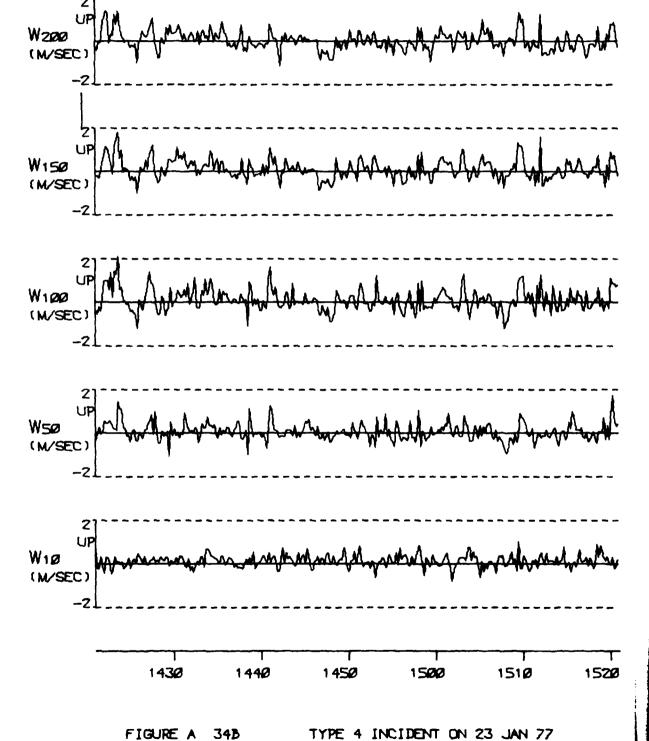
FIGURE A 34A (CONT) TYPE 4 INCIDENT ON 23 JAN 77

FIGURE A 34A (CONT) TYPE 4 INCIDENT ON 23 JAN 77

FIGURE A 34B   TYPE 4 INCIDENT ON 23 JAN 77

FIGURE A 34B (CONT) TYPE 4 INCIDENT ON 23 JAN 77
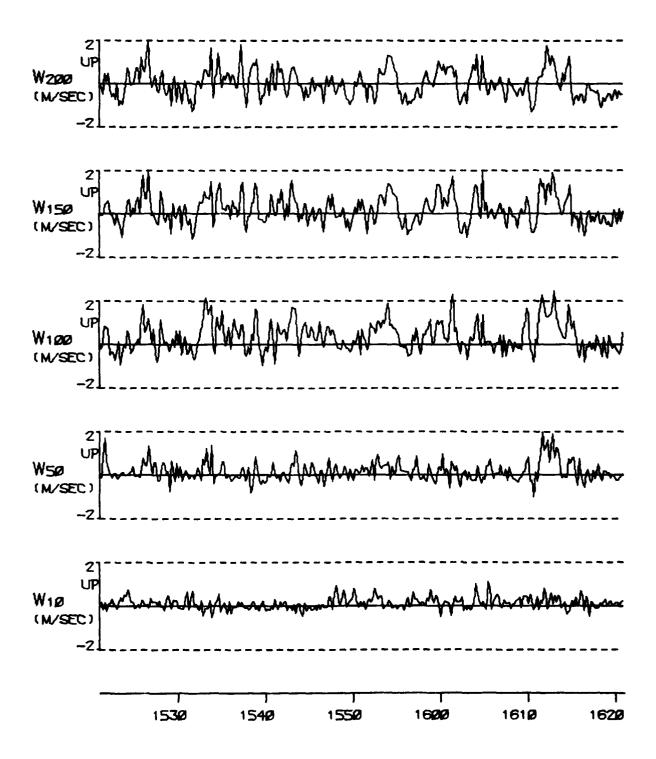
FIGURE A 34B (CONT) TYPE 4 INCIDENT ON 23 JAN 77
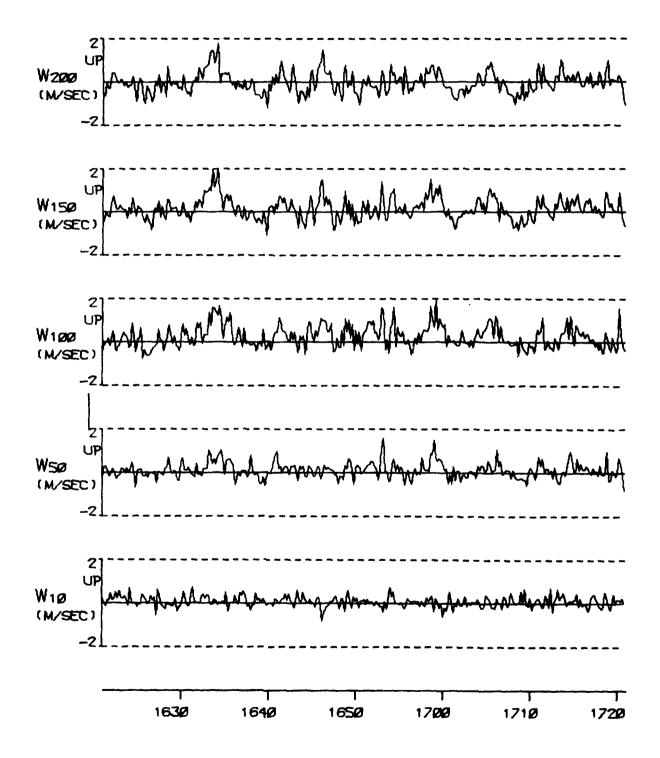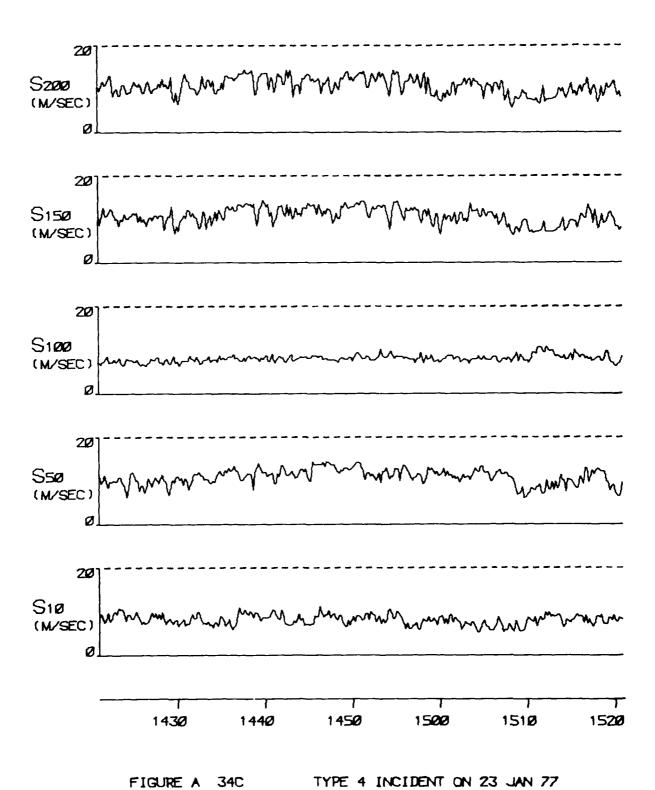
FIGURE A 34C   TYPE 4 INCIDENT ON 23 JAN 77
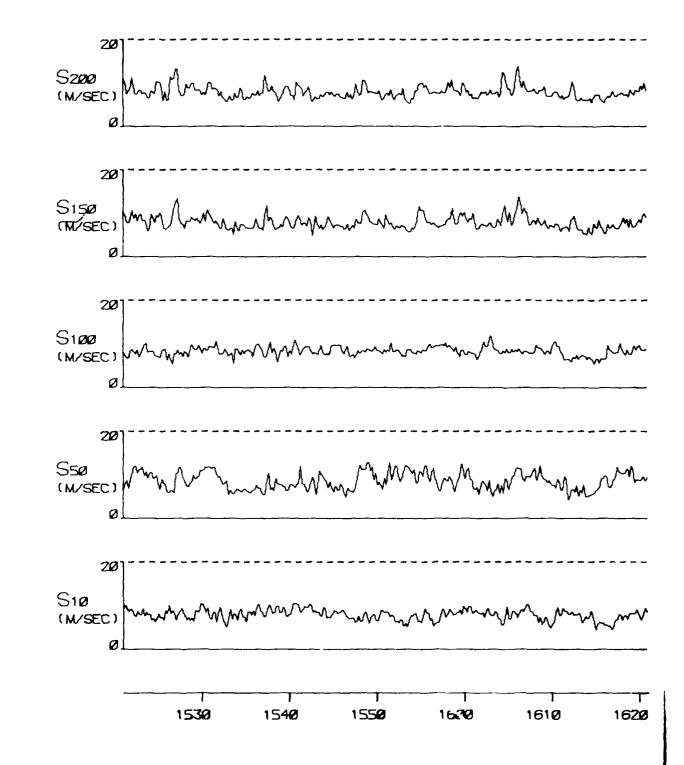
FIGURE A 34C (CONT) TYPE 4 INCIDENT ON 23 JAN 77
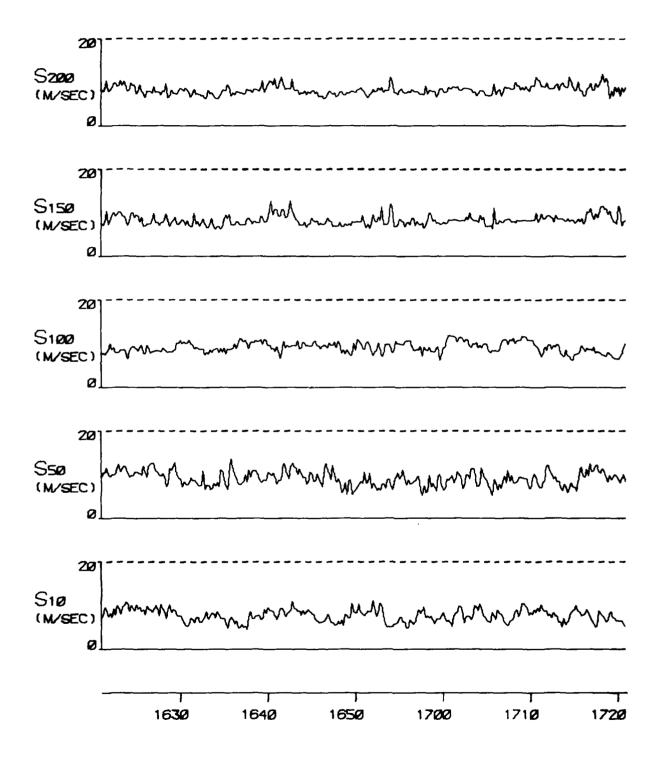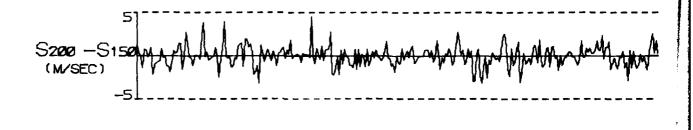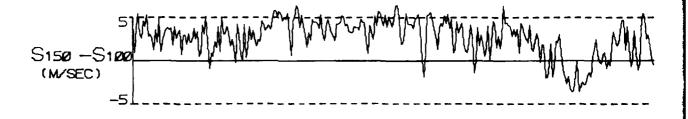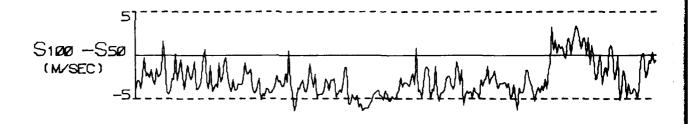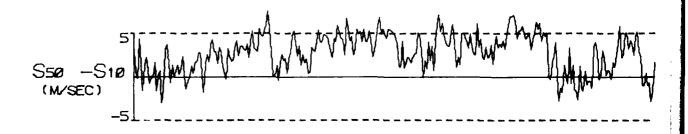
FIGURE A 34C (CONT) TYPE 4 INCIDENT ON 23 JAN 77
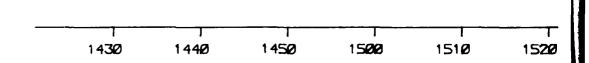
FIGURE A 34D   TYPE 4 INCIDENT ON 23 JAN 77
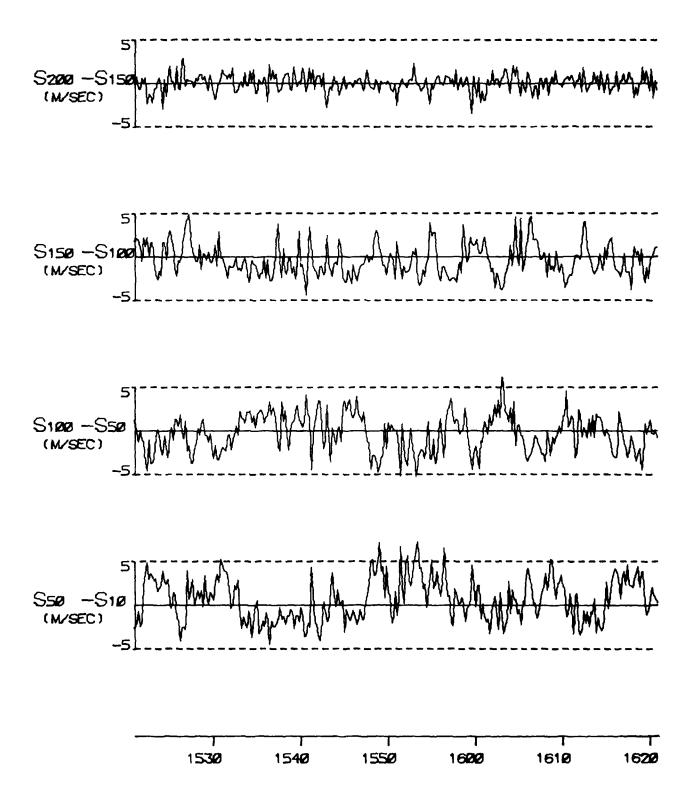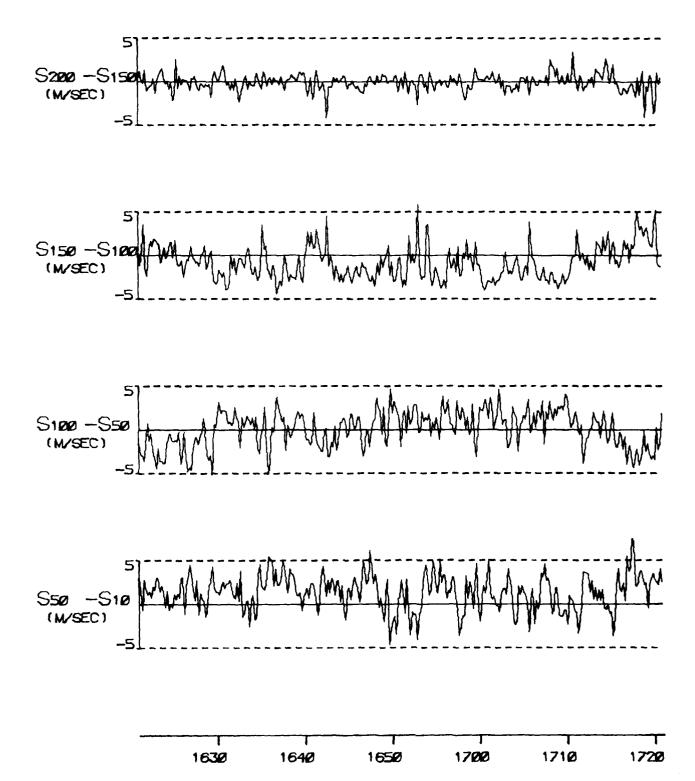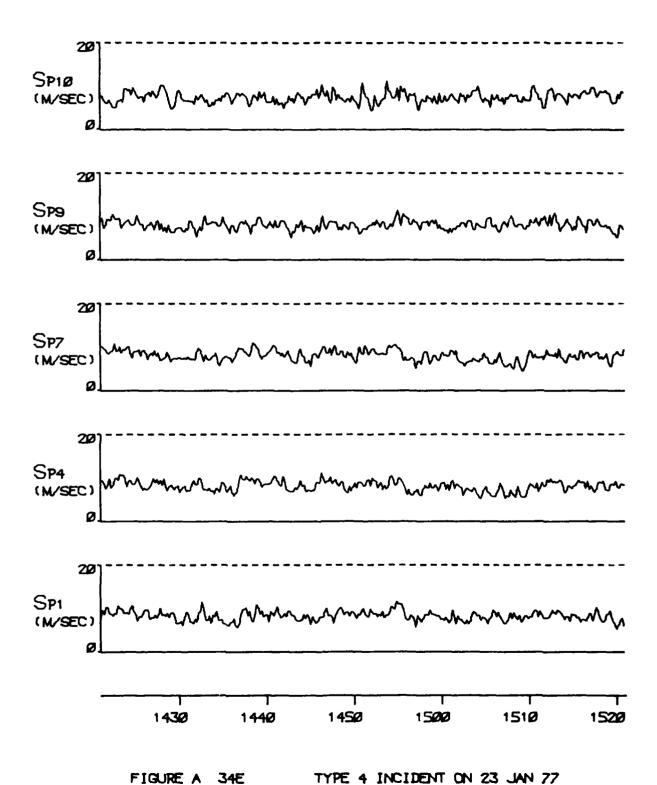
FIGURE A 34D (CONT) TYPE 4 INCIDENT ON 23 JAN 77

FIGURE A 34D (CONT) TYPE 4 INCIDENT ON 23 JAN 77

FIGURE A 34E   TYPE 4 INCIDENT ON 23 JAN 77

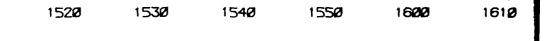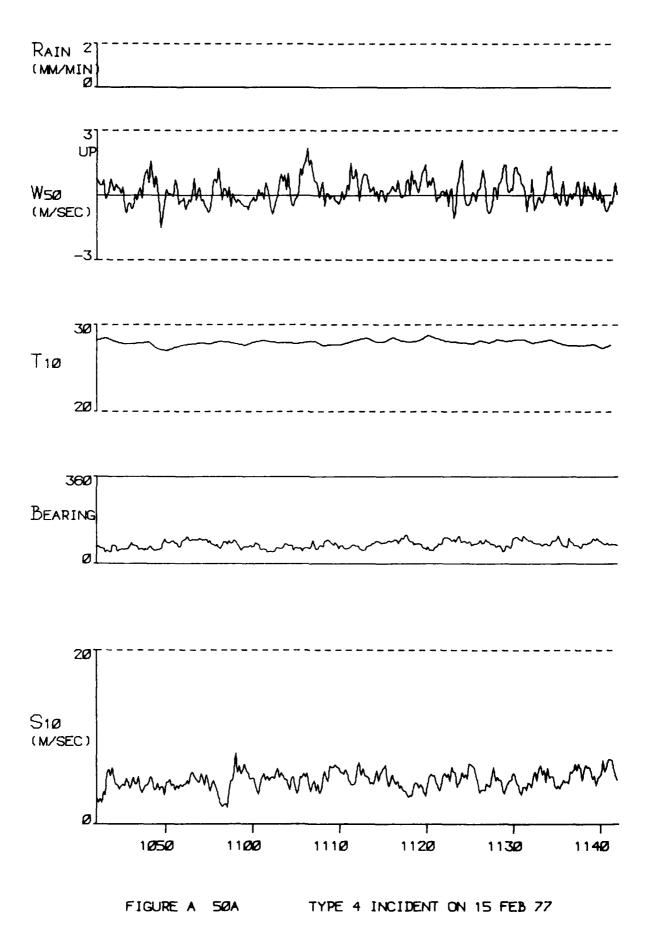FIGURE A 34E (CONT) TYPE 4 INCIDENT ON 23 JAN 77
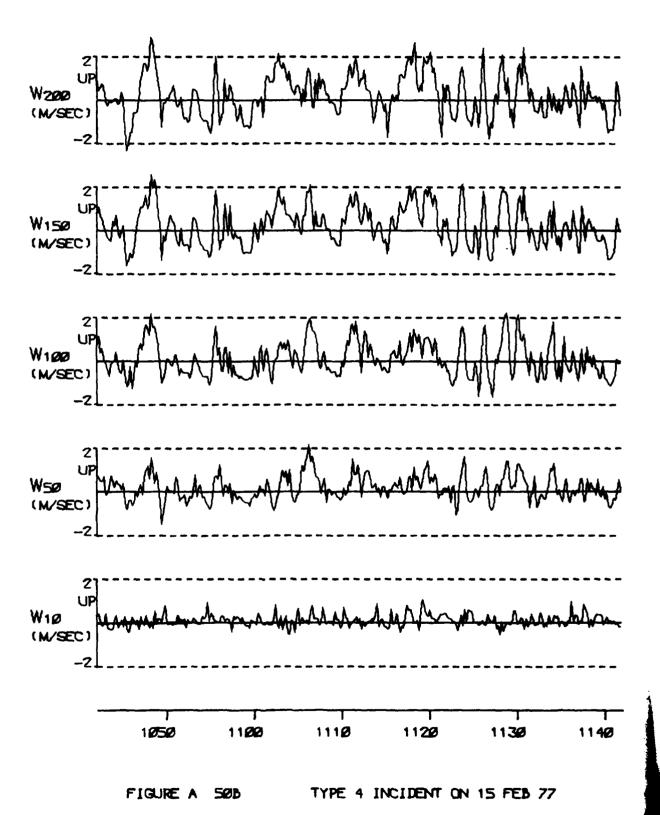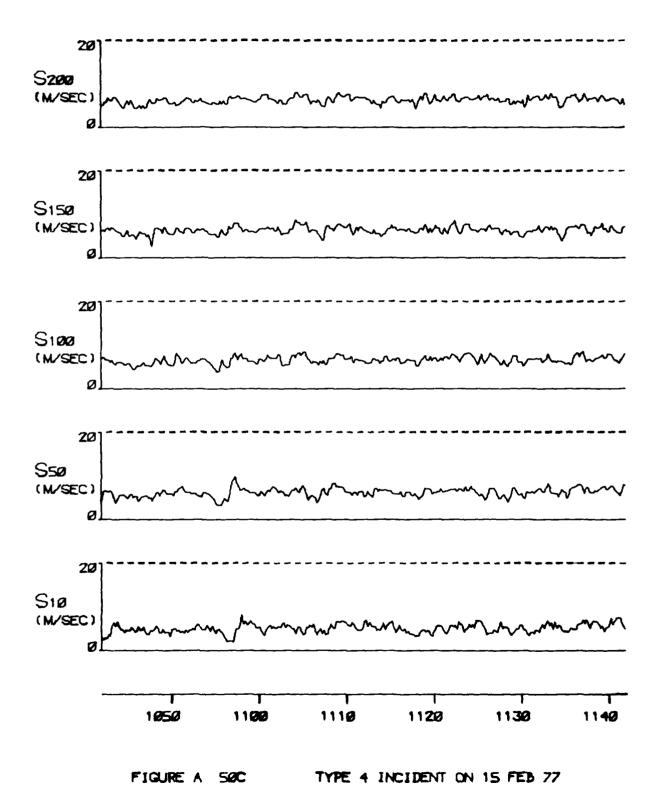
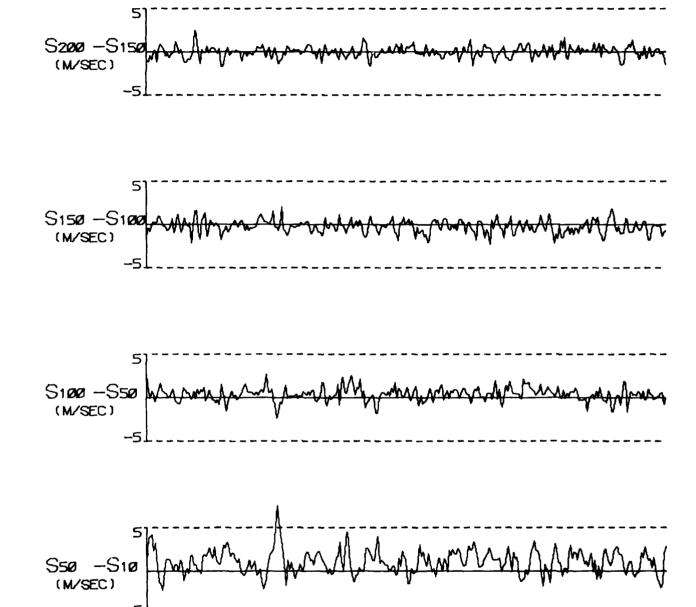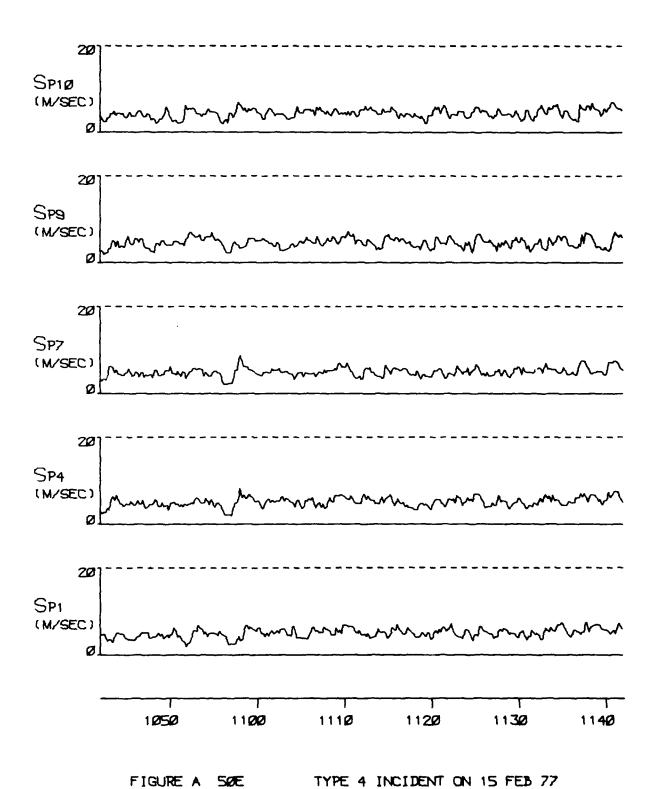FIGURE A 34E (CONT) TYPE 4 INCIDENT ON 23 JAN 77

FIGURE A 34F   TYPE 4 INCIDENT ON 23 JAN 77

FIGURE A 34F (CONT) TYPE 4 INCIDENT ON 23 JAN 77

FIGURE A 34F (CONT) TYPE 4 INCIDENT ON 23 JAN 77

FIGURE A 35A   TYPE 2 INCIDENT ON 24 JAN 77

FIGURE A 35B   TYPE 2 INCIDENT ON 24 JAN 77

FIGURE A 35C   TYPE 2 INCIDENT ON 24 JAN 77

FIGURE A   35D   TYPE 2 INCIDENT ON 2, JAN 77
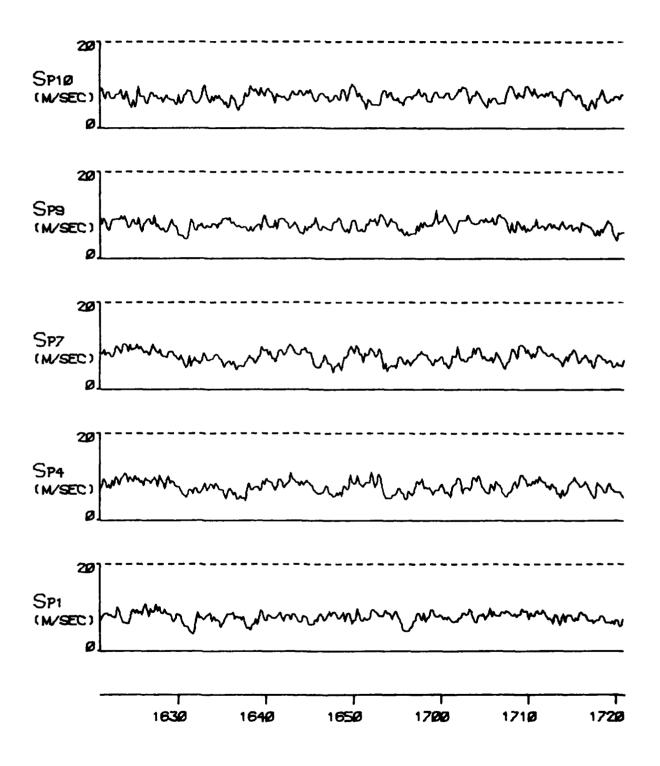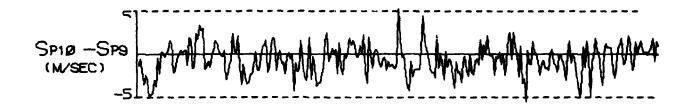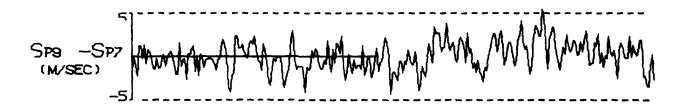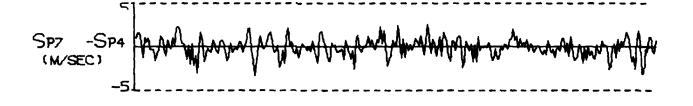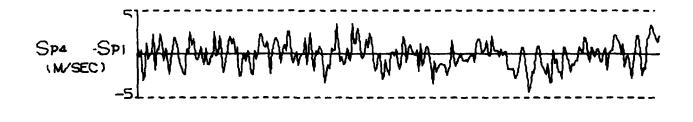
FIGURE A   35E   TYPE 2 INCIDENT ON 24 JAN 77

FIGURE A 35F   TYPE 2 INCIDENT ON 24 JAN 77
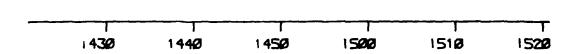
FIGURE A   36A   TYPE 3 INCIDENT ON 24 JAN 77
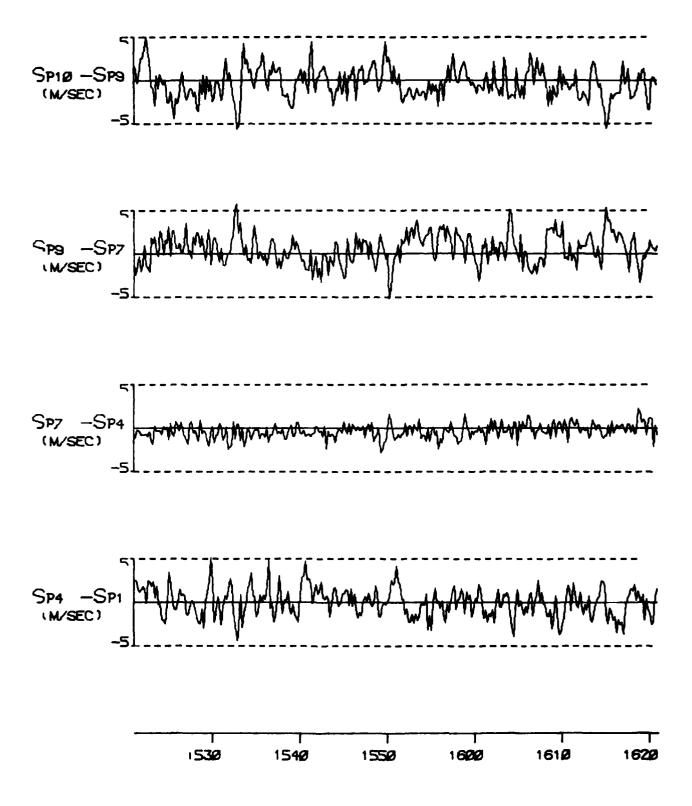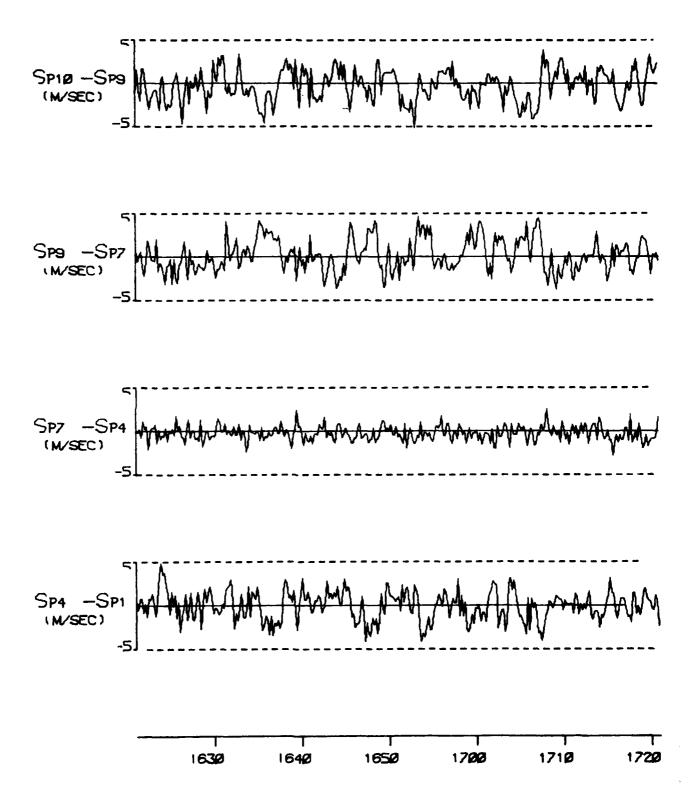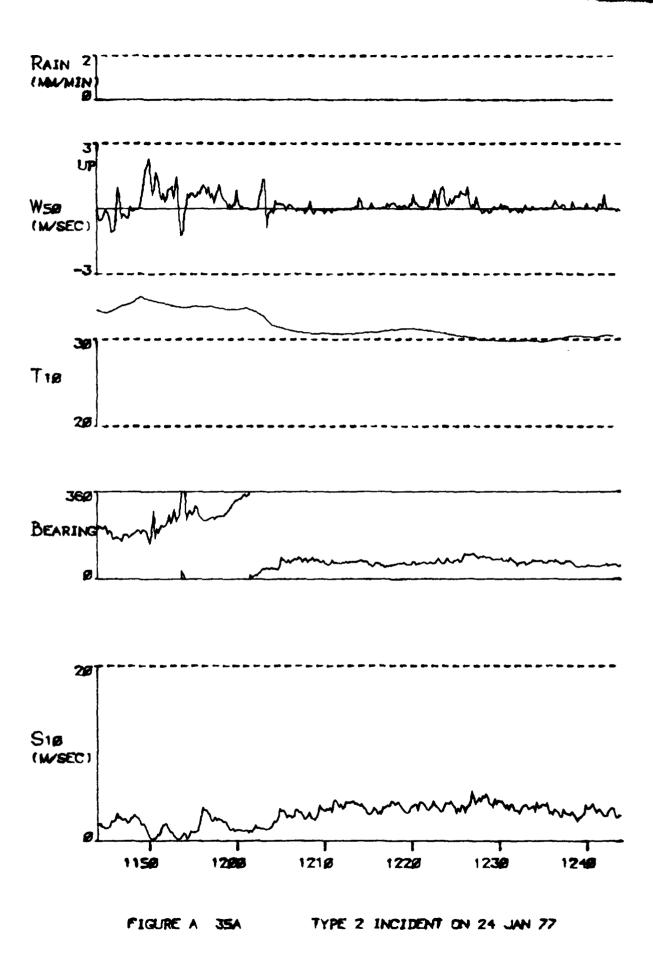
FIGURE A 36B   TYPE 3 INCIDENT ON 24 JAN 77
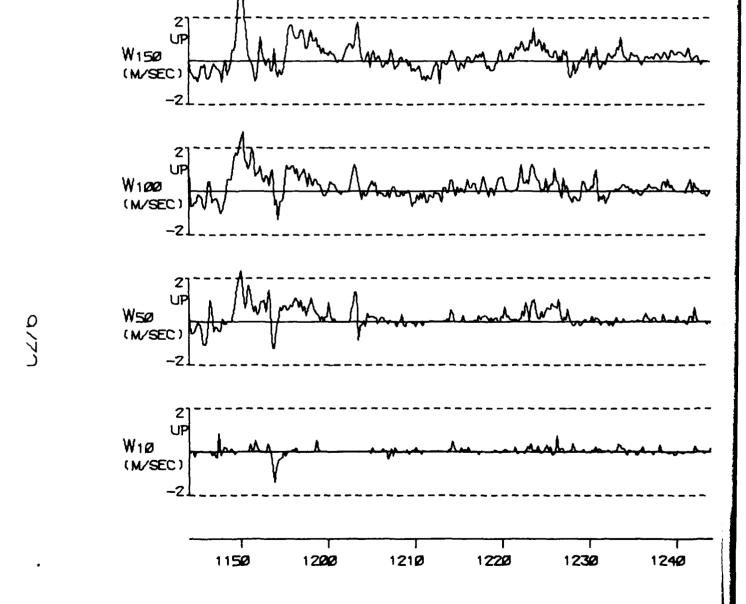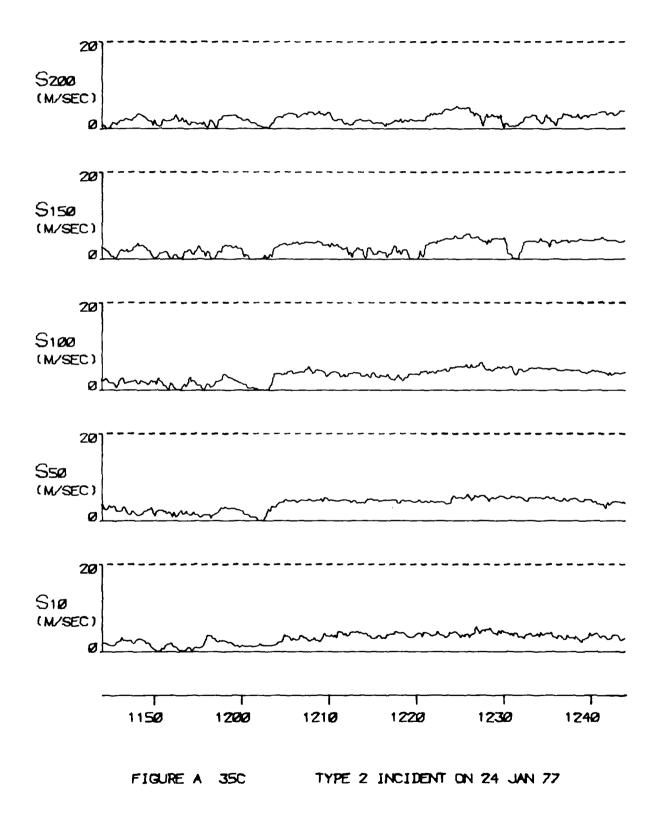
FIGURE A 36C   TYPE 3 INCIDENT ON 24 JAN 77
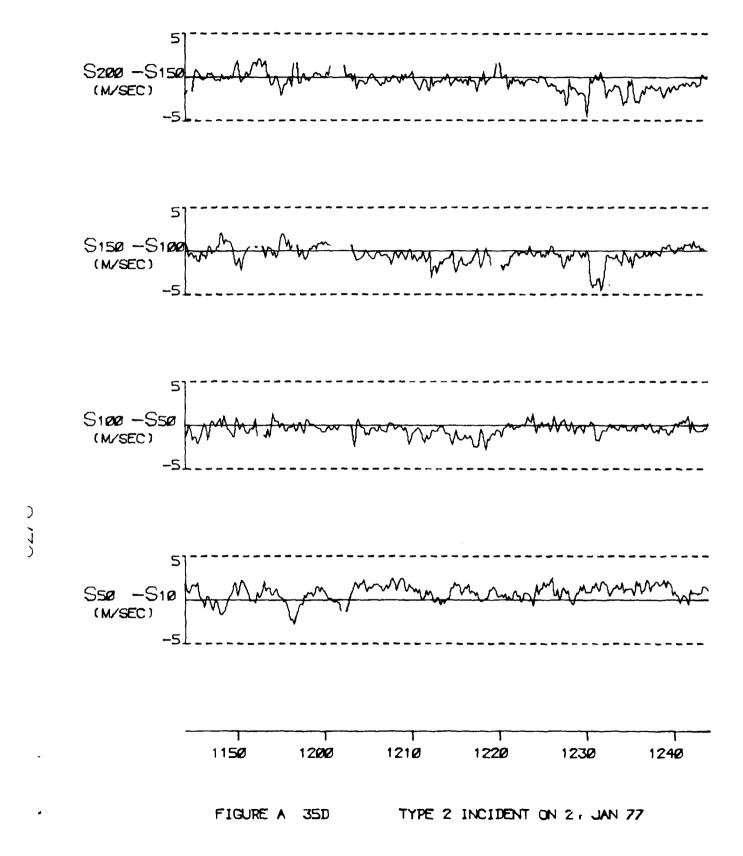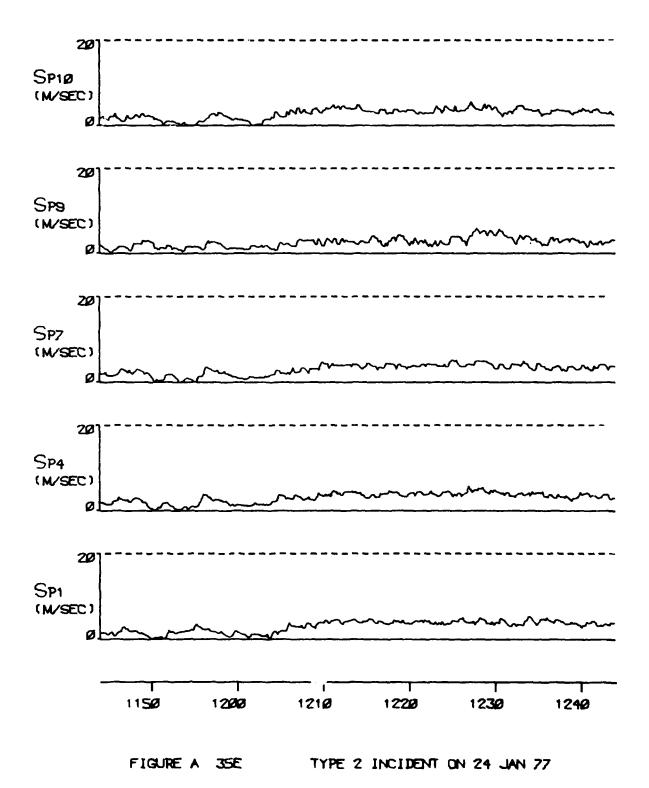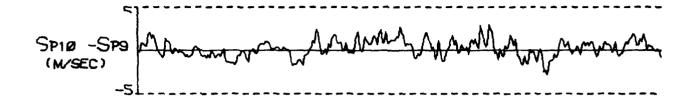
FIGURE A 38D   TYPE 3 INCIDENT ON 24 JAN 77
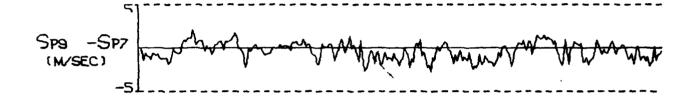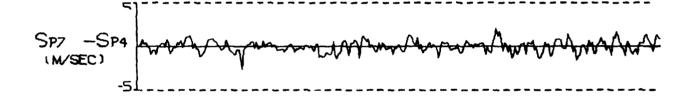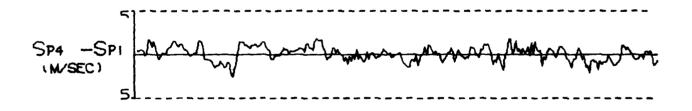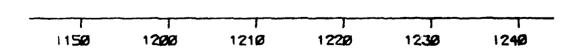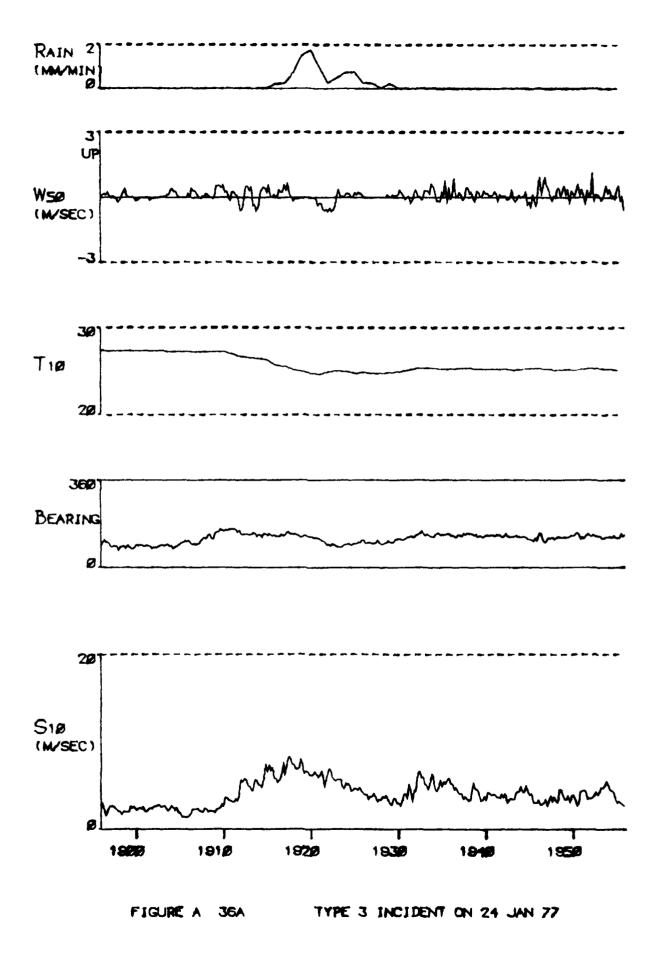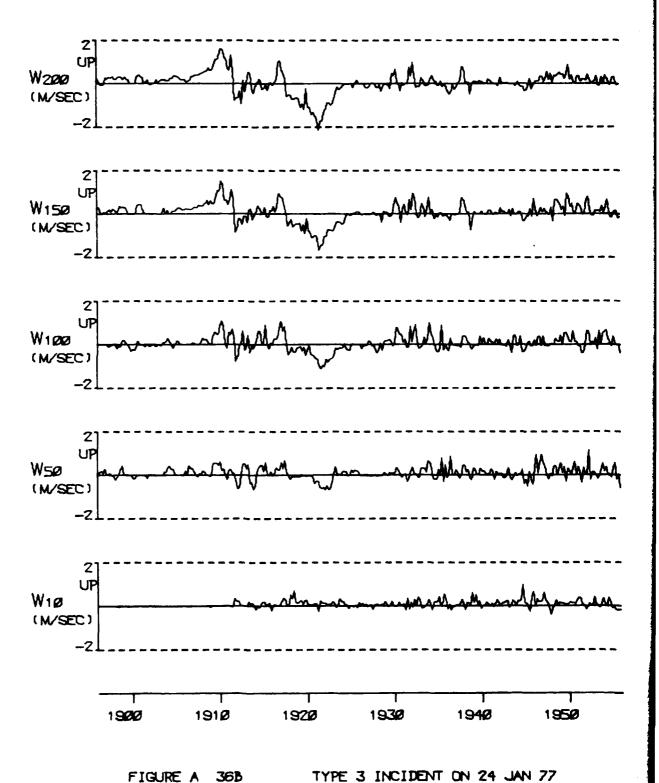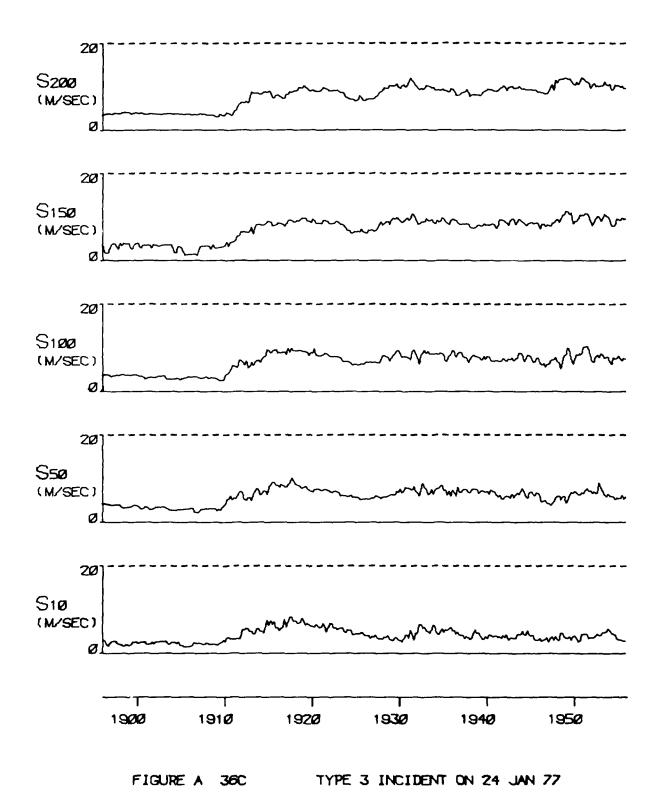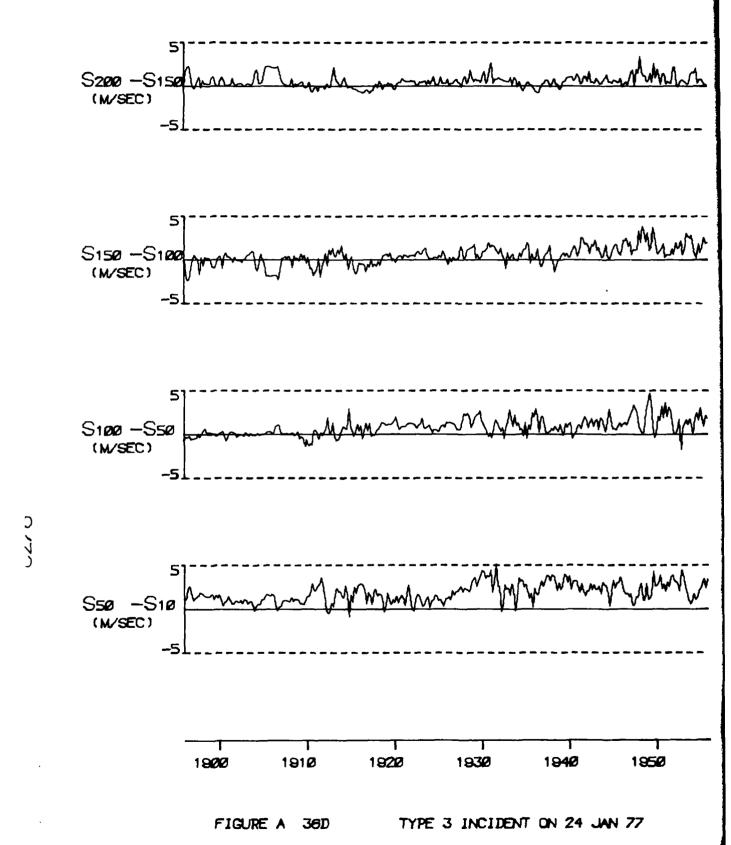
FIGURE A 36E   TYPE 3 INCIDENT ON 24 JAN 77
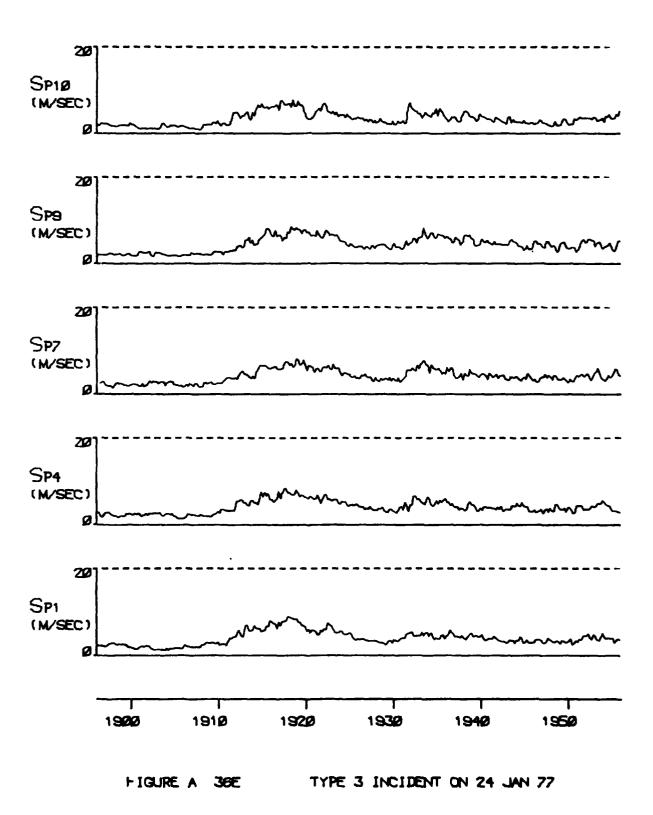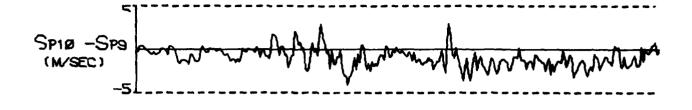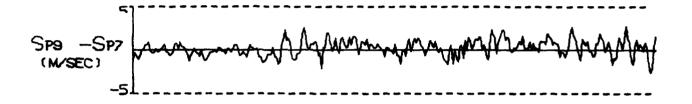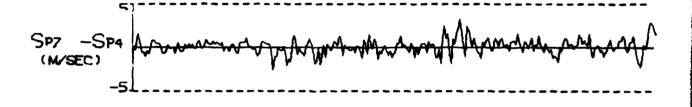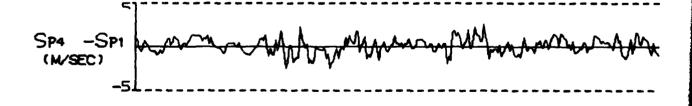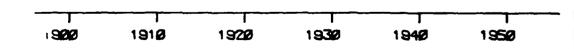
FIGURE A 36F   TYPE 3 INCIDENT ON 24 JAN 77
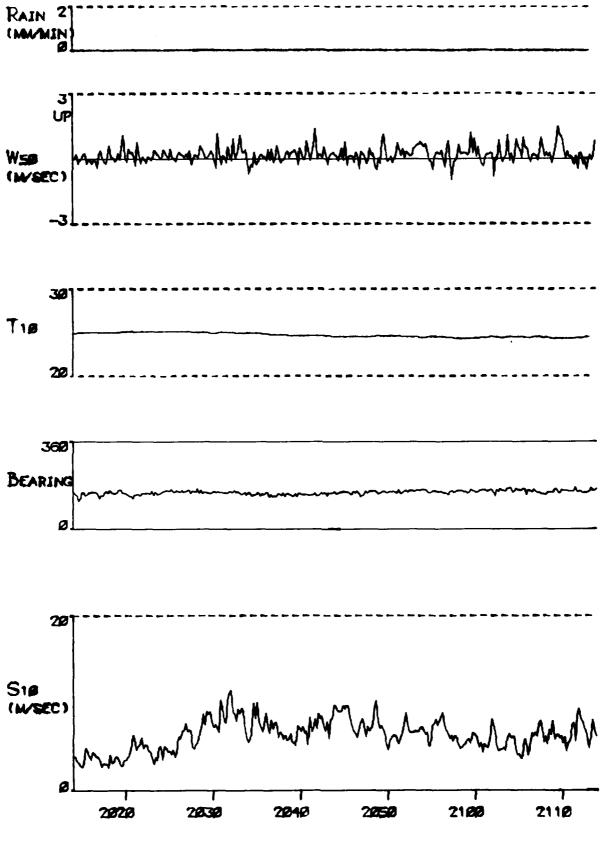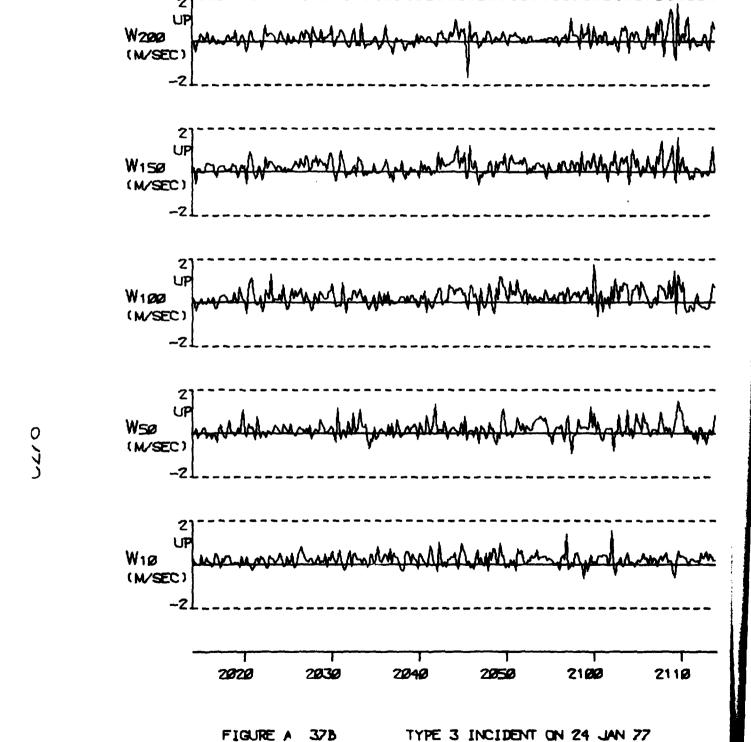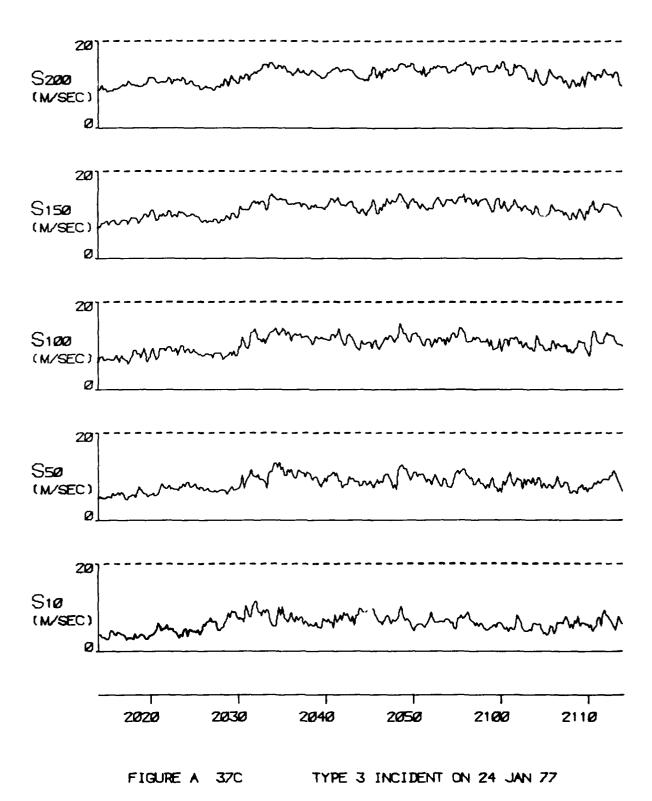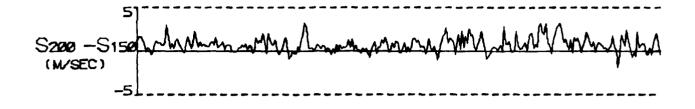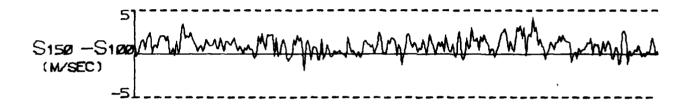
FIGURE A 37A   TYPE 3 INCIDENT ON 24 JAN 77

FIGURE A 37B   TYPE 3 INCIDENT ON 24 JAN 77
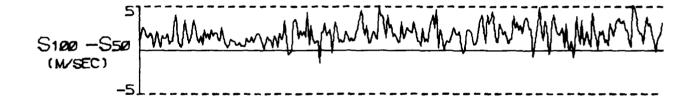
FIGURE A 37C   TYPE 3 INCIDENT ON 24 JAN 77
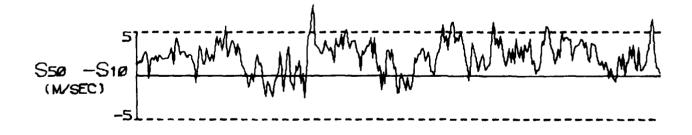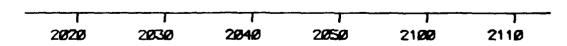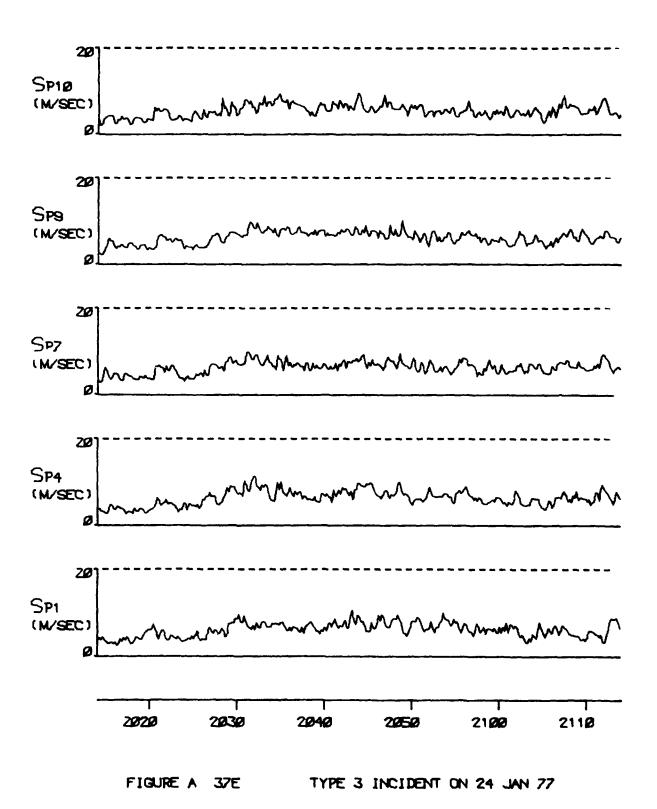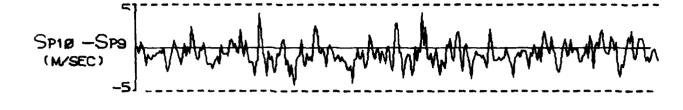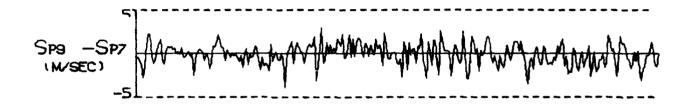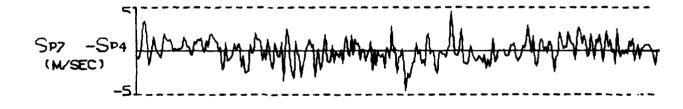
FIGURE A 37D   TYPE 3 INCIDENT ON 24 JAN 77

SP10 (M/SEC)

SP9 (M/SEC)

SP7 (M/SEC)

SP4 (M/SEC)

SP1 (M/SEC)

2020   2030   2040   2050   2100   2110
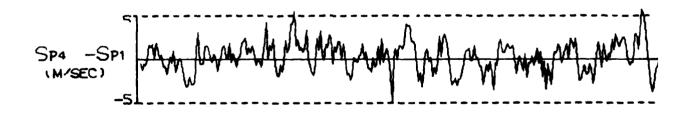
FIGURE A 37E   TYPE 3 INCIDENT ON 24 JAN 77
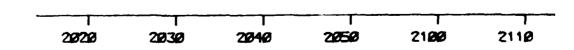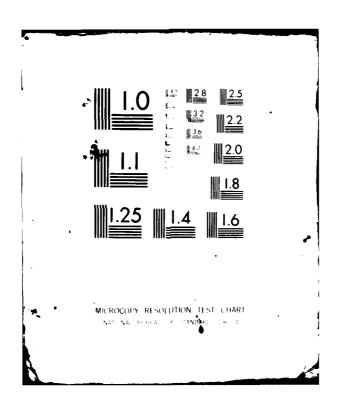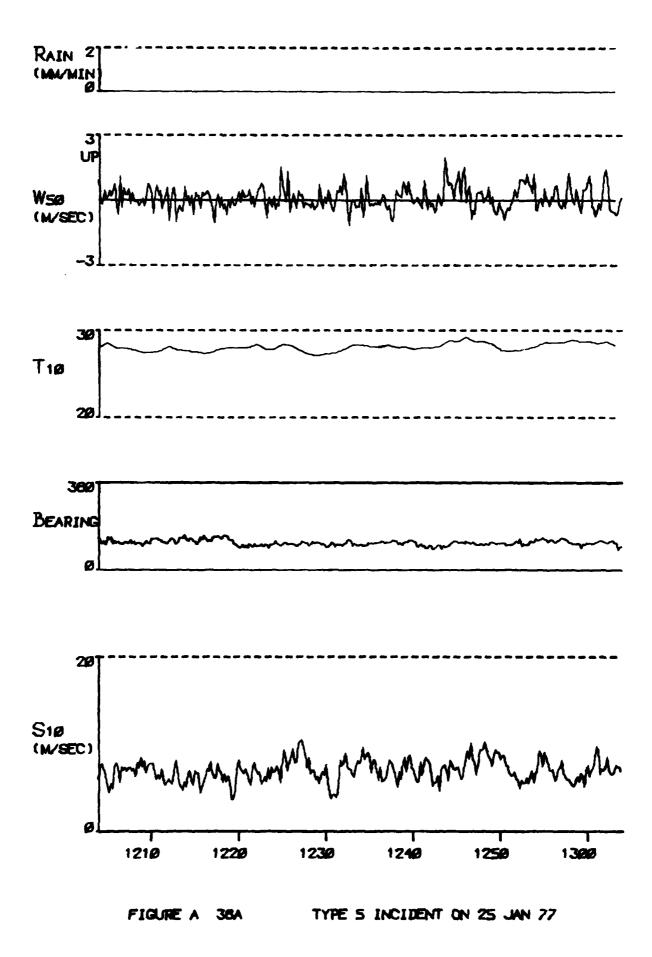
FIGURE A 37F   TYPE 3 INCIDENT ON 24 JAN 77

1.0

1.1

1.25   1.4   1.6

2.8   2.5

3.2   2.2

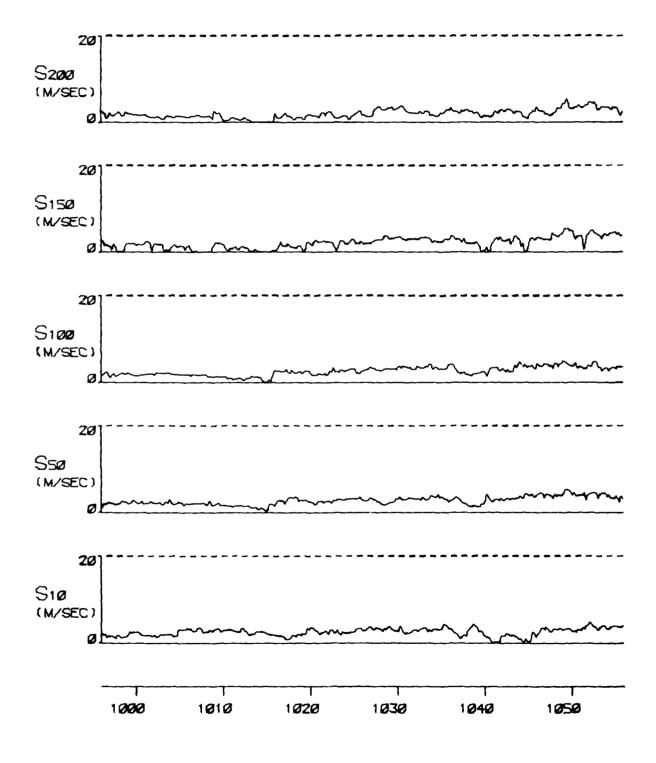3.6

4.0   2.0

1.8

MICROCOPY RESOLUTION TEST CHART

NATIONAL BUREAU OF STANDARDS

FIGURE A 38A   TYPE 5 INCIDENT ON 25 JAN 77

FIGURE A 38A (CONT) TYPE 5 INCIDENT ON 25 JAN 77

FIGURE A 38A (CONT) TYPE 5 INCIDENT ON 25 JAN 77

FIGURE A 38B   TYPE 5 INCIDENT ON 25 JAN 77
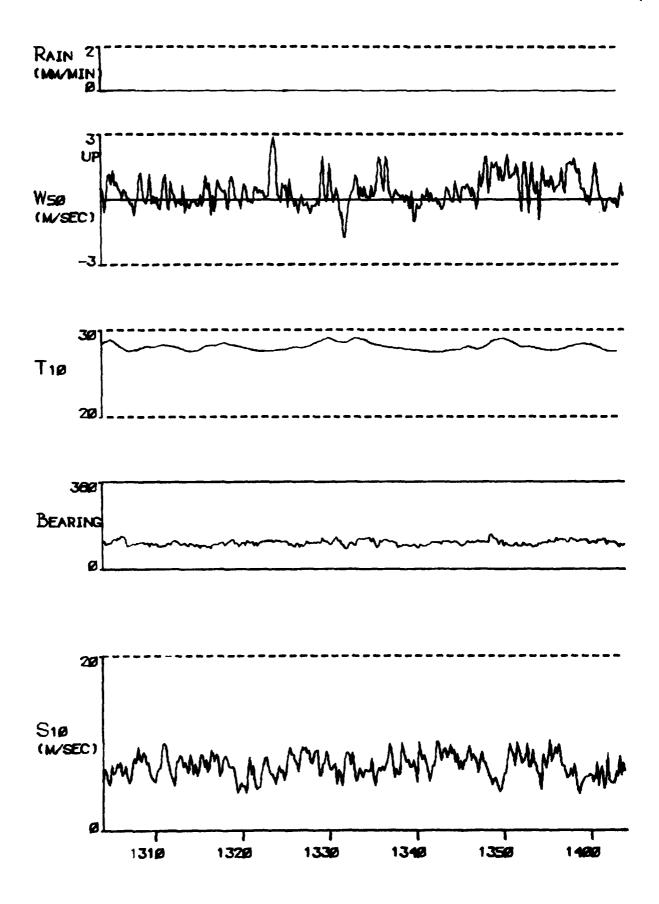
FIGURE A 38b (CONT) TYPE 5 INCIDENT ON 25 JAN 77
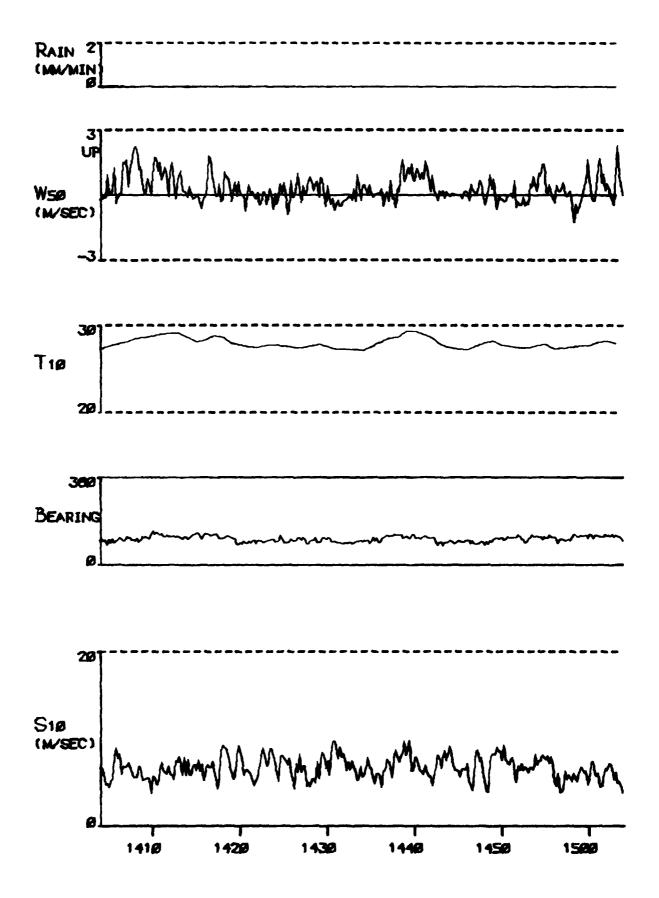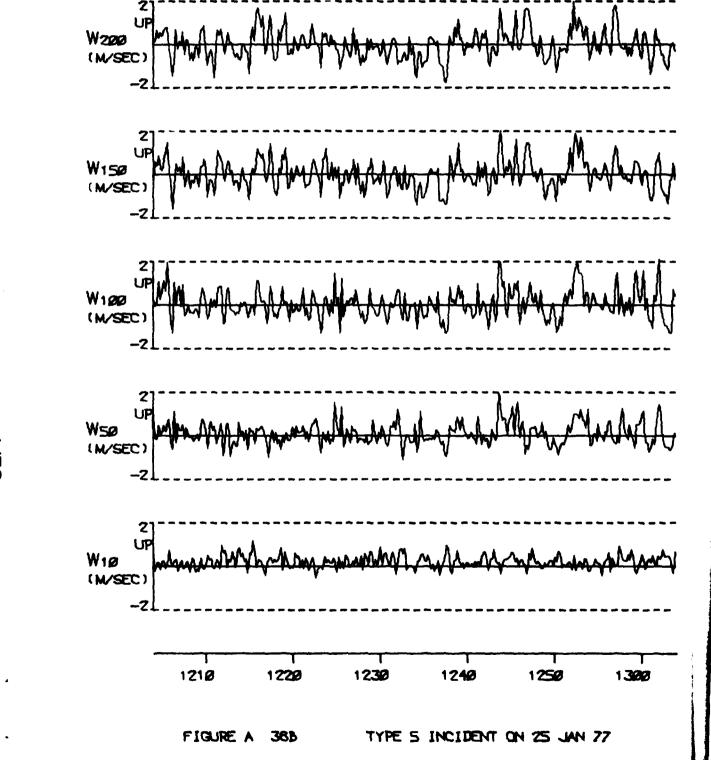
FIGURE A 38B (CONT) TYPE 5 INCIDENT ON 25 JAN 77
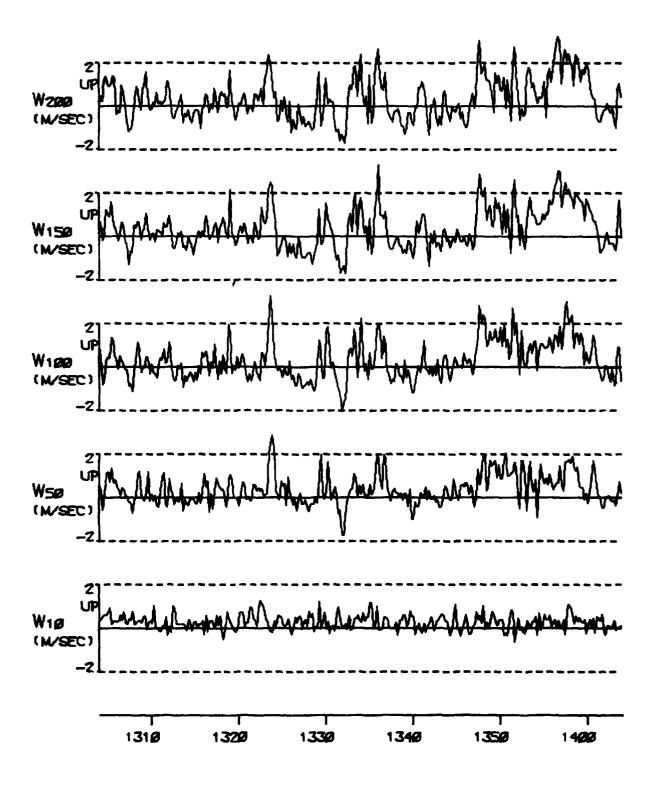
FIGURE A 38C   TYPE 5 INCIDENT ON 25 JAN 77
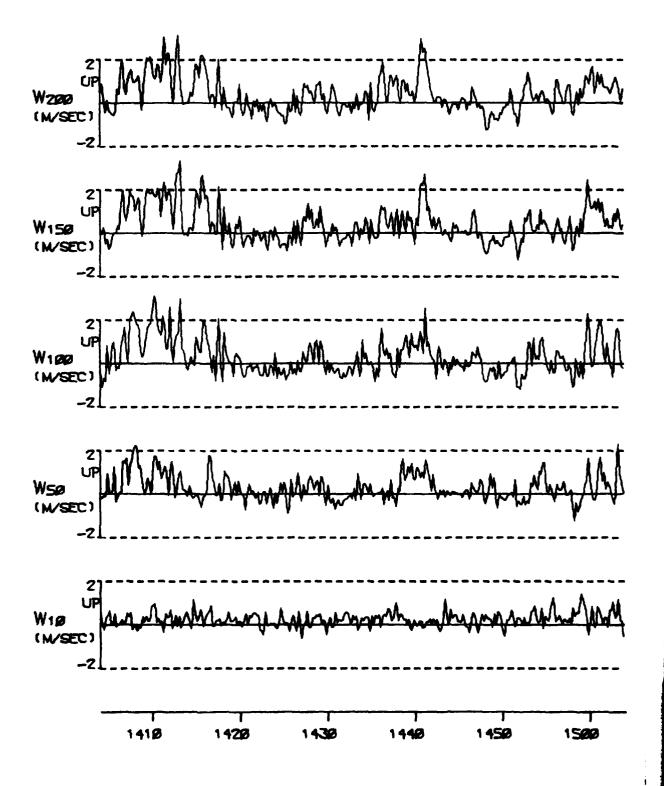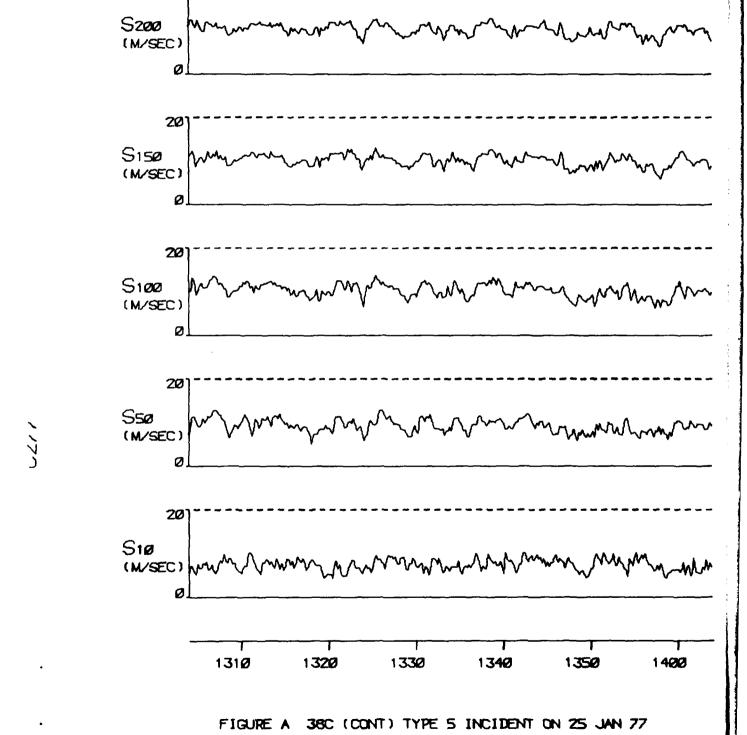
FIGURE A 38C (CONT) TYPE 5 INCIDENT ON 25 JAN 77

FIGURE A 38C (CONT) TYPE 5 INCIDENT ON 25 JAN 77

FIGURE A 38D   TYPE 5 INCIDENT ON 25 JAN 77

FIGURE A 38D (CONT) TYPE 5 INCIDENT ON 25 JAN 77
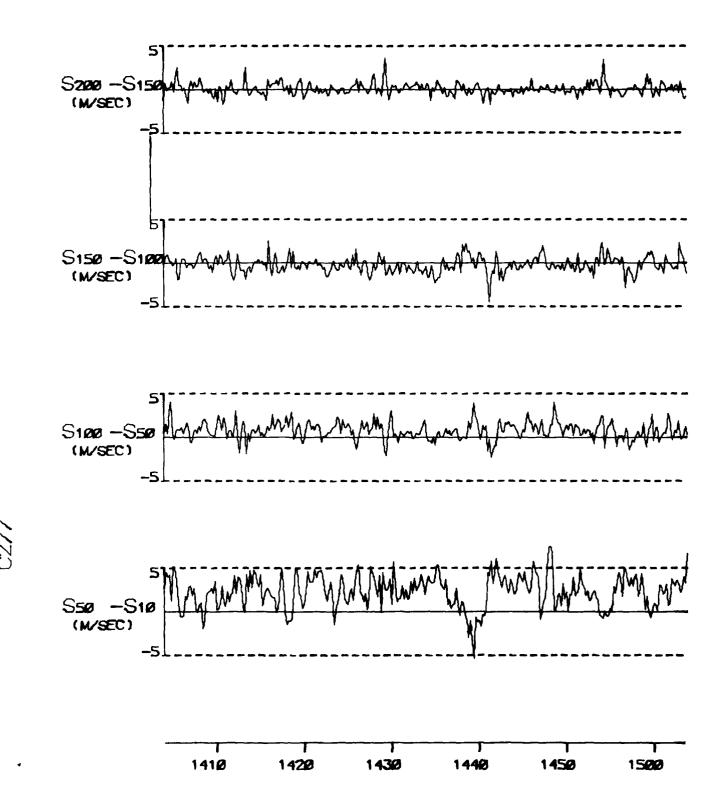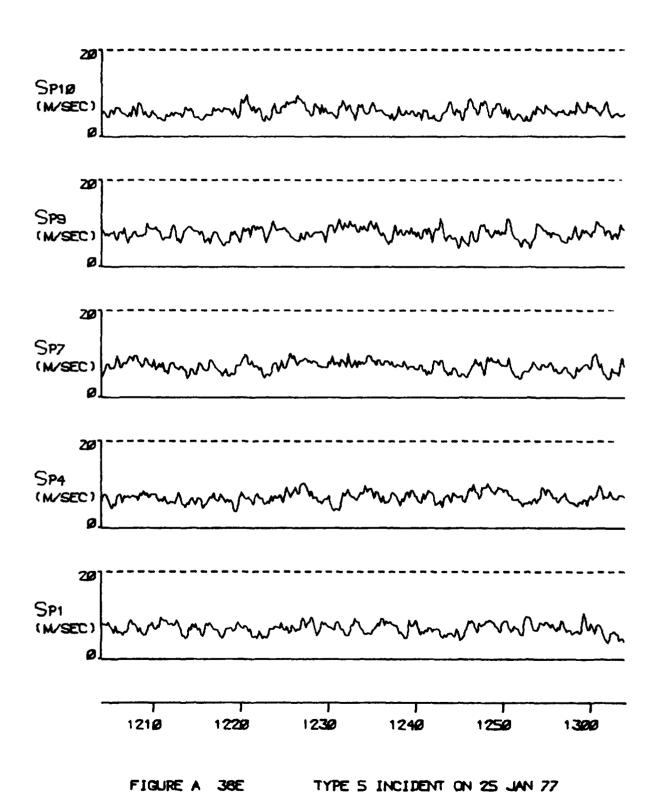
FIGURE A 38D (CONT) TYPE 5 INCIDENT ON 25 JAN 77

FIGURE A 38E   TYPE 5 INCIDENT ON 25 JAN 77
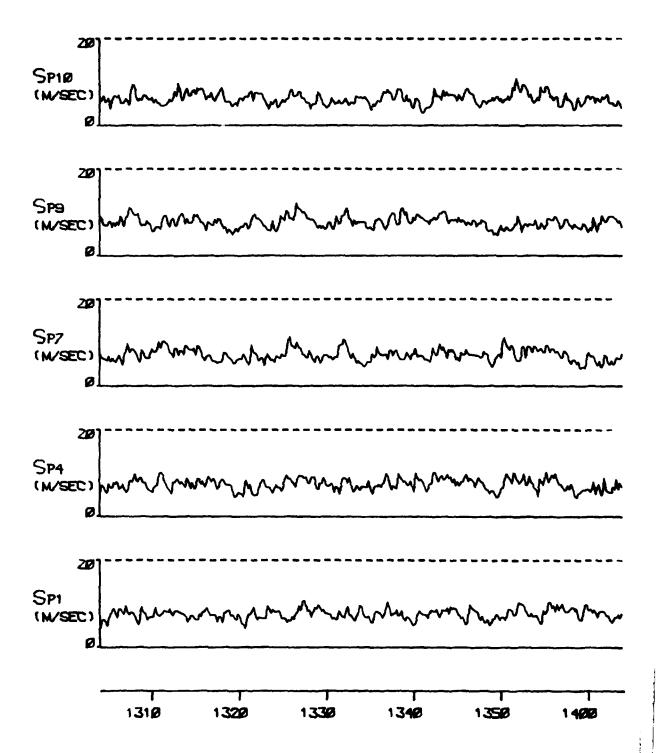
FIGURE A 36E (CONT) TYPE 5 INCIDENT ON 25 JAN 77

C277

FIGURE A 36E (CONT) TYPE S INCIDENT ON 25 JAN 77

FIGURE A 38F   TYPE 5 INCIDENT ON 25 JAN 77

FIGURE A 38F (CONT) TYPE S INCIDENT ON 25 JAN 77
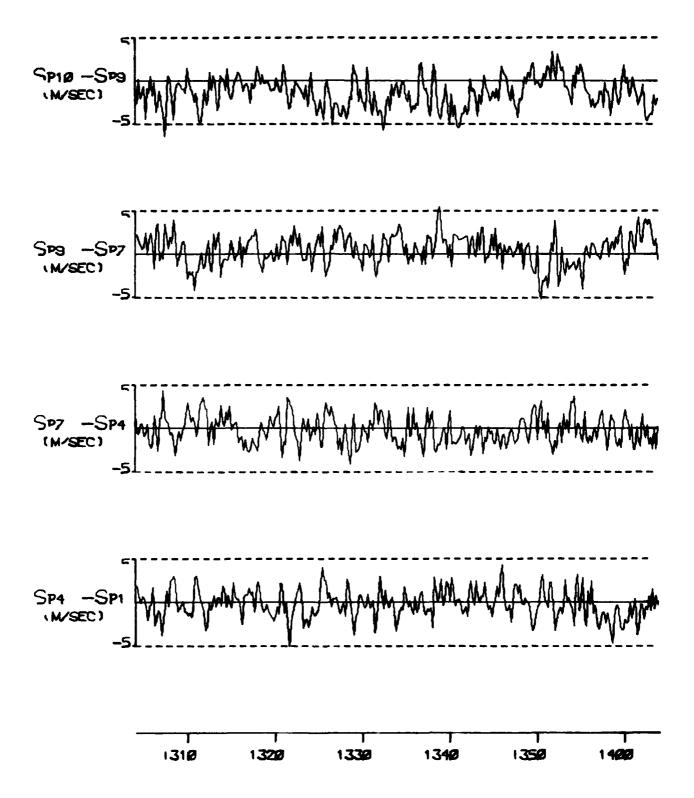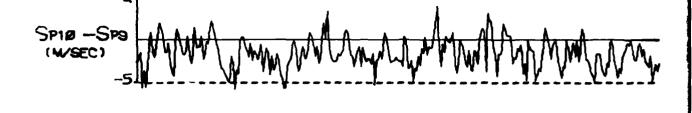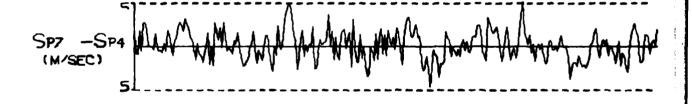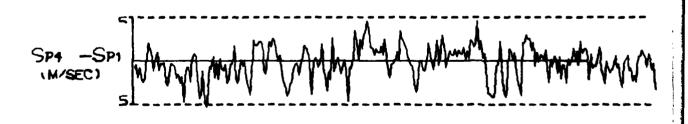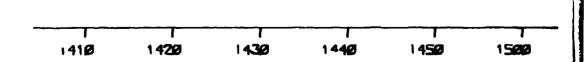
FIGURE A 38F (CONT) TYPE 5 INCIDENT ON 25 JAN 77
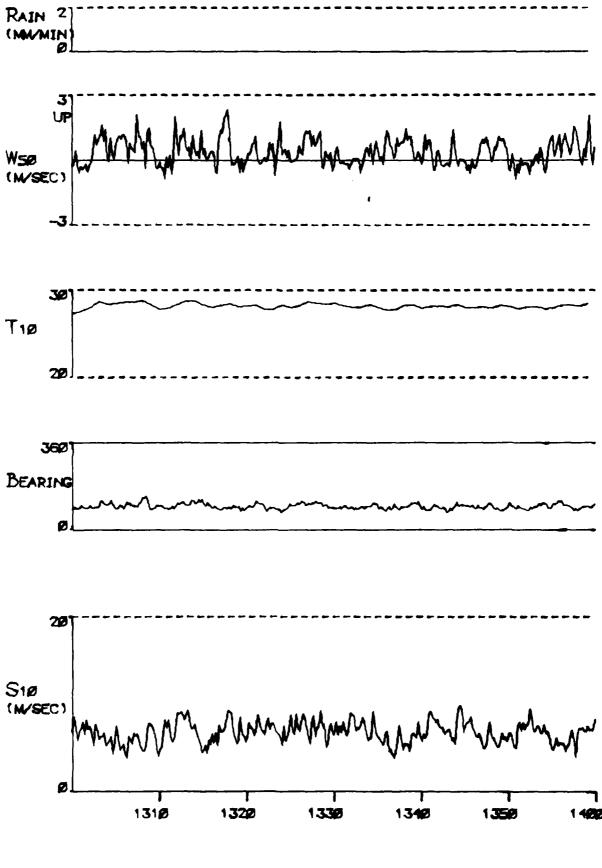
FIGURE A 39A   TYPE 4 INCIDENT ON 26 JAN 77

FIGURE A 39B   TYPE 4 INCIDENT ON 26 JAN 77

FIGURE A 39C   TYPE 4 INCIDENT ON 26 JAN 77

FIGURE A 39D   TYPE 4 INCIDENT ON 26 JAN 77

C278

FIGURE A 39E   TYPE 4 INCIDENT ON 26 JAN 77

C278
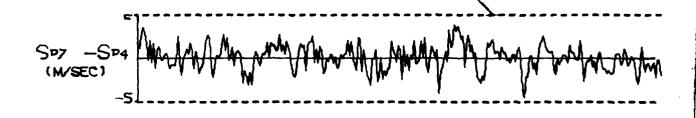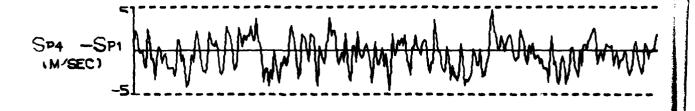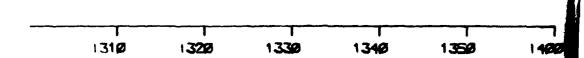
FIGURE A 39F   TYPE 4 INCIDENT ON 28 JAN 77
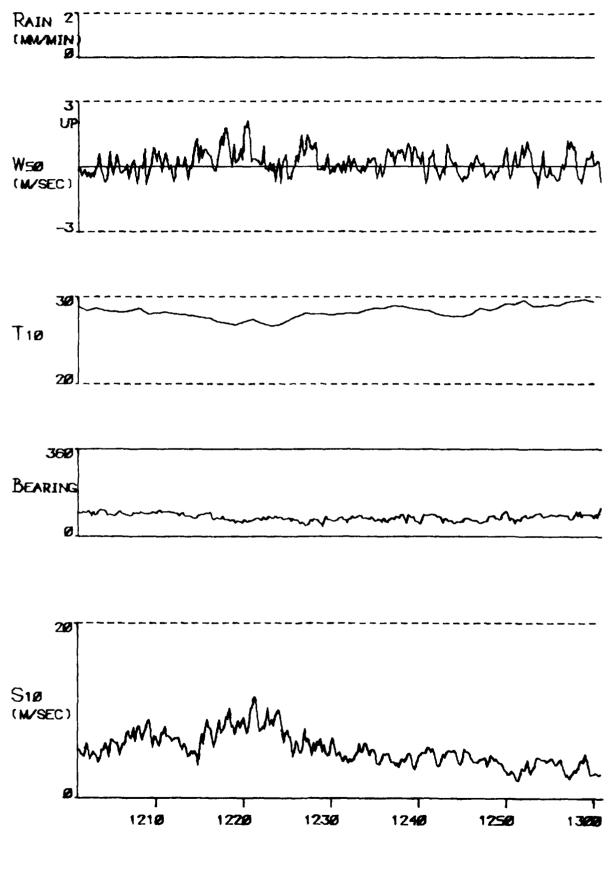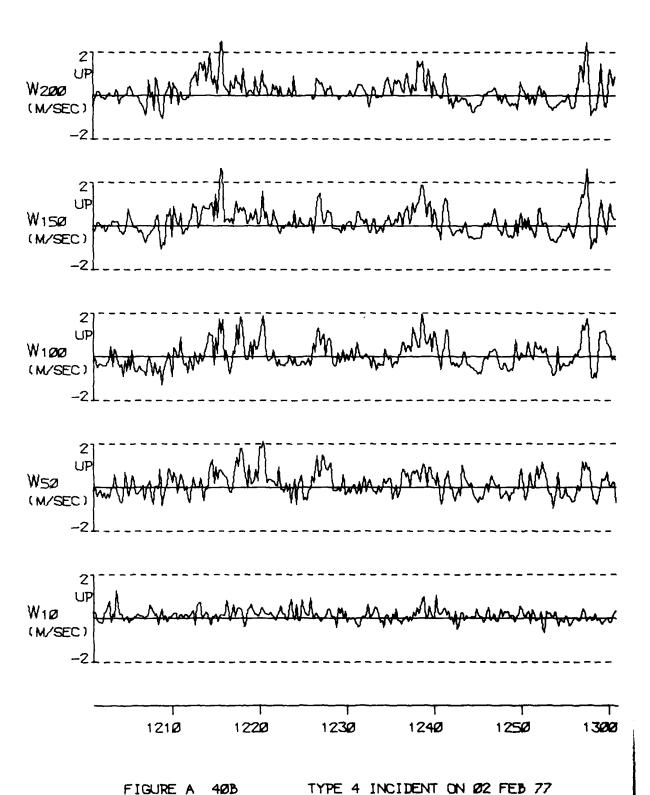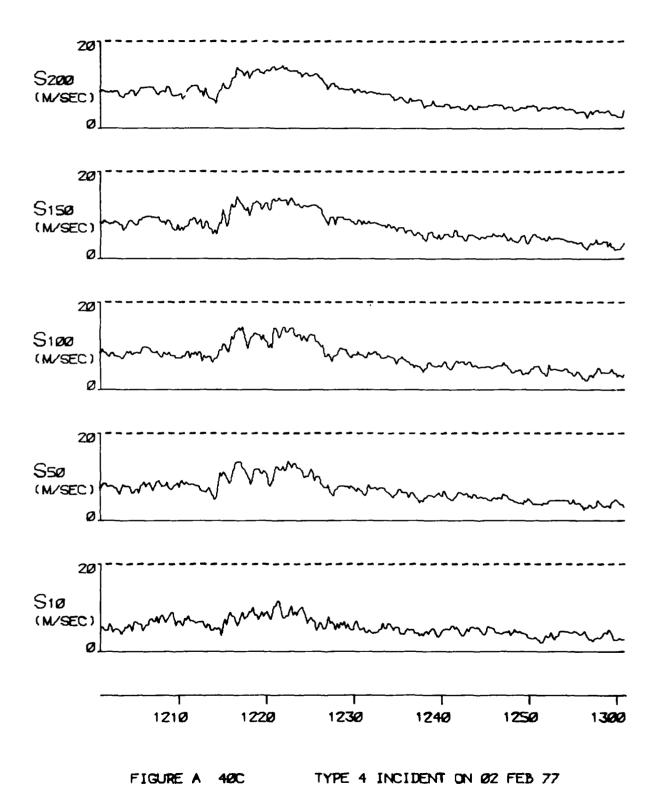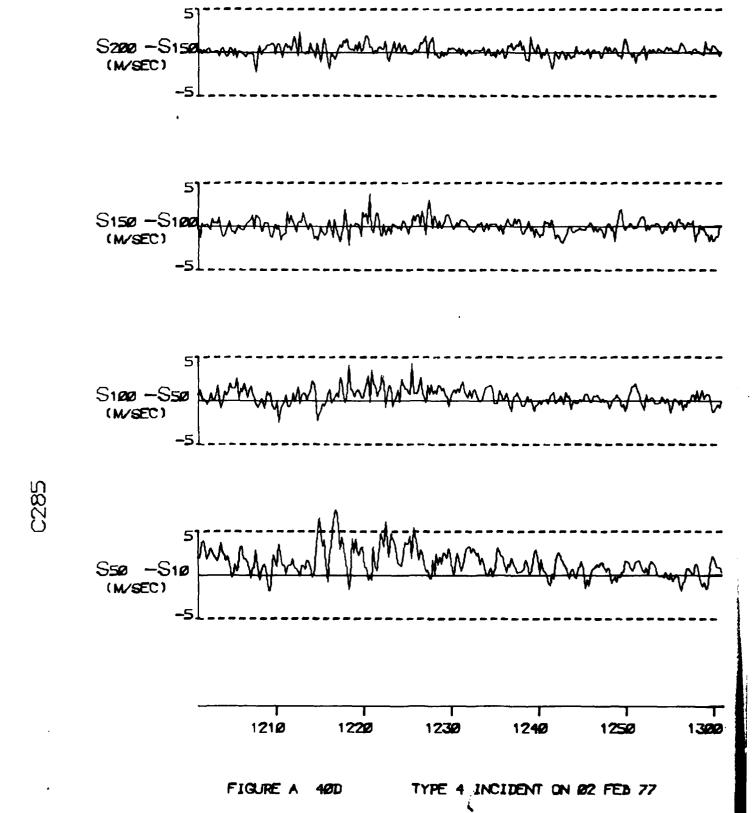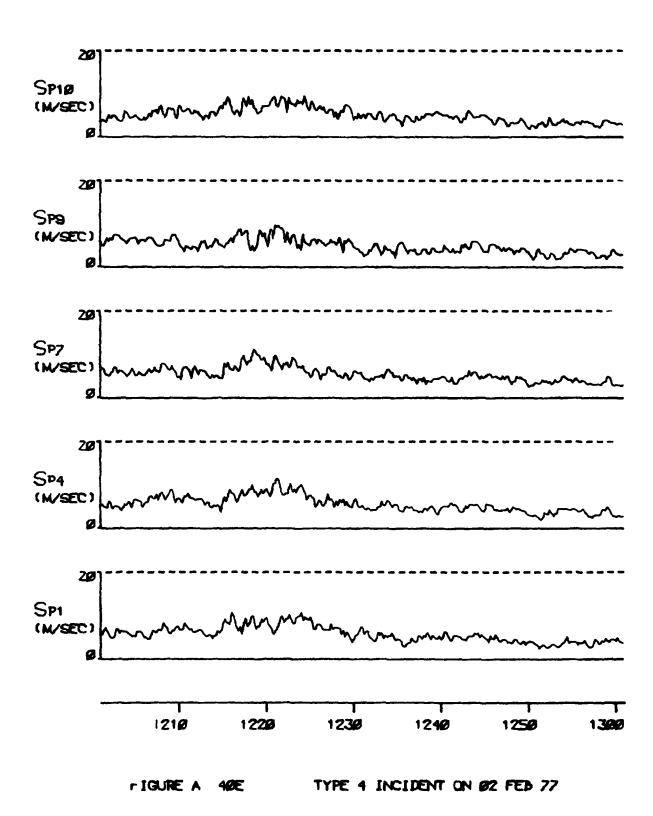
FIGURE A 40A   TYPE 4 INCIDENT ON 02 FEB 77

FIGURE A 40B   TYPE 4 INCIDENT ON 02 FEB 77

FIGURE A 40C   TYPE 4 INCIDENT ON 02 FEB 77
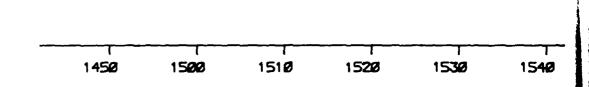
C285

FIGURE A 40D   TYPE 4 INCIDENT ON 02 FEB 77

FIGURE A 40E   TYPE 4 INCIDENT ON 02 FEB 77
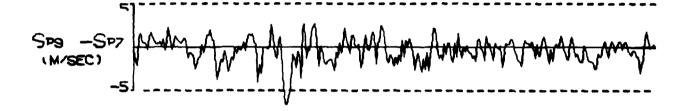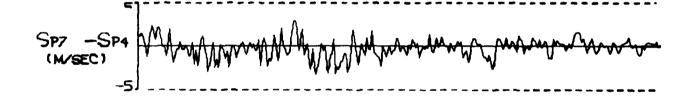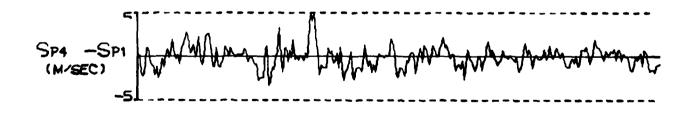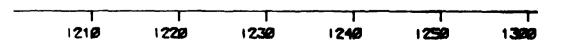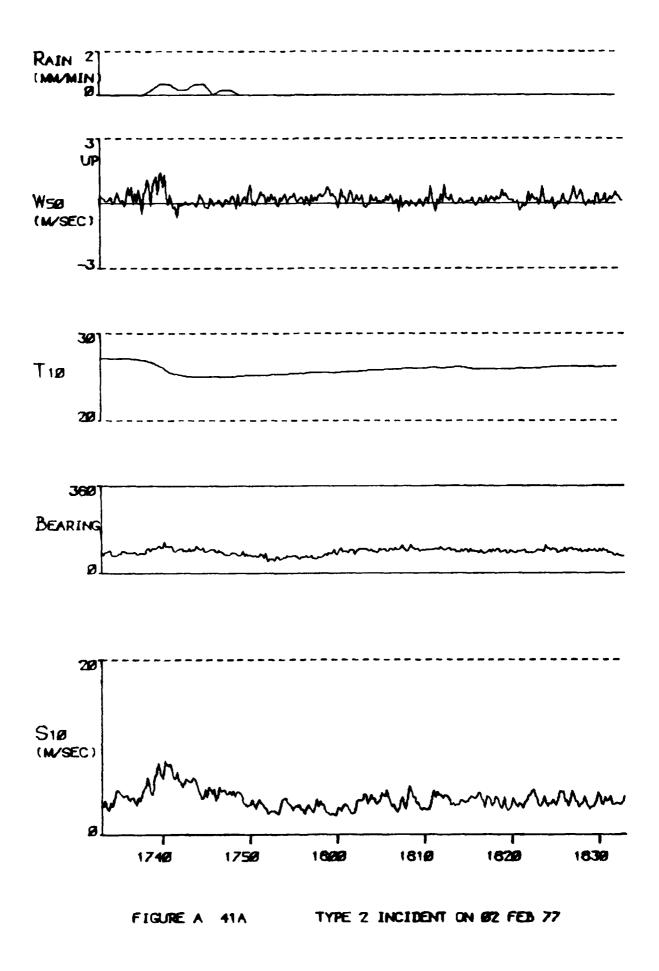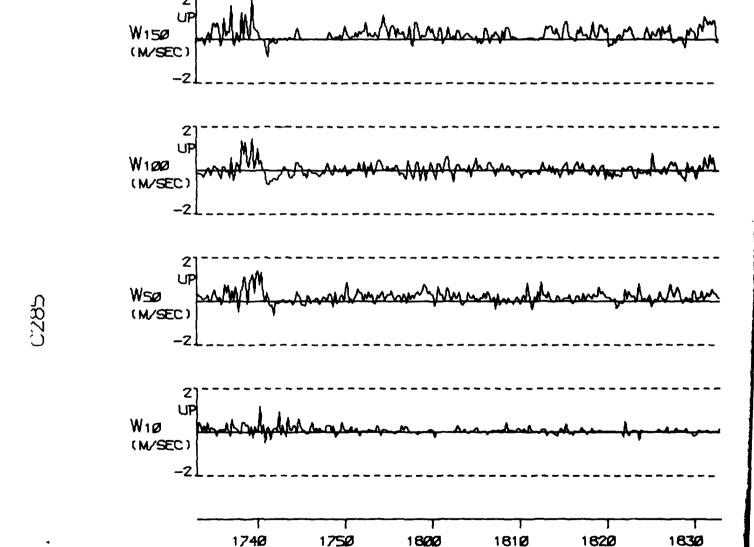
C285

FIGURE A 40F   TYPE 4 INCIDENT ON 02 FEB 77

FIGURE A 41A   TYPE 2 INCIDENT ON 02 FEB 77

C285

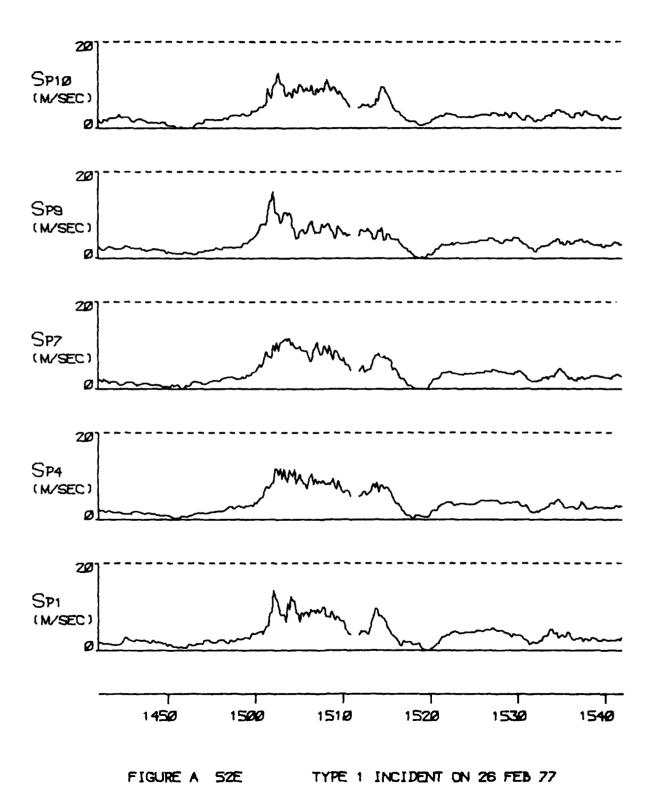FIGURE A 41B   TYPE 2 INCIDENT ON 02 FEB 77
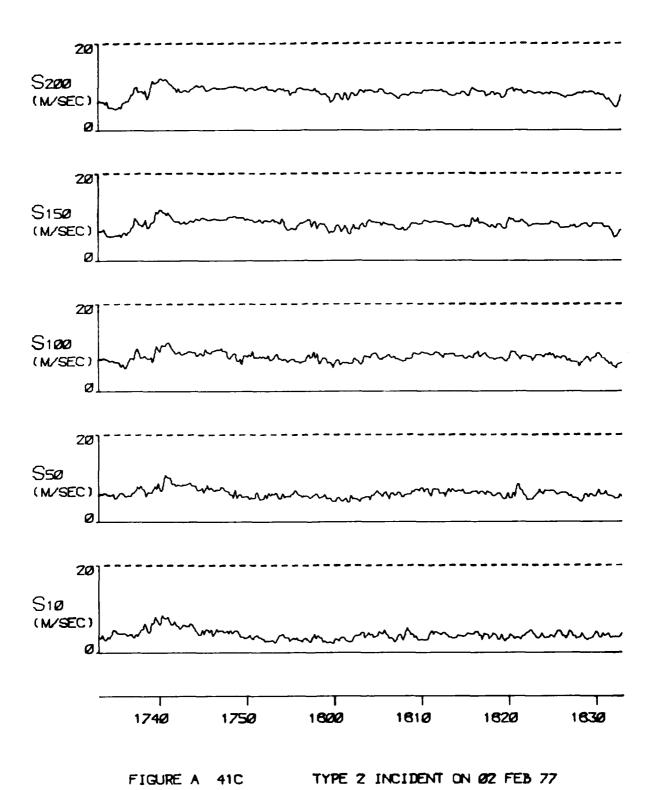
FIGURE A 41C   TYPE 2 INCIDENT ON 02 FEB 77
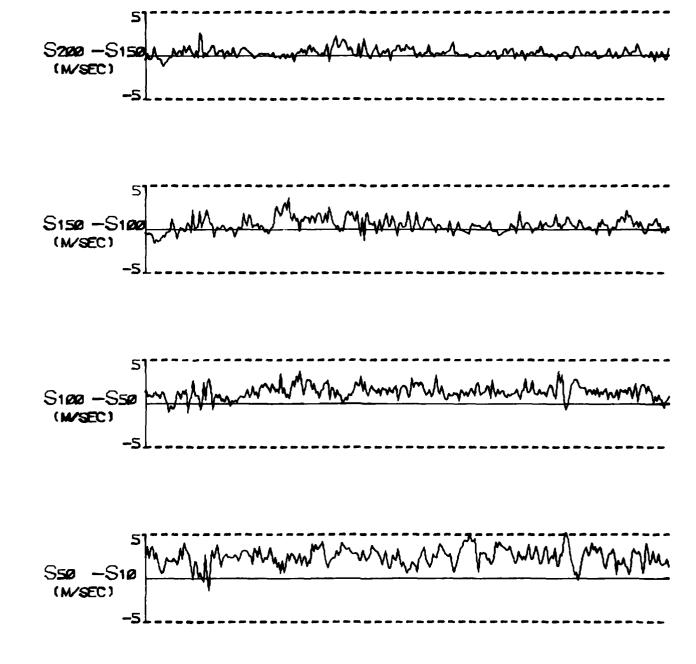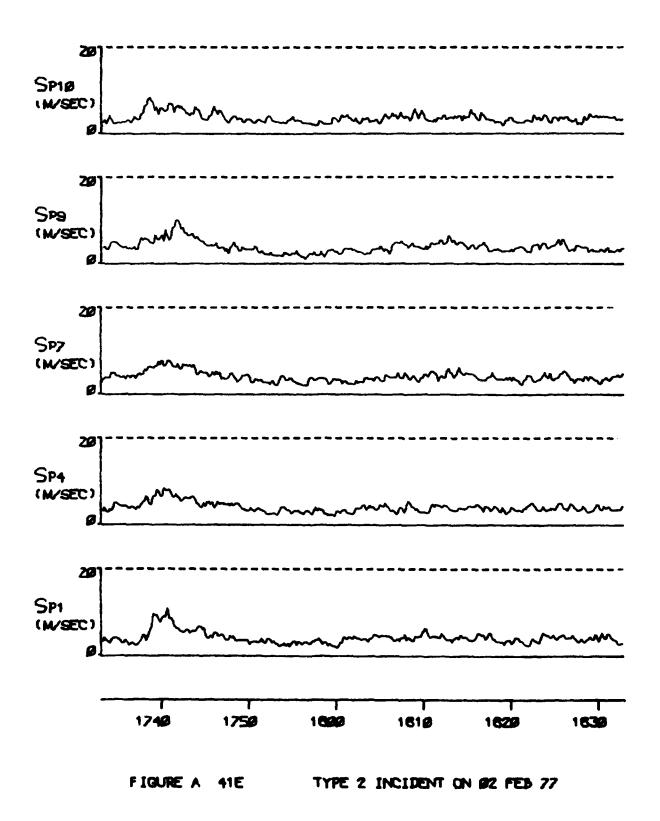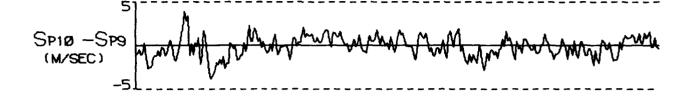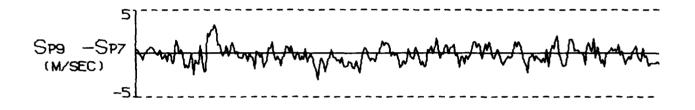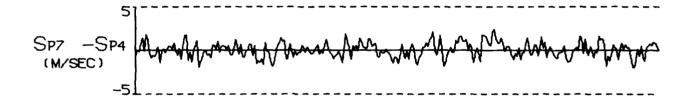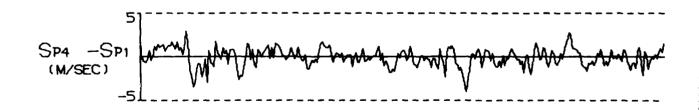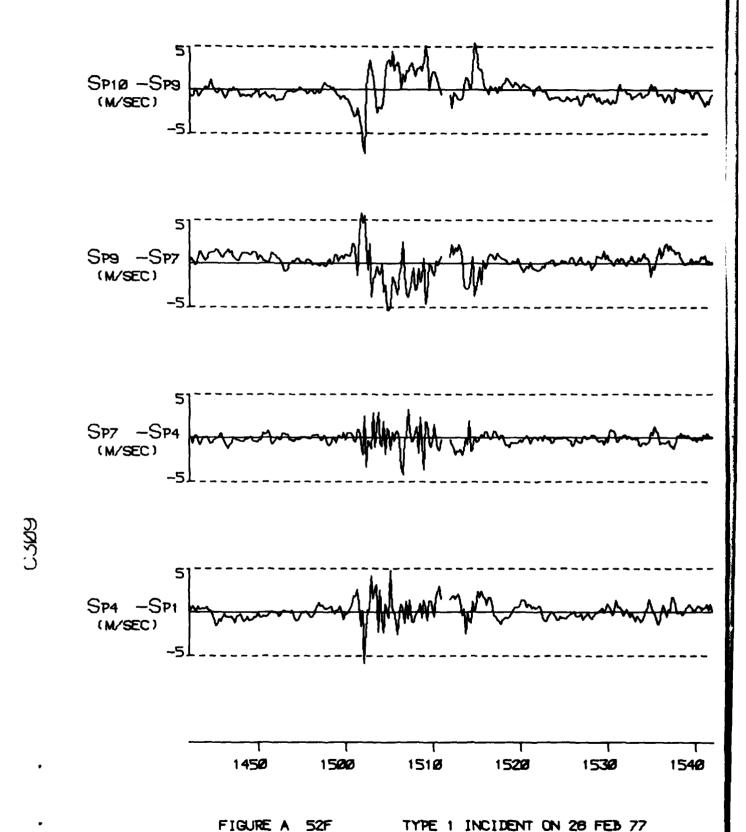
FIGURE A 41D   TYPE 2 INCIDENT ON 02 FEB 77

FIGURE A 41E   TYPE 2 INCIDENT ON 02 FEB 77
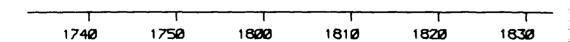
FIGURE A 41F   TYPE 2 INCIDENT ON 02 FEB 77
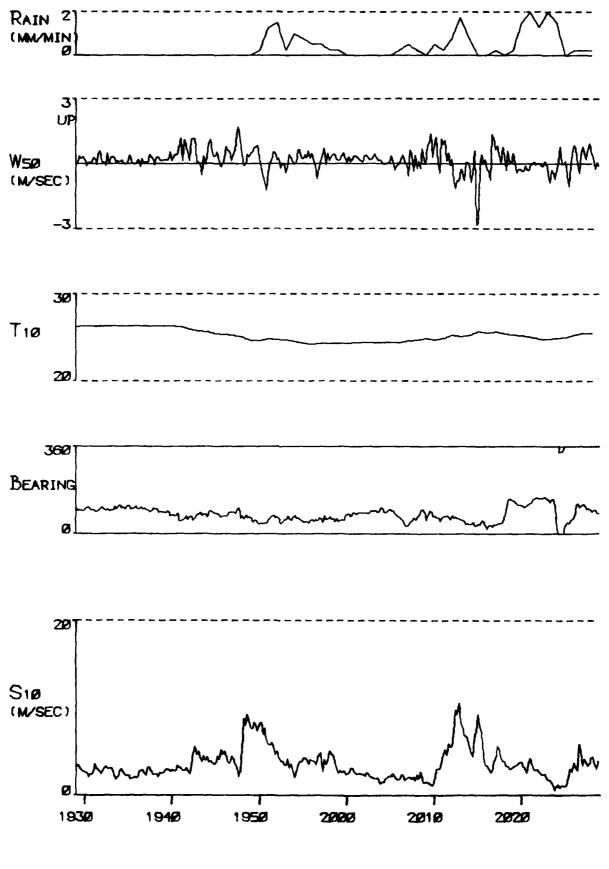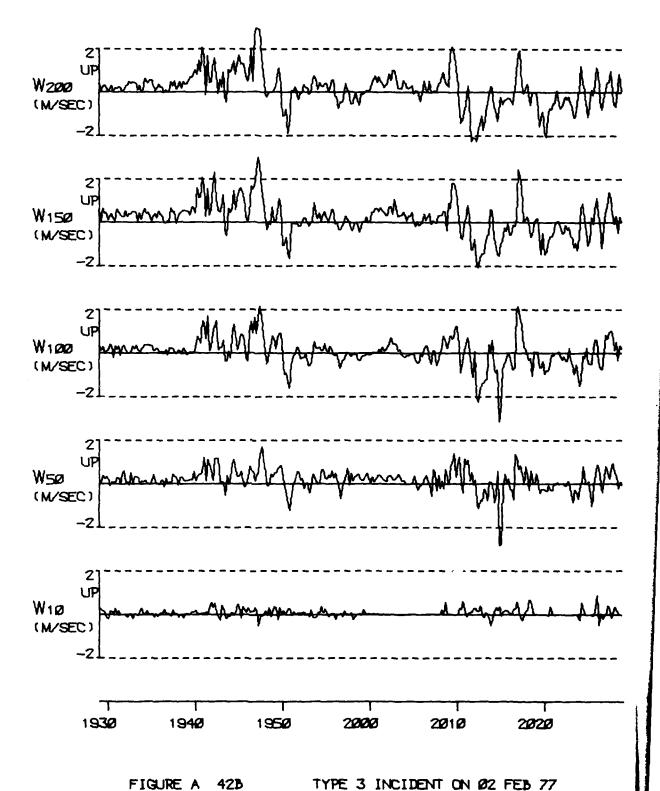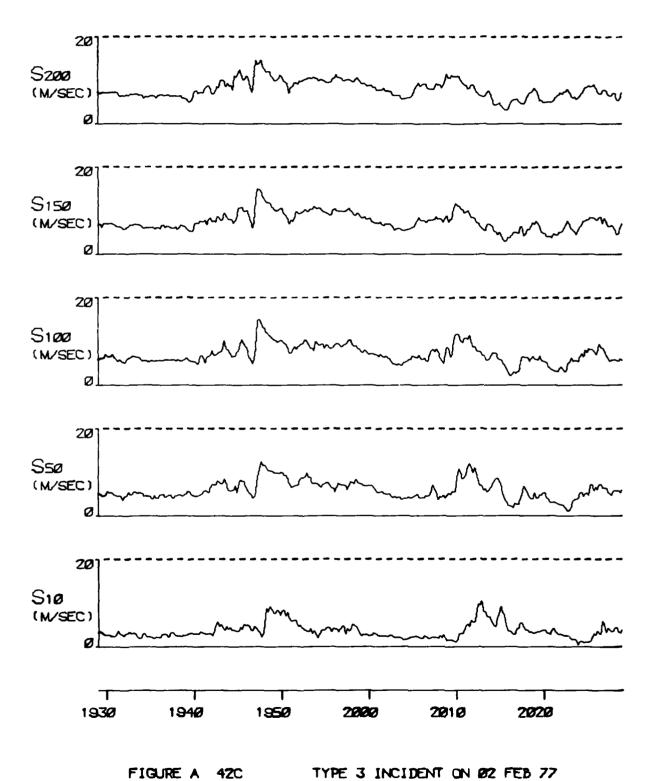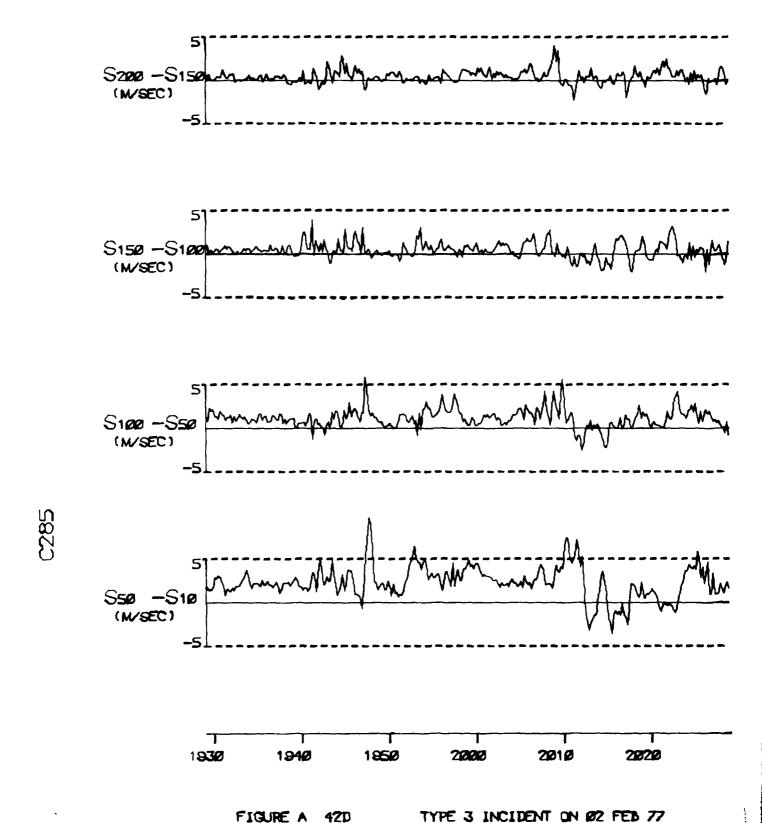
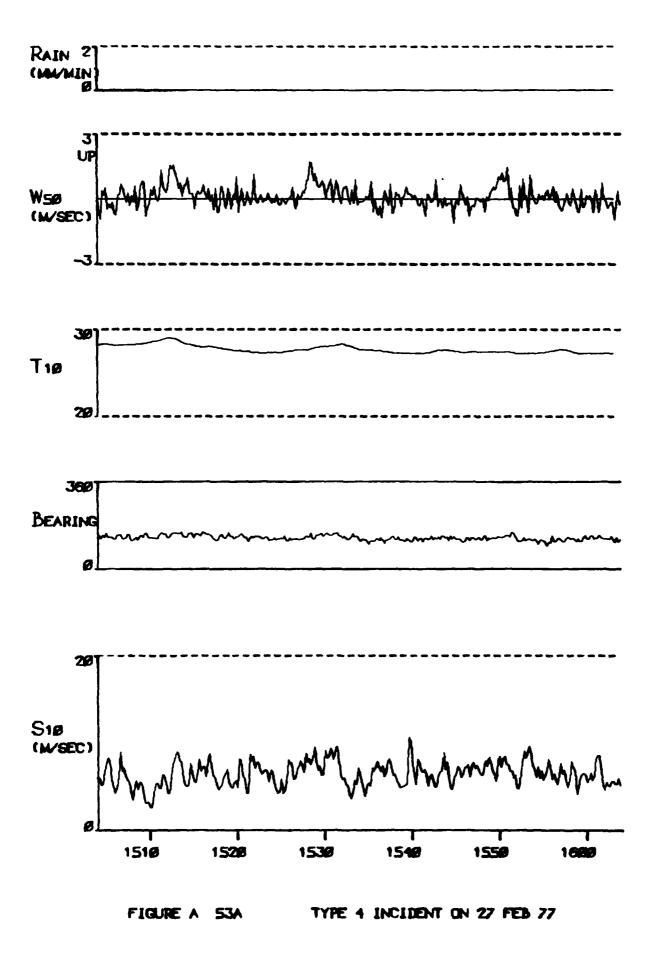FIGURE A 42A   TYPE 3 INCIDENT ON 02 FEB 77

FIGURE A 42B   TYPE 3 INCIDENT ON 02 FEB 77

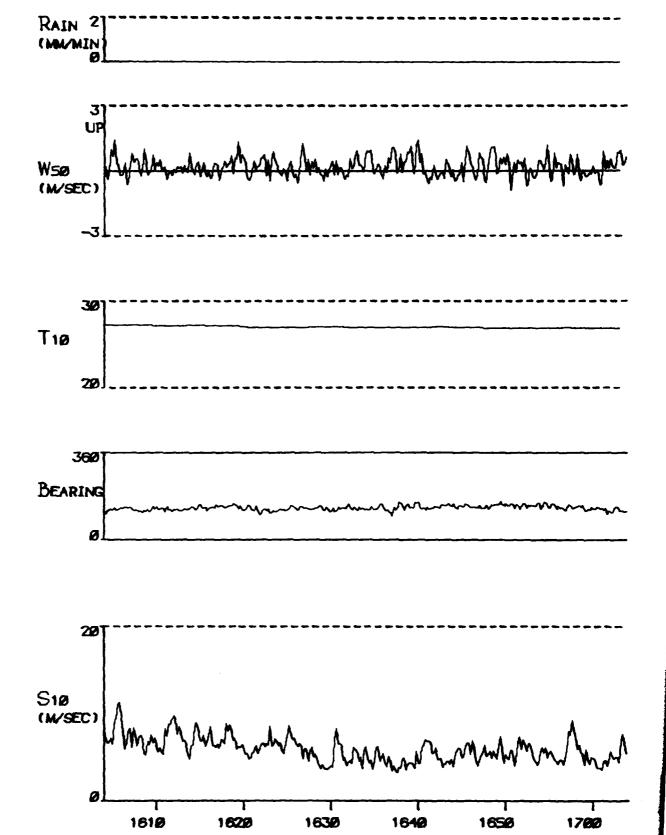FIGURE A   42C   TYPE 3 INCIDENT ON 02 FEB 77

C285

FIGURE A 42D   TYPE 3 INCIDENT ON 02 FEB 77

rIGURE A 42E   TYPE 3 INCIDENT ON 02 FEB 77

SP10 −SP9
(M/SEC)

SP9 −SP7
(M/SEC)

SP7 −SP4
(M/SEC)

SP4 −SP1
(M/SEC)

1930   1940   1950   2000   2010   2020
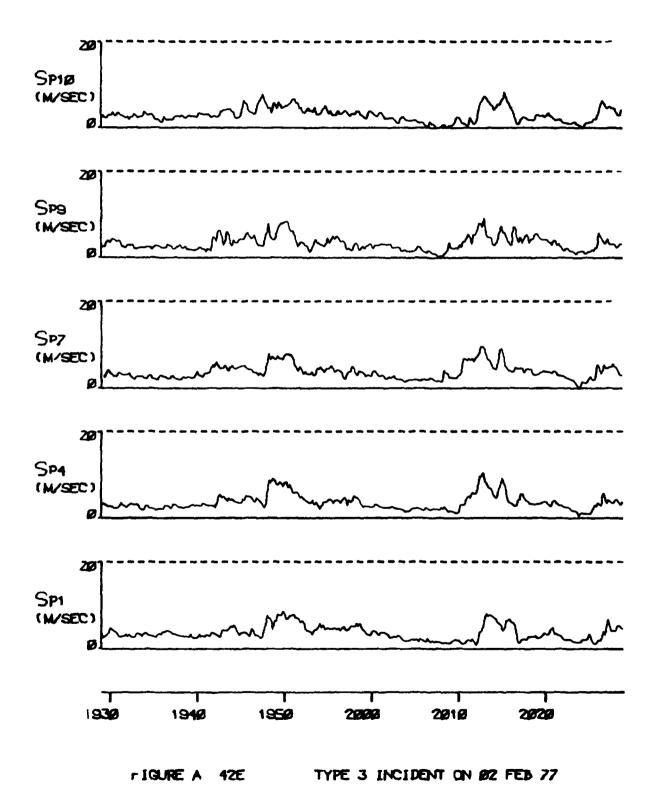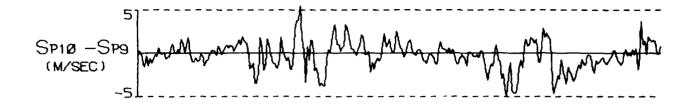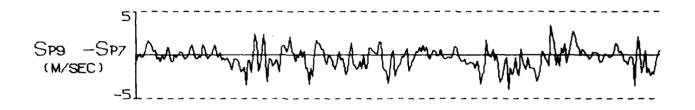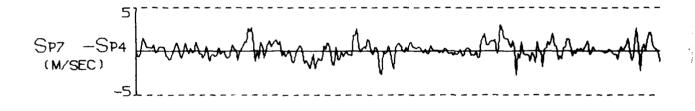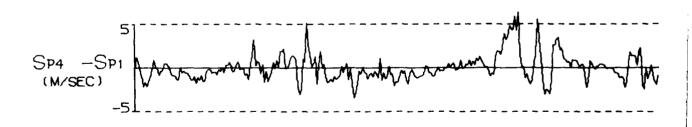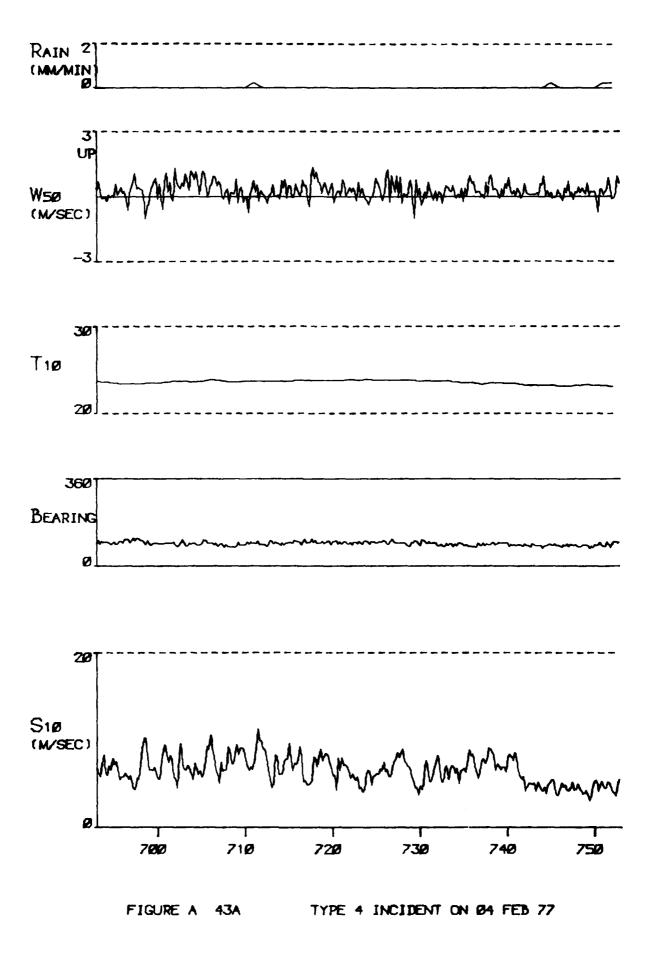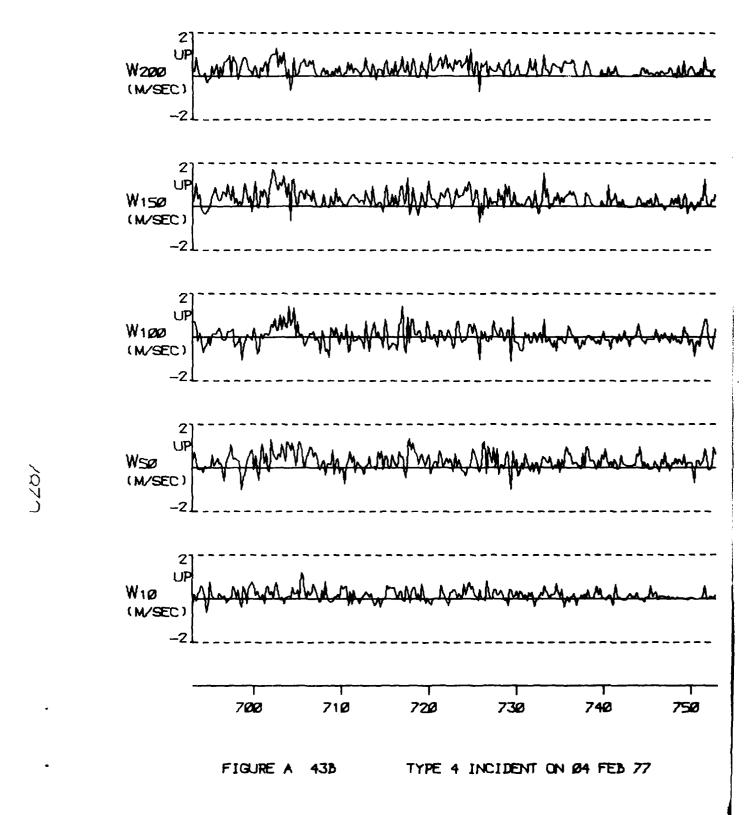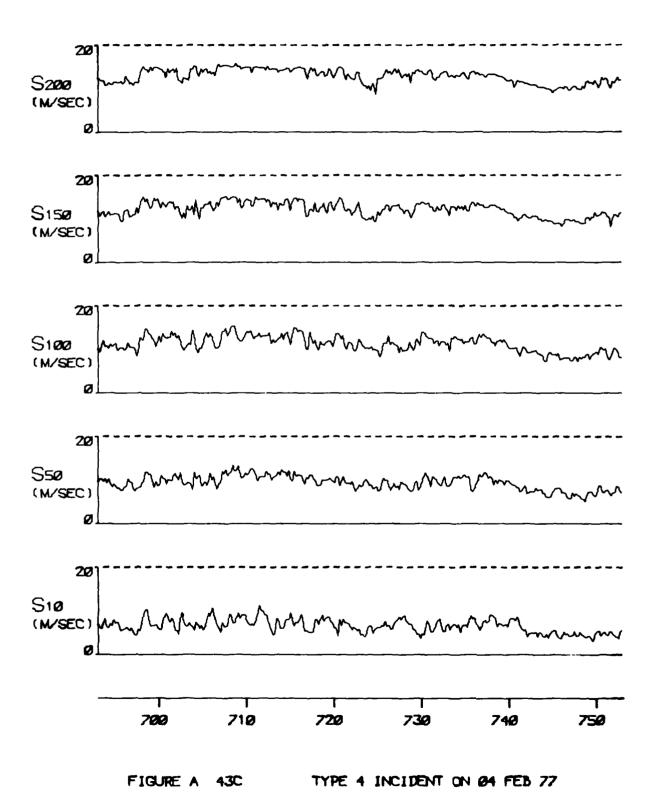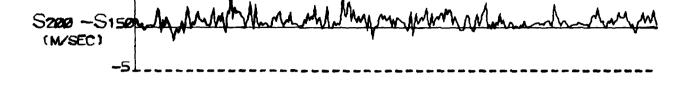
FIGURE A 42F   TYPE 3 INCIDENT ON 02 FEB 77

FIGURE A   43A   TYPE 4 INCIDENT ON 04 FEB 77
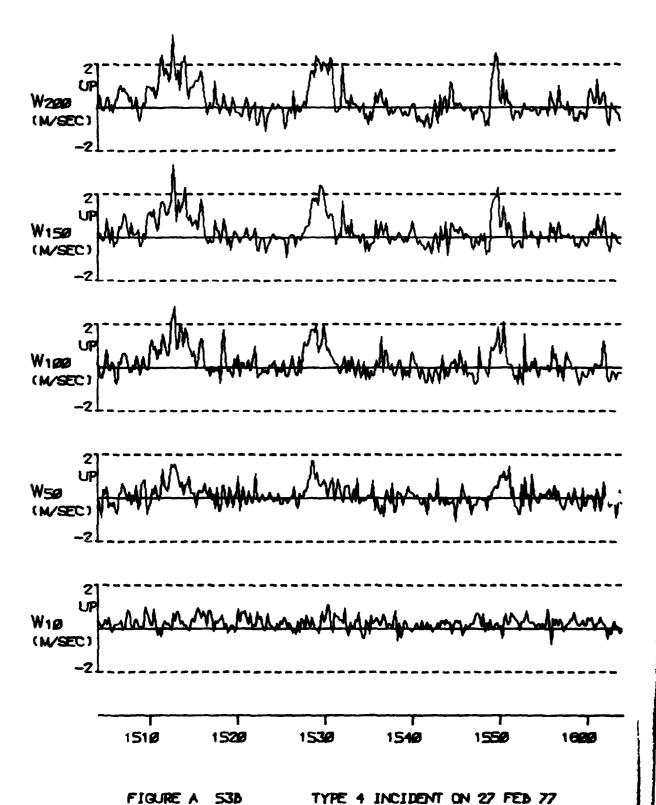
FIGURE A 43B   TYPE 4 INCIDENT ON 04 FEB 77
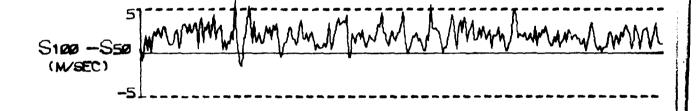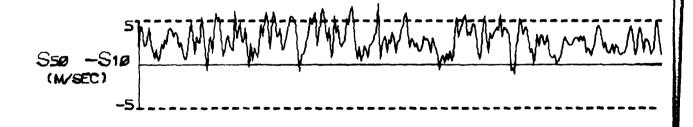
FIGURE A 43C   TYPE 4 INCIDENT ON 04 FEB 77
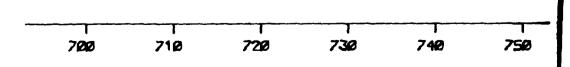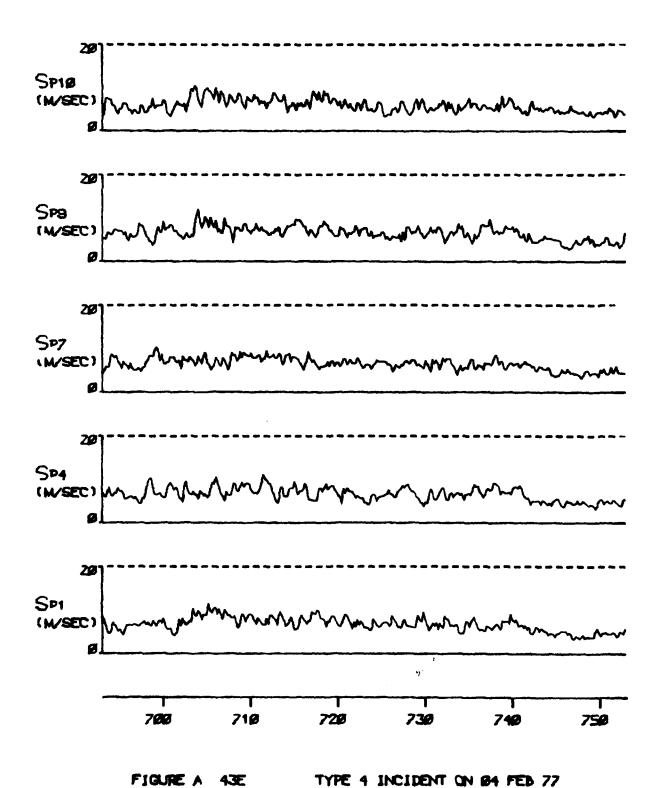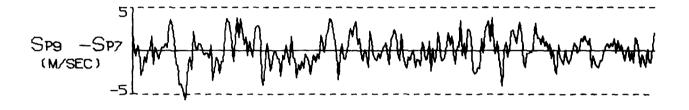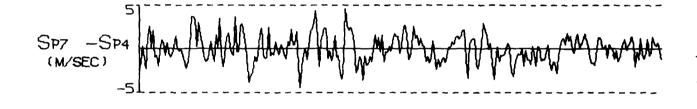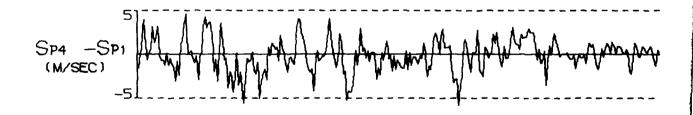
FIGURE A 43D   TYPE 4 INCIDENT ON 04 FEB 77

C287

FIGURE A 43E   TYPE 4 INCIDENT ON 04 FEB 77

SP10 −SP9 (M/SEC)

SP9 −SP7 (M/SEC)

SP7 −SP4 (M/SEC)

SP4 −SP1 (M/SEC)

700   710   720   730   740   750

C281
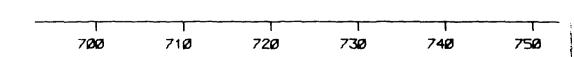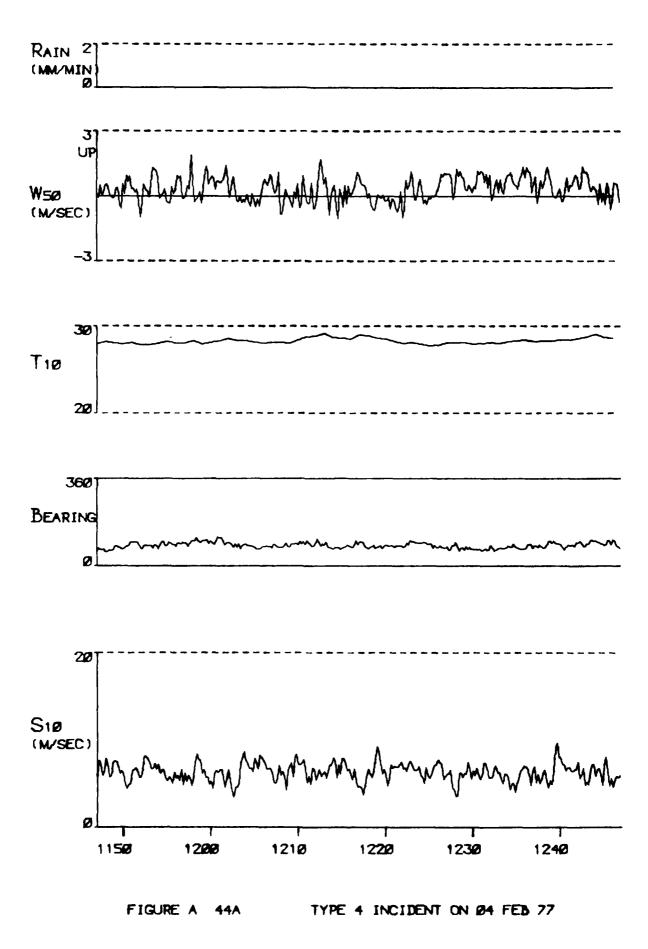
FIGURE A 43F   TYPE 4 INCIDENT ON Ø4 FEB 77

FIGURE A   44A   TYPE 4 INCIDENT ON 04 FEB 77

FIGURE A   44B   TYPE 4 INCIDENT ON 04 FEB 77

FIGURE A 44C   TYPE 4 INCIDENT ON 04 FEB 77

FIGURE A 44D   TYPE 4 INCIDENT ON 04 FEB 77
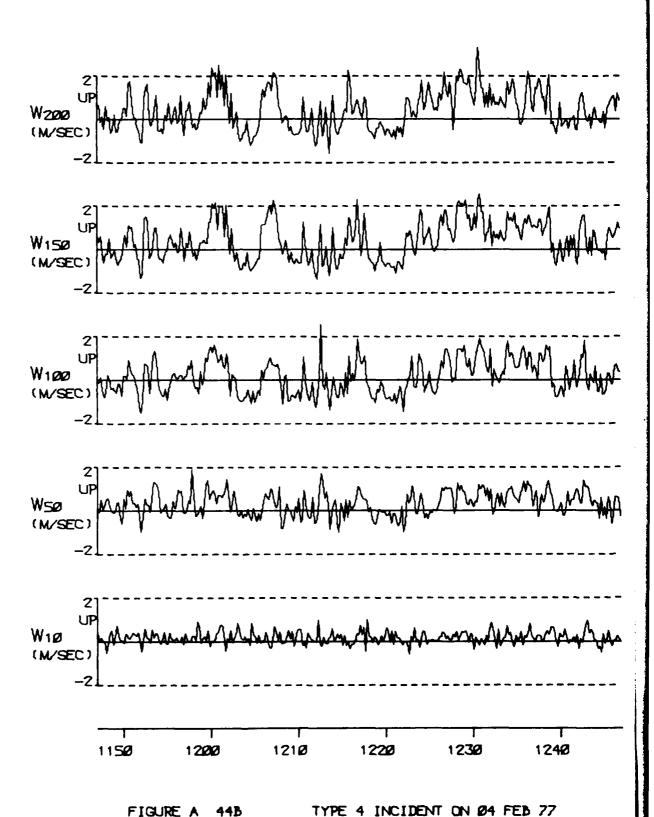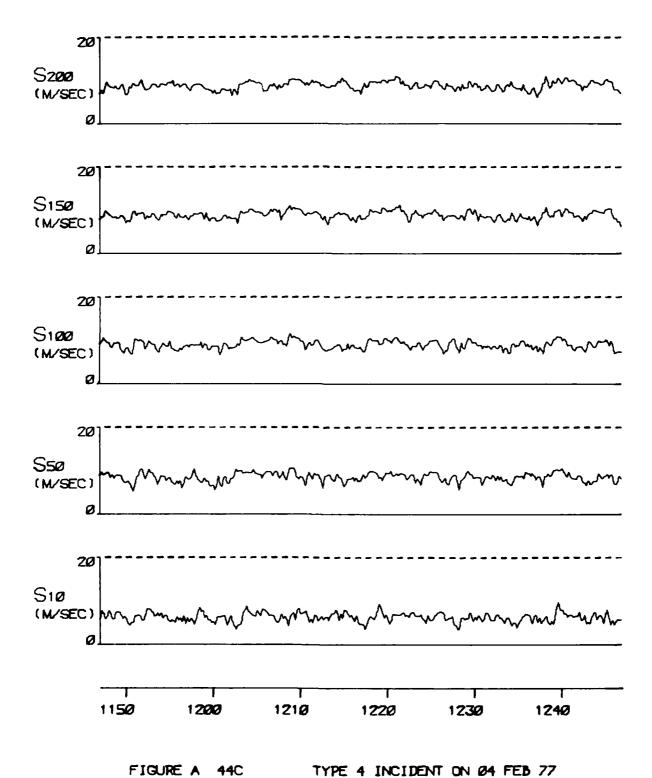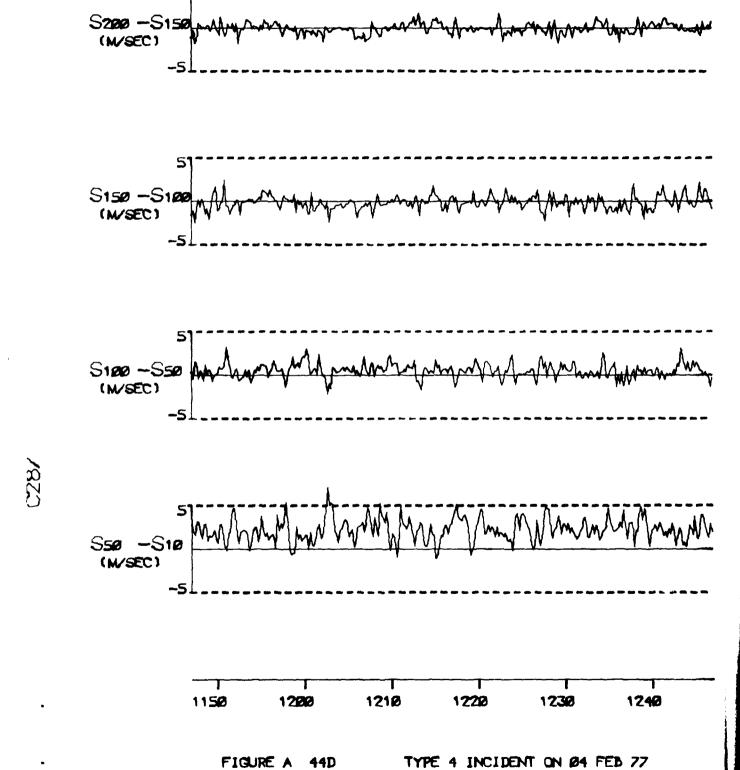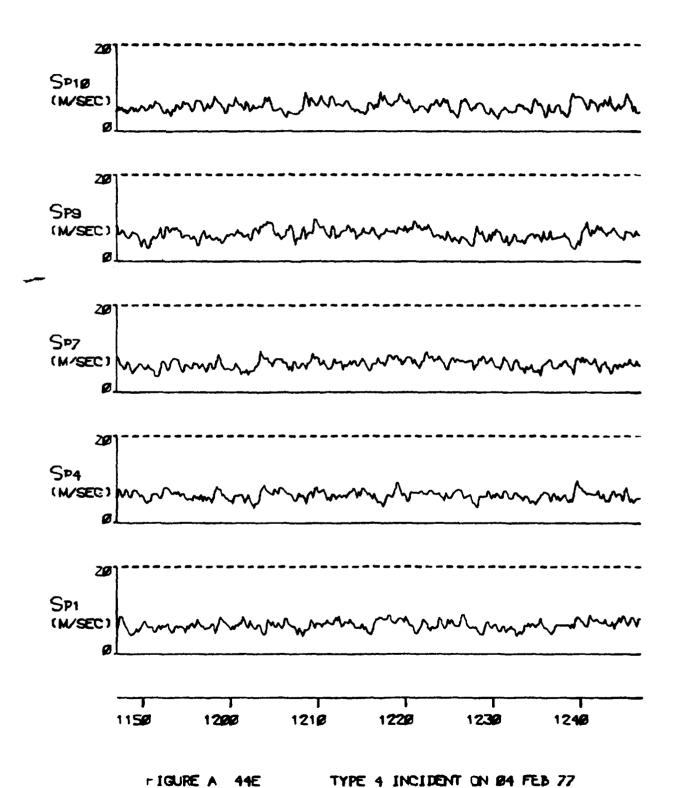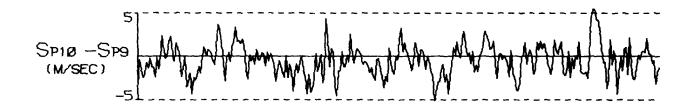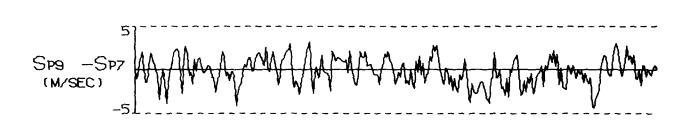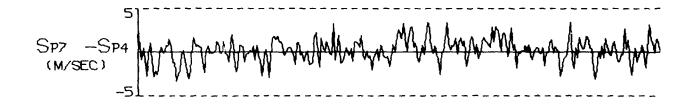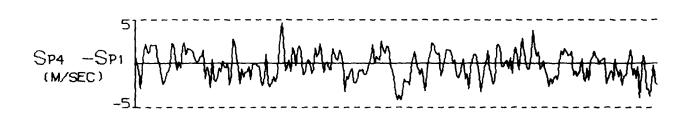
FIGURE A 44E   TYPE 4 INCIDENT ON 04 FEB 77
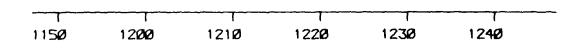
FIGURE A 44F   TYPE 4 INCIDENT ON 04 FEB 77
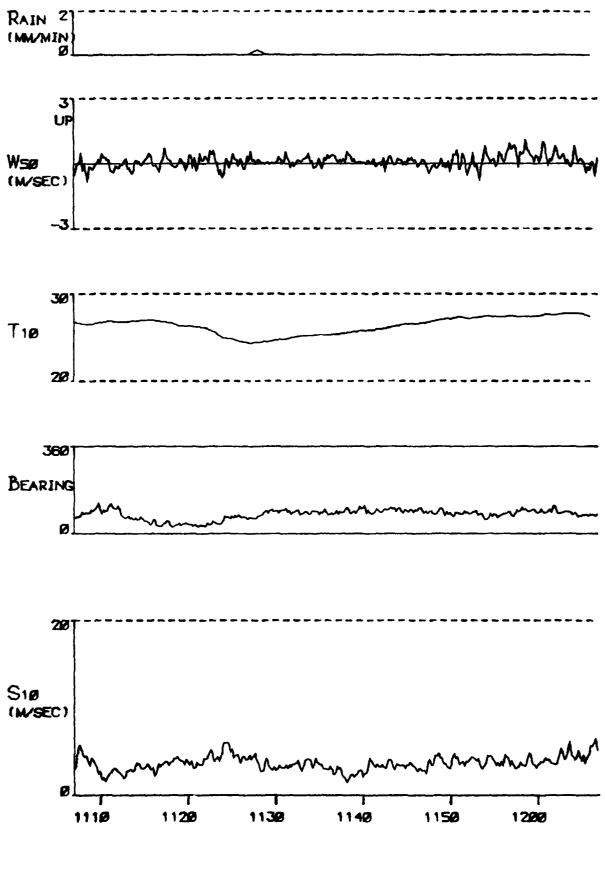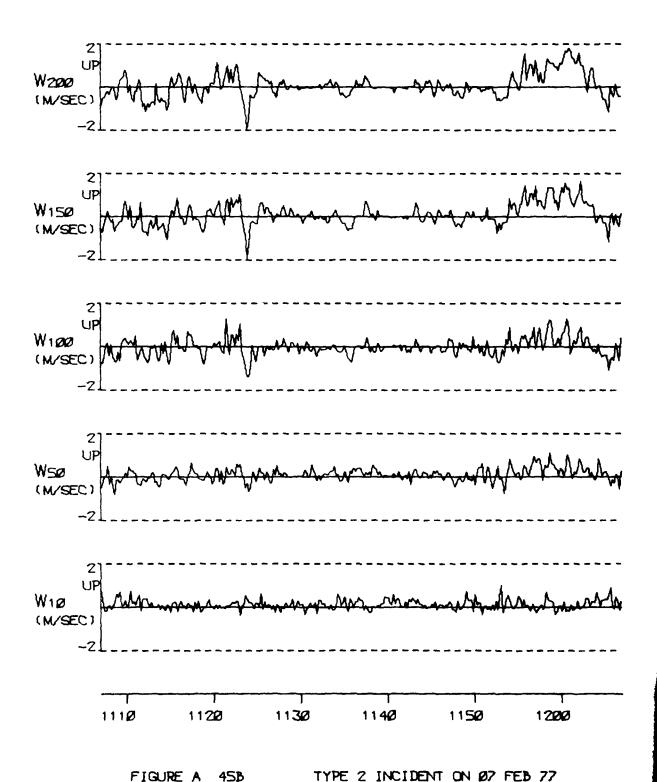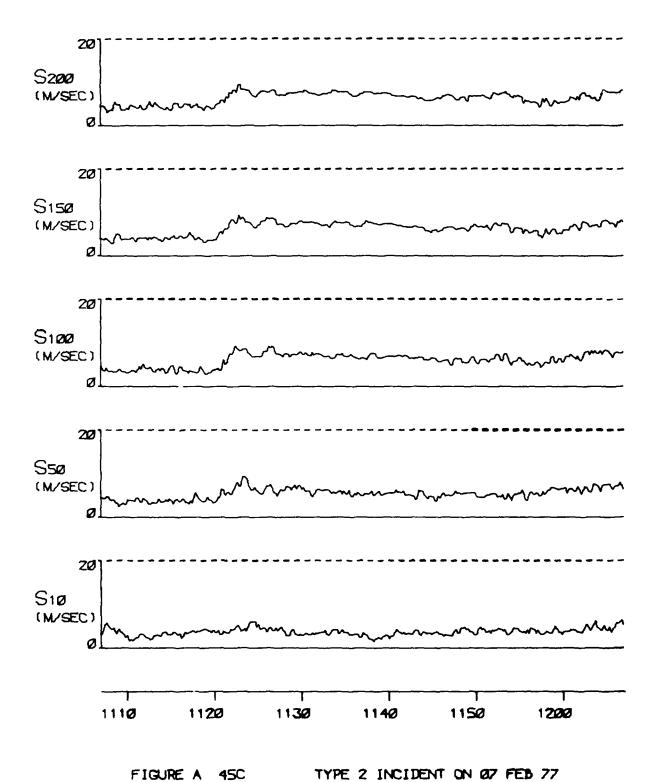
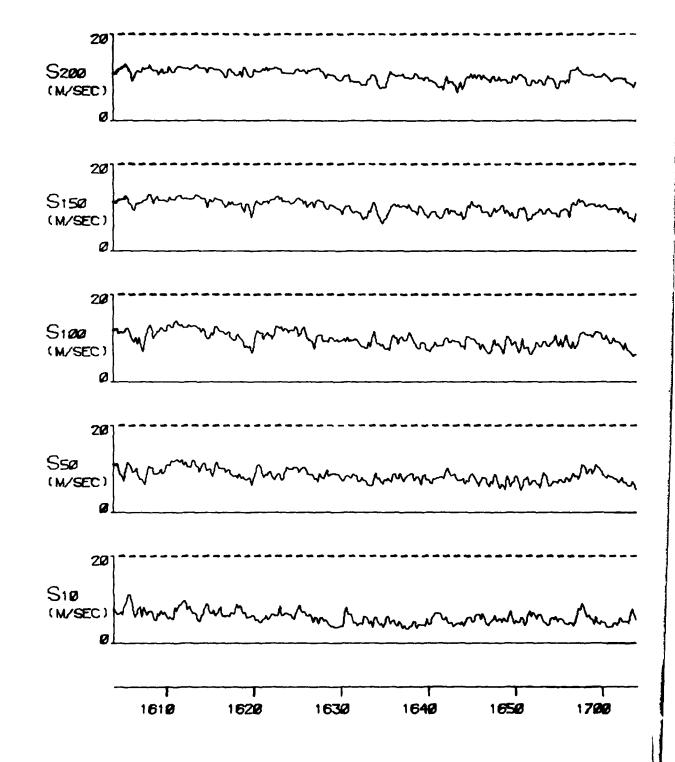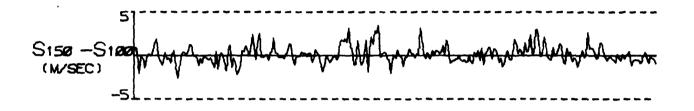FIGURE A 45A   TYPE 2 INCIDENT ON 07 FEB 77

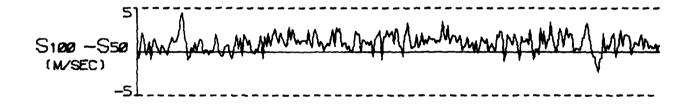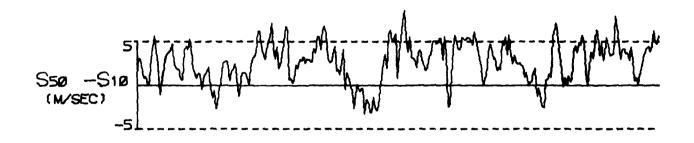FIGURE A 45B   TYPE 2 INCIDENT ON 07 FEB 77
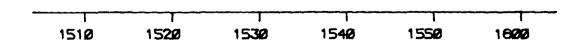
FIGURE A 45C   TYPE 2 INCIDENT ON 07 FEB 77
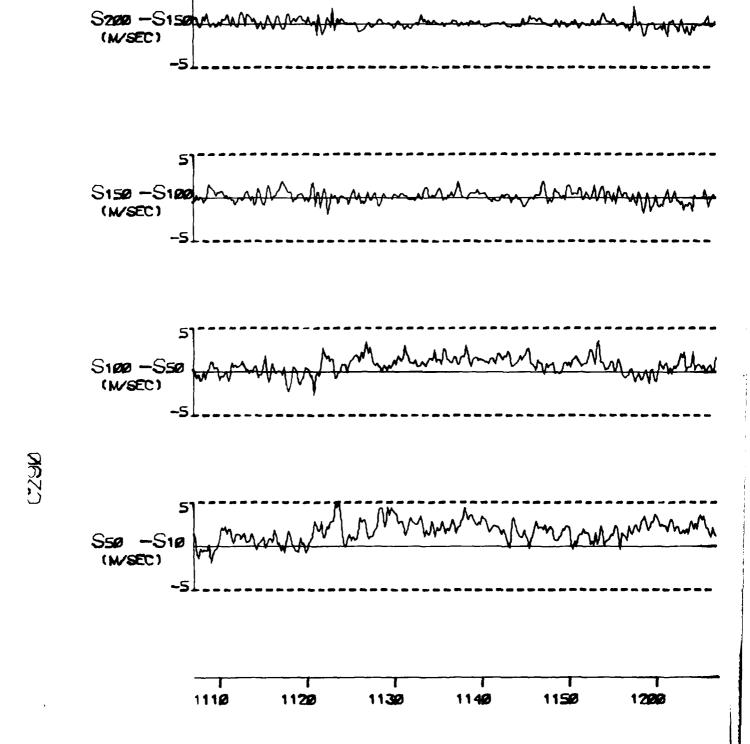
FIGURE A   45D   TYPE 2 INCIDENT ON 07 FEB 77
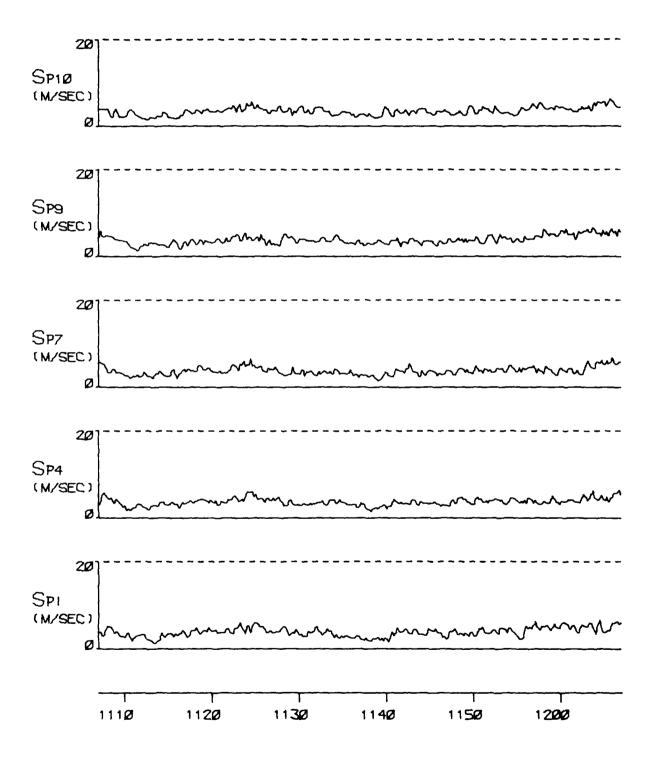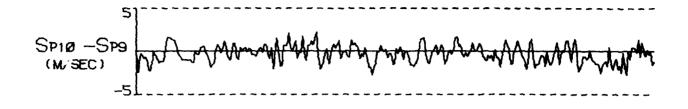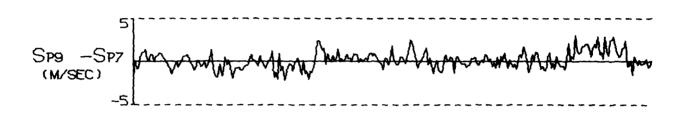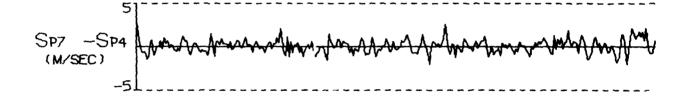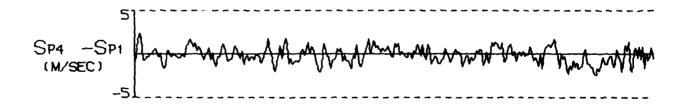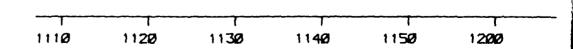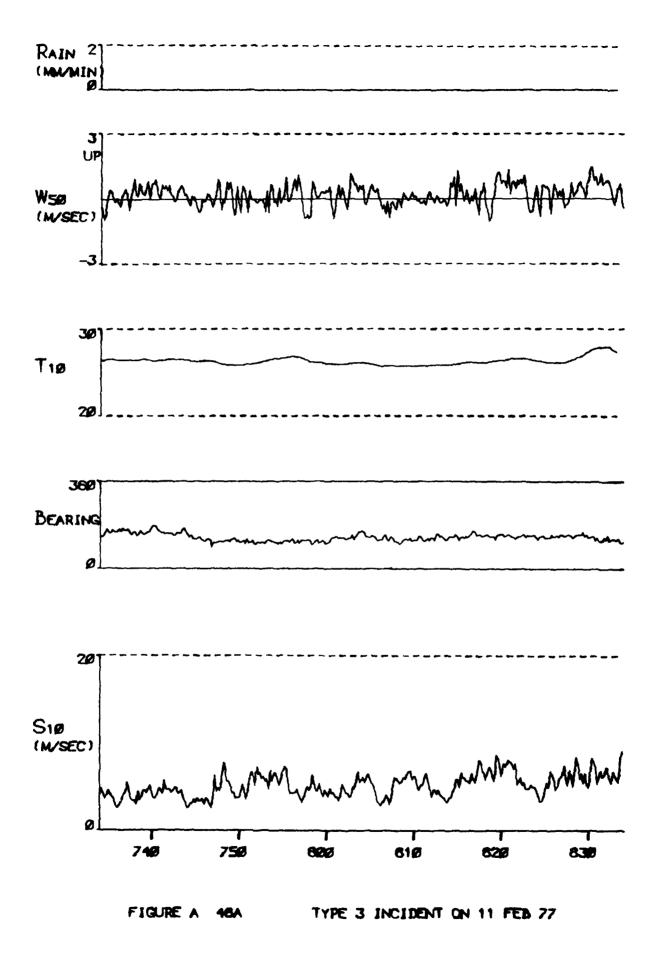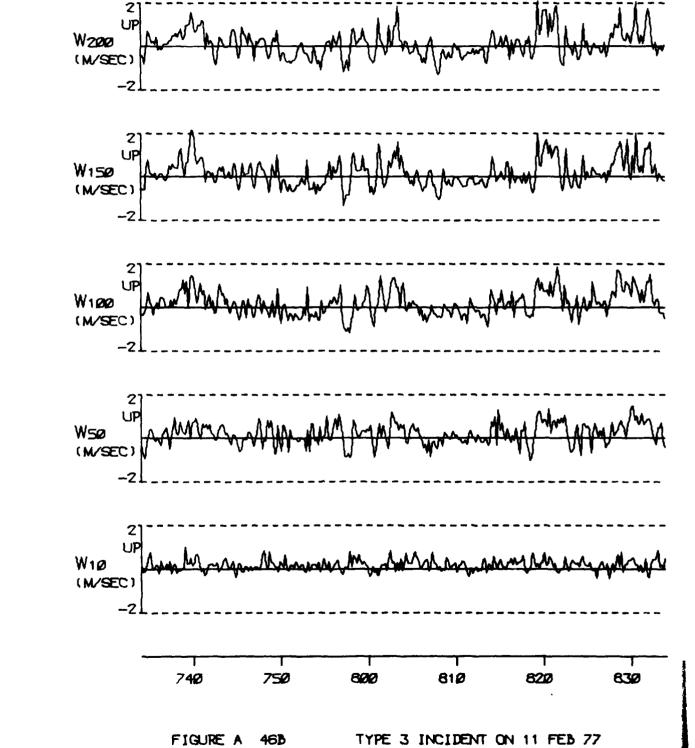
FIGURE A 4SE   TYPE 2 INCIDENT ON 07 FEB 77

FIGURE A .45F   TYPE 2 INCIDENT ON 07 FEB 77
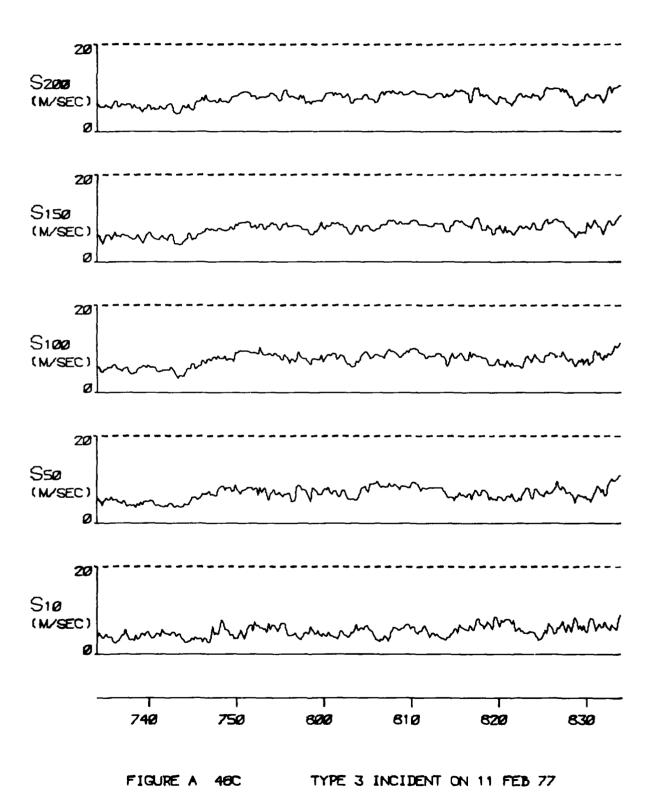
FIGURE A 46A   TYPE 3 INCIDENT ON 11 FEB 77

FIGURE A 46B   TYPE 3 INCIDENT ON 11 FEB 77

FIGURE A 46C   TYPE 3 INCIDENT ON 11 FEB 77

FIGURE A 48D   TYPE 3 INCIDENT ON 11 FEB 77
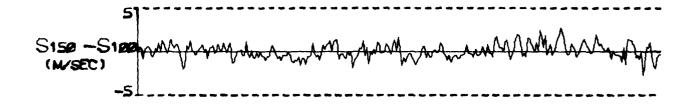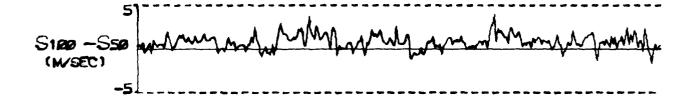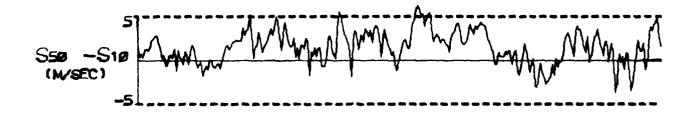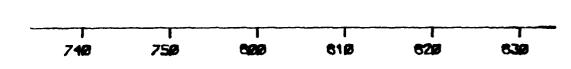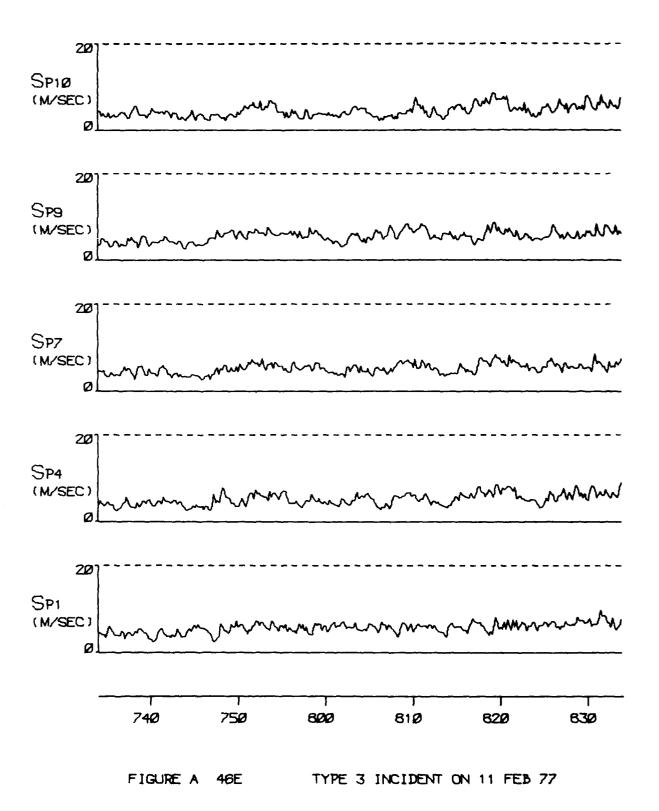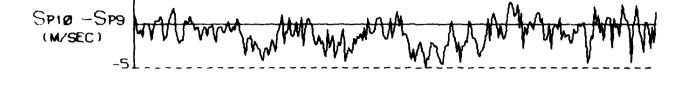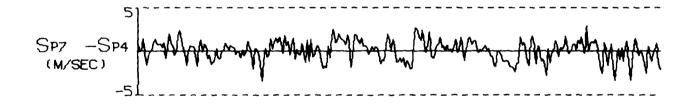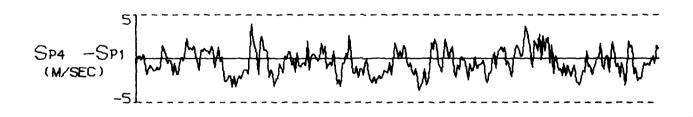
FIGURE A 46E   TYPE 3 INCIDENT ON 11 FEB 77
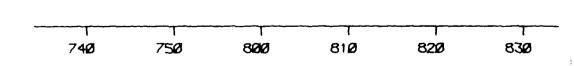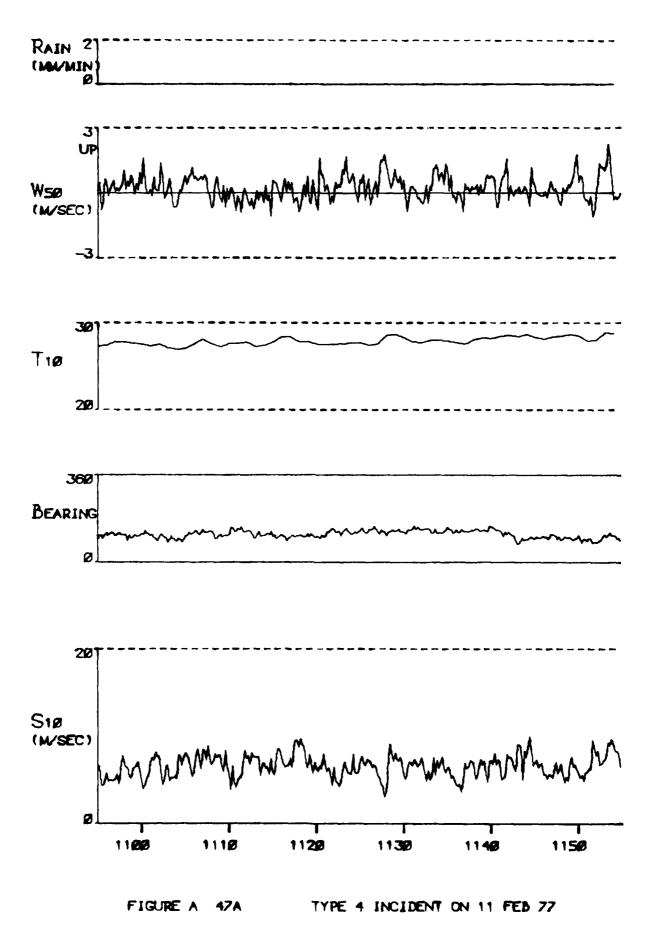
C294

FIGURE A   46F   TYPE 3 INCIDENT ON 11 FEB 77

FIGURE A 47A   TYPE 4 INCIDENT ON 11 FEB 77
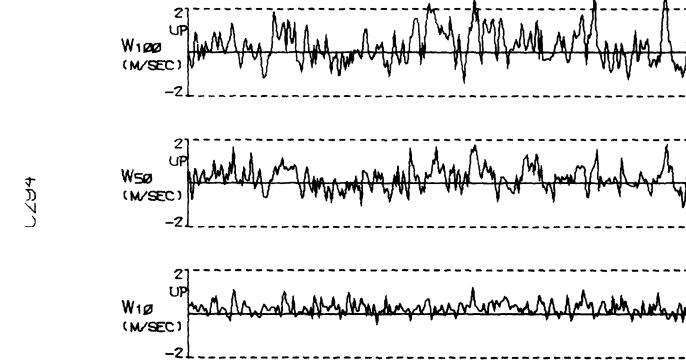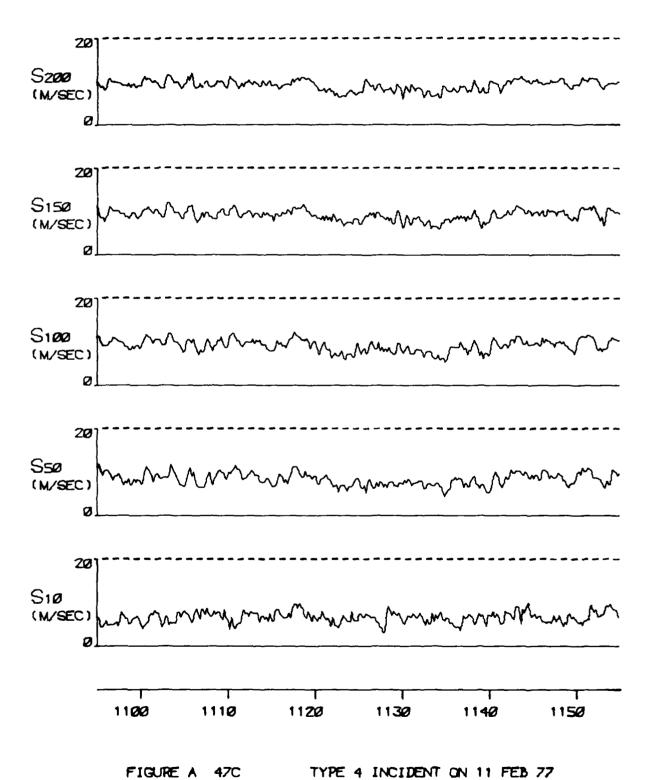
FIGURE A 47B   TYPE 4 INCIDENT ON 11 FEB 77

FIGURE A   47C   TYPE 4 INCIDENT ON 11 FEB 77
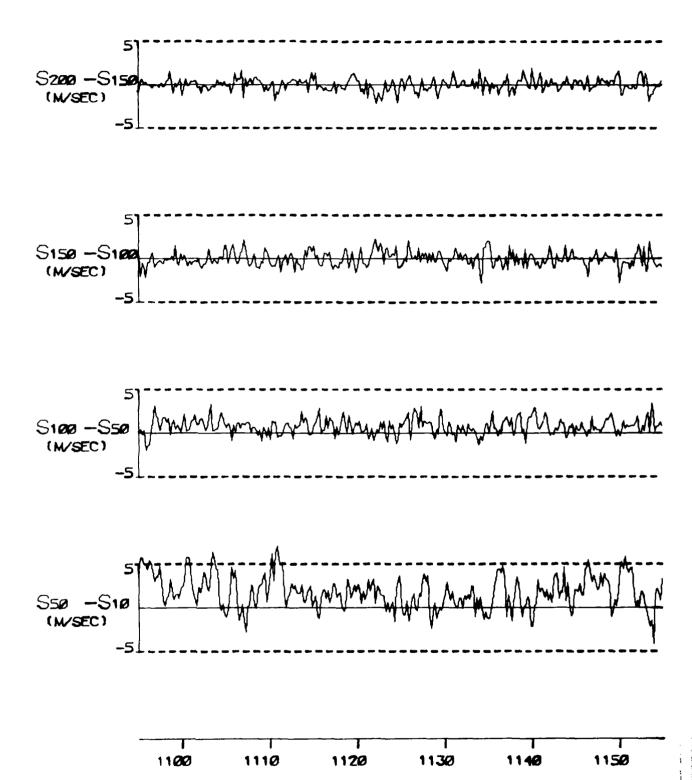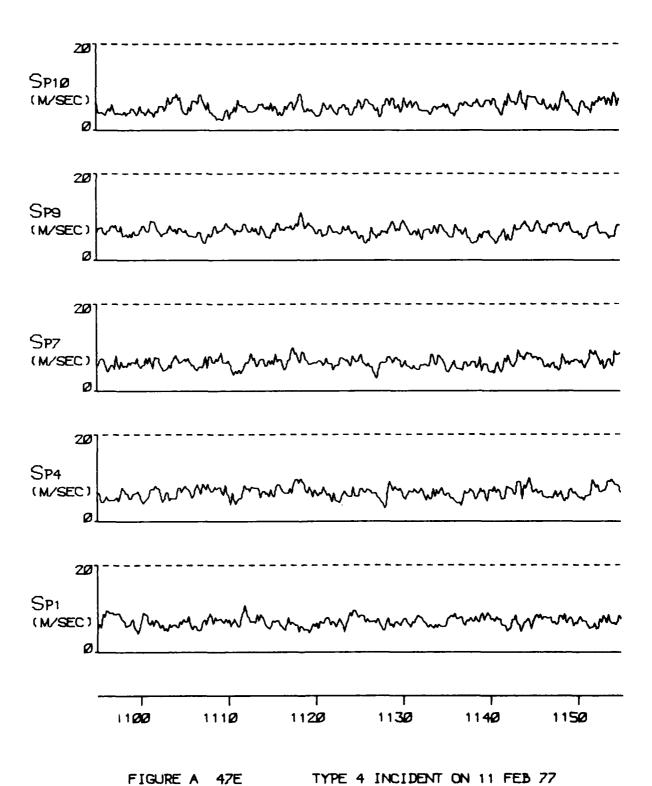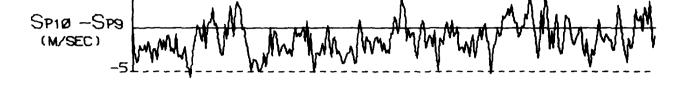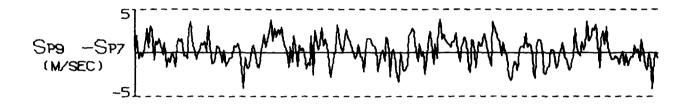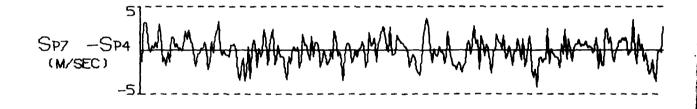
FIGURE A 47D   TYPE 4 INCIDENT ON 11 FEB 77

FIGURE A 47E   TYPE 4 INCIDENT ON 11 FEB 77

SP10 −SP9
(M/SEC)

SP9 −SP7
(M/SEC)

SP7 −SP4
(M/SEC)

SP4 −SP1
(M/SEC)

C294

1100   1110   1120   1130   1140   1150
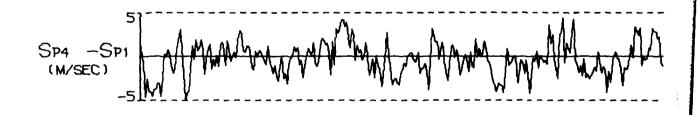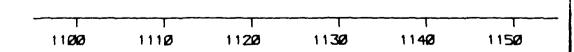
FIGURE A 47F   TYPE 4 INCIDENT ON 11 FEB 77
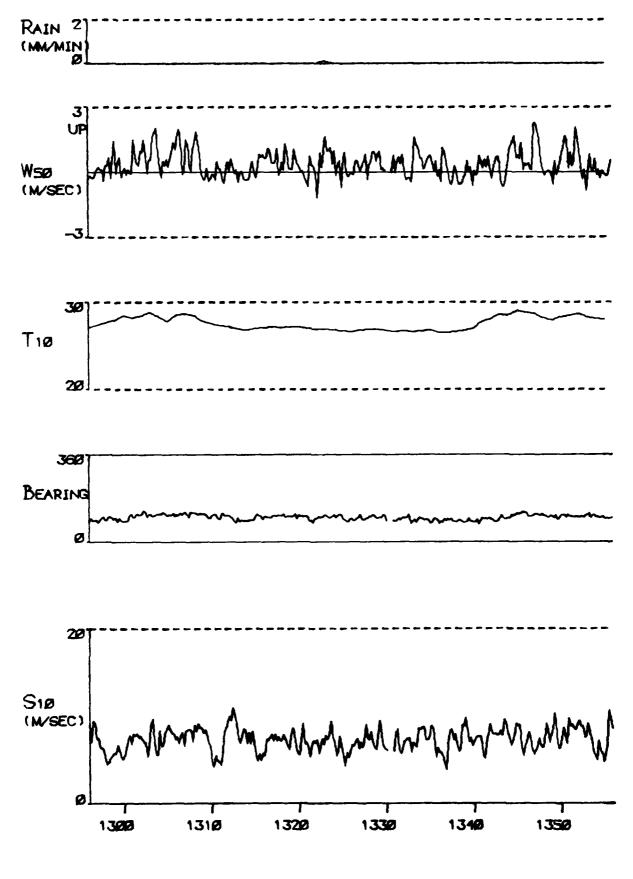
FIGURE A 48A   TYPE 5 INCIDENT ON 12 FEB 77

FIGURE A 48B   TYPE 5 INCIDENT ON 12 FEB 77
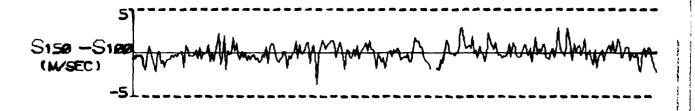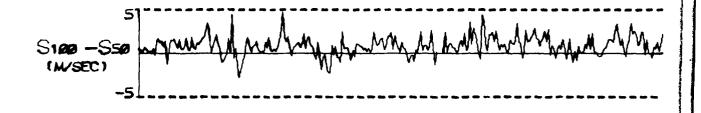
FIGURE A 48C   TYPE 5 INCIDENT ON 12 FEB 77

FIGURE A 46D   TYPE 5 INCIDENT ON 12 FEB 77

FIGURE A   48E   TYPE 5 INCIDENT ON 12 FEB 77

FIGURE A 48F   TYPE 5 INCIDENT ON 12 FEB 77

FIGURE A 49A   TYPE 4 INCIDENT ON 12 FEB 77
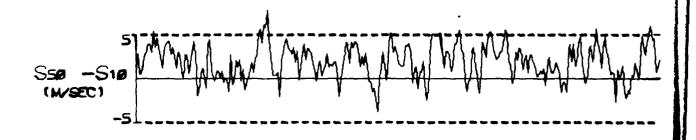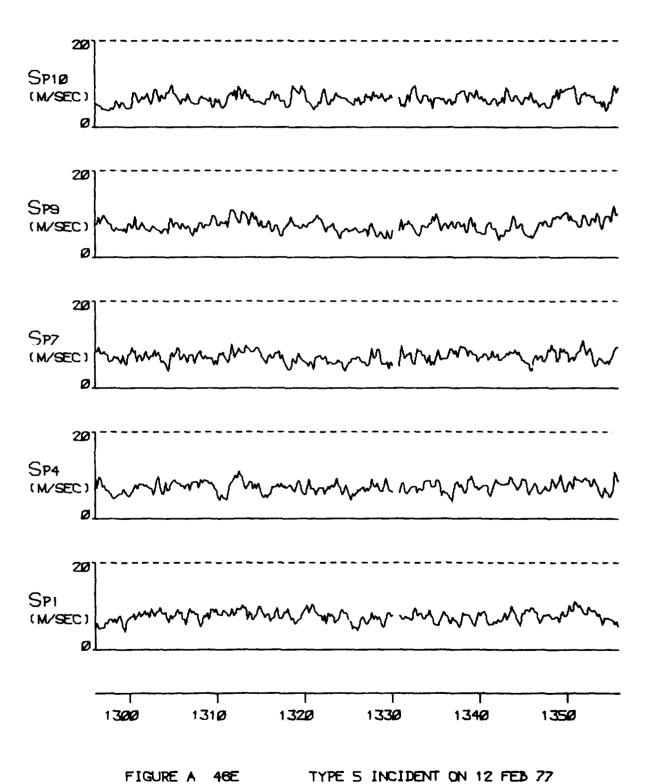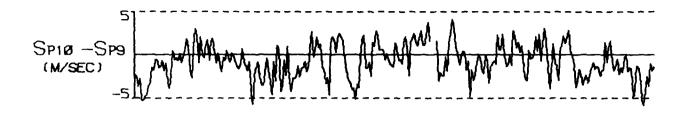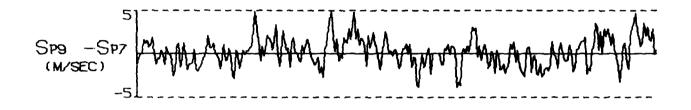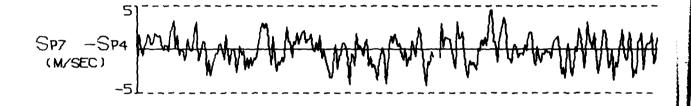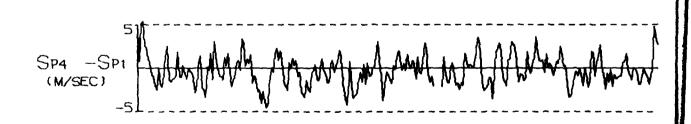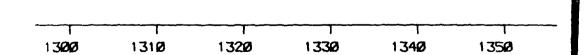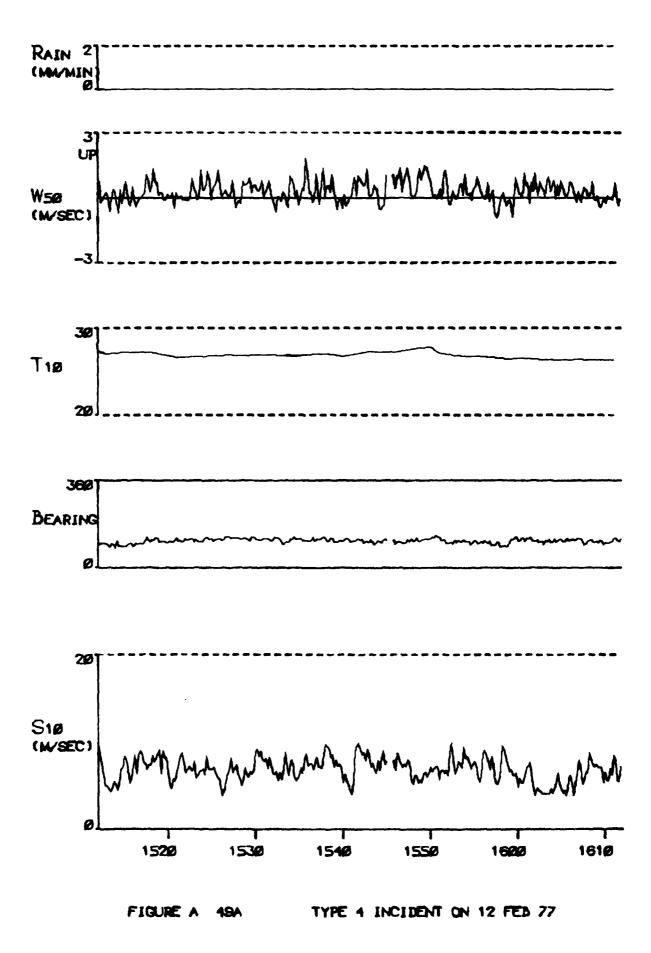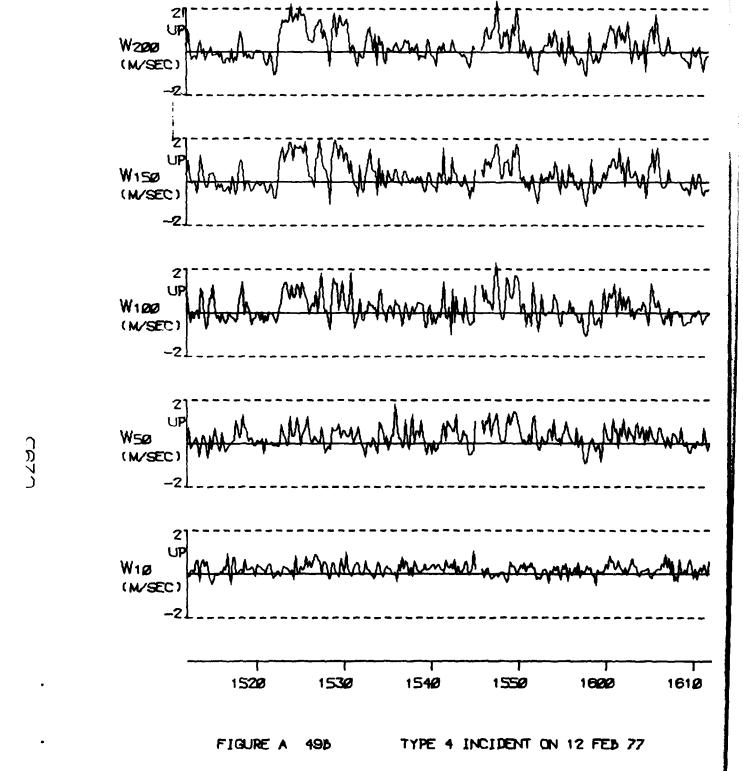
FIGURE A 49b TYPE 4 INCIDENT ON 12 FEB 77
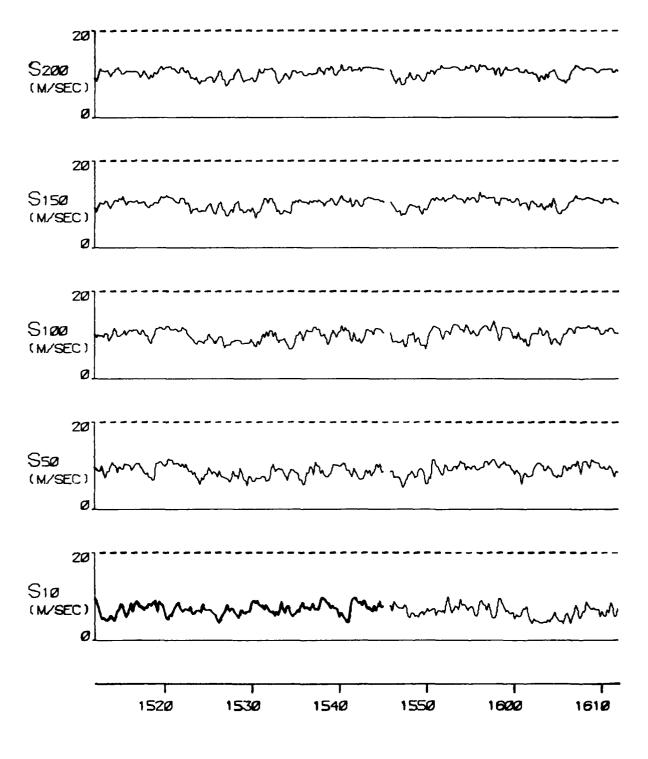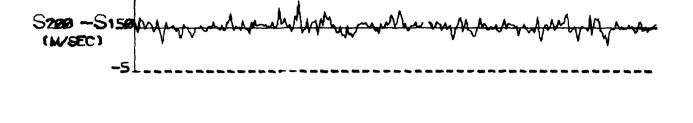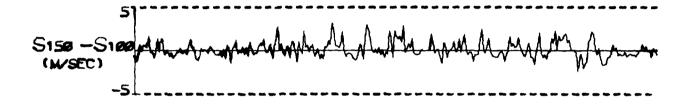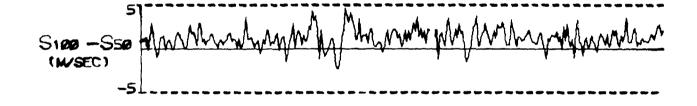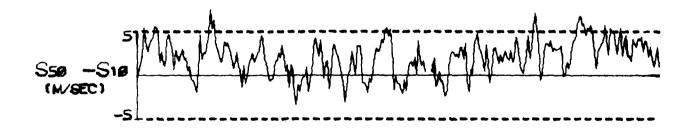
FIGURE A 49C   TYPE 4 INCIDENT ON 12 FEB 77

C295

FIGURE A 49D   TYPE 4 INCIDENT ON 12 FEB 77

FIGURE A 4SE   TYPE 4 INCIDENT ON 12 FEB 77

SP10 −SP9 (M/SEC)

SP9 −SP7 (M/SEC)

SP7 −SP4 (M/SEC)

SP4 −SP1 (M/SEC)

C295
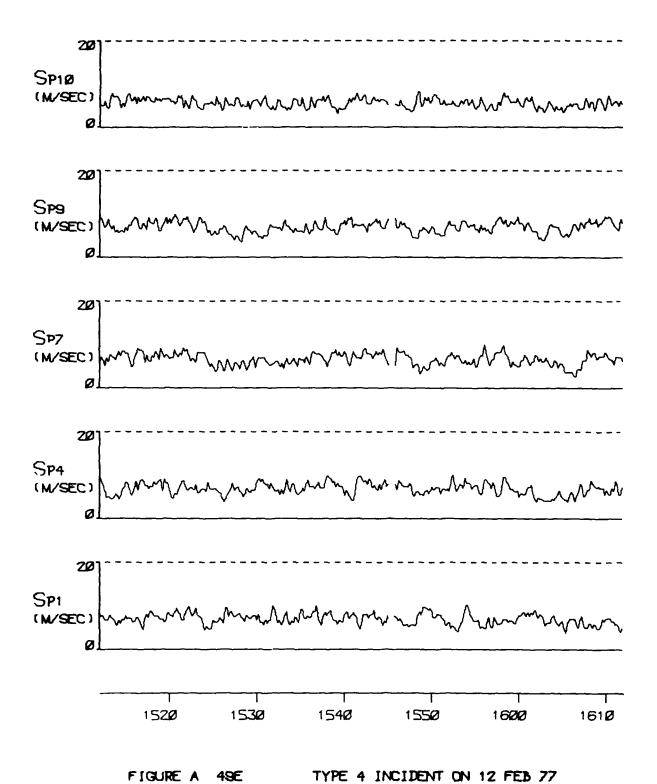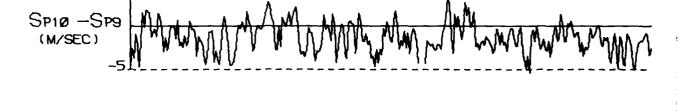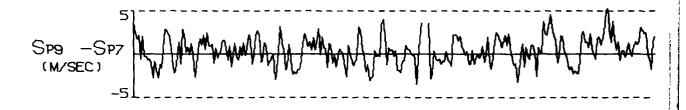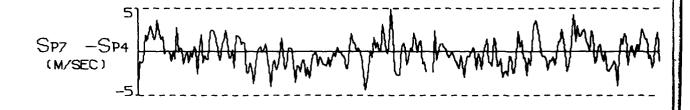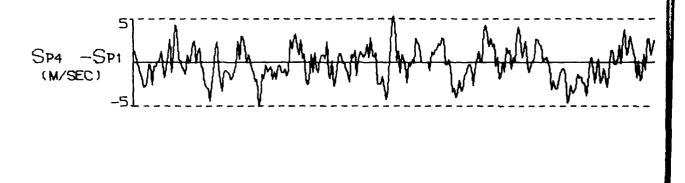
FIGURE A 49F   TYPE 4 INCIDENT ON 12 FEB 77

FIGURE A 50A   TYPE 4 INCIDENT ON 15 FEB 77

FIGURE A 50B   TYPE 4 INCIDENT ON 15 FEB 77

FIGURE A 50C   TYPE 4 INCIDENT ON 15 FEB 77

FIGURE A 50D   TYPE 4 INCIDENT ON 15 FEB 77

FIGURE A 50E   TYPE 4 INCIDENT ON 15 FEB 77

C298
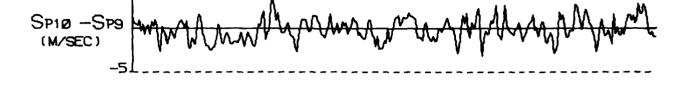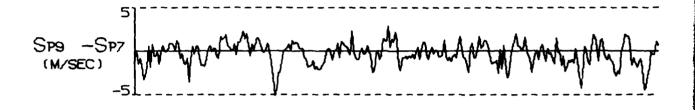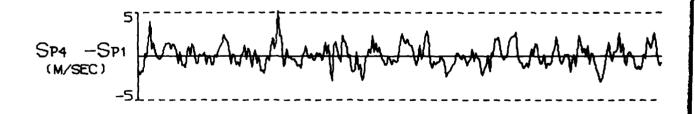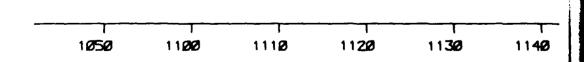
FIGURE A· 50F   TYPE 4 INCIDENT ON 15 FEB 77

FIGURE A 51A   TYPE 5 INCIDENT ON 25 FEB 77
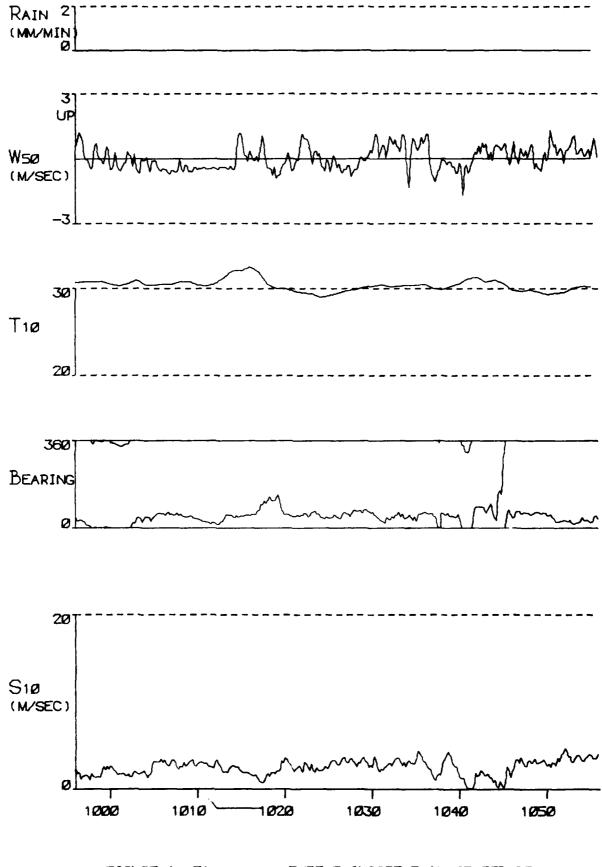
FIGURE A 51B   TYPE 5 INCIDENT ON 25 FEB 77
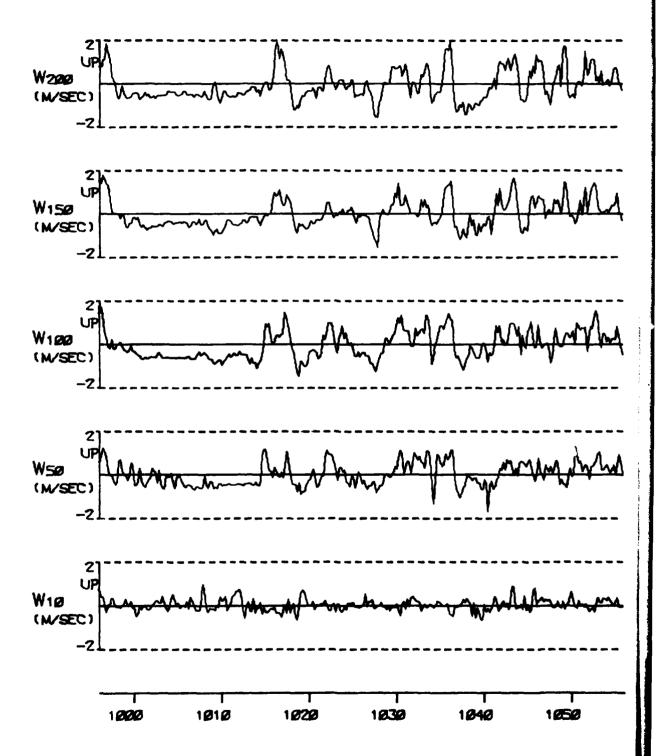
FIGURE A 51C   TYPE 5 INCIDENT ON 25 FEB 77

FIGURE A 51D   TYPE 5 INCIDENT ON 25 FEB 77

FIGURE A 51E   TYPE 5 INCIDENT ON 25 FEB 77

SP10 – SP9 (M/SEC)

SP9 – SP7 (M/SEC)

SP7 – SP4 (M/SEC)

SP4 – SP1 (M/SEC)

C3008

1000   1010   1020   1030   1040   1050

FIGURE A 51F   TYPE 5 INCIDENT ON 25 FEB 77

1.0

2.8 2.5
3.2 2.2
3.6
4.0 2.0

1.1

1.8

1.25 1.4 1.6

MICROCOPY RESOLUTION TEST CHART
NATIONAL BUREAU OF STANDARDS 1963 A

FIGURE A 52A   TYPE 1 INCIDENT ON 26 FEB 77

FIGURE A 52B   TYPE 1 INCIDENT ON 26 FEB 77

FIGURE A 52C   TYPE 1 INCIDENT ON 26 FEB 77

C309

S200 −S150 (M/SEC)

S150 −S100 (M/SEC)

S100 −S50 (M/SEC)

S50 −S10 (M/SEC)

1450   1500   1510   1520   1530   1540

FIGURE A 52D   TYPE 1 INCIDENT ON 26 FEB 77
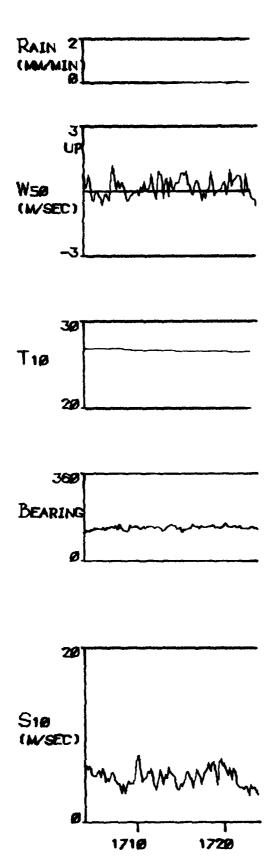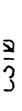
FIGURE A 52E   TYPE 1 INCIDENT ON 26 FEB 77

FIGURE A 52F   TYPE 1 INCIDENT ON 28 FEB 77

FIGURE A 53A   TYPE 4 INCIDENT ON 27 FEB 77

FIGURE A 53A (CONT) TYPE 4 INCIDENT ON 27 FEB 77

FIGURE A ' 53A (CONT) TYPE 4 INCIDENT ON 27 FEB 77

FIGURE A 53B   TYPE 4 INCIDENT ON 27 FEB 77

FIGURE A 53B (CONT) TYPE 4 INCIDENT ON 27 FEB 77
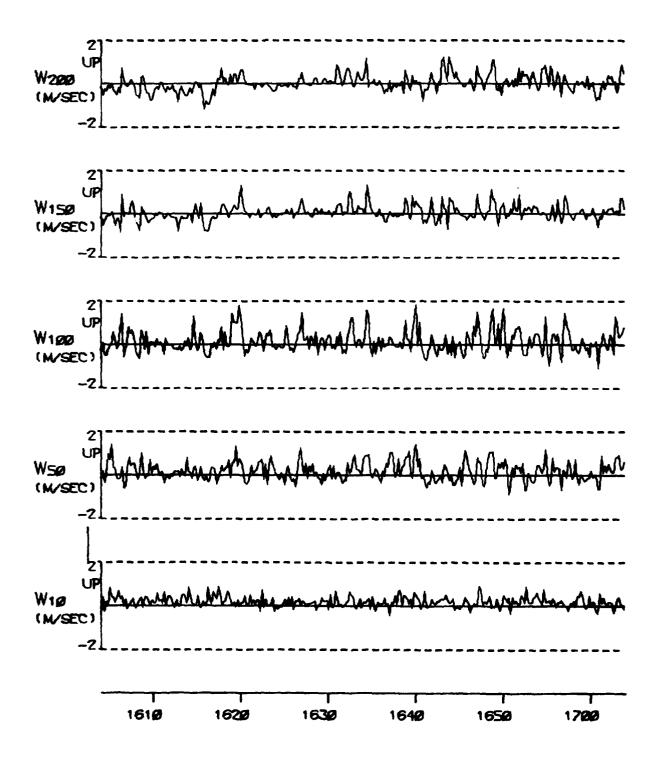
FIGURE A 53B (CONT) TYPE 4 INCIDENT ON 27 FEB 77
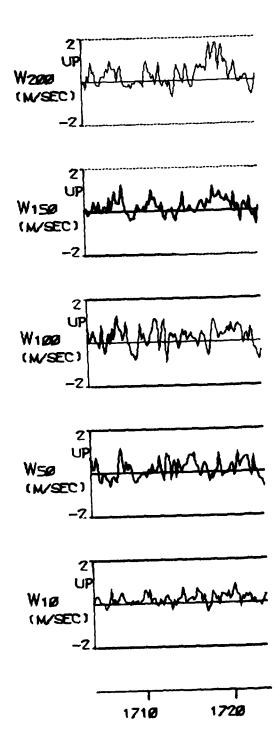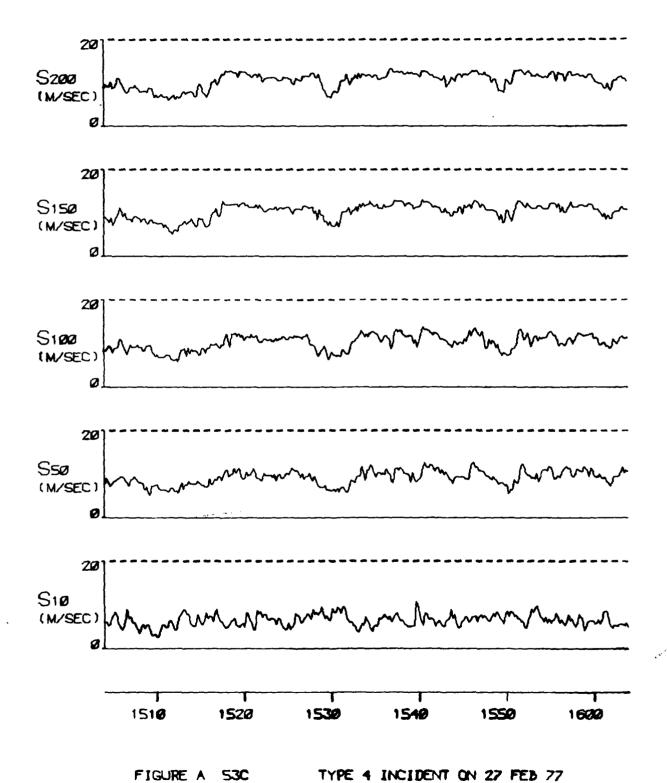
FIGURE A 53C   TYPE 4 INCIDENT ON 27 FEB 77

FIGURE A 53C (CONT) TYPE 4 INCIDENT ON 27 FEB 77
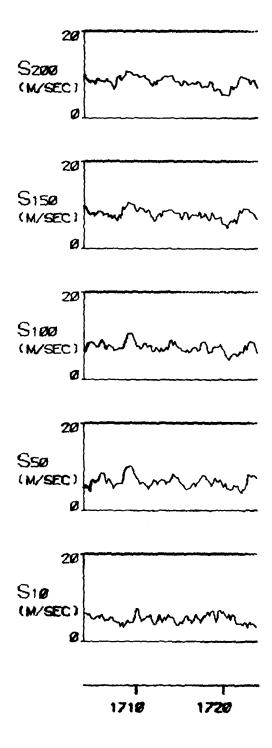
FIGURE A 53C (CONT) TYPE 4 INCIDENT ON 27 FEB 77

FIGURE A 53D   TYPE 4 INCIDENT ON 27 FEB 77
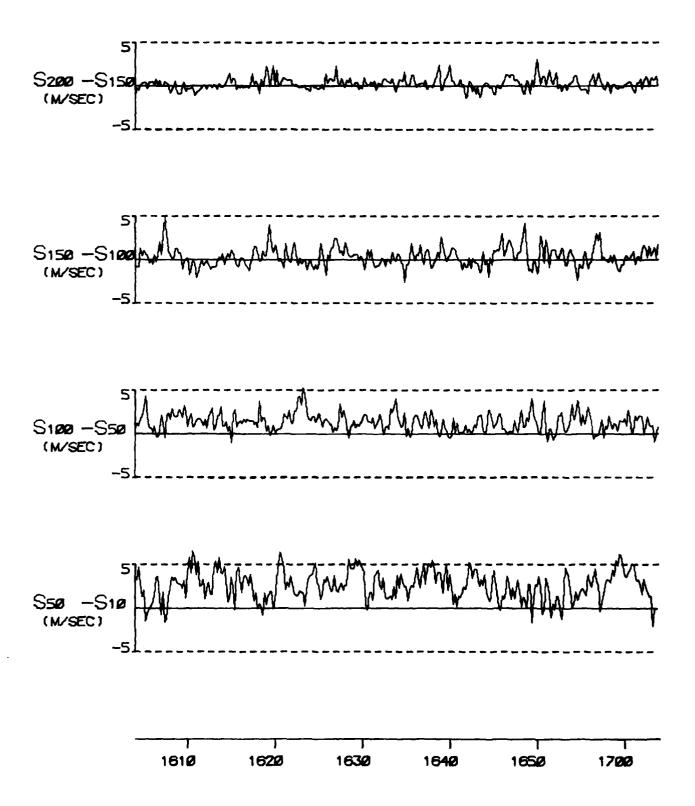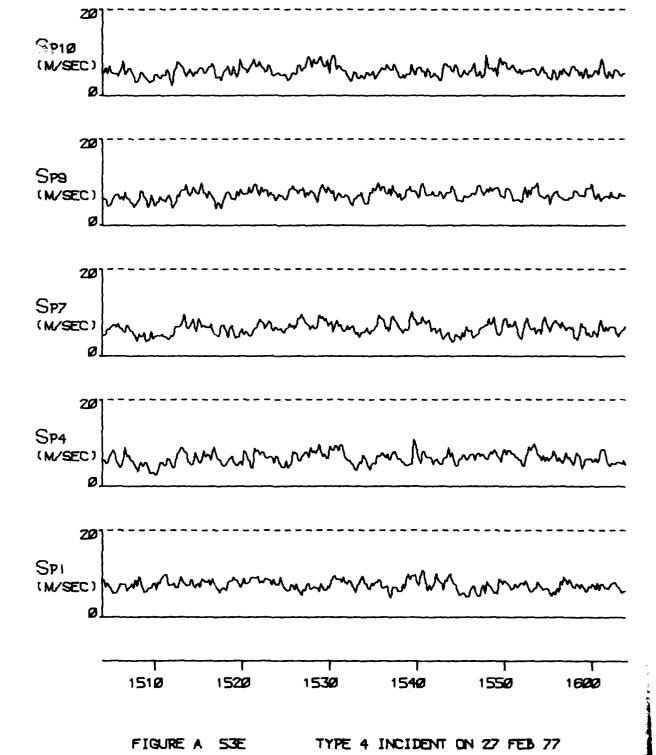
FIGURE A 53D (CONT) TYPE 4 INCIDENT ON 27 FEB 77
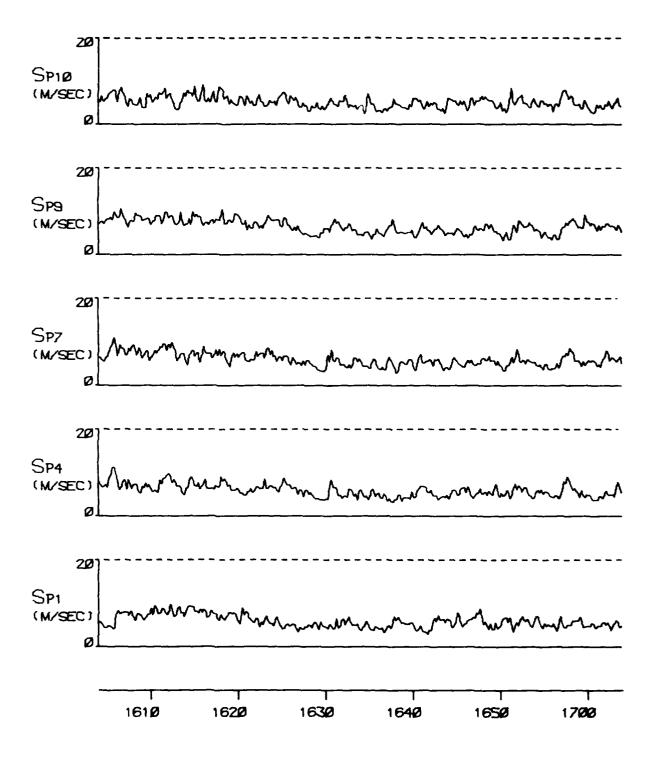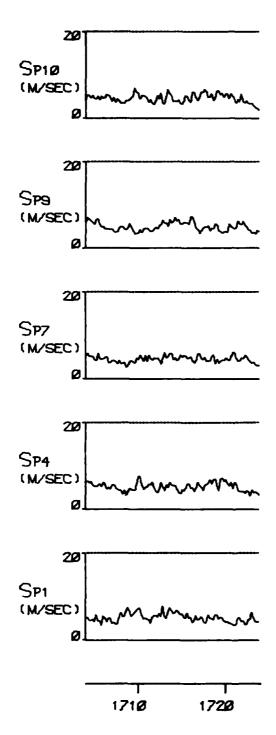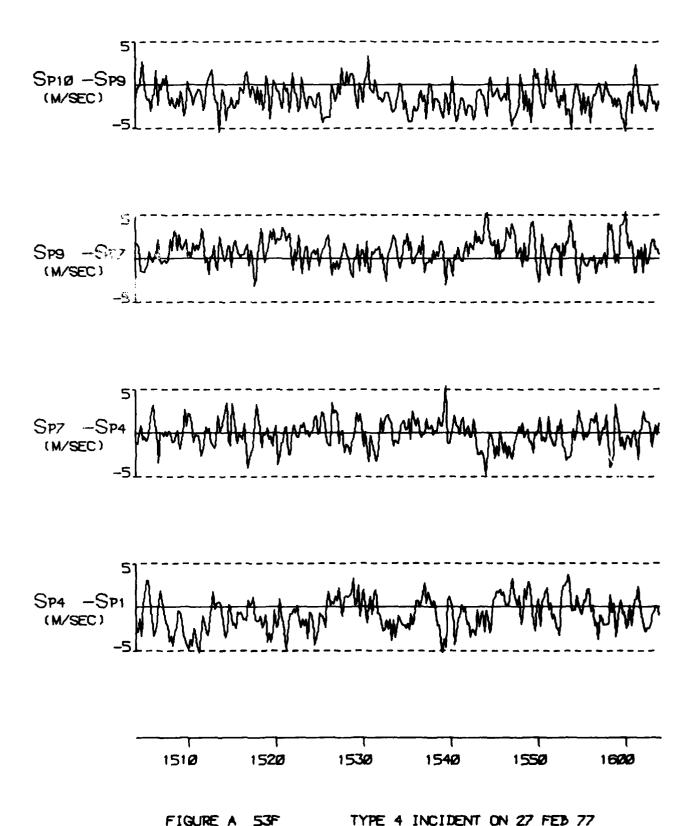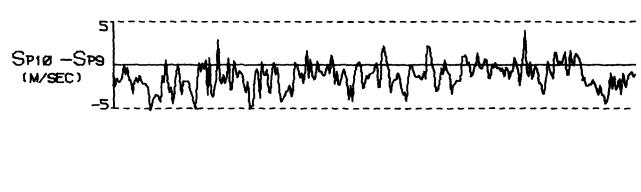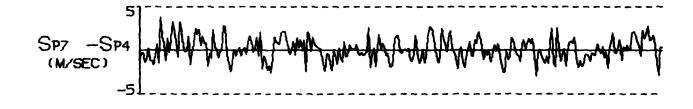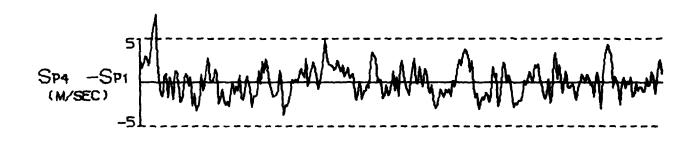
FIGURE A 53E   TYPE 4 INCIDENT ON 27 FEB 77

FIGURE A 53E (CONT) TYPE 4 INCIDENT ON 27 FEB 77

FIGURE A 53E (CONT) TYPE 4 INCIDENT ON 27 FEB 77

FIGURE A 53F   TYPE 4 INCIDENT ON 27 FEB 77

FIGURE A 53F (CONT) TYPE 4 INCIDENT ON 27 FEB 77

FIGURE A 53F (CONT) TYPE 4 INCIDENT ON 27 FEB 77

RAIN 2
(MM/MIN)
0

3
UP
WS0
(M/SEC)
-3

30
T10
20

360
BEARING
0

20
S10
(M/SEC)
0

1630   1640   1650   1700   1710   1720

C312

FIGURE A 54A   TYPE 4 INCIDENT ON 01 MAR 77

FIGURE A 54B   TYPE 4 INCIDENT ON 01 MAR 77

FIGURE A 54C   TYPE 4 INCIDENT ON 01 MAR 77

FIGURE A 54D   TYPE 4 INCIDENT ON 01 MAR 77

FIGURE A 54E   TYPE 4 INCIDENT ON 01 MAR 77
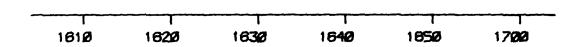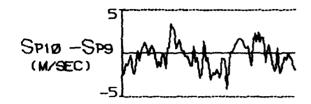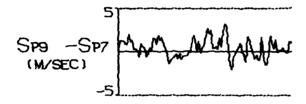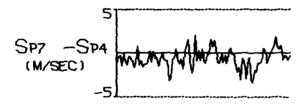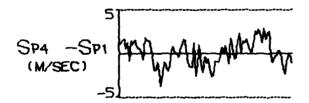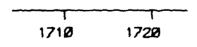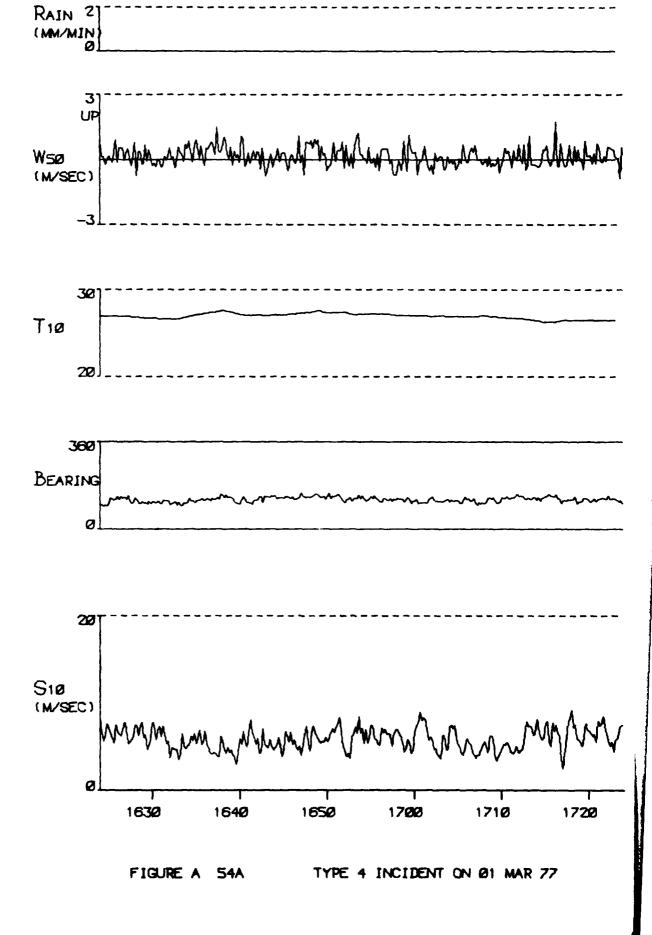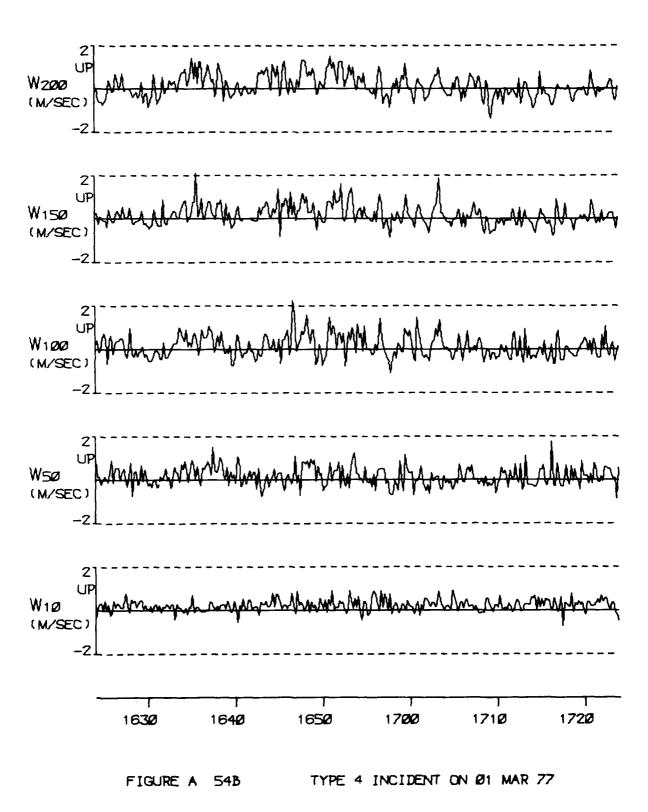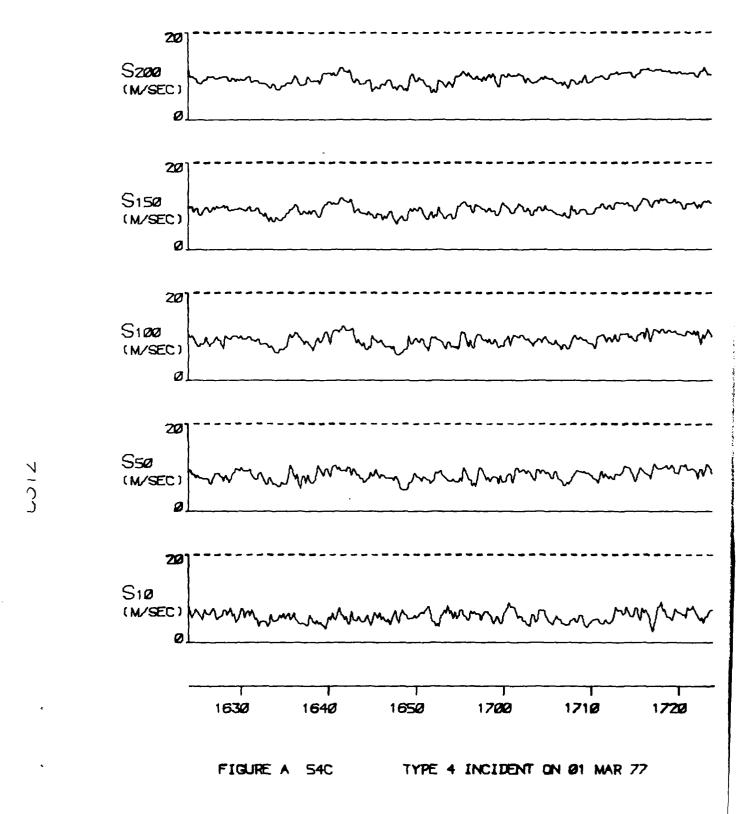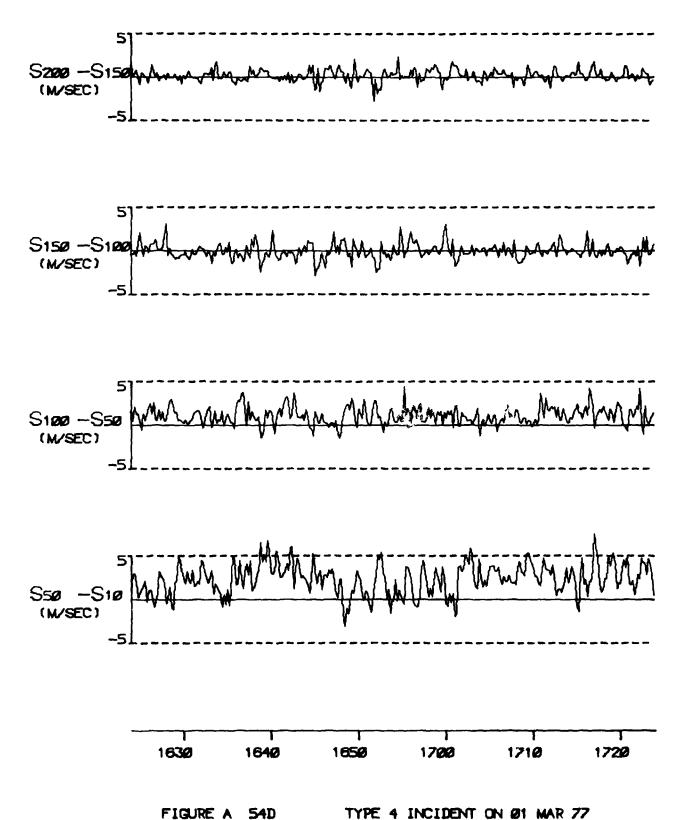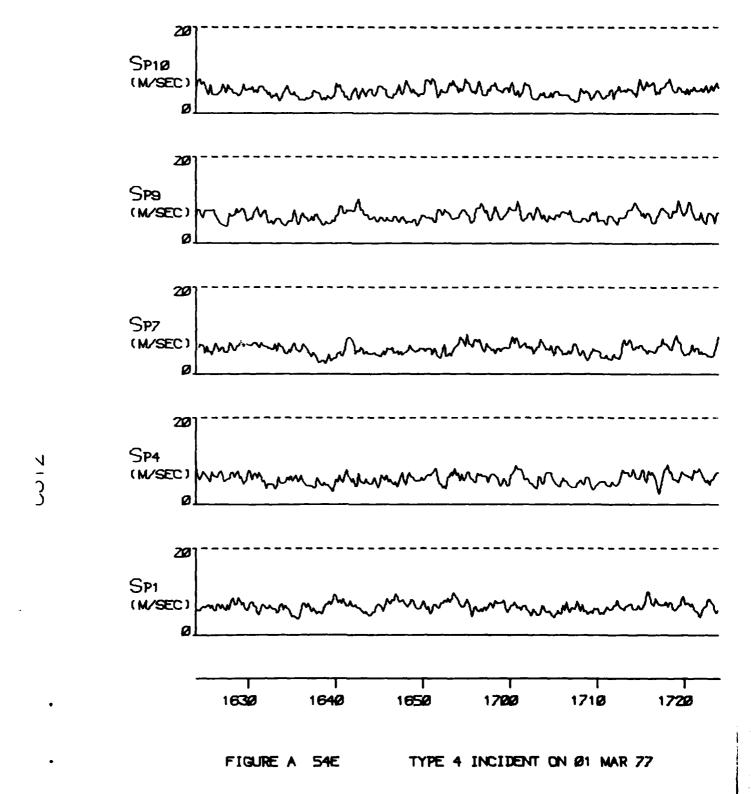
FIGURE A S4F   TYPE 4 INCIDENT ON 01 MAR 77
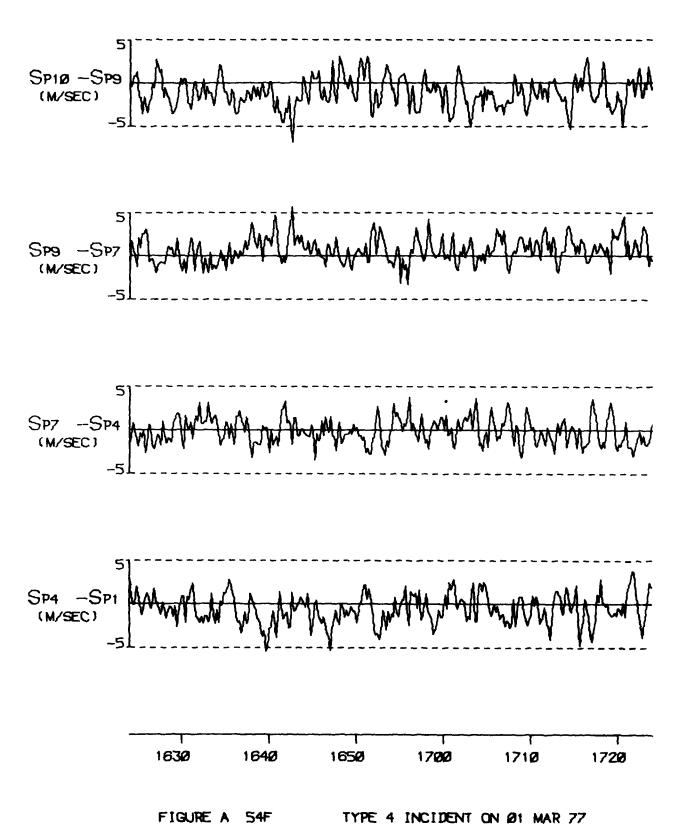
DISTRIBUTION

Copy No.

AUSTRALIA

Department of Defence

Central Office
Chief Defence Scientist	1
Deputy Chief Defence Scientist	2
Superintendent, Science and Technology Programs	3
Australian Defence Scientific and Technical Representative (UK)	—
Counsellor, Defence Science (USA)	—
Defence Central Library	4
Document Exchange Centre, D.I.S.B.	5–21
DGAD (NCO)	22
Joint Intelligence Organisation	23

Aeronautical Research Laboratories
Chief Superintendent	24
Library	25
Superintendent — Structures Division	26
Divisional File — Structures	27
Authors: C. K. Rider	28
D. J. Sherman	29
M. R. Thomson	30

Materials Research Laboratories
Library	31

Defence Research Centre
Library	32

Central Studies Establishment
Information Centre	33

RAN Research Laboratory
Library	34

Victorian Regional Office
Library	35

Air Force Office
Air Force Scientific Adviser	36
Director General Operational Requirements — Air Force	37

Department of Science and The Environment

Bureau of Meteorology, Melbourne
Publications Officer	38
Library	39
Dr R. R. Brook	40
Dr P. A. Barclay	41
Mr P. J. Meighen	42

UNITED STATES OF AMERICA